



Universitat de Girona

# ANALYTICAL STRATEGIES BASED ON INDUCTIVELY COUPLED PLASMA SPECTROSCOPY (ICP) AND DIFFUSIVE GRADIENTS IN THIN FILMS (DGT) TECHNIQUES FOR THE ASSESSMENT OF ENVIRONMENTAL POLLUTION INDICATORS

**Mireia COLON I BOSCH**

**Dipòsit legal: GI. 1378-2012**

<http://hdl.handle.net/10803/84050>

**ADVERTIMENT.** L'accés als continguts d'aquesta tesi doctoral i la seva utilització ha de respectar els drets de la persona autora. Pot ser utilitzada per a consulta o estudi personal, així com en activitats o materials d'investigació i docència en els termes establerts a l'art. 32 del Text Refós de la Llei de Propietat Intel·lectual (RDL 1/1996). Per altres utilitzacions es requereix l'autorització prèvia i expressa de la persona autora. En qualsevol cas, en la utilització dels seus continguts caldrà indicar de forma clara el nom i cognoms de la persona autora i el títol de la tesi doctoral. No s'autoritza la seva reproducció o altres formes d'explotació efectuades amb finalitats de lucre ni la seva comunicació pública des d'un lloc aliè al servei TDX. Tampoc s'autoritza la presentació del seu contingut en una finestra o marc aliè a TDX (framing). Aquesta reserva de drets afecta tant als continguts de la tesi com als seus resums i índexs.

**ADVERTENCIA.** El acceso a los contenidos de esta tesis doctoral y su utilización debe respetar los derechos de la persona autora. Puede ser utilizada para consulta o estudio personal, así como en actividades o materiales de investigación y docencia en los términos establecidos en el art. 32 del Texto Refundido de la Ley de Propiedad Intelectual (RDL 1/1996). Para otros usos se requiere la autorización previa y expresa de la persona autora. En cualquier caso, en la utilización de sus contenidos se deberá indicar de forma clara el nombre y apellidos de la persona autora y el título de la tesis doctoral. No se autoriza su reproducción u otras formas de explotación efectuadas con fines lucrativos ni su comunicación pública desde un sitio ajeno al servicio TDR. Tampoco se autoriza la presentación de su contenido en una ventana o marco ajeno a TDR (framing). Esta reserva de derechos afecta tanto al contenido de la tesis como a sus resúmenes e índices.

**WARNING.** Access to the contents of this doctoral thesis and its use must respect the rights of the author. It can be used for reference or private study, as well as research and learning activities or materials in the terms established by the 32nd article of the Spanish Consolidated Copyright Act (RDL 1/1996). Express and previous authorization of the author is required for any other uses. In any case, when using its content, full name of the author and title of the thesis must be clearly indicated. Reproduction or other forms of for profit use or public communication from outside TDX service is not allowed. Presentation of its content in a window or frame external to TDX (framing) is not authorized either. These rights affect both the content of the thesis and its abstracts and indexes.



**University of Girona**  
Chemistry Department  
Analytical Chemistry Unit

**DOCTORAL THESIS**

**ANALYTICAL STRATEGIES BASED ON  
INDUCTIVELY COUPLED PLASMA  
SPECTROSCOPY (ICP) AND DIFFUSIVE  
GRADIENTS IN THIN FILMS (DGT) TECHNIQUES  
FOR THE ASSESSMENT OF ENVIRONMENTAL  
POLLUTION INDICATORS**

**Mireia Colon i Bosch**

**BIOTECHNOLOGY**

July 2010

Directed by Dra. Manuela Hidalgo Muñoz and Dra. Mònica Iglesias Juncà

PhD dissertation presented in candidacy for the degree of doctor in Chemistry at the  
University of Girona



Departament de Química  
Àrea de Química Analítica

La **Dra. Manuela Hidalgo Muñoz**, Professora Titular, i la **Dra. Mònica Iglesias Juncà**, Professora Agregada, del Departament de Química de la Universitat de Girona,

**CERTIFIQUEM:**

Que aquest treball, titulat “*Analytical strategies based on Inductively Coupled Plasma Spectroscopy (ICP) and Diffusive Gradients in Thin Films (DGT) techniques for the assessment of environmental pollution indicators*”, ha estat realitzat sota la nostra direcció i que compleix els requeriments per poder optar a Menció Europea.

I perquè així consti, signem la present certificació.

Dra. Manuela Hidalgo Muñoz

Dra. Mònica Iglesias Juncà

Girona, 29 de juliol de 2010

The development of this thesis has been funded by two research projects from the Spanish Government:

- *“Estudio integrado de la calidad del agua en zonas de abandono minero. Evaluación de los efectos sobre el medio hídrico superficial y subterráneo y de las posibles acciones para su atenuación”* (Ref. CGL2004-05963-C04-03/HID).
- *“Movilidad y redistribución de metales en la zona no saturada y sus efectos sobre cambios de calidad de aguas subterráneas”* (Ref. CGL-2007-66861-C04-02/HID).

Mireia Colon i Bosch gratefully acknowledges a PhD research grant from the Spanish Government (BES-2005-6962) and its associated research mobility grants. Part of the experimental work of this thesis was performed in:

- Departamento de Química Analítica, Nutrición y Bromatología, University of Alicante, Spain.
- Department of Environmental Science, Lancaster University, United Kingdom

*A la meva família,  
especialment a en Ton*

# CONTENTS

<b>SUMMARY</b> .....	<b>1</b>
<b>RESUM</b> .....	<b>7</b>
<b>RESUMEN</b> .....	<b>13</b>
<b>INTRODUCTION</b> .....	<b>19</b>
<b>I.1 Inductively Coupled Plasma</b> .....	<b>23</b>
I.1.1 Overview .....	23
I.1.1.1 Plasma source .....	24
I.1.1.2 Sample introduction devices .....	27
I.1.2 Inductively coupled plasma – atomic emission spectroscopy (ICP-AES) .....	31
I.1.2.1 Interferences .....	32
<i>I.1.2.1.1 Non-spectral interferences</i> .....	32
<i>I.1.2.1.2 Spectral interferences</i> .....	34
I.1.2.2 Spectrometers .....	32
I.1.3 Inductively coupled plasma – mass spectrometry (ICP-MS) .....	37
I.1.3.1 Interferences .....	38
<i>I.1.3.1.1 Non-spectral interferences</i> .....	38
<i>I.1.3.1.2 Spectral interferences</i> .....	39
I.1.3.2 Collision/reaction cells .....	41
I.1.3.3 Interface devices .....	43
I.1.3.4 Mass analyzers .....	43
<b>I.2. The technique of diffusive gradients in thin films (DGT)</b> .....	<b>46</b>
I.2.1 General approaches .....	46
I.2.1.1 Gel types.....	47
<i>I.2.1.1.1 Diffusive gels</i> .....	47
<i>I.2.1.1.2 Resin gels</i> .....	47
I.2.1.2 Theory .....	48
<i>I.2.1.2.1. Diffusion coefficients</i> .....	49
I.2.2 DGT applications.....	50
I.2.2.1 Applications to water samples.....	50
I.2.2.2 Applications in sediments and soils .....	52

I.2.2.2.1 <i>General considerations</i> .....	52
I.2.2.2.2 <i>Homogeneous systems (bulk deployments)</i> .....	53
I.2.2.2.3 <i>Heterogeneous systems (high-resolution deployments)</i> .....	54
<b>I.3. Sulfide in the environment .....</b>	<b>55</b>
I.3.1 Sulfide in sediments .....	55
I.3.2 Sulfide determination .....	56
I.3.2.1 Spectrophotometric methods .....	57
I.3.2.2 Electrochemical methods .....	58
I.3.2.3 Other methods for sulfide determination.....	59
<b>I.4. Arsenic in the environment .....</b>	<b>60</b>
I.4.1 Arsenic in the aquatic environment.....	62
I.4.2 Arsenic determination .....	62
I.4.2.1 Electrochemical methods .....	63
I.4.2.2 Spectrometric methods .....	64
<b>I.5 References .....</b>	<b>67</b>
 <b>OBJECTIVES.....</b>	 <b>81</b>
 <b>CHAPTER 1 .....</b>	 <b>85</b>
<b>1.1 Introduction .....</b>	<b>87</b>
1.1.1 Sulfide in the environment: the importance of being determined .....	87
1.1.2 Determination of sulfide by ICP-based spectroscopic techniques.....	89
1.1.2.1 Vapor generator .....	90
1.1.3 Method Optimization.....	91
1.1.3.1 Experimental design .....	91
1.1.3.1.1 <i>Complete factorial design</i> .....	92
1.1.3.1.2 <i>Fractional factorial design</i> .....	94
1.1.3.2 The simplex method .....	94
<b>1.2 Experimental.....</b>	<b>96</b>
1.2.1 Reagents and solutions.....	96
1.2.2 Sampling procedure .....	96
1.2.3 Instrumentation .....	98
1.2.4 ICP-MS method optimization.....	100

1.2.5 ICP-AES method development.....	101
<b>1.3 Results and discussion .....</b>	<b>101</b>
1.3.1 Sulfide determination by ICP-MS .....	101
1.3.1.1 Experimental design and optimization .....	102
1.3.1.2 Method performance.....	105
1.3.2 SEM/AVS relationship in Mar Menor sediments.....	107
1.3.3 Sulfide determination by ICP-AES.....	109
1.3.3.1 Buffer selection.....	109
1.3.3.2 Operating parameters.....	109
1.3.3.3 Solvent plasma load.....	109
1.3.3.4 Method Performance .....	116
1.3.3.5 Sulfate and sulfide determination .....	119
<b>1.4 Conclusions .....</b>	<b>120</b>
<b>1.5 References.....</b>	<b>122</b>
<b>CHAPTER 2.....</b>	<b>125</b>
<b>2.1 Introduction .....</b>	<b>127</b>
2.1.1 Determination of arsenic by ICP-MS .....	128
2.1.1.1 Mathematical corrections.....	130
2.1.1.2 Internal standard methodology .....	130
2.1.1.3 Effect of carbon-containing compounds on ICP-MS .....	130
<b>2.2 Experimental.....</b>	<b>131</b>
2.2.1 Reagents and solutions.....	131
2.2.2 Instrumentation .....	132
2.2.3 Effect of collision/reaction gases flow rates .....	132
2.2.4 Interference equation evaluation.....	133
2.2.5 Alcohol effect on m/z signal.....	133
2.2.6 Internal standard studies .....	133
2.2.7 Sample preparation .....	134
<b>2.3 Results and discussion .....</b>	<b>134</b>
2.3.1 Effect of collision/reaction gas flow rates .....	134
2.3.2 Interference equation evaluation.....	136
2.3.3 Effect of alcohol on the m/z signal .....	137



2.3.4 Internal standard evaluation.....	140
2.3.5 Analysis of spiked samples, CRM and real samples .....	143
<b>2.4 Conclusions .....</b>	<b>147</b>
<b>2.5 References.....</b>	<b>149</b>
<b>CHAPTER 3.....</b>	<b>153</b>
<b>3.1 Introduction .....</b>	<b>158</b>
3.1.1 Assessment of metal availability .....	156
<b>3.2 Experimental.....</b>	<b>158</b>
3.2.1 DGT gel preparation .....	158
3.2.2 Experiments with synthetic water.....	158
3.2.3 Sampling and analysis of acidic mine drainage waters .....	160
3.2.4 Sampling and characterisation of mining wastes.....	161
3.2.5 Deployment of DGT in mining residues.....	162
3.2.6 DGT calculations .....	163
3.2.7 Modeling with WHAM VI .....	163
3.2.8 Pot Experiments.....	164
<b>3.3 Results and discussion.....</b>	<b>164</b>
3.3.1 DGT performance in acidic aqueous solution .....	164
3.3.1.1 Effect of pH on DGT measurements of Co, Ni, Cu, Zn, Cd and Pb ....	164
3.3.1.2 Effect of calcium on DGT measurements of Co, Ni, Cu, Zn, Cd and Pb	
.....	166
3.3.1.3 Effect of fulvic acid on DGT measurements of Co, Ni, Cu, Zn, Cd and	
Pb .....	168
3.3.1.4 Acidic mine drainage (AMD) waters .....	169
3.3.2 DGT performance in acidic mining wastes .....	172
3.3.2.1 pH of mining wastes .....	172
3.3.2.2 Pseudototal heavy metal content .....	173
3.3.2.3 Single Extractions .....	174
3.3.2.4 DGT-measured metal concentration in mining wastes.....	178
3.3.2.5 Metal content in vegetation specimens ( <i>Crithmum maritimum</i> ).....	181
3.3.2.6 DGT-plant relationships .....	182
<b>3.4 Conclusions .....</b>	<b>183</b>

<b>3.5 References.....</b>	<b>185</b>
<b>GENERAL DISCUSSION .....</b>	<b>189</b>
<b>GENERAL CONCLUSIONS.....</b>	<b>199</b>
<b>AGRAÏMENTS .....</b>	<b>203</b>



## SUMMARY

Environmental pollution is the modification of the natural contents of chemicals, particulate matter or biological materials that damages the natural environment. Some metals, metalloids and other species such as sulfides or oxides have been introduced into the environment through natural and anthropogenic sources over the years and they are now a threat to human health, animals and plants. Thus, environmental pollution is an issue of serious international concern and it requires immediate attention.

The aim of this thesis is to apply analytical existing methodologies and the development of novel procedures based on spectroscopic inductively coupled plasma (ICP) spectroscopy which can be used for the determination of relevant environmental inorganic contaminants such as sulfide, metals and metalloids. Moreover, the use of diffusive gradients in thin films (DGT) technique has been proved in acidic contaminated mining samples. The developed methodologies have been applied to the analysis of different types of samples from the abandoned Cartagena mining area.

On one hand, it is well known that the detection of sulfide has gained importance, mainly as a consequence of the toxicity of hydrogen sulfide. Sulfide is usually determined in natural and waste waters because at certain pH conditions, hydrogen sulfide can be generated in a sufficient amount to present a danger to either human health or environment. This interest in the analytical community has resulted in a large number of developed protocols. Nevertheless, the need to determine this compound at very low levels of concentration has forced to find more sensitive techniques. ICP quadrupole mass spectrometry (ICP-QMS) has been used as a sensitive technique for the simultaneous determination of trace elements in different matrices due to its good performance in terms of robustness, sample throughput and simplified sample preparation. However, sulfur isotopes are particularly difficult to measure accurately by ICP-QMS due to the large interference from  $^{16}\text{O}^{16}\text{O}^+$  on  $^{32}\text{S}^+$  as well as  $^{16}\text{O}^{17}\text{O}^+$  on  $^{33}\text{S}^+$  and  $^{16}\text{O}^{18}\text{O}^+$  on  $^{34}\text{S}^+$ . The introduction of the reaction cell and/or collision cell technique has proved to be an effective method for alleviating spectroscopic interferences in the ICP-QMS analysis, removing interfering ions by using gases such as hydrogen, helium or oxygen. In the same way, ICP atomic emission spectrometry (ICP-AES) has also been used for the determination of elementary sulfur. However, as sulfur emission lines

are below 190 nm, its determination by means of ICP-AES requires purging the path between the plasma and the monochromator with nitrogen.

In this thesis, simple methods to determine sulfide at low levels ( $\mu\text{g L}^{-1}$ ) in aqueous samples and sediments by water free hydrogen sulfide vapor generation using a commercially available vapor generation accessory have been developed. The hydrogen sulfide is then introduced in the ICP-QMS, equipped with an octopole collision/reaction cell which is pressurized with hydrogen and helium gases, or in the ICP-AES where the optical path between the plasma and the monochromator is purged with nitrogen. When using ICP-QMS, experimental designs have been carried out in order to select the instrumental parameters related with the collision/reaction cell that significantly affects sulfur isotopes determination. The operating conditions were then optimized to obtain the best signal to background ratio for  $^{32}\text{S}$ . When using ICP-AES, the sulfur emission has been monitored at the 180.669 nm line. Moreover, further experiments have demonstrated that the gas/liquid separator of the vapor generator can be replaced by a commercial nebulization chamber obtaining also a sensitive and reliable method. This methodology permits the determination of sulfide and sulfate components in aqueous samples using hydrochloric acid and water in the reaction tube of the vapor generator respectively. Since certified reference material of natural water with a certified value for  $\text{S}^{2-}$  is not commercially available, the ICP developed methods have been evaluated by comparison with the well-established potentiometric method. In all cases detection limits achieved were lower than those obtained by the sulfide electrode.

On the other hand, arsenic is a naturally occurring element present in the environment in both organic and inorganic forms and its determination has gained importance within environmental community due to its high toxicity to flora, fauna and humans. During the last forty years, many methods based on different techniques have been developed for arsenic determination in a variety of matrices. Among them, spectrometric techniques and electrochemical methods have been usually employed. However, it is well known that arsenic determination by ICP-MS suffers from both spectral and non-spectral interferences. Possibly, the most important drawback of ICP-QMS equipped with a pneumatic nebulizer is the formation of  $^{40}\text{Ar}^{35}\text{Cl}^+$  interference obtained when moderate chloride ( $\text{mg L}^{-1}$ ) matrices are introduced in the ICP-MS. As this interference has the same mass charge ratio ( $m/z$ ) as arsenic, results can be inaccurate, especially

when low levels of arsenic are determined. As it has been mentioned, the introduction of ICP-MS equipped with collision/reaction cell technology has been demonstrated to be a useful way to overcome problems linked with polyatomic interferences. Furthermore, it is well known that matrix effects can be very important in plasma based atomic spectrometric techniques, since moderate amounts of matrix ions can significantly change the analyte signal, especially when using ICP-MS. Several techniques can be used to correct these matrix effects, including standard addition, isotope dilution or internal standard techniques.

In this thesis different studies have been conducted for the determination of arsenic by ICP-MS in natural waters with high sodium and chloride content and spectral and non-spectral interferences on arsenic measurement have been investigated. The optimization of collision/reaction gas flow rates has been carried out and a mixture of 2.9 mL min<sup>-1</sup> of hydrogen and 0.5 mL min<sup>-1</sup> of helium has been found to be suitable for the removal of <sup>40</sup>Ar<sup>35</sup>Cl<sup>+</sup> interference. Although the use of arithmetic corrections is necessary when no gas is used in the collision/reaction cell, it does not completely eliminate persistent interferences produced in the plasma. Moreover, modification of arithmetic corrections must be made when this correction is used together with a pressurised collision/reaction cell due to the formation of additional interferences. The effect of the introduction of small amounts of alcohol has also been studied in this part of the thesis and has been compared under vented and pressurized cell conditions. It has been verified that the presence of 4% (v/v) of ethanol or methanol results in an increase in arsenic sensitivity, being more important under pressurized cell conditions. Moreover, under vented cell conditions the addition of alcohol also results in a decrease of the formation of the polyatomic interference (<sup>40</sup>Ar<sup>35</sup>Cl<sup>+</sup>). However, this decrease was not observed under pressurized cell conditions as the interference is almost totally eliminated. Finally, different elements have been studied as possible internal standards for arsenic determination in the presence of high amounts of sodium. Rhodium has been found to be the most suitable element for arsenic determination in the presence of sodium, under both vented and pressurized cell conditions. The presence of alcohol in the sample matrix also affects the internal standards behaviour, but rhodium is again the most adequate internal standard for arsenic determination in such condition.

## SUMMARY

---

The last part of this thesis focuses on the use of diffusive gradients in thin films (DGT) technique in acidic samples. This technique has already been used for labile metal measurement in waters with pH ranging from 5-10. However, a limitation of DGT is the reduced performance of the chelating Chelex resin at low pH, due to the competition between metals and hydrogen ions for the binding agent. In this thesis, the effect of pH, calcium and fulvic acid on the adsorption of different metals on the resin gel in the pH range 1.5-5.5 has been studied under controlled laboratory conditions. Laboratory results showed that DGT can be used in water with pH as low as 3.5 for cobalt, zinc and cadmium, 3.0 for nickel and lead and 2.0 for copper, without the need for correcting for reduced adsorption. However, below these pH values, concentration given by DGT must be corrected using a sigmoid 5 parameters curve obtained for each metal. On the other hand, the effect of calcium concentration on DGT measured concentrations of the transition metals has also been studied at pH 2.5 and 3.5. Calcium has little effect on metal-Chelex binding at low pH values for almost all metals studied. However, at pH 3.5 the presence of calcium at high concentrations affected cadmium adsorption, with the concentration of cadmium determined by DGT being about 25% lower than the expected concentration. Experiments with added fulvic acid demonstrate that DGT measured concentrations of copper and lead are affected by fulvic acid presence even at very low pH due to the high affinity of these metals for organic matter. The other metals studied are in inorganic form at low pH and so fulvic acid does not influence the DGT measurement. The experimental results have compared well with predictions of speciation made using the speciation program WHAM VI. DGT has been used with correction for low pH to measure metals in waters from acid mine drainage containing high amounts of lead, zinc and cadmium.

For the first time, DGT have been deployed in acidic mining wastes with pH ranging from 2 to 7 to assess zinc, lead and cadmium availability to vegetation. For this purpose, eight residues from the abandoned mining area of Cartagena, Spain, have been studied. The results obtained with the DGT device have been compared with other bioavailability tests such as metal concentration in pore water or in selective extracts. In this way, the DTPA (Diethylene triamine pentaacetic acid) extraction protocol and the first steps of BCR (Community Bureau of Reference) and NIST (National Institute of Standards and Technology) standardized sequential extraction procedures have been carried out. Pseudototal metal content has been also determined at the eight studied

sites. Measurements using DGT correlated well with magnesium chloride extraction procedure (first step of NIST) and the pseudototal metal content. The DGT-recovered metal concentration has been also correlated with metal content in *Crithmum maritimum* species grown on the mining wastes under controlled laboratory conditions. Results indicated significant correlations for lead and zinc at pH above 5, but not a direct relationship between DGT measurements and cadmium content in plants.





## RESUM

La contaminació ambiental és la modificació del contingut natural de components químics, partícules o matèria biològica que afecta negativament al medi ambient. Alguns metalls, metal·loides i altres espècies com sulfurs o òxids s'han introduït al medi ambient durant anys a través de fonts naturals i antropogèniques, i ara representen un greu problema per a la salut humana, els animals i les plantes. Així, la contaminació ambiental és un tema d'interès internacional que requereix una atenció immediata.

L'objectiu d'aquesta tesi és aplicar metodologies analítiques existents i desenvolupar nous procediments basats en l'espectrometria amb font de plasma induït per alta freqüència, la qual es pot utilitzar per a la determinació de contaminants inorgànics rellevants. D'altra banda, la tècnica de DGT (diffusive gradients in thin films) s'ha aplicat a mostres àcides procedents de zones mineres. Les metodologies desenvolupades s'han utilitzat per analitzar diferents tipus de mostres de la zona minera abandonada de Cartagena.

Per una banda, se sap que la determinació de sulfur ha guanyat importància a causa de l'alta toxicitat del sulfur d'hidrogen. Normalment, el sulfur es determina en aigües naturals i residuals ja que, en determinades condicions de pH, es pot generar una quantitat suficient de sulfur d'hidrogen que pot arribar a ser perillosa tant per a la salut humana com per al medi ambient. Aquest interès entre la comunitat analítica ha fet que s'hagin desenvolupat un gran nombre de protocols per a la determinació de sulfur. Tot i així, la necessitat de determinar aquest component a molt baixes concentracions ha provocat que s'hagi hagut de recórrer a tècniques cada vegada més sensibles. L'espectrometria de masses amb font de plasma induït per alta freqüència i analitzador de masses quadripolar (ICP-QMS) s'ha utilitzat com una tècnica molt sensible per a la determinació simultània d'elements a nivells traça, en diferents matrius, gràcies al seu bon funcionament en termes de robustesa, rendiment i preparació senzilla de la mostra. Tanmateix, els isòtops de sulfur són particularment difícils de mesurar amb ICP-QMS a causa de les importants interferències provocades per  $^{16}\text{O}^{16}\text{O}^+$  sobre  $^{32}\text{S}^+$  així com també  $^{16}\text{O}^{17}\text{O}^+$  sobre  $^{33}\text{S}^+$  i  $^{16}\text{O}^{18}\text{O}^+$  sobre  $^{34}\text{S}^+$ . S'ha demostrat que amb la utilització de cel·les de col·lisió/reacció es pot eliminar gran part d'aquestes interferències espectroscòpiques, reduint la presència de ions poliatòmics interferents mitjançant gasos

com hidrogen, heli o oxigen. Així mateix, la tècnica d'ICP amb espectrometria d'emissió atòmica (ICP-AES) també s'ha utilitzat per a la determinació de sulfur, però, com que les línies d'emissió del sofre estan per sota de 190 nm, la determinació d'aquest element requereix purgar el pas entre el plasma i el monocromador amb gas nitrogen.

En la present tesi, s'han desenvolupat mètodes senzills per a la determinació de sulfur a baixes concentracions ( $\mu\text{g L}^{-1}$ ) en mostres aquoses i sediments mitjançant la generació de sulfur d'hidrogen utilitzant un accessori de generació d'hidrurs comercial. Un cop format el sulfur d'hidrogen, aquest es pot introduir a l'ICP-QMS, equipat amb una cel·la de col·lisió/reacció pressuritzada amb hidrogen i heli, o a l'ICP-AES purgant amb nitrogen el pas entre el plasma i el monocromador. En el cas del mètode mitjançant ICP-QMS, s'ha dut a terme un disseny experimental per seleccionar els paràmetres instrumentals relacionats amb la cel·la de col·lisió/reacció que afecten la determinació dels isòtops de sofre. S'han optimitzat les condicions de treball per tal d'obtenir la millor relació senyal/soroll per l'isòtop  $^{32}\text{S}$ . Amb l'ICP-AES, s'ha mesurat l'emissió del sofre a 180,669 nm. A més, s'ha demostrat que el separador gas/líquid del generador d'hidrurs es pot substituir per un nebulitzador comercial, d'aquesta manera també s'obté un mètode sensible i fiable; a més, aquesta configuració permet la determinació simultània de sulfur i sulfat en mostres aquoses utilitzant àcid clorhídric i aigua, respectivament, en el tub de reacció. Com que no existeix cap material aquós de referència amb un valor certificat per a la concentració de sulfur, els tres mètodes desenvolupats basats en ICP s'han avaluat per comparació amb el mètode potenciomètric de referència. En tots els casos s'han obtinguts límits de detecció més baixos que quan s'utilitza l'elèctrode de sulfur.

Per altra banda, l'arsènic és un element que es troba en el medi tant en forma orgànica com en forma inorgànica. A causa de la seva alta toxicitat per a la flora, fauna i éssers humans, la determinació d'aquest element ha anat guanyant importància. Durant els últims quaranta anys s'han desenvolupat nombrosos mètodes basats en tècniques diverses per determinar arsènic en diferents matrius. Les tècniques espectromètriques i els mètodes electroquímics han estat els més utilitzats per aquest propòsit. No obstant això, se sap que la tècnica de ICP-MS presenta problemes d'interferències, tant espectrals com no espectrals i, possiblement, l'inconvenient més important de l'ICP-

QMS equipat amb un nebulitzador neumàtic és la formació de la interferència  $^{40}\text{Ar}^{35}\text{Cl}^+$  que s'obté en matrius amb un contingut moderat de clor ( $\text{mg L}^{-1}$ ). Com que aquesta interferència té la mateixa relació massa/càrrega ( $m/z$ ) que l'arsènic, els resultats poden ser inexactes, especialment quan es determinen quantitats baixes d'arsènic. Tal com s'ha dit anteriorment, la introducció d'una cel·la de col·lisió/reacció és una bona estratègia per solucionar problemes relacionats amb les interferències poliatòmiques. A més, també se sap que els efectes provocats per la matriu poden ser molt importants en les tècniques d'ICP, ja que la presència, més o menys moderada, d'alguns ions de la matriu pot modificar el senyal analític significativament, especialment quan s'utilitza ICP-MS. Per tal de corregir aquests efectes matriu s'han utilitzat diferents tècniques com l'addició estàndard, la dilució isotòpica o la utilització de patrons interns.

En aquesta tesi s'han fet alguns estudis per determinar arsènic mitjançant ICP-MS en aigües naturals amb alt contingut de sodi i clor, i s'han investigat les interferències espectrals i no espectrals sobre aquest element. S'ha optimitzat el cabal de gasos de la cel·la de col·lisió/reacció i s'ha trobat que, per eliminar la interferència  $^{40}\text{Ar}^{35}\text{Cl}^+$ , es pot utilitzar una barreja de  $2,9 \text{ mL min}^{-1}$  d'hidrogen i  $0,5 \text{ mL min}^{-1}$  d'heli. Tot i que les correccions matemàtiques són necessàries quan no es pressuritza la cel·la de col·lisió/reacció, aquestes no eliminen completament les interferències que es produeixen en el plasma. A més, s'han de fer algunes modificacions d'aquestes correccions quan s'utilitzen amb la cel·la pressuritzada, ja que es formen interferències addicionals. En aquesta part de la tesi, també s'ha estudiat l'efecte que produeix la presència de petites quantitats d'alcohol a les mostres quan s'utilitza una cel·la pressuritzada i sense pressuritzar. S'ha verificat que la presència d'un 4% (v/v) d'etanol o metanol produeix un increment de la sensibilitat de l'arsènic, que és més important quan es pressuritza la cel·la. A més, quan no es pressuritza la cel·la, la presència d'alcohol fa que disminueixi la interferència poliatòmica ( $^{40}\text{Ar}^{35}\text{Cl}^+$ ). Tanmateix, aquesta disminució no s'observa amb cel·la pressuritzada ja que gran part d'aquesta interferència és eliminada. Finalment, s'han estudiat diferents elements com a possibles patrons interns per a la determinació d'arsènic en presència d'altres concentracions de sodi. S'ha observat que el rodi és l'element que es comporta millor per a la determinació d'arsènic en presència de sodi, tant amb cel·la pressuritzada com sense pressuritzar. La presència d'alcohol també afecta el comportament dels patrons interns, però el rodi

continua essent el patró intern més adequat per a la determinació d'arsènic en aquestes condicions.

L'última part d'aquesta tesi se centra en l'estudi de l'aplicabilitat de la tècnica de DGT (diffusive gradients in thin films) en mostres àcides. Aquesta tècnica ha estat utilitzada per mesurar metall làbil en aigües amb valors de pH entre 5 i 10. No obstant això, una limitació del DGT és la competència amb els ions hidrogen per l'agent complexant a valors de pH baixos. En aquesta tesi s'ha estudiat l'efecte del pH, del calci i de l'àcid fúlvic en l'adsorció de diferents metalls sobre la resina Chelex en l'interval de pH de 1,5 a 5,5 al laboratori. Aquests estudis demostren que els dispositius de DGT es poden utilitzar, sense necessitat de corregir els resultats, en aigües amb pH de fins a 3,5 per determinar cobalt, zinc i cadmi; 3,0 per níquel i plom i 2 per coure. Tot i així, per sota d'aquests valors de pH, la concentració obtinguda a partir de la tècnica de DGT s'ha de corregir utilitzant les corbes sigmoïdals de 5 paràmetres ajustades per a cada metall. Per altra banda, també s'ha estudiat l'efecte del calci sobre les concentracions de metall determinades mitjançant la tècnica de DGT tant a pH 2,5 com a pH 3,5. S'ha observat que, per a gairebé tots els elements, la presència de calci afecta, tot i que de manera poc important, la interacció metall-Chelex a valors de pH baixos i, a més, a pH 3,5 el calci també afecta la determinació del cadmi de manera que el resultat obtingut amb el DGT és un 25% més baix del que s'esperava. Els experiments amb àcid fúlvic han demostrat que l'especiació del plom i del coure es veu afectada per la presència d'aquest àcid, fins i tot a valors de pH molt baixos, a causa de la gran afinitat d'aquests metalls per la matèria orgànica. Els altres metalls que s'han estudiat, en canvi, es troben en forma inorgànica a valors de pH baixos. Els resultats experimentals s'han comparat amb les prediccions fetes pel programa d'especiació WHAM VI. La tècnica de DGT, amb les corresponents correccions de pH, s'ha utilitzat per analitzar aigües àcides de mineria que contenien grans quantitats de plom, zinc i cadmi.

Per primera vegada, el DGT s'ha utilitzat en residus àcids de mineria per avaluar la disponibilitat de zinc, plom i cadmi per a la vegetació. Amb aquest propòsit, s'han estudiat vuit residus (amb valors de pH entre 2 i 7) de la zona minera, actualment abandonada, de Cartagena, Espanya. Els resultats obtinguts s'han comparat amb altres tests de biodisponibilitat com la concentració de metall en aigua de porus o en diferents dissolucions extractants. Així, s'han utilitzat el protocol d'extracció simple amb DTPA

(Diethylene triamine pentaacetic acid) i els primers passos dels procediments d'extracció seqüencial BCR (Community Bureau of Reference) i NIST (National Institute of Standards and Technology). També s'ha determinat el metall pseudototal en aquests vuit residus. Els resultats obtinguts mitjançant la tècnica de DGT es correlacionen bé amb el metall pseudototal i el metall extret amb clorur de magnesi (NIST). La concentració calculada mitjançant els dispositius de DGT també s'ha correlacionat amb el metall determinat a l'espècie *Crithum maritimum*, desenvolupada en aquests residus en condicions controlades de laboratori. Els resultats indiquen que hi ha una correlació significativa pel plom i el zinc a valors de pH superiors de 5, però no s'observa una relació directa entre les concentracions observades mitjançant el DGT i el contingut de cadmi a les plantes.



## RESUMEN

La contaminación ambiental es la modificación del contenido natural de componentes químicos, partículas o materia biológica que afecta negativamente al medio ambiente. Algunos metales, metaloides y otras especies como sulfuros u óxidos se han introducido en el medio ambiente durante años a través de fuentes naturales y antropogénicas, y ahora representan un grave problema para la salud humana, los animales y las plantas. Así, la contaminación ambiental es un tema de interés internacional que requiere una atención inmediata.

El objetivo de esta tesis es aplicar metodologías analíticas existentes y desarrollar nuevos procedimientos basados en la espectrometría con fuente de plasma inducido por alta frecuencia, la cual se puede utilizar para la determinación de contaminantes inorgánicos relevantes. Por otro lado, la técnica de DGT (diffusive gradients in thin films) se ha aplicado a muestras ácidas procedentes de zonas mineras. Las metodologías desarrolladas se han utilizado para analizar diferentes tipos de muestras de la zona minera abandonada de Cartagena.

Por un lado, se sabe que la determinación de sulfuro ha ganado importancia debido a la alta toxicidad del sulfuro de hidrógeno. Normalmente, el sulfuro se determina en aguas naturales y residuales ya que, en determinadas condiciones de pH, se puede generar una cantidad suficiente de sulfuro de hidrógeno que puede llegar a ser peligrosa tanto para la salud humana como para el medio ambiente. Este interés entre la comunidad analítica ha hecho que se hayan desarrollado un gran número de protocolos para la determinación de sulfuro. No obstante, la necesidad de determinar este compuesto a muy bajas concentraciones ha hecho que se haya tenido que recorrer a técnicas cada vez más sensibles. La espectrometría de masas con fuente de plasma inducido por alta frecuencia y espectrómetro de masas de cuadrupolo (ICP-QMS) se ha utilizado como una técnica muy sensible para la determinación simultánea de elementos a nivel traza, en distintas matrices, gracias a su buen funcionamiento en términos de robustez, rendimiento y preparación sencilla de la muestra. Sin embargo, los isótopos de sulfuro son particularmente difíciles de medir mediante ICP-QMS debido a las importantes interferencias provocadas por  $^{16}\text{O}^{16}\text{O}^+$  sobre  $^{32}\text{S}^+$  así como también  $^{16}\text{O}^{17}\text{O}^+$  sobre  $^{33}\text{S}^+$  y  $^{16}\text{O}^{18}\text{O}^+$  sobre  $^{34}\text{S}^+$ . Se ha demostrado que con la utilización de celdas de



colisión/reacción se puede eliminar gran parte de estas interferencias espectroscópicas, reduciendo la presencia de iones poliatómicos interferentes mediante gases como hidrógeno, helio u oxígeno. Asimismo, la técnica de ICP con espectrometría de emisión atómica (ICP-AES) también se ha utilizado para la determinación de sulfuro pero, como las líneas de emisión del azufre están por debajo de 190 nm, la determinación de dicho elemento requiere purgar el paso entre el plasma y el monocromador con gas nitrógeno.

En la presente tesis, se han desarrollado métodos sencillos para la determinación de sulfuro a bajas concentraciones ( $\mu\text{g L}^{-1}$ ) en muestras acuosas y sedimentos mediante la generación de sulfuro de hidrógeno, utilizando un accesorio de generación de hidruros comercial. Una vez formado el sulfuro de hidrógeno, este puede introducirse en el ICP-QMS equipado con una celda de colisión/reacción presurizada con hidrógeno o helio, o en el ICP-AES purgando con nitrógeno el trayecto entre el plasma i el monocromador. En el caso del método mediante ICP-QMS, se ha llevado a cabo un diseño experimental para seleccionar los parámetros instrumentales relacionados con la celda de colisión/reacción que afectan a la determinación de los isótopos de azufre. Se han optimizado las condiciones de trabajo para obtener la mejor relación señal/ruido para el isótopo  $^{32}\text{S}$ . Con ICP-AES se ha medido la emisión del azufre a 180,669 nm. Además, se ha demostrado que el separador gas/líquido del generador de hidruros se puede substituir por un nebulizador comercial, de esta forma también se obtiene un método sensible y fiable; además, esta configuración permite la determinación simultánea de sulfuro y sulfato en muestras acuosas utilizando ácido clorhídrico y agua, respectivamente, en el tubo de reacción. Como no existe ningún material acuoso de referencia con un valor certificado para la concentración de sulfuro, los tres métodos desarrollados basados en ICP se han evaluado por comparación con el método potenciométrico de referencia. En todos los casos el límite de detección obtenido ha sido inferior al que se obtiene cuando se usa el electrodo de sulfuro.

Por otro lado, el arsénico es un elemento que se encuentra en el medio tanto en forma orgánica como en forma inorgánica. Debido a su alta toxicidad para la flora, fauna y seres humanos, la determinación de dicho elemento ha ido ganando importancia. Durante los últimos cuarenta años se han desarrollado numerosos métodos basados en técnicas distintas para determinar arsénico en diferentes matrices. Las técnicas espectrométricas y los métodos electroquímicos han sido las más utilizadas para este

propósito. No obstante, se sabe que la técnica de ICP-MS presenta problemas de interferencias, tanto espectrales como no espectrales y, posiblemente, el inconveniente más importante del ICP-QMS equipado con un nebulizador neumático es la formación de la interferencia  $^{40}\text{Ar}^{35}\text{Cl}^+$  que se obtiene en matrices con un contenido moderado de cloro ( $\text{mg L}^{-1}$ ). Dado que esta interferencia tiene la misma relación masa carga ( $m/z$ ) que el arsénico, los resultados pueden ser inexactos, especialmente cuando se determinan cantidades bajas de arsénico. Tal y como se ha mencionado anteriormente, la introducción de una celda de colisión/reacción es una buena estrategia para solucionar problemas relacionados con las interferencias poliatómicas. Además, también se sabe que los efectos de la matriz pueden ser muy importantes en las técnicas de ICP, ya que la presencia, más o menos moderada, de algunos iones de la matriz puede modificar la señal analítica significativamente, especialmente cuando se utiliza ICP-MS. Para corregir estos efectos de la matriz se han utilizado diferentes técnicas como la adición estándar, la dilución isotópica o el uso de patrones internos.

En esta tesis se han hecho diferentes estudios para determinar arsénico mediante ICP-MS en aguas naturales con alto contenido de sodio y cloro, y se han investigado las interferencias espectrales y no espectrales sobre este elemento. Se ha optimizado el caudal de gases de la celda de colisión/reacción y se ha encontrado que para eliminar la interferencia  $^{40}\text{Ar}^{35}\text{Cl}^+$  se puede utilizar una mezcla de  $2,9 \text{ mL min}^{-1}$  de hidrógeno y  $0,5 \text{ mL min}^{-1}$  de helio. Aunque las correcciones matemáticas son necesarias cuando no se presuriza la celda de colisión/reacción, estas no eliminan completamente las interferencias que se producen en el plasma. Además, se deben hacer algunas modificaciones de estas correcciones cuando se utilizan con la celda presurizada ya que se forman interferencias adicionales. En esta parte de la tesis, también se ha estudiado el efecto que produce la presencia de pequeñas cantidades de alcohol en las muestras empleando una celda presurizada y sin presurizar. Se ha verificado que la presencia de un 4% (v/v) de etanol o metanol produce un incremento de la sensibilidad para el arsénico que es más importante cuando se presuriza la celda. Además, cuando no se presuriza la celda, la presencia de alcohol hace que disminuya la interferencia poliatómica ( $^{40}\text{Ar}^{35}\text{Cl}^+$ ). No obstante, esta disminución no se observa con la celda presurizada ya que gran parte de esta interferencia es eliminada. Finalmente, se han estudiado distintos elementos como posibles patrones internos para la determinación de arsénico en presencia de altas concentraciones de sodio. Se ha observado que el rodio es

el elemento que mejor se comporta para la determinación de arsénico en presencia de sodio, tanto cuando se emplea la celda presurizada como sin presurizar. La presencia de alcohol también afecta al comportamiento de los patrones internos, pero el rodio continúa siendo el patrón interno más adecuado para la determinación de arsénico en estas condiciones.

La última parte de esta tesis se centra en el estudio de la aplicabilidad de la técnica de DGT (diffusive gradients in thin films) a muestras ácidas. Esta técnica ha sido ampliamente utilizada para medir metal lábil en aguas con valores de pH entre 5 y 10. No obstante, una limitación de la técnica de DGT es la competencia con los iones hidrógeno por el agente complejante a valores de pH bajos. En esta tesis se ha estudiado el efecto del pH, del calcio y del ácido fúlvico en la adsorción de distintos metales sobre la resina Chelex en el intervalo de pH de 1,5 a 5,5 en el laboratorio. Estos resultados demuestran que los dispositivos de DGT se pueden utilizar, sin necesidad de corrección, en aguas con pH de hasta 3,5 para determinar cobalto, zinc y cadmio; 3,0 para níquel y plomo y 2 para cobre. Sin embargo, por debajo de estos valores de pH, la concentración obtenida a partir de la técnica de DGT se debe corregir utilizando las curvas sigmoidales de 5 parámetros ajustadas para cada metal. Por otro lado, también se ha estudiado el efecto del calcio sobre las concentraciones de metal determinadas mediante la técnica de DGT tanto a pH 2,5 como a pH 3,5. Se ha observado que, para la mayoría de elementos, la presencia de calcio afecta, aunque de forma poco importante, la interacción metal-Chelex a valores de pH bajos y, además, a pH 3,5 el calcio también afecta a la determinación del cadmio de manera que el resultado obtenido mediante la técnica de DGT es un 25% inferior de lo esperado. Los experimentos con ácido fúlvico han demostrado que la especiación de plomo y cobre se ve afectada por la presencia de este ácido incluso a valores de pH muy bajos debido a la gran afinidad de estos metales por la materia orgánica. El resto de los metales estudiados, en cambio, se encuentran en forma inorgánica a valores de pH bajos. Los resultados experimentales se han comparado con las predicciones hechas por el programa de especiación WHAM VI. La técnica de DGT, con las correspondientes correcciones de pH, se ha utilizado para analizar aguas ácidas de minería que contenían grandes cantidades de plomo, zinc y cadmio.

Por primera vez, la técnica de DGT se ha aplicado a residuos ácidos de minería para evaluar la disponibilidad de zinc, plomo y cadmio a la vegetación. Con este propósito, se han estudiado ocho residuos (con valores de pH entre 2 y 7) de la zona minera, actualmente abandonada, de Cartagena, España. Los resultados obtenidos se han comparado con otros tests de biodisponibilidad como la concentración de metal en agua de poro o en diferentes disoluciones extractantes. Así, se ha utilizado el protocolo de extracción simple con DTPA (Diethylene triamine pentaacetic acid) y los primeros pasos de los procedimientos de extracción secuencial BCR (Community Bureau of Reference) y NIST (National Institute of Standards and Technology). También se ha determinado el metal pseudototal en estos ocho residuos. Los resultados obtenidos mediante la técnica de DGT se correlacionan bien con el metal pseudototal y el metal extraído con cloruro de magnesio (NIST). La concentración calculada mediante los dispositivos de DGT también se ha correlacionado con el metal determinado en la especie *Crithum maritimum* desarrollada sobre estos residuos en condiciones controladas de laboratorio. Los resultados indican que hay una correlación significativa para el plomo y el zinc a valores de pH superior a 5, pero no se observa una relación directa entre las concentraciones observadas mediante el DGT y el contenido de cadmio en las plantas.



# INTRODUCTION





Environmental pollution can be defined as the discharge of contaminants into the water, soil or the air that can alter ecosystems and subsequently reduce the quality of life of their inhabitants. Pollutant discharges can occur naturally or unnaturally. Naturally occurring pollutants include dust, pollen, salt particles, smoke from forest fires, gases from decaying organisms or gases from volcanic eruptions; they are considered contaminants when they exceed natural levels. Unnatural pollution is always related to human activities.

At the beginning of history, human activities did not affect the ecological balance of the Earth, but as knowledge and development of humanity increased, the environment received more adverse effects. Thus, common activities such as fertilization, deforestation or industry now result in general environmental contamination.

Mining activities also represent a current source of pollution by introducing trace elements into atmospheric, terrestrial and aquatic ecosystems. Discharges from abandoned mines and spoil heaps are a major source of surface and groundwater pollution worldwide. This is supported by reported chemical contamination in areas where mining and smelting were carried out in the past. Mineral extraction generates important volumes of waste dumps, which in contact with air and water can cause acid drainage. Moreover, there are mineral processing plants that produce mineral concentrates that in turn also generate waste [I.1-I.3].

The Cartagena-La Unión Mining District, situated in the south-east of the Iberian Peninsula, was an important mining area from ancient times until 1991, when due to the lower yield and the depletion of the most important ores, the mining exploitations were closed. During the years of mining activity, high amounts of mining dust and residues were dumped into the water streams that drain the Sierra of Cartagena. Nowadays, almost 60% of the residues produced are located by the water streams that flow to the Mar Menor Lagoon while the remaining 40% lead to the Mediterranean Sea [I.4]. The ore deposits of this zone contain large amounts of iron, lead and zinc (the main metal components), but they also have small amounts of cadmium and arsenic which appear as impurities in the main minerals.

Mining wastes, which were dumped indiscriminately in the past, have now become a great environmental problem due to the potential mobilization and bioavailability of their metal content. Although some metals, such as cobalt, copper or zinc, are essential for living organisms, an excess may have serious consequences. On the other hand,



## INTRODUCTION

---

exposure to low concentrations of some metals such as arsenic or cadmium can be fatal for living organisms.

The mobility and availability of metals depends on their physico-chemical characteristics and the specific binding to the solid phase. In anoxic sediments, metals can be bound to sulfide, forming an insoluble species and limiting their mobility [1.5]. However, the mining wastes which are still located in this area have a remarkably low pH that could lead to easy metal mobility.

Environmental pollution is a serious problem, and several techniques have been developed to identify pollutants in air, soil and water. However, the constant need to reach lower detection limits in more complicated matrices has created several as yet unresolved issues. And more information is needed about the mobility and availability of metals to determinate their toxicity in living organisms.

The aim of this thesis is twofold: the development of analytical methods to determine relevant environmental species based on spectroscopic ICP techniques and the application of the DGT technique in acidic waters and mining wastes to assess metal accumulation and the potential metal availability.

## I.1 INDUCTIVELY COUPLED PLASMA

### I.1.1 Overview

Spectroscopy is the study of the interaction between electromagnetic radiation and matter, and has both physical and analytical applications. Physical spectroscopists use emitted, absorbed or scattered light to understand the mechanics of a chemical system while analytical spectroscopists use the same physical processes to determine the occurrence and concentration of the atomic and molecular species present in a chemical system. The basic aim of analytical atomic spectroscopy is to identify elements and quantify their concentrations in various media. In the case of atomic emission spectroscopy, the procedure consists of three general steps: atom formation, excitation, emission and, sometimes, ionization. An energy source is needed to achieve them.

The perfect atomic source should have the following characteristics:

1. Complete removal of the analyte from its original matrix to minimize interferences.
2. Complete atomization of all elements to be determined.
3. A controllable energy source for excitation, which allows the proper energy needed to excite all elements.
4. An inert chemical environment, which avoids the formation of undesirable molecular species (e.g. oxides, carbides, etc.) that affect the accuracy of the measurement.
5. No background radiation from the source. Background radiation is defined as unwanted atomic or molecular emissions that could interfere with analytical wavelengths.
6. Ability to handle a range of solvents, both organic and inorganic in nature.
7. Adjustable to handle solids, slurries, liquids, or gases.
8. Inexpensive to purchase and maintain.
9. Easy to operate.

Inductively coupled plasma (ICP) spectroscopy is an energy source used in atomic emission spectroscopy, as well as in atomic mass spectrometry, to detect trace metals and metalloids in a wide range of matrix samples. The technology of the ICP techniques was first employed in the early 1960s [I.6].

Moreover, ICP techniques have been used in combination with other techniques such as gas chromatography (GC), liquid chromatography (LC) and hydride generation (HG). GC-ICP provides a specific and highly sensitive system to determine and identify trace organic, inorganic and organometallic compounds in environmental, industrial, biological and pharmaceutical samples. LC-ICP has become the most popular technique for elemental speciation studies of samples and matrices, including environmental, biological and clinical [I.7,I.8].

### **I.1.1.1 Plasma source**

ICP-based spectroscopy uses plasma as the atomization and excitation source. The energy is supplied by an induced magnetic field produced by a high frequency generator. Plasmas are highly ionized gases that contain molecules, radicals and ions [I.6]. The ability of the positive and negative charges to move somewhat independently makes the plasma electrically conductive so that it responds strongly to electromagnetic fields. Radiofrequency generators are required to supply power to the ICPs. These are oscillators that generate an alternating current at a desired frequency. The basic circuit consists of a capacitor and an inductor in parallel. A number of commercial instruments use generators with nominal powers of 2 kW and frequency of 27.12 MHz [I.9]. A higher frequency of oscillation may lead to lower excitation and ionization temperatures, lower electron densities and lower and more stable backgrounds that give improved detection limits, which can be clearly seen as the frequency is increased from 27 to 40 MHz. Nowadays a frequency of 40.68 MHz is commonly used. Most analytical plasmas operate with pure argon or helium, which makes combustion impossible. However, inductively coupled plasmas are divided into two main groups: high-power nitrogen-argon ICPs and low- or medium-power argon ICPs. Plasmas are characterized by their temperature and their electron and ion densities. Analytical plasmas typically range in temperature from 6000 to 10000 K.

The plasma is formed in a stream of gas flowing through three concentric quartz tubes known as a plasma torch (shown in Figure I.1). The sample, as aerosol, is led with its carrier gas through the central tube. Between the outer and the intermediate tube a gas flow is introduced tangentially. The torch is encircled at the top by an induction coil made from copper, also called the load coil, connected to a free-running or crystal-controlled radiofrequency generator. Plasma is formed almost instantaneously when the

gas is seeded with energetic electrons. A stable and self-sustaining plasma is maintained as long as the magnetic field strength is sufficiently high and the gas flows in a symmetrical pattern. The largest current flow occurs on the periphery of the plasma, which gives the ICP a distinctive annular configuration that sets it apart from other discharges; this structure ensures the efficient introduction of sample aerosol into the central channel of the plasma resulting in the efficient desolvation, vaporization, atomization, excitation and ionization of the sample. However, gas flow rates are critical parameters as they can influence the residence time of analyte in the plasma as well as the amount of analyte reaching the plasma, both of which affect signal intensity. The Ar-ICP is capable of the excitation-ionization of a wide range of elements, particularly metals, and therefore of simultaneous multi-element determination.

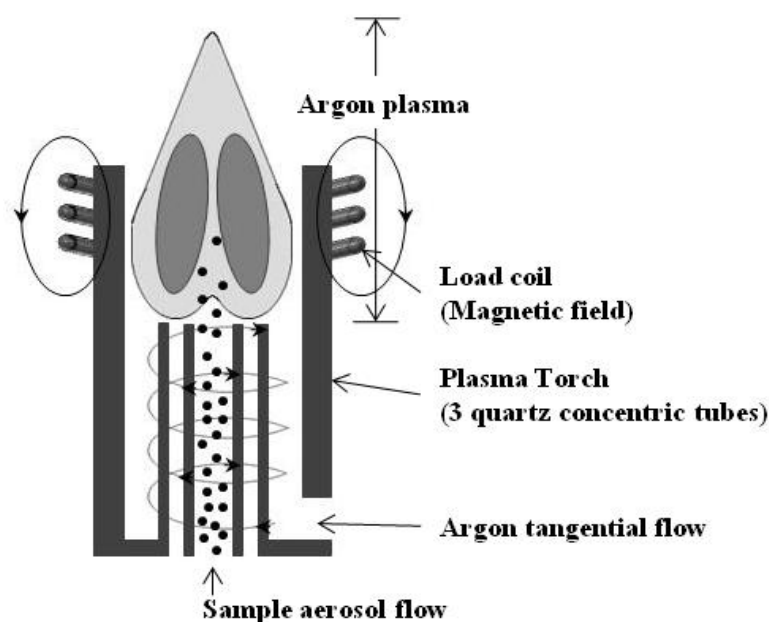


**Figure I.1** Scheme of an inductively coupled plasma torch.

There are two ways to observe plasma: radial viewing and axial viewing. For both ways, the emission of interest occurs in the central channel of the plasma. When using radial viewing ICP, the spectrometer views the analyte emission from the side of the plasma through the background argon emission. Viewing height is a very important parameter with radial viewed plasmas because the element distribution along the plasma is not homogenous. An axially viewed plasma system looks down the central channel of the plasma and collects the entire analyte emission over the entire length of the plasma. The net effect is that the emission path length is increased relative to radial viewed

plasma. This increases the measured analyte emission and improves sensitivity [I.10-I.13].

The processes that take place in the plasma are shown in Figure I.2. In a first step, dry particles are obtained as a result of solvent evaporation. Molecules present in these remaining particles are vaporized and then atomized. Obtained atoms undergo different processes such as excitation, ionization or a combination of both (ionization followed by excitation). At the highest part of the plasma, recombination processes also take place, as depicted in the figure.

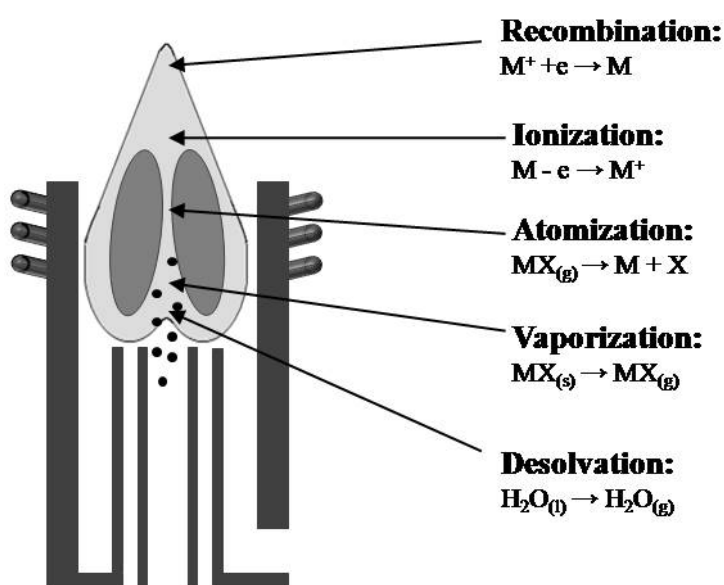


**Figure I.2** Analyte processes that take place in the plasma.

Several mechanisms for analyte excitation and ionization are described in the literature. Some of them are summarized in Table I.1 [I.14].

**Table I.1.** Mechanisms for analyte excitation and ionization in ICP [I.14].

MECHANISM	REACTIONS
Penning ionization	$M + Ar^m \rightarrow M^{+*} + e^-$
Electron-impact ionization	$M + e^- \rightarrow M^{+*} + 2e^-$
Electron impact excitation	$M + e^- \rightarrow M^* + e^-$
Radiative ion-electron recombination	$M^+ + e^- \rightarrow M^* + h\nu_c$
Three-body ion-electron recombination	$M^+ + 2e^- \rightarrow M^* + e^-$
Energetic Ar collisional excitation	$M^+ + e^- + Ar \rightarrow M^* + Ar$
	$M^+ + Ar^m \rightarrow M^* + Ar + h\nu$
	$M^+ + Ar^m + Ar \rightarrow M^* + 2Ar$
	$M^+ + Ar^m + e^- \rightarrow M^{+*} + Ar + e^-$
Charge transfer reaction	$M^+ + Ar^+ \rightarrow M^{+*} + Ar$

### I.1.1.2 Sample introduction devices

In plasma spectrometry, the sample must be introduced into the plasma as a fine aerosol. Liquid sample introduction is the most common way to present samples to plasmas. Generally, liquids are dispersed into fine aerosols before being introduced into the ICP. The analytical performance of ICP spectrometries are directly affected by the quality of the aerosol generated. Typically, the quality of the aerosol is improved by removing the large droplets from the aerosol stream via a spray camber. The most commonly used sample introduction devices for ICP spectrometry are pneumatic nebulizers, which are already well known from early work on flame spectrometry. The pneumatic nebulization of liquids is based on the viscous drag forces of a gas flow passing over a liquid surface, which produce small independent droplets. This may occur when the liquid is forced through a capillary tube and, at the exit, the gas then flows concentrically around the tube (concentric type) or perpendicularly with respect to the liquid stream (cross-flow type). The concentric design is more suitable for clean samples, while the cross-flow is generally more tolerant of samples containing higher levels of particulate matter [I.15]. A diagram of each nebulizer type is shown in Figure I.3.

**Concentric nebulizers:** Concentric nebulizers work by having the liquid solution introduced through a capillary tube into a region of low pressure created by a concentric gas flowing rapidly past the end of the capillary. The flow of liquid and flow

of gas are parallel to each other and the liquid breaks up into a fine mist as it exits the capillary tip. The typical nebulizer gas flow rate is about 1 L/min. The concentric nebulizers have very small orifices, which result in highly efficient aerosol formation, from 2 to 5%, this results in excellent sensitivity and stability. They can be made of metal, plastic or glass and they are often self-aspirating [I.12]. Concentric nebulizers are sensitive to high salt concentrations due to ion-exchange phenomena at the glass wall. The most common glass concentric nebulizer is the Meinhard nebulizer which is easily clogged by solutions containing as little as 0.1% dissolved solids.

**Cross-flow nebulizers:** This type is less sensitive to salt concentration as the sample capillary has a larger diameter that minimizes clogging of the nebulizer by salt deposits. However, it is not self-aspirating and to introduce the sample it needs a peristaltic pump, which originates a low-frequency noise. The cross-flow nebulizer uses a high-speed gas flow perpendicular to the sample flow capillary tip to form the aerosol. Droplets formed by cross-flow nebulizers are larger than those from concentric nebulizers, so the cross-flow nebulizer is not as efficient. They can also be made of metal, plastic or glass.

Concentric nebulizers are more frequently used for ICP spectrometry than cross-flow designed devices because the adjustment of the gas and liquid capillaries is not necessary.

**Babington nebulizer:** the Babington nebulizer is a variation of the cross-flow nebulizer [I.16]. It works by allowing the liquid to flow over a smooth surface with a small hole in it. High speed argon gas emanating perpendicularly shears the liquid into small drops. This working mode, where the sample does not need to pass through a capillary, allows the analysis of very viscous liquids and solutions containing high salt concentrations without the risk of clogging [I.12].

**Ultrasonic nebulizers** have also been built for ICP techniques. Ultrasounds can be used instead of a gas to break up a liquid mass into smaller particles. These nebulizers use an ultrasonic generator at a frequency between 200 kHz and 10 MHz to drive a piezoelectric crystal. The surface of the liquid sample will break down into an aerosol when the longitudinal wave propagates from the surface of the crystal toward the liquid-air interface. This aerosol is of very fine, uniform droplets, unlike the aerosol from a pneumatic nebulizer. Ultrasonic nebulizers are significantly more expensive than pneumatic designs but their efficiency is 5-10 times greater. This results in improved

sensitivities and better detection because more sample reaches the plasma. However, they are prone to carry over memory effects from one sample to the next due to the ease of adsorption of certain elements on the nebulizer surface [I.17,I.18].

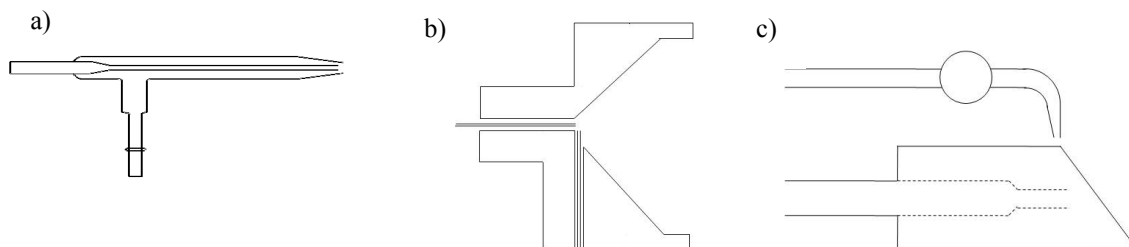


**Figure I.3** Typical concentric (a), cross-flow (b) and Babington (c) nebulizers.

A nebulizer must produce droplets less than 10  $\mu\text{m}$  in diameter in order to achieve a high aerosol transport efficiency and rapid desolvation, volatilization and atomization of the aerosol droplets. Pneumatic nebulizers usually produce highly polydisperse aerosols with droplets up to 100  $\mu\text{m}$  in diameter. Thus, nebulizers are generally placed in a nebulization chamber with a drain to separate off the large droplets and remove inappropriate liquid deposits. The drainage characteristics are important in part due to pressure changes that can occur during drainage. It is also important that the drainage process be smooth and continuous. The most common types of spray chambers are the double-pass (the so-called Scott-type) and the cyclonic. It is known that the Scott-type spray chamber transports less analyte to the plasma than the cyclonic type. Moreover, the double-pass spray chamber has higher memory effects. When less than 5% of the nebulized analyte is transported to the atomizer, the spray chamber, rather than the nebulizer, determines the characteristics (fineness and amount) of the aerosol injected into the plasma. Some characteristics of an ideal spray chamber are:

- It should be able to transport as much analyte mass to the atomization cell as possible without deteriorating its excitation properties.
- The aerosol entering the plasma should be as fine as possible.
- It should be robust.
- The memory effects should be minimal in order to increase the sample throughput.
- It should be mechanically simple and have a low production cost [I.19-I.21].



Over the years, many changes have been introduced in these types of nebulizers to improve the aerosol transport efficiency, stability and response time. So far, other types of nebulizers and cloud chambers and/or their combination have been investigated, including thermospray, micro-concentric or micro-flow ultrasonic nebulizers [I.22,I.23]. To this end, a total sample introduction system has been designed. In this system an evaporation cavity is used to completely vaporize the solvent before entering the plasma. Thus, a micronebulizer has been associated to a low inner volume spray chamber. This device has been called TISIS (Torch Integrated Sample Introduction System). With this configuration, low delivery rates (*i.e.*, below  $20 \mu\text{l min}^{-1}$ ) are used and evaporation in aerosol phase is achieved. However, when using TISIS, heating the chamber is required to promote the complete solvent evaporation. This introduction system provides superior performances over the conventional devices and the main advantages of this system are higher sensitivities, lower detection limits, fewer non-spectroscopic interferences and lower memory effects [I.24,I.25]. However, the use of common spray chambers is not always advisable because a large mass of nebulized sample can be lost there. Moreover, spray chambers can enhance matrix effects and be a source of signal flicker noise. As a result, nebulizers especially designed to introduce the aerosol directly into the plasma at very low liquid flow rates have been developed. These are the so-called direct injection nebulizers (DINs) or the direct injection high-efficiency nebulizers (DIHEN) [I.26-I.28].

On the other hand, other sample introduction tools are also being used and investigated to enhance the practical capabilities of ICP. Among them, laser ablation, electrothermal vaporization and chromatography techniques are the most important. Laser ablation is a microanalytical technique for the introduction of solid material with a growing number of applications in fields such as geochemistry, material science or environmental studies. In such tool, a pulsed laser beam is used to ablate a small quantity of sample material which is transported into the argon plasma by a stream of argon carrier gas [I.29]. Electrothermal vaporization (ETV) has high transport efficiency ( $\sim 80\%$ ) which results in a promotion of the detection limits. Moreover, the steps of sample vaporization and its excitation/ionization are separated and, therefore, matrix is removed reducing non-spectroscopic and spectroscopic interferences. Furthermore, ETV is also quite suitable for direct analysis of solid samples [I.30]. The combination of ICP with high performance liquid chromatography (HPLC) and gas chromatography (GC) has

gained relevance in the past ten years. The main advantage of HPLC-ICP combination is the possibility of speciation analysis of a variety of environmentally, toxicologically and/or biochemically relevant elements. GC-ICP provides high resolving power and introduction efficiency into the ICP. At the same time, as a consequence of the dry plasma conditions, the plasma is more stable and exhibits fewer spectral interferences. In both configurations (HPLC-ICP and CG-ICP) matrix effect are avoided due to the separation of the analyte from the matrix [I.31].

### **I.1.2 Inductively coupled plasma – atomic emission spectroscopy (ICP-AES)**

Inductively coupled plasma-atomic emission spectrometry (ICP-AES) instruments have been commercially available since 1974. The primary goal of ICP-AES is to get elements to emit characteristic wavelengths which can then be measured. The role of the radiation source in AES is not just to produce free atoms but to produce different excitation levels from which transitions with high emission efficiency are possible. Ionization also occurs in ICP-AES making it possible to use ionic lines. Ideal sources for AES should have a very robust geometry, high electron temperatures, and low spectral background intensities.

Atoms and ions present in the plasma can be in their ground states or an excited state and radiation can be emitted or absorbed when transitions from one state to another occur. The wavelength of the radiation can be obtained from Planck's law while the intensities of the discrete lines depend on the number densities of the species and the states involved [I.12]. The population of a particular excited state is proportional to the Boltzmann factor,  $e^{-E/kT}$ , where E is the energy of the upper state of the spectroscopic transition (usually between 3 and 7 eV for the most sensitive lines emitted by the ICP), k is the Boltzmann constant, and T is temperature. Excited states are so extensively populated in the ICP that intense emission is produced from many lines simultaneously. As a result, rapid simultaneous analysis can be performed. Emission lines can be classified as "soft" or "hard". Atomic lines of elements with low to medium ionization potential (I.P.  $\leq 8$  eV) are, in general, soft lines. Ionic lines and atomic lines of elements with high ionization potential (I.P.  $> 8$  eV) are, in general, hard lines [I.32]. Soft emission lines exhibit their maximum intensity  $< 10$ mm above the load coil while hard emission lines exhibit their maximum intensity at higher viewing heights [I.16].

Unlike a flame, in which only a very limited number of metals emit light because of the low temperature, virtually all metals present in a sample emit their line spectrum from the ICP torch. ICP-AES can determine 60 or more elements at once by monitoring at pre-set wavelengths. This includes halogens and some other non-metals and metalloids, as well as metals [I.33]. In ICP-AES, sequential and simultaneous instruments are used. In sequential spectrometers special attention is given to the speed of the wavelength access and in simultaneous spectrometers to the provision of background correction facilities. The main sources of continuum background in ICP-AES are the radiative recombination of electrons and ions and the loss or gain of energy by electrons accelerated in a field of ions, called bremsstrahlung radiation. Molecular species are not prevalent in the plasma, and most molecular species are not strong emitters. However, some molecular emission is observed from species produced from aqueous or organic solvents. The recombination of matrix ions and electrons can also produce large increases in the ICP-AES continuum background [I.10,I.12,I.33,I.34].

### **I.1.2.1 Interferences**

Most interferences in ICP-AES are of spectral origin because of a high plasma temperature. Other types of interference are often the result of high concentrations of certain elements or compounds in the sample matrix, which can modify different processes such as nebulization, atomization or ionization. Thus, interferences in ICP-AES can be divided into the non-spectral and the spectral.

#### ***I.1.2.1.1 Non-spectral interferences***

Non-spectral interferences may be defined as matrix-induced signal enhancement or suppression due to the presence of major elements or reagents. The origin of these effects is difficult to determine as they can occur during aerosol formation, transport and filtration and during the processes of atomization, excitation and ionization [I.35]. The most important non-spectral interferences are:

**Nebulization effects.** Differences in the physical properties of the different sample and calibration solutions lead to variations in the aerosol droplet size and thus also in the efficiency of the nebulizer and the sample introduction. These effects are usually more important at low liquid flow rates.

**Transport effects.** Sample uptake rates and transport rates are affected due to differences in the viscosity of the solutions; the amount of the sample reaching the plasma decreases when the solution viscosity increases.

**Plasma effects.** Variations in plasma conditions produce differences in atomization, excitation and ionization processes [I.12,I.36,I.37,I.38].

This interference is not limited to a single element but a combination of different elements present in the matrix. Easily ionized elements, organic compounds and acids have been found to be the most important interfering species in ICP-AES.

**Easily ionized elements.** Easily ionized elements can cause enhancement or depression of the analyte emission signal. Several authors have studied interference effects from easily ionized elements such as Na, K, Li or Cs in ICP. Mechanisms that have been proposed to explain the effects of such elements include reduction in analyte volatilization, enhancement of excitation temperature and shifts in the ionization equilibrium. An increase in electron collisions has also been suggested because of the resulting increased electron density. Ambipolar diffusion, changes in plasma thermal conductivity, cooling of the plasma, quenching of Ar metastable atoms, charge transfer involving Ar species, direct electron impact ionization, excitation, autoionization and dielectric recombination are also processes described in the literature [I.12,I.39,I.40].

**Organic compounds.** It has been demonstrated that the presence of organic compounds can lead to changes in analyte emission. Transport efficiency in sample introduction, efficiency of nebulization, desolvation and ionization of analyte are affected by the presence of organic compounds [I.41-I.43]. These changes are attributed to differences in density, viscosity and surface tension.

**Acid interferences.** Acid, which is normally present in liquid samples as a result of previous sample preparation steps, is known to be one of the most important sources of interference when using atomic spectrometry techniques. It has been demonstrated that acids can produce a reduction in the nebulization aspiration rate and a modification of the mass of solution transported to the plasma. Moreover, it has been reported that primary aerosols originating from nitric acid and water have similar drop size distributions, while the amount of finer droplets in tertiary aerosols drastically increases when acid solutions are nebulized [I.44].

Interferences present in the matrix can manifest themselves in either suppression or enhancement of the analyte signal. In general, the presence of a high concentration of a concomitant suppresses the analyte signal, although under certain experimental conditions enhancements have been reported.

Some of these interferences can also affect the stability of signals and analysis precision, but in all cases the extent of the matrix effect depends on the absolute amount of the matrix element present, not on the relative amount of matrix element to analyte. Therefore, by reducing the absolute concentration of the matrix components (by dilution or extraction), suppression effects can be reduced to an insignificant level. Another way to avoid matrix effects is by the use of internal standards, which are also suitable for overcoming drift caused by instrument fluctuations that limit the precision of the analysis. The application of standard additions or isotope dilution instead of external calibration has also been applied in ICP-MS to overcome non-spectral interferences and improve the precision and accuracy of the ICP-MS measurements.

### *1.1.2.1.2 Spectral interferences*

Light emission from spectral sources other than the element of interest may increase the apparent signal intensity. Spectral interferences are caused by:

- Overlap of a spectral line from another element.
- Unresolved overlap of molecular spectra.
- Background contribution.
- Stray light from the line emission of high-concentration elements.

In common with other emission techniques, there is the problem of spectral overlap from different elements, as an element will produce many more lines in its emission spectrum than in its corresponding absorption spectrum. The large number of emission lines produced in the ICP-AES (often hundreds or thousands for a single element) is one of the most serious disadvantages of the ICP-AES technique. Spectral overlaps arise when emission lines from two elements are sufficiently close in energy. In some cases higher resolution spectrometers can resolve partially overlapping emissions, but often the peaks are nearly coincident. In other cases, alternative line selection can be used to avoid interferences, but this is not always possible and generally leads to a loss of sensitivity. In addition, molecular bands also occur. It has been demonstrated that water and acid are pyrolyzed in the plasma and make various polyatomic species such as OH,

NO and NH, which interfere with analytical lines and peaks. For example, NH emission occurs around 336 nm and NO bands are intense from 200 to 280 nm.

Stray light is produced by elements such as alkaline earths that produce relatively high levels of light. The light enters the spectrometer and can cause problems in isolating the required wavelength. Shifts in background can also be observed due to stray light [I.12,I.45,I.46].

### **I.1.2.2 Spectrometers**

Because excited species in the plasma emit light at different wavelengths, the emission from the plasma is polychromatic. This polychromatic radiation must be separated into individual wavelengths. However, the fact that all the elements present in the plasma emit their spectra at the same time makes multi-element analysis possible, sequentially or simultaneously. For this purpose, atomic emission from the plasma is focused on to the entrance slit of the wavelength selector using a combination of convex and plano-convex lenses and a concave mirror. The combination of focusing optics, wavelength selector and detector is generally referred to as a spectrometer. A monochromator is an optical device that is used to select a single wavelength of an emission spectrum. Monochromators need to be optimized for only one wavelength at the time. This allows the use of larger gratings and mirrors leading to a better optical quality. The most common monochromators are the Czerny-Turner (Figure I.4a) and Ebert models with which the lines can be rapidly selected and measured one after another. While the Czerny-Turner monochromator consists of two spherical mirrors and one plane diffraction grating, the Ebert configuration uses just one large spherical mirror and the plane grating. In both cases, light passing through the entrance slit is directed towards the first concave mirror. This mirror collimates the reflected light, which is directed towards the plane grating. Each ray of the collimated light is then diffracted from the grating into several wavelengths and reflected towards the second mirror. The second mirror focuses the spectrum at the exit slit, where the different wavelengths of the light are spread out. Due to the fact that the entrance slit is finite in width, wavelengths can overlap. The range of wavelengths leaving the exit slit is a function of the width of the slits. By rotating the grating element or by moving the exit slit across the light beam from the monochromator, the wavelength range passing through the exit slit can be changed [I.12,I.47].

## INTRODUCTION

Mountings with a concave grating are also used. Here, the radius of the grating determines the so-called Rowland circle. In the direction of the dispersion, the spectral lines are focused on the Rowland circle and monochromatic images of the entrance slit are reflected, which allows simultaneous determination. One of the most useful polychromators is the Paschen-Runge mounting, shown in Figure I.4b. In this mounting, the grating, the entrance slit, and all the exit slits are fixed on the Rowland circle. Paschen-Runge is most often used in large simultaneous polychromators with photoelectric detection.

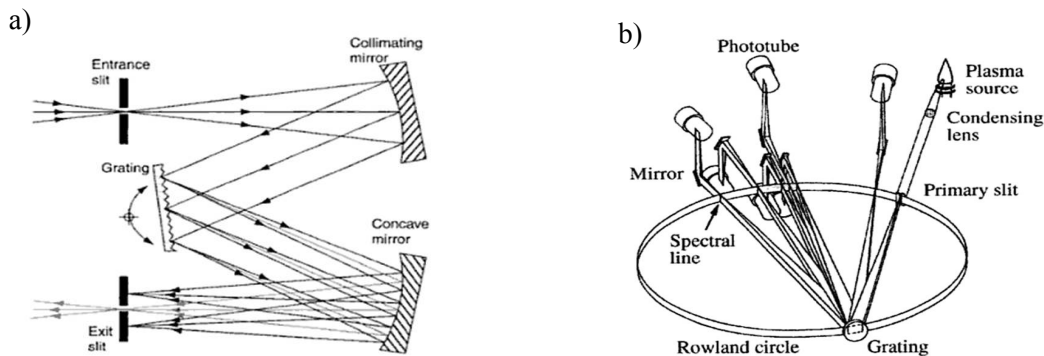


**Figure I.4** The Czerny-Turner (a) and the Paschen-Runge (b) mounts [I.16,I.47].

Echelle gratings are widely used nowadays in ICP-AES instruments. This configuration is accomplished by placing a dispersive element before an Echelle grating using a Czerny-Turner mounting. The Echelle grating configuration is capable of maximizing the intensity of the separated incident radiation at the optimum order. This is accomplished by using a prism to order separate the radiation, and the Echelle grating to wavelength separate the radiation. The result is a two-dimensional array on which exit slits can be positioned to measure the emitted radiation [I.48].

Detectors measure the intensity of the light that emerges from a sample. Normally, they do this by converting radiation energy into electrical energy. The amount of energy produced is usually low and must be amplified. The signal from the detector must be steady and representative of the intensity of radiation falling on it. The most common form of detector is a photomultiplier tube (PMT). This consists of a sealed tube covered by a photoemissive surface, which converts light in the form of photons into an electrical signal. This electrical signal is amplified by successively accelerating the electrons through a series of anodes. In the past, the number of elements that could be

determined simultaneously on a direct-reading spectrometer with photomultiplier tube (PMT) detection depended on the number of fixed exit slits and PMT assemblies. Typical PMT-based simultaneous ICP-AES systems had between 20 and 60 channels [I.18,I.47]. Solid-state detectors were introduced in ICP-AES in the ninety's. Nowadays, charge-transfer device (CTD) detectors are the alternative to photomultiplier tubes. These devices are solid-state, array detectors also sensitive to photons from the far-infrared to the x-ray region. The use of arrays provides a means to record the entire spectrum in a very short time, and produce the complete output of an entire spectral region. Hence, the main advantage that CTDs offer over the single channels achieved by PMT detection is multichannel solid-state detection. [I.48].

### **I.1.3 Inductively coupled plasma – mass spectrometry (ICP-MS)**

ICP-MS instruments became commercially available in 1983. In comparison to other atomic spectroscopic techniques, such as flame atomic absorption, electrothermal atomization and ICP-AES, ICP-MS has clear advantages in terms of its multi-element characteristics, speed of analysis, detection limits and isotopic capability.

In ICP-MS, elements are ionized by ICP in the same way as in ICP-AES. However, in ICP-AES the plasma is used to generate photons of light by exciting the electrons of a ground-state atom to a higher energy level, while in ICP-MS plasma is used to generate positively charged ions. When energy is applied to a ground-state atom in the form of heat from a plasma discharge, one of the orbiting electrons of the atom is stripped off the outer shell. Thus, the atom loses a negative charge and becomes a positively charged ion. Rather than separating emission light according to their wavelengths, the mass spectrometer separates ions according to their mass-to-charge ratios ( $m/z$ ). Since most of the ions in mass spectrometers are singly charged, the  $m/z$  ratio is simply equal to the mass of the ion. Because ions are counted in ICP-MS, the number (abundance) of ions is used as the basis for quantitative measurements. The mass spectrum is therefore a plot of abundance versus  $m/z$ , unlike the optical UV-VIS spectrum in ICP-AES, which is a plot of light emission versus wavelength.

ICP-MS is routinely employed in diverse fields such as geochemistry, environmental and life sciences, industry, forensic science and archeology. Its applications can be attributed to the robustness, low detection limits and high spectral resolution for multi-element isotope detection that ICP-MS instruments exhibit. ICP-MS can provide



chemical information on a basic level, such as total single elemental contents, or elemental and isotope ratios. Without preconcentration, detection limits are usually in the nanogram per liter range when detecting with a high-resolution ICP-MS instrument. As a large proportion of elements (80%) is composed of several isotopes, naturally occurring stable as well as unstable isotopes are routinely measured in nuclear research. Measuring at least two isotopes of the same element allows not only safe element identification but also recognition of the contributions from interfering masses by means of the deviation in natural isotopic ratios. Furthermore, the ability to independently measure intensities of individual stable isotope ions provides the opportunity to perform analysis by classical isotope dilution quantization [I.49-I.54].

### **I.1.3.1 Interferences**

Interferences in ICP-MS are generally classified in the same way as ICP-AES interferences, i.e. non-spectral and spectral. Each has the potential to be problematic, but modern instrumentation and optimized analytical methodologies have minimized their negative impact on trace element determination by ICP-MS.

#### ***I.1.3.1.1 Non-spectral interferences***

As pointed out in the ICP-AES section, the matrix can induce changes in signal intensity which are related not to the presence of a spectral component but to the presence of certain components affecting nebulization, transport and ionization processes.

When using organic solutions in ICP-MS, it has been found that small amounts of organic compounds enhance the element signal while higher amounts reduce the signal due to the resultant cooling of the plasma. To explain this enhancement, three mechanisms have been described: (1) charge transfer reaction from  $C^+$ -species to analyte atoms, (2) improvement in the nebulization transport of the sample, and (3) shift of the zone of maximum ion density in the plasma [I.42,I.43].

The deposition of solids in the optic cones can also cause unwanted changes in the analytical response because the amount of analyte arriving at the detector can be reduced [I.13,I.55-I.58].

### *1.1.3.1.2 Spectral interferences*

Spectral interferences in ICP-MS occur in two forms, the overlap of one isotope with another (isobaric interference), or the overlap of one isotope with a species derived from the ion beam sampling process (polyatomic interference). Isobaric interference is a result of equal mass isotopes of different elements present in the sample solution. Overlap is a serious problem when quadrupole based ICP-MS instruments are used as such analyzers have only unit mass resolution. For elements having more than one isotope, the quickest solution is to use another isotope of that element. For monoisotopic elements, it must be mentioned that there are no elemental singly charged isotopes that overlap with monoisotopic elements. However, monoisotopic elements can overlap with polyatomic interferences. Polyatomic interferences are due to the recombination of sample and matrix ions with other matrix components or elements from the air such as O, N, H, etc or with Ar from the plasma. The background of the mass spectrum is the count rate in absence of any specific species at the  $m/z$  value where an analyte ion is to be measured for quantitative analysis. Typical background count rates with modern mass spectrometers equipped with well-designed electron multiplier detectors and stable electronic circuitry are 10 counts per second (Hz) or less. Because of the very sensitivity of ICP-MS measurements, and the relatively constant background count rate, background correction procedures are not required in ICP-MS measurements for accurate and sensitive analysis. However, some background species can produce serious overlaps as  $N_2^+$  on  $^{28}Si^+$  or  $Ar_2^+$  on  $^{80}Se^+$ . Typical ICP-MS background species and those arising from the use of specific acids are summarized in Table I.2 [I.13,I.55,I.59].

Another type of spectral interference is doubly charged interferences. These are species are formed when an ion is generated with a double positive charge as opposed to a normal single charge, and produces an isotopic peak at half its mass. The level of doubly charged species is related to the ionization conditions in the plasma and can usually be minimized by careful optimization of the nebulizer gas flow, RF power and sampling position within the plasma [I.50].

## INTRODUCTION

Table I.2. Common spectral interferences in ICP-MS.

SOLVENT SYSTEM	INTERFERING SPECIES	ANALYTE	MASS
H <sub>2</sub> O/NO <sub>3</sub> <sup>-</sup>	N <sub>2</sub> <sup>+</sup> , N <sub>2</sub> H <sup>+</sup> , NO <sup>+</sup> , NOH <sup>+</sup> , O <sub>2</sub> <sup>+</sup> , O <sub>2</sub> H <sup>+</sup>	Si, P, S	28-33
	CO <sub>2</sub> <sup>+</sup>	K, Ca	39-41
	ArH <sup>+</sup> , Ar <sup>+</sup> , ArH <sup>+</sup>	Ca	44
	ArN <sup>+</sup> , ArNH <sup>+</sup> , ArO <sup>+</sup> , ArOH <sup>+</sup>	Mn, Fe	54-57
	Ar <sub>2</sub> <sup>+</sup>	Se	76, 78, 80
Cl <sup>-</sup>	ClO <sup>+</sup> , ClOH <sup>+</sup>	V, Cr, Fe	51-54
	ArCl <sup>+</sup>	As, Se	75, 77
	Cl <sub>2</sub> <sup>+</sup>	Ge	70-74
SO <sub>4</sub> <sup>2-</sup>	SO <sup>+</sup> , SOH <sup>+</sup>	Ti, V	48-51
	S <sub>2</sub> <sup>+</sup> , SO <sub>2</sub> <sup>+</sup>	Zn	64
	ArS <sup>+</sup>	Ge	72, 74
PO <sub>4</sub> <sup>3-</sup>	PO <sup>+</sup> , POH <sup>+</sup>	Ti	47-48
	PO <sub>2</sub> <sup>+</sup>	Cu	63
	ArP <sup>+</sup>	Ge	71

There are several methods for bringing about the resolution of or a reduction in spectral interferences, such as the use of mathematical corrections, the use of cool plasma, desolvation of the aerosol, matrix elimination, collision or reaction cells and the use of high resolution (HR) mass spectrometers. Mathematical corrections can be used when the natural isotopic distribution of the interference and the analyte is known, but it may be complicated to set up, time consuming, and may introduce errors if sample matrix components vary. Aerosol desolvation can add excessive cost and complexity and introduce new problems of poorer analyte washout and loss of volatile species. Cool plasma leads to less efficient decomposition of the sample matrix and a reduced signal for poorly ionized analytes. The use of HR-ICP-MS eliminates many of the spectral interferences seen with quadrupoles because the overlaps do not occur. Furthermore, the resolution is sufficient to separate the exact masses of the polyatomic species and analyte elements. However, high resolution mass spectrometers are more costly and more complicated to operate than quadrupole-based ICP-MS [I.12,I.13,I.17,I.60,I.61].

### I.1.3.2 Collision/reaction cells

A collision/reaction cell is a device which was introduced into the ICP-MS technique when there was a need to determine trace elements which overlapped with different spectral interferences. The development of collision/reaction cells for ICP-MS has extended the capability of the technique by allowing the selective attenuation or removal of previously problematic spectral interferences. The first experiment to attenuate polyatomic ion interferences was described by Douglas in 1989.

A reaction cell is mounted in the mass spectrometer, positioned after the ion optics and prior to the mass analyzer. The sample ion beam produced by the ICP is collimated by the ion lens and is extracted under vacuum into the reaction/collision cell through an aperture. Once there, noble gases such as He, Xe or Ar, molecular gases such as H<sub>2</sub>, O<sub>2</sub>, CH<sub>4</sub>, NH<sub>3</sub>, or a combination of the two types, are bled into the cell, which consists of a multipole (octopole, hexapole or quadrupole) usually operated in the rf-only mode. Collision/reaction gas is introduced to promote ion-molecule reactions or collisions with the aim of eliminating spectral interferences arising from air, argon, matrix or solvent. This process is schematized in Figure I.5.

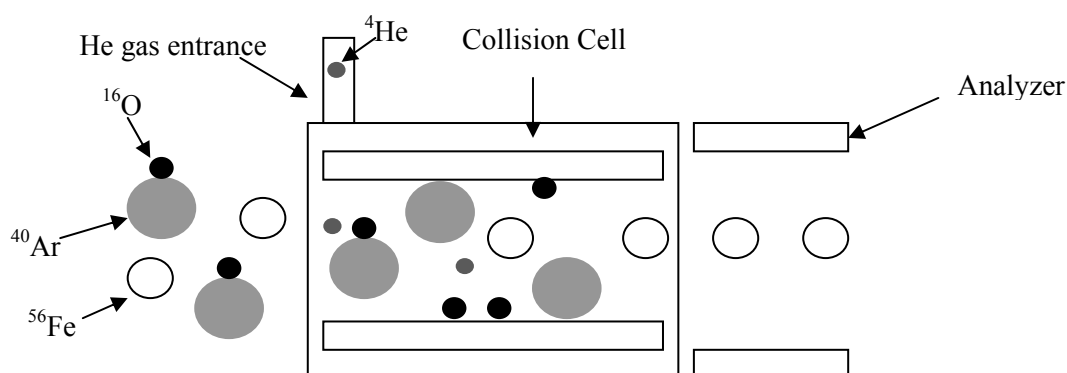


**Figure I.5** Collision cell working scheme

The three main types of ion-molecule reactions that take place are charge transfer, proton transfer and hydrogen ion transfer. The instrument manufacturers have stated that this process is so efficient that the magnitude of the polyatomic molecules can be reduced by as much as a factor of  $10^6$ . Moreover, due to collisions between ions formed in the ICP and gas atoms or molecules of the collision gas, the kinetic energy of the ions

is reduced from several eV to less than 0.1 eV, which results in an increased sensitivity to analyte ions because of the higher transmission of ions. In this way, detection limits can be improved by several orders of magnitude. Kinetic energy discrimination can usually be achieved by setting the collision cell potential slightly more negatively than the mass filter potential. This allows the collision/product ions generated in the cell (which have a lower kinetic energy as a result of the collision process) to be rejected, while the analyte ions (which leave the cell with a higher kinetic energy) are transmitted [I.13,I.62].

Two potentially undesirable processes must be considered for a successful use of a collision/reaction cell. Scattering losses can be severe if the mass of the collision or reaction gas is high compared to that of the analyte ion mass, and reaction product ions can produce new spectral overlaps. They can also react further through a series of reactions to produce other potentially interfering background ions. Impurities in the reaction-collision gases can also contribute to the formation of new interferences. The products of those interactions must be eliminated by the use of energy discrimination methods or mass filters. However, if too many collisions occur, the kinetic energy of both the analyte and the collision/product ion becomes too small and they cannot be discriminated. Thus, heavier gases like ammonia and methane, which are more efficient at reducing the ion kinetic energy after each collision, are not suitable for the kinetic energy discrimination of a collision cell. Therefore, low-reactivity gases such as H<sub>2</sub> or He are recommended in this case [I.60,I.63].

Another way to eliminate the products of secondary reactions is to discriminate by mass. However, higher-order multipoles such as hexapoles or octopoles cannot be used for efficient mass discrimination as sequential secondary reactions are not easily intercepted. To solve that problem, a quadrupole has been introduced in collision/reaction cells and has been used as a selective bandpass filter allowing the use of highly reactive gases. The advantage of using a quadrupole in the reaction cell is that the stability regions are well defined compared with those of a hexapole or an octopole, and the quadrupole can therefore act as a bandpass filter, not just as an ion guide. When a hexapole or an octopole is used the device is known as a collision/reaction cell, and when a quadrupole is used, it is called a dynamic reaction cell.

### I.1.3.3 Interface devices

Since plasma is generated at atmospheric pressure whereas for its operation the mass spectrometer generally requires low pressures, an interface is required to extract ions into a vacuum system. This can be done by a cone with a sampling orifice in its top, placed directly in the analytical zone of the plasma. Because of the pressure differential over the cone (atmospheric pressure on one side, low pressure on the other side), gas flows through the orifice and carries some ions with it. The sampling cone has a 0.8-1.2 mm orifice, so the gas flow is large enough to puncture the boundary layer in front of the sampling orifice. A second cone, called skimmer, is placed several mm behind the sampler orifice and opens directly into the vacuum chamber of the mass spectrometer. Skimmer cone is generally smaller and more pointed than a sampler cone and also has a much smaller orifice (typically 0.4-0.8 mm). Both cones are usually made of Ni, because of its high thermal conductivity and because it is fairly robust and resistant against corrosion. Other materials, such as Pt, which is far more tolerant to corrosive liquids, have also been used. To reduce the effects of high temperature plasma on the cones, the interface housing is water cooled and made from a material such as copper or aluminum that dissipates heat easily. Between the cones a pressure of about 2.5 mbar is obtained with a mechanical vacuum pump. Ions crossing the skimmer cone are guided in a vacuum through cylindrical lenses by electric and magnetic fields to the spectrometer compartment [I.45,I.51,I.54].

In general, a number of voltages must be set with respect to the ion optics. The exact extent of the dependence of the signal on these voltages depends on the design and type of ion optics used. Ion optics vary from manufacturer to manufacturer and are under continued development and modification [I.13].

### I.1.3.4 Mass analyzers

A mass analyzer separates the ions formed in the plasma according to their  $m/z$  value. The selection of a mass analyzer depends upon the resolution, mass range, and detection limits required for an application. Analyzers are typically described as “static ion separation systems” or “dynamic ion separation systems”. The proposed classification is related to the time dependence of the mass spectrometric ion separation systems during the separation process of the ions. Static separation systems combine magnetic and electrical fields, while dynamic separation systems are based on another physical

## INTRODUCTION

---

principle and use the different flight time of ions with different masses and different velocities.

The quadrupole mass filter, a dynamic separation system, is clearly the most popular mass analyzer in ICP-MS, due to its relatively low cost and easy handling. It is extremely good for multi-element analysis and can also be used for isotopic analyses. As shown in Figure I.6, it consists of four hyperbolic electrodes where opposite electrodes have potentials of the same sign. Ions move through these electrodes in the  $z$  direction and are focused in one plane, but defocused in the perpendicular plane. By applying different voltages, ions of a certain  $m/z$  ratio pass through the electrode system without touching the rods, while ions of both higher and lower masses are filtered out and lost from the system, and subsequently ejected to waste via the vacuum system.

The main problem of a quadrupole-based mass spectrometer is its limited resolution in the mass spectrum, which leads to the presence of spectral interferences that cannot be resolved. The resolution,  $R$ , is defined as the ratio  $m/\Delta m$  where  $\Delta m$  is the peak width measured in mass units at a given fraction of the maximum peak height. Typical quadrupole mass spectrometers used in ICP-MS have resolutions between 0.7-1.0 amu. This is sufficient for most routine applications. However, there are some instances where this resolution is not sufficient to separate overlapping molecular or isobaric interferences from the elemental isotope of interest. In addition, another major limitation of quadrupole-based mass analyzers is that they are inherently sequential instruments [I.64,I.65,I.66].

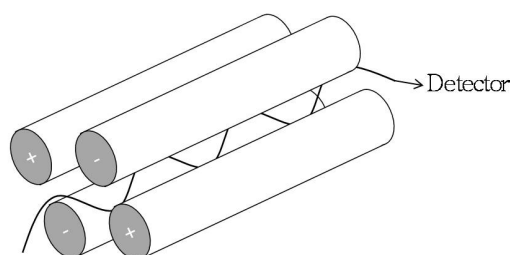


**Figure I.6** Diagram showing the important elements of a quadrupole mass filter. The four parallel rods receive DC and RF voltages allowing ions of sequential  $m/z$  ratios to attain stable trajectories.

Time-of-flight (TOF) mass analyzers, which are also dynamic systems, have also been used with good results. As in quadrupole analyzers, positive ions are extracted from the ICP ion source and then guided in a straight line by a series of lenses to accelerate the

ions to uniform velocities in a pulsed mode. The ions then move into a field-free flight tube where they travel at different velocities depending on their mass. The lower the ion mass, the faster they travel along the tube, reaching the end at different times. These instruments have high transmission efficiency, very low detection limits and fast scan rates, but low resolution [I.66].

The use of high resolution or magnetic sector mass spectrometers, examples of static separation, has become more common in ICP-MS, as this is the best strategy to overcome signal overlap in ICP-MS. This configuration allows proper interpretation of spectral interferences in elemental analysis and also permits the operation of the plasma in its normal mode, so levels of oxides are not preferentially raised as occurs in a cold plasma mode. With the most common high resolution configuration, both a magnetic sector and an electric sector are used to separate and focus the ions. The magnetic sector is dispersive with respect to both ion energy and mass, and focuses all the ions with diverging angles of motion coming from the entrance slit of the spectrometer. The electric sector is dispersive only to ion energy and focuses the ions into the exit slit. Such an arrangement is called a double-focusing high resolution mass spectrometer. Another type of HR-ICP-MS instrument uses multiple detectors, which are usually used for high-precision isotope ratio analyses. Since an array of 5-10 detectors can be positioned around the exit slit of a double-focusing system, the isotopes of a single element can generally all be determined simultaneously, leading to a high level of precision. The disadvantage of this type of system is that the isotopes must all be in a narrow mass range, as the magnetic sector settings remain fixed while only the electric sector settings are scanned.

However, high resolution instruments have some limitations. They are quite expensive, costing between two and three times more than a quadrupole ICP-MS instrument. They are also more complex to operate and to maintain and, for every 10-fold increase in resolving power, there is a concomitant decrease in signal intensity. Moreover, they are much slower than a quadrupole system [I.13,I.67].



### I.2. THE TECHNIQUE OF DIFFUSIVE GRADIENTS IN THIN FILMS (DGT)

#### I.2.1 General approaches

The technique of diffusive gradients in thin films (DGT) emerged in the mid-1990s as a potential general procedure for in situ dynamic trace metal measurement. The first reported use of an improved DGT device, for measuring Zn in sea-water, was in 1994. Later, it was developed as a general monitoring tool for transition and heavy metals [I.68]. Nowadays, it has become a successful tool for cesium and strontium measurement [I.69], radioactive cesium measurements [I.70], inorganic As determination [I.71], calcium and magnesium determination [I.72], uranium and uranium speciation measurements [I.73,I.74], and the determination of mercury and methylmercury in aquatic systems [I.75,I.76]. Dissolved phosphate and sulfate have been also measured by the DGT methodology [I.77,I.78]. The DGT technique has also been applied in solid systems such as soils and sediments, and metal fluxes in sediments and soils as well as concentrations of metals in pore waters have been determined by the use of DGT units [I.79].

The DGT technique is based on the principle of diffusion of hydrated metal cations, dissolved inorganic complexes and small labile organic complexes through an outer filter membrane and a diffusive gel of a known thickness. Once diffused through the outer layers, solutes are irreversibly fixed at the back side of the diffusive gel, where a selective binding agent is immobilized in a second layer of hydrogel. A polyacrylamide hydrogel, of known thickness is commonly used as the diffusive layer, while, depending on the application, different binding agents can be used. The outer surface of the diffusive gel is covered by a 0.45  $\mu\text{m}$  membrane filter in order to protect it from particles adhering to it. The gels are enclosed in a small plastic device as shown in Figure I.7 [I.68,I.80].

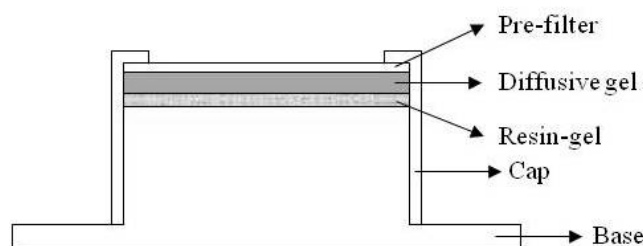


**Figure I.7** Schematic representation of a piston type DGT device.

### **I.2.1.1 Gel types**

#### ***I.2.1.1.1 Diffusive gels***

The pore size of the diffusive gel can be controlled by adding different amounts of cross-linked acrylamide monomer. Restricted gels (RG) have also been obtained by using higher amount of cross-linker agent, ammonium persulfate and N,N,N',N'-Tetramethylethylenediamine (TEMED). Restricted gels have a smaller pore size, which results in a delay in the diffusion of complexes with fulvic and humic acids. A cellulose dialysis membrane (CDM) has also been used as a diffusive layer for DGT performance [I.68,I.81].

#### ***I.2.1.1.2 Resin gels***

Chelex-100 is generally used as a binding agent as it can bind a large number of metals. However, other binding phases have been studied for trace metal speciation. A DGT device using a solution phase poly(4-styrenesulfonate) (PSS) binding layer combined with a dialysis membrane diffusive layer was characterized for copper and cadmium and was found to have good reproducibility [I.81]. The use of a commercially available solid ion exchange membrane (Whatman P81) was also tested as a binding phase in DGT analysis, with simple preparation, ease of handling, and reusability being found to be some of its advantages [I.82].

Some authors have investigated the possibility of using DGT devices with different binding phases to determine DGT labile fractions of Cd and Cu in laboratory solutions and in natural waters. Several binding phases have been studied, including conventional Chelex-100, poly(acrylamide-co-acrylic acid) (PAM-PAA) gel, poly(acrylamidoglycolic acid-co-acrylamide) (PAAG-PAM) gel, Whatman P81 cellulose phosphate ion-exchange membrane (P81), and PSS aqueous solution. The DGT devices with different binding phases were found to be capable of measuring inorganic metal fractions in solutions containing complexing ligands, EDTA and humic acid. However, in natural waters, of a more complex composition, metal concentrations measured by DGT devices with different binding phases were different [I.83].

Phosphate, molybdate and arsenic can be measured by the DGT technique when using a binding layer of ferrihydrite embedded in gel. Some investigators have used a mixed

binding layer (MBL) consisting of ferrihydrite and Chelex-100 combined in a binding gel to measure cations and anions in a single assay [I.84].

A combined DGT was designed to measure sulfide and metals simultaneously. This DGT probe consisted of a layer of gel impregnated with AgI, overlain by a layer of gel containing Chelex-100 (1), a diffusive gel layer (2) and a filter membrane (3). Diffusion of sulfide was controlled by layers (1) to (3) and the AgI gel trapped sulfide through the formation of AgS. The Chelex gel trapped metals were measured after elution with acid [I.85].

### I.2.1.2 Theory

DGT generally responds to both labile inorganic and organic species with different sensitivities depending on their mobility. When the plastic holder is placed in the water, cations diffuse across the filter and the diffusive gel layer and concentrate in the resin gel. Figure I.8 shows a schematic representation of the concentration gradients of a solute in a typical DGT sampler configuration. A diffusion boundary layer (DBL) is present between the filter and the bulk solution, whose thickness depends on the degree of agitation of the water.

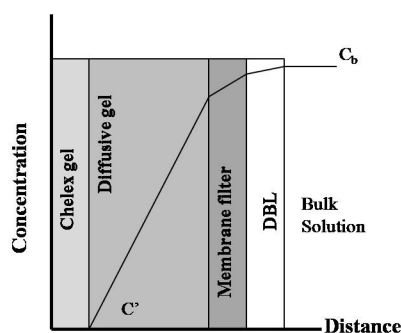


**Figure I.8** Schematic representation of the concentration gradients of a solute in a DGT device.

If the metal ions bind rapidly and efficiently to the resin and the resin is not saturated, it can be assumed that the free cation concentration at the resin/layer interface is effectively zero and a linear concentration gradient is quickly established across the diffusive gel layer. This diffusion is governed by Fick's first law:

$$F = D \frac{dC}{dx} \quad (I.1)$$

where  $F$  is the flux of ions per time unit and,  $D$  is the diffusion coefficient, and  $dC/dx$  is the concentration gradient of the dissolved ion in the hydrogel.

The flux can also be determined directly from the measured mass ( $M$ ) diffused through an area ( $A$ ) after a given time ( $t$ ):

$$F = \frac{M}{At} \quad (I.2)$$

In a sufficiently stirred solution where the DBL in the solution can be considered negligible compared to the thickness of the diffusive gel, the total thickness of the diffusive layer is the sum of the thickness of the diffusive gel and the cellulose membrane filter ( $\Delta g$ ). Thus, the concentration given by DGT can be calculated with Eq. (I.3):

$$C_b = \frac{F\Delta g}{D} \quad (I.3)$$

After a known deployment time, the DGT device is removed from the solution and the resin layer is retrieved and placed in a known volume of dilute  $HNO_3$  to extract the metal ions from the resin for at least 24 h. The acid extract can then be analyzed after an appropriate dilution to determine the mass of accumulated metals:

$$M = \frac{C_e(V_{HNO_3} + V_{gel})}{f_e} \quad (I.4)$$

where  $C_e$  is the concentration measured in the acid extract,  $V_{gel}$  is the volume of gel provided by the manufacturer,  $V_{HNO_3}$  is the volume of added acid for metal extraction and  $f_e$  is the extraction efficiency of the acid (0.8 for many metals).

If Eq (I.1) and Eq. (I.3) are combined, the concentration in the bulk solution during the in situ deployment can be calculated as:

$$C_b = \frac{M\Delta g}{DtA} \quad (I.5)$$

#### ***1.2.1.2.1 Diffusion coefficients***

Since diffusion coefficients play an important role in the DGT technique for metal determination, several studies have been developed to determine the diffusion coefficients of metal ions and metal-ligand complexes in different gels. Zhang and Davison used Fick's first and second laws to measure the diffusion coefficients of trace

metals and fulvic and humic substances in five different hydrogels used in DGT devices [I.86]. The diffusion coefficients of metal ions and metal-ligand complexes in gels obtained with acrylamide monomer cross-linked with a patented agarose derivative (APA1, APA2 and APA3) were measured at different ionic strengths. These studies demonstrated that diffusion coefficients are independent of ionic strength above 1 mmol L<sup>-1</sup>. Moreover, diffusion coefficients of metal complexes decrease when the size of the ligand increases [I.87]. Lead et. al. measured the diffusion coefficients of five different humic substances in water and in agarose hydrogels at several pH values. It was found that at low pH values, some humic substances form large aggregates that cannot penetrate into the gel, and therefore cannot be defined by a single diffusion coefficient value. A decrease was observed in the diffusion coefficient for other humic acids when the pH decreased [I.88]. These studies lead to the establishment and tabulation of different diffusion coefficients of metal and metal-ligands at different temperatures in different types of gels commonly used in the DGT technique.

### **I.2.2 DGT applications**

#### **I.2.2.1 Applications to water samples**

DGT has been successfully used for transition and heavy metal determination in many different natural waters.

Many studies confirm the suitability of the DGT technique for trace metal speciation in lake water. DGT has been used as a tool to determine Cu, Zn, Ni, Cd, Pb and Mn concentrations and speciation in a hardwater eutrophic lake. In this study, the technique was used in situ during six sampling periods [I.89]. Fe, Mn, Cu and Zn were measured in five different lakes by DGT, dialysis and filtration techniques. In this case, filtration, dialysis, DGT and model predictions all provided the same result, suggesting metals were present mainly as inorganic species [I.90]. By the use of an ammonium molybdophosphate (AMP) binding agent, cesium radionuclides could be determined in a freshwater lake. The use of DGT for monitoring radionuclides has several advantages over traditional methods, such as simplicity, provision of time-averaged mean concentrations, and automatic in-situ concentration [I.91]. The major cations Ca and Mg were determined in the laboratory in filtered and modified lake water [I.72]. By using a resin gel consisting of a polyacrylamide gel impregnated with 3-mercaptopropyl

functionalized silica gel, methylmercury could be determined in the dissolved phase of a stratified boreal lake [I.76].

The DGT technique has also been applied in river waters. In the first studies, DGT was compared to anodic stripping voltammetry (ASV) measurements. While DGT allowed in situ measurement of solution speciation, ASV was used to measure labile Cu, Cd and Zn in the laboratory. Such studies concluded that, in the absence of strong complexation, DGT measurements were equivalent to ASV measurements. Moreover, DGT was much easier to use than ASV and was less susceptible to calibration problems [I.92]. Later, Cu, Cd and Mn were measured in situ in two river systems using DGT as a pre-concentration tool [I.93]. The DGT technique was also used to estimate the bioavailable metal concentration that can interact with aquatic organisms [I.94]. DGT has been proven to be a robust tool in routine monitoring of trends in water quality. In this study Ni, Cu and Pb were measured in European rivers under different hydrological conditions [I.95]. Ni, Cu, Zn, Cd and Pb were measured in an urban river in Tokyo with DGT under dry and wet weather conditions. DGT measurements were compared with the prediction of a WHAM VI speciation model and were found to be similar to the model-computed results [I.96].

Recently, the DGT technique has been used in an estuary to determine labile metals in situ under different hydrological conditions. The results demonstrate the sensitivity of DGT to metal speciation and the feasibility of using the DGT technique in highly dynamic estuarine waters to obtain a time-integrated record of labile trace metals [I.97]. Different studies with sea water evidenced the applicability of DGT technique to trace metal speciation in salty waters. Using the technique, Mn, Co, Cd, Cu, Ni and Pb have been successfully determined in sea water [I.98,I.99]. DGT devices can be used as tracking tools to detect episodic sources of seawater contamination [I.100]. The availability of trace metals such as Cd, Cu, Ni, and Pb has been investigated in the Mediterranean Sea by the use of DGT. Results obtained in those experiments were compared with mussel bioaccumulation. This study demonstrated the usefulness of a combination of biomonitoring and DGT techniques for a better understanding of trace metal availability in coastal waters [I.101].

### 1.2.2.2 Applications in sediments and soils

#### 1.2.2.2.1 General considerations

When DGT is deployed in water solutions, it is assumed that the system is well stirred and that the bulk concentration will therefore remain constant. However, in soils and sediments there is a lack of mixing. When a DGT device is deployed in soils or sediments, it must therefore be assumed that pore water concentrations adjacent to the DGT device will become depleted. To overcome this depletion, there are two main ways of resupplying solutes: diffusion and solid-to-liquid phase remobilization. Usually, the concentration of the interfacial pore water between the solid and the DGT device ( $C_a$ ) is greater than the concentration of the bulk pore water. This indicates that there is a significant resupply of solutes coming from the solid phase. In this case, the concentration given by DGT is higher than the bulk pore water solute concentration. However, sometimes there is no resupply of solutes from the solid phase, and the DGT device is supplied only by the diffusion of solutes through the pore water.

The ratio of DGT measured concentration to bulk concentration ( $R$ ) can be used as a tool to estimate the relative mobility of the elements from the solid phase to the pore water and the kinetics of this transfer. For a deployment time of 24 h, three main conditions of solid supply have been established [I.102-I.104]:

- **$R > 0.8$** : there is a rapid and sustained supply from the solid phase. This can occur when solute mixing rates are fast or the resupply from the solid phase is faster than removal to the DGT.
- **$0.1 < R < 0.8$** : there is a partial resupply of the solid phase to the pore water, but this is insufficient to maintain fully pore water concentrations.
- **$R < 0.1$** : there is virtually no resupply of solutes to the pore water. The DGT device is supplied only by diffusion.

For a better interpretation of these measurements, a numerical model of trace metal reaction and transport in sediments is required. The DIFS (DGT induced fluxes in sediments) model permits quantitative interpretation of DGT measurements in terms of kinetic and equilibrium resupply parameters. The DIFS model quantifies the dependence of  $R$  on the resupply of trace metals from solid phase to solution, coupled to the diffusional supply to the interface and across the diffusion layer to the resin gel.

DIFS was developed as a software tool to simulate temporal and spatial changes in concentrations of trace metals in solid and solution phases in sediments during in situ DGT deployments, and estimate resupply parameters from experimental data. DIFS was at first a one-dimensional (1D) model operating along the axis perpendicular to the DGT interface. However, there were big errors with the 1D model, especially in non-sustained cases, and the errors were bigger when simulated deployment times were longer. To overcome this problem, the 2D-DIFS model was developed. The 2D description has reasonably short calculation times with almost any laboratory computer and provides a good approximation of 3D behavior, except for the diffusive case and long simulation times [I.105,I.106].

The DGT technique has also been used in metal bioavailability studies and compared to a plant's uptake processes. For a given device and deployment time, the interfacial concentration can be related directly to the effective concentration ( $C_E$ ) of labile metal.  $C_E$  can be considered the supply concentration of metal to a sink such as DGT or an organism. This parameter has been shown to correlate very well with uptake by biota. In this sense, DGT mimics a plant's uptake mechanism by lowering the concentration locally and inducing diffusive supply and release from the solid phase [I.102].

The application of DGT in sediments and soils can be subdivided into two types based on objectives and methodologies: homogeneous and heterogeneous systems.

#### ***1.2.2.2 Homogeneous systems (bulk deployments)***

Here the objective is to measure directly the flux to the DGT device and interpret it as an effective concentration experienced by the device. The one used in such systems is the piston type, used also in solution.

Several studies have been developed with this configuration. DGT has been used to investigate the resupply kinetics of Cu, Zn, Ni, Cd and Pb under in-situ and laboratory conditions in polluted and unpolluted soils and sediments. Some results have been compared with metal plant uptake. In the same way, results obtained with DGT have been compared to concentrations found in other organisms, such as mussels and chironomids [I.107]. Such comparisons have proved that the bioavailability of metals can be estimated by the use of the DGT technique [I.108-I.110]. The use of different diffusive gels with different pore sizes allows the assessment of inorganic and organic complexes as well as the bioavailability of different metals [I.111].



The Fe-oxide gel has been used in DGT devices to measure phosphorus availability in fertilized soils. This methodology has proved to be an excellent alternative to extraction procedures, which can be affected by the presence of other anions such as chloride, nitrate, sulfate or bicarbonate [I.112,I.113]. The availability of As to roots has also been assessed in old contaminated soils using the DGT technique. The Fe-oxide gel with impregnated ferrihydrite allows the absorption of both As (III) and As (V) [I.114]. The DGT technique has also been used as an additional value in assessing uranium bioavailability. In this study, the uranium concentration found by the use of DGT correlated well with plant uptake [I.115]. Chelex gel and AgI gel have been used simultaneously in sediments for Fe, Mn, Ni, Zn and sulfide release, indicating that there are some active zones in sediments where the reduction in manganese oxides, iron oxides and sulfate occurs simultaneously. These results help us to understand the nature of trace metals and sulfide in sediments [I.116].

### *1.2.2.3 Heterogeneous systems (high-resolution deployments)*

The main objective of this configuration is to provide a vertical pore water concentration profile at a very high resolution. The DGT assembly used in this type is designed to be used in situ. As can be observed in Figure I.9, rectangular gels and a filter membrane are placed on a rectangular plastic support. In this configuration, the resin-gel layer can be sliced on retrieval. The metal in each slice can then be measured, making it possible to observe local variations in concentrations and properties.

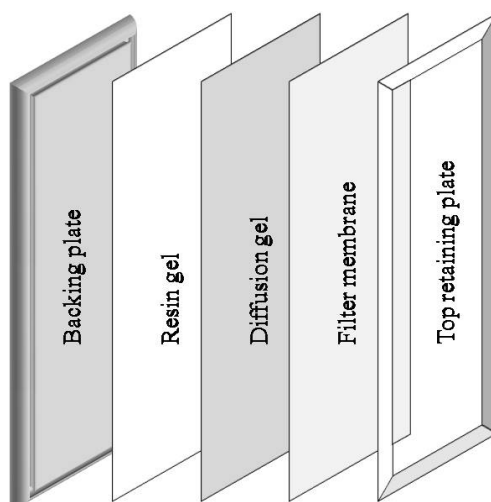


**Figure I.9** Schematic representation of a section through the high resolution DGT assembly for soils and sediments.

This configuration was developed in 1994 and was successfully used in 1995 to measure in situ fluxes of metals (Zn, Cd, Ni, Fe, Cu and Mn) at fine spatial resolution (1.25 mm) in surface sediments (0-9 cm) [I.117].

Since then, several studies with DGT have been carried out to determine the high resolution pore water profiles of trace metals such as Cd, Co, Cr, Cu, Mn, Ni, Pb, Zn and Tl [I.118-I.120].

### **I.3. SULFIDE IN THE ENVIRONMENT**

Sulfide is present in aquatic systems as a result of organic matter decomposition and a reduction in sulfate due to bacterial activity. There are two ways by which sulfate can be reduced to sulfide: assimilatory sulfate reduction, where sulfate is reduced with an organism's energy consumption, and dissimilatory sulfate reduction, where the organism gains energy from such a reduction [I.121-I.123].

Industrial processes have also contributed to the introduction of sulfide and hydrogen sulfide in the environment by the direct use of these components as reagents or producing them as by-products. The petrol industry and its derivatives, and mineral processing, are examples of the effect of industry on the presence of sulfide. The leather and paper industries, which produce wastewaters that can contain around  $20 \mu\text{gL}^{-1}$  of sulfide, are also a source of sulfide compounds [I.124].

Once sulfide is released, it can react with metals at a low pH to form metal sulfides which can then be oxidized as well. Metal sulfide oxidation is a process with a major environmental impact, causing acid rock drainage and acid mine drainage, and aquifer contamination [I.125]. Under some pH conditions, metal sulfide can turn into hydrogen sulfide ( $\text{pK}_{\text{a}1} = 6.88$ ,  $\text{pK}_{\text{a}2} = 14.15$ ), a toxic gas which represents a significant danger to health and the environment. At concentrations higher than  $20 \text{ mg L}^{-1}$ , hydrogen sulfide has a narcotic effect on olfactory receptor cells. At over  $100 \text{ mg L}^{-1}$  it can cause death by asphyxiation. At low concentrations, hydrogen sulfide causes irritation of eyes, the respiratory system and the throat [I.126].

#### **I.3.1 Sulfide in sediments**

Sediments are very important environmental compartments for aquatic ecosystems. In such compartments, a large number of toxic species can accumulate through complex physical or chemical adsorption mechanisms. Accumulation can be affected by different

parameters such as pH, oxidative-reductive potentials, dissolved oxygen or organic matter content [I.127-I.129].

Sulfides have an important role in metal transport and distribution between aqueous and solid phases in the aquatic environment. Due to the low solubility of some of them, a large number of cations are immobilized in anoxic sediments. When these sediments are exposed to oxygen, metal sulfides can be oxidized, thereby releasing metal cations to the aqueous phase which are then available to living organisms. This release can also occur when pH decreases [I.130]. Because of this, sulfide is recognized as having ecotoxicological significance through its affinity for heavy metals. Moreover, acid volatile sulfide (AVS) has the potential to be an indicator of toxicity in both marine and freshwater sediments [I.131]. AVS is defined as the source of H<sub>2</sub>S evolved from sediments by adding 1 N HCl. Hydrogen sulfide measured by this method includes HCl-reactive sulfide minerals and sulfide dissolved in pore waters. Simultaneously, by the addition of HCl, some metals are extracted from the solid phase which are operationally defined as SEM (simultaneous extracted metals). The measurement of the SEM/AVS ratio in sediments is technically simple and has therefore been widely used in sediment contamination assessment [I.132]. In general, sediments with a SEM/AVS ratio (on a molar basis) higher than one are considered potentially toxic, while sediments with a SEM/AVS ratio lower than one can be considered free of toxic effects. The general idea is that, due to the low solubility of metal sulfides, where there is an excess of available sulfide ion, heavy metals are not available for uptake by organisms. However, the AVS model is only reliable when it indicates “non toxicity” ( $AVS \geq SEM$ ). Otherwise, when  $AVS \leq SEM$ , it only indicates that sulfide is not the major binding agent for metals [I.132,I.133].

### **I.3.2 Sulfide determination**

Due to its importance for the environmental community and its high reactivity, different strategies have been developed for the determination of sulfide, involving classical and instrumental techniques. The most common classical method is the reaction of sulfide with iodide to oxidize it to sulfate using starch as an indicator agent. However, the presence of other compounds capable of reducing iodide (such as tiosulfate, sulfite or different organic compounds) can produce substantial errors in the results. Thus, more

selective and sensitive instrumental methods have been developed for sulfide determination [I.122].

### I.3.2.1 Spectrophotometric methods

The Fischer test is probably the most widely used reaction to determine sulfide in different aqueous matrices. In the presence of Fe(III), N,N-dimethylphenyl-1,4-diamine (DMPD) reacts with sulfide to obtain methylene blue, which has maximum absorbance at 670 nm. This reaction is characterized by its high selectivity and sensitivity [I.134].

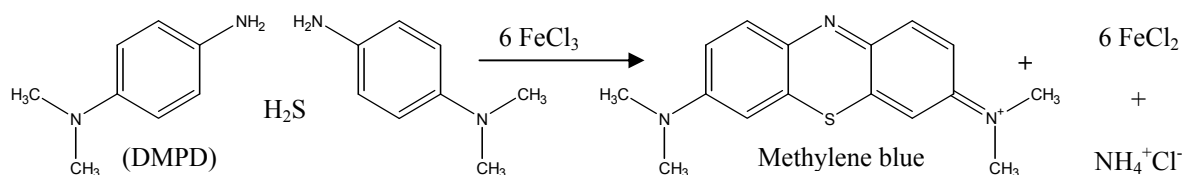


**Figure I.10** Fischer reaction for methylene blue formation.

The need for achieving lower detection limits has led to modifications of the methylene blue method, such as the introduction of FIA (Flow Injection Analysis) [I.135-I.137], fluorescence detection [I.138] and the use of HPLC, which is especially useful when sample turbidity can disturb methylene blue measurement [I.139-I.140]. With the preconcentration of methylene blue into a C18 cartridge and the elimination of organic matter interferences by HPLC in a gradient elution, nanomolar levels of dissolved sulfide were determined [I.140].

Other chromogenic species, apart from DMPD, that react irreversibly with sulfide have been studied. These include aromatic amines such as 4-amino-dimethyl-aniline and N,N-diethyl-p-phenylenediamine (DPD), nitrosylpentacyanoferrate (II) and ferrophenantroline [I.134,I.137,I.141,I.142]. The Schiff reaction has also been studied in depth. Sulfide reacts with formaldehyde to obtain a product which forms a pink specie in the presence of pararosaniline, whose absorbance can be measured at 520 nm [I.143].

The affinity of sulfide for co-ordinated mercuric ion has been used for fluorometric protocol development. The reaction of sulfide to the mercury complex 2,2-pyridylbenzimidazole leads to the formation of mercuric sulfide with subsequent radiation emission. Other methods use fluorescein-mercury acetate complexes whose intensity emission decreases when sulfide concentration increases. Recently, the use of

Hg (II)-2-(2'-hydroxyphenyl) benzoimidazole (HPBI) fluorescence quenching system has been described for the determination of trace amounts of sulfides [I.134,I.144].

Chemiluminescence reactions have also been used for sulfide determination, with reagents such as luminol, hydrogen peroxide, N-bromosuccinimide and N-chlorosuccinimide being successfully applied in sulfide determination protocols. Moreover, some authors have investigated the use of fiber optic sensors for hydrogen sulfide determination by solid surface fluorescence. This approach allows simple miniaturization, simultaneous analysis, and is applicable to a large number of complex matrices [I.145].

Recently, the turbidimetry technique has been also used for sulfide determination. H<sub>2</sub>S was generated in situ in the sample and then extracted in a Zn(II)-containing alkaline microdrop. Turbidimetric measurements were carried out at 275 nm [I.146].

### **I.3.2.2 Electrochemical methods**

The most common electrochemical method is the potentiometric system, which uses silver sulfide as the main sensing element. It is based on the low solubility of the salt and its dissociation influenced by a sulfide solution. Commercially available sulfide electrodes usually consist of polycrystalline Ag<sub>2</sub>S pressed in disc form and embedded in an epoxy resin electrode body. Such electrodes have been successfully applied to a large number of aqueous and gas matrices. A Ag<sub>2</sub>S electrode is sensitive to potential created by S<sup>2-</sup> and Ag<sup>+</sup> ions, it has a very low detection limit, a long lifetime and a wide dynamic working range. However, it suffers from several interferences such as bromide, iodide, cyanide and thiocyanate. Moreover, its long response time, deviation from ideal Nernstian behavior and poisoning of the reference electrode by sulfide are other problems that have limited the use of conventional sulfide selective electrodes [I.134,I.147]. As a way of overcoming such problems, some authors have described pervaporation-potentiometric detection, where sulfide is converted to hydrogen sulfide. This leads to an improvement of the detection limit as well as a decrease in interferences and analysis time [I.148].

The Fischer reaction for methylene blue formation has been used for the development of a potentiometric method which uses a methylene blue detector. This procedure takes advantage of the remarkable selectivity of this reaction in converting sulfide ions into

methylene blue cation, and the high selectivity and sensitivity of the potentiometric sensor for measuring methylene blue [I.149].

The electrochemical behavior of sulfide allows its determination by voltammetric procedures. The oxidation of  $S^{2-}$  at a mercury electrode occurs with the participation of the electrode material and the formation of either a soluble salt or a soluble mercury complex of the anion. The determination of sulfide by stripping voltammetry is based on the reduction of HgS formed in the anodic oxidation of  $S^{2-}$  [I.150]. Because of its relatively simple and portable instrumentation, no need for sample preparation and rapid analysis time, stripping voltammetry is a very suitable method for field analysis. However, conventional batch-mode stripping voltammetry suffers from a loss of dissolved sulfide as a result of reaction with the waste mercury pool in the voltammetric cell during analysis, due to formation of insoluble mercuric sulfide salts [I.151,I.152].

Xerogels have also been used for the preparation of screen-printed electrodes that can be used in the development of highly selective amperometric sensors for the determination of sulfide [I.153].

Biosensors have been applied as useful monitoring devices due to their other advantages, such as low sample pre-treatment, low cost and short analysis time, sensitivity and selectivity. An inhibition biosensor for the detection of sulfides was developed on the basis of their inhibition to horseradish peroxidase, which was immobilized on cysteamine self-assembled monolayer. Sulfides inhibited the activity of the enzyme, with the effect of decreasing the reduction current [I.154].

### **I.3.2.3 Other methods for sulfide determination**

Both gas chromatography (GC) and high performance liquid chromatography (HPLC) have been used for sulfide determination in a large number of matrices, including pharmaceutical preparations, environmental samples, soil samples, etc. The most important advantage of these techniques when working with complex matrices is the separation capabilities of both GC and HPLC. Several detectors have been used in combination with chromatography, including conductivity detectors, flame photometers, UV-visible fluorometric systems, and more recently, mass detectors. Although almost all of them directly determine sulfide, a large number of procedures which use derivatization reactions based on the methylene blue formation have also been described [I.134,I.140,I.155].

Ion chromatography systems vary from simple ion exchange columns to gel-based separation columns. They usually use visible absorption spectrometers as a detector. The most common method uses a solid lead (II) chromate loaded column for sulfide ion removal and detection [I.134]. Another way to determine sulfide in liquid samples is by converting it to hydrogen sulfide, which can be determined by GC-FPD (flame photometric detector) or by ionic chromatography after oxidation to sulfate [I.156].

A more robust alternative to ion chromatography involves capillary electrophoresis. Capillary electrophoresis is a powerful separation technique with high selectivity and efficiency. This methodology has also been applied to the determination of sulfide with direct ultraviolet detection at 229 nm [I.124].

Although ICP-AES has been used to measure total sulfur content in a variety of samples such as wine or fuels [I.157,I.158], it has never been used to measure sulfide directly in water. The situation is similar with ICP-MS, which has been used to determine sulfur species in combination with other analytical techniques such as gas chromatography, ion chromatography and HPLC [I.159,I.160]. However, ICP-QMS has never been used for the direct determination of sulfide in aqueous samples.

### **I.4. ARSENIC IN THE ENVIRONMENT**

Arsenic is the 20<sup>th</sup> most abundant of the 92 naturally occurring elements in the Earth's crust. It is associated with igneous and sedimentary rocks, particularly with sulfidic ores. There are more than 300 arsenic minerals in nature. Of these, approximately 60% are arsenates, 20% sulfides and sulfosalts, 10% oxides and the rest are arsenides, native elements and metal alloys [I.161]. Arsenic has often been described as a heavy metal in the environmental community, while it is actually a metalloid with a predominantly non-metallic character.

Arsenic was the first chemical element to which carcinogenic properties were attributed, after a large number of miners contracted lung cancer due to inhaling it. It has been recognized as the most carcinogenic substance named in current drinking water regulations. Several types of cancer, such as skin cancer, lung cancer and urinary-tract cancer have also been related to exposure to arsenic. Moreover, cardiovascular effects, diabetes, dermal diseases (hyperpigmentation and keratosis), respiratory effects, hepatotoxic effects and neuronal effects have been commonly attributed to long-term

exposure to arsenic in drinking water. To protect people against such exposure, governments around the world have decreased the maximum contaminant level permitted in drinking water during the last ten years. In Spain, in 1992, an initial drinking water limit for arsenic of  $50 \mu\text{g L}^{-1}$  was established, but this was lowered to  $10 \mu\text{g L}^{-1}$  in 2002 [I.162]. However,  $2 \mu\text{g L}^{-1}$  has been suggested on safety grounds, but this has been rejected due to financial implications [I.163].

Although arsenic is well known as being carcinogenic, it has also been found to be essential for some organisms and promote their growth. For this reason it is often added to pig and poultry feed [I.164,I.165].

Arsenic is found in a wide variety of chemical forms throughout the environment. It can be transformed by microbiological activity, changes in geochemical conditions, as well as changes in redox potential, pH and other environmental processes. It is stable in four oxidation states (+5, +3, 0, -3) but its normal valence states are +3 and +5. For instance, trivalent arsenite is more toxic to animals and humans and also more mobile in the environment than pentavalent arsenate. However, plants can reduce arsenate to arsenite, so arsenate is more toxic to plants. Organisms affect the distribution of arsenic by accumulating, transporting and transforming it, and the mobilization of arsenic in natural ecosystems is basically carried out by microbiological activity. The microbial reduction of arsenic (V) to arsenic (III) species occurs via detoxification or respiration processes [I.166,I.167]. A wide range of bacteria have the ability to synthesize arsenite oxidases and thus to oxidize arsenic (III) enzymatically. Certain fungi, yeasts and bacteria are known to methylate arsenic to gaseous derivatives of methyl arsines [I.168].

While arsenic occurs naturally, it may also be found as a result of human activities. Arsenic has been widely used in pesticides, fungicides, herbicides and insecticides and especially as a wood preservative. Moreover, large quantities of arsenic are released into the environment through industrial activities including leather and metal treatments (alloys and bronze) and the production of some pharmaceuticals [I.169]. Another important source of anthropogenic arsenic emissions is the burning of oil and coal [I.164,I.166].



### **I.4.1 Arsenic in the aquatic environment**

Higher concentrations of arsenic tend to be found in groundwater than in surface water and, in general, fresh water concentrations are higher than those in local seawater. The arsenic concentration present in aquatic systems depends on local geology and soil type, as well as chemical conditions. The geochemistry of arsenic is complex. Important processes that control its partitioning between aqueous and solid phases include mineral precipitation/dissolution, oxidation/reduction, biological transformation and adsorption/desorption. These are the most significant processes and they are all dependant on the pH [I.163].

As previously stated, arsenic can occur in waters in four valency states: +5, +3, 0 and -3. Elemental arsenic is very rare and  $\text{As}^{3-}$  is found only at extremely low Eh values in highly reducing environments. Arsenate and arsenite are the dominant forms of inorganic arsenic in aqueous ecosystems and are soluble over a wide range of pH and Eh conditions.  $\text{As}^{5+}$  species are more stable and predominant in oxidizing environmental conditions whereas  $\text{As}^{3+}$  species are predominant in reducing environmental conditions. Under anaerobic conditions, arsenite can be reduced to arsine by microorganisms. Arsenic species may be methylated as monomethylarsonic acid (MMAA), dimethylarsinic acid (DMAA) and trimethylamine oxide (TMAO) by microorganisms, humans and animals. The trivalent compounds are generally more toxic than the pentavalent ones. Other arsenical compounds also exist but they are generally nontoxic [I.170]. The co-deposition of hydrous ferric oxides containing adsorbed arsenic was first proposed as the cause of arsenic groundwater enrichment, on the basis that when organic matter caused a reductive dissolution of ferric oxides, both iron and arsenic were released. Later, the metabolic effects of Fe-reducing bacteria and Mn-reducing bacteria were also taken into account in the release of iron and arsenic and other trace elements. However, some studies reported that  $\text{SO}_4^-$ -reducing bacteria removed arsenic and iron, by co-precipitating them in biogenic pyrite [I.171].

### **I.4.2 Arsenic determination**

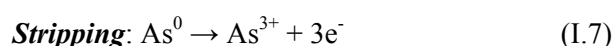
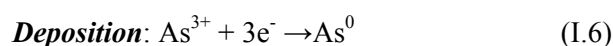
The toxic and carcinogenic properties of inorganic and organic arsenic species make their determination in natural water vitally important. For this reason, several different methodologies have been developed for arsenic determination in a wide variety of environmental sample matrices. These include total arsenic determination methods and

speciation techniques. Probably the cheapest and easiest are the colorimetric methods, which have been widely used for in situ arsenic determination. Most of them are based on the “Gutzei” method and involve treating the water sample with a reducing agent to form arsenic trihydride (arsine gas). The gas is then exposed to paper impregnated with mercuric bromide and a highly colored compound is produced. Quantification can be done by the use of a calibrated color scale. However, sulfur, selenium and tellurium compounds have the potential of interfering with this assay [I.165].

#### I.4.2.1 Electrochemical methods

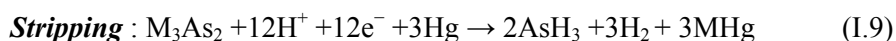
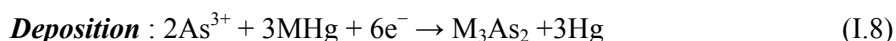
Stripping voltammetric techniques for trace metal analysis have been used for more than 50 years. Nowadays, with advances in computer science and the introduction of new pulse voltammetric techniques, much better control of the experiments is possible as well as the enhancement of signal-to-noise ratio.

One of the most common electrochemical methodologies for the determination of arsenic in water is anodic stripping voltammetry (ASV), which is based on the deposition of metal arsenic on the electrode surface with subsequent anodic stripping. Determination of arsenic by ASV has been investigated in detail using various electrode materials such as graphite [I.172], platinum, gold [I.173], boron and diamond [I.174].



To ensure sufficient mass transfer to the working electrode, a magnetic stirrer is usually used. However, novel mass transfer techniques such as a gas-driven rotating gold film electrode or gold microelectrode placed at the end of a teflon tube integrated with a low frequency sound vibration source have been recently used for arsenic determination. These methodologies have been shown to increase the mass transfer, and thus the arsenic stripping signal, by several orders of magnitude [I.175].

Cathodic stripping voltammetry (CSV) with mercury as the working electrode is a classical technique for the analysis of anions. Cathodic stripping analysis of arsenic at the hanging drop mercury electrode (HDME) is based on arsenic pre-concentration in highly acidic media, with further scanning in the cathodic direction to obtain a peak due to the formation of arsine.

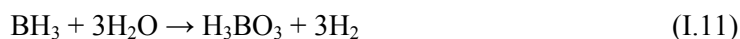


(where M = Cu or Se)

Most cathodic stripping techniques are carried out by using an HMDE, as this electrode does not suffer from the disadvantages of solid electrodes. Generally, methods involving mercury electrodes for arsenic analysis are complicated and require more reagents and careful sample preparation, and are prone to interferences from the adsorption of naturally occurring organic matters. On the other hand, the advantage is that an HDME does not require electrode conditioning and cleaning [I.175].

### I.4.2.2 Spectrometric methods

Atomic absorption spectrometry and atomic fluorescence spectrometry have been widely used for arsenic determination, and their combinations with hydride generation are recognized as powerful analytical tools for trace determinations. Hydride generation is probably the most popular sample derivatization method used for inorganic arsenic detection. It can be used for total inorganic arsenic determination as well as for differential determination of arsenic (III) and arsenic (V), based on the fact that arsenic (III) reacts with tetrahydroborate at a higher pH than arsenic (V). Tetrahydroborate acts as a reductant for arsenic (V) as well as a hydride source, and hydride generation can be used to avoid matrix effects and also as a pre-concentration tool. However, these methodologies also present some interference, in that some matrix elements can also react with the hydride reactive and suppress the volatile hydride of the analyte. Matrix elements such as transition metals, transported to the atomizer in the form of an aerosol, can cause atomization interference, which can also be due to the formation of another volatile hydride forming element [I.176,I.177].



Electrothermal atomic absorption spectrometry (ETAAS) is one of the spectrometric methods which can run without hydride generation. However, most reported methods for arsenic detection based on ETAAS require pre-concentration in order to increase sensitivity. Some modifiers have been successfully studied and applied to the

determination of arsenic in real samples by ETAAS. Some of the benefits that they introduce are shorter time consumption, leading to simpler and faster heating programs, elimination of volatile impurities and lower detection limits. [I.176,I.178]

Inductively coupled plasma has also been used for arsenic determination, and this technique can also be combined with hydride generation. ICP-AES with ultrasonic nebulization is widely utilized for the determination of arsenic as its high sample throughput ensures lower detection limits in comparison to ICP-AES with pneumatic nebulization [I.179]. However, ICP-AES suffers from spectral interferences in arsenic at high concentrations of titanium, manganese, chromium and iron, due to vacuum ultraviolet lines, and from high concentrations of vanadium and chromium, due to ultraviolet lines.

The ICP-MS technique is one of the most widely applied techniques in analytical protocols for arsenic determination. Its main advantages over ICP-AES are isotope analysis, its high precision capability and lower detection limits. However, when using a direct nebulizer at high levels of chloride, the formation of argon chloride ( $^{40}\text{Ar}^{35}\text{Cl}$ ), which has a similar mass to arsenic ( $^{75}\text{As}$ ), occurs in the plasma. Electrothermal vaporization has been used to overcome this interference, a technique which has the additional advantages of requiring small sample sizes, as well as increased sensitivity and lower detection limits. High resolution detectors can also be used to overcome  $^{40}\text{Ar}^{35}\text{Cl}$  signal interference, by using both pneumatic and ultrasonic nebulizers [I.180]. Collision/reaction cells devices have been introduced in ICP-MS instruments to eliminate polyatomic interferences produced in the plasma [I.181].

The poor ionization efficiency of ICP for arsenic hinders the determination of low concentrations of arsenic in real samples. In order to overcome this problem, several ICP-MS applications combined with hydride generation have been applied for arsenic determination using these instruments [I.176].

High performance liquid chromatography (HPLC) has also been used in combination with ICP-MS for the simultaneous speciation analysis of different elements, and different HPLC columns have been successfully applied to arsenic speciation. A C30 reversed-phase column has been used for the identification of various arsenic and antimony species in biological and environmental samples [I.182]. An ion exchange HPLC column has been found to enhance the separation and selectivity of arsenic

## INTRODUCTION

---

species and has been successfully applied to water samples [I.183,I.184]. Mixed mode columns have also been proven to separate arsenite, arsenate, monomethylarsenate, dimethylarsinate, arsenobetaine and arsenocholine in one chromatographic run [I.176]. Recently, capillary microextraction coupled on line with ICP-MS has been developed for the sequential determination of inorganic arsenic (III), arsenic (V), selenium (IV) and selenium (VI) [I.185].

**I.5 REFERENCES**

- I.1. C.J. Gandy, J.W.N. Smith, A.P. Jarvis, Attenuation of mining-derived pollutants in the hyporheic zone: A review, *Sci. Total Environ.* 373 (2007) 435–446
- I.2. B. Passariello, V. Giuliano, S. Quaresima, M. Barbaro, S. Caroli, G. Forte, G. Carelli, I. Iavicoli, Evaluation of the environmental contamination at an abandoned mining site, *Microchem. J.* 73 (2002) 245–250
- I.3. M.G. Bagur, S. Morales, M. López-Chicano, Evaluation of the environmental contamination at an abandoned mining site using multivariate statistical techniques - The Rodalquilar (Southern Spain) mining district, *Talanta* 80 (2009) 377–384
- I.4. J. García Guinea, J. Martínez Frías, *Recursos minerales de España* (1ª ed.) Madrid: Consejo Superior de Investigaciones Científicas, 1992
- I.5. A. Kot, J. Namiesńik, The role of speciation in *Anal. Chem. Trends Anal. Chem.* 19 (2000) 69-79
- I.6. T. J. Manning, W. R. Grow, Inductively coupled plasma - atomic emission spectrometry, *The Chemical Educator*, 2 (1997) S1430-4171
- I.7. P.C. Uden, Element-specific chromatographic detection by atomic absorption, plasma atomic emission and plasma mass spectrometry, *J. Chromatogr. A* 703 (1995) 393-416
- I.8. T. Wang, Liquid chromatography - inductively coupled plasma mass spectrometry (LC-ICP-MS), *J. Liq. Chromatogr. R. T.* 30 (2007) 807-831
- I.9. L.H.J. Lajunen, *Spectrochemical analysis by atomic absorption and emission*, The Royal Society of Chemistry, 1992, ISBN: 0-85186-873-8
- I.10. J.W. Olesik, Elemental analysis using ICP-OES and ICP/MS. An evaluation and assessment of remaining problems, *Anal. Chem.* 63 (1991) 12A-21A
- I.11. N.P. Vela, L.K. Olson, J.A. Caruso, Elemental speciation with plasma mass spectrometry, *Anal. Chem.* 65 (1993) 585A-597A
- I.12. J.A.C., Broekaert, *Analytical Atomic Spectrometry with Flames and Plasmas*, Wiley-VCH, 2005, ISBN: 978-3-527-31282-5
- I.13. A. Montaser, *Inductively Coupled Plasma Mass Spectrometry*, Wiley-VCH, 1998, ISBN: 0-471-18620-1
- I.14. S.A. Lehn, G.M. Hieftje, Experimental evaluation of analyte excitation mechanisms in the inductively coupled plasma, *Spectrochim. Acta B* 58 (2003) 1821–1836
- I.15. R. Thomas, A beginner's guide to ICP-MS Part II: The sample-introduction system, on line: [www.spectroscopyonline.com](http://www.spectroscopyonline.com)

- I.16. P.H.J. Lajunen, P. Perämäki, *Spectrochemical Analysis by Atomic Absorption and Emission 2nd Edition*, Royal Society of Chemistry, 2004, ISBN: 978-0-85404-624-9
- I.17. B. Gammelgaard, O. Jøns, Comparison of an ultrasonic nebulizer with a cross-flow nebulizer for selenium speciation by ion-chromatography and inductively coupled plasma mass spectrometry, *J. Anal. At. Spectrom.* 15 (2000) 499-505
- I.18. James W. Robinson, E. M. S. Frame, George M. Frame II, *Undergraduate instrumental analysis*, Marcel Dekker, Inc., 2004, ISBN: 978-0-824-75359-7
- I.19. L. Ebdon, E. Hywel Evans, Andy S. Fisher, S. J. Hill, *An Introduction to Analytical Atomic Spectrometry*, Wiley, 1998, ISBN: 978-0-471-97418-5
- I.20. S. Maestre, J. Mora, J.L. Todolí, A. Canals, Evaluation of several commercially available spray chambers for use in inductively coupled plasma atomic emission spectrometry, *J. Anal. At. Spectrom.* 14 (1999) 61–67
- I.21. J.W. Olesik, J.A. Kinzer, B. Harkleroad, Inductively coupled plasma optical emission spectrometry using nebulizers with widely different sample consumption rates, *Anal. Chem.* 66 (1994) 2022-2030
- I.22. M.A. Tarr, G. Zhu, R.F. Browner, Microflow ultrasonic nebulizer for inductively coupled plasma atomic emission spectrometry, *Anal. Chem.* 65 (1993) 1689-1695
- I.23. H. Isoyama, T. Uchida, T. Nagashima, O. Ohira, Modified Babington nebulizer for inductively coupled plasma atomic emission spectrometry, *Anal. Sci.* 19 (2003) 593-597
- I.24. E. Paredes, M. Grotti, J.M. Mermet, J. L. Todolí, Heated-spray chamber-based low sample consumption system for inductively coupled plasma spectrometry, *J. Anal. At. Spectrom.* 24 (2009) 903-910
- I.25. M. Grotti, F. Soggia, J.L. Todolí, Ultratrace analysis of Antarctic snow samples by reaction cell inductively coupled plasma mass spectrometry using a total-consumption micro-sample-introduction system, *Analyst* 133 (2008) 1388-1394
- I.26. K.E. Lawrence, G.W. Rice, V.A. Fassel, Direct liquid sample introduction for flow injection analysis and liquid chromatography with inductively coupled argon plasma spectrometric detection, *Anal. Chem.* 56 (1984) 289-292
- I.27. J.A. McLean, H. Zhang, A. Montaser, A direct injection high-efficiency nebulizer for inductively coupled plasma mass spectrometry, *Anal. Chem.* 70 (1998) 1012-1020
- I.28. J.L. Todolí, J.M. Mermet, Evaluation of a direct injection high-efficiency nebulizer (DIHEN) by comparison with a high-efficiency nebulizer (HEN) coupled to a cyclonic spray chamber as a liquid sample introduction system for ICP-AES, *J. Anal. At. Spectrom.* 16 (2001) 514–520
- I.29. P.J. Potts, J.F.W. Bowles, S.J.B. Reed, M.R. Cave, *Microprobe Techniques in the Earth Sciences*, Chapman & Hall, 1995, ISBN: 978-0-412-55100-0
- I.30. B. Hu, S. Li, G. Xiang, M. He, Z. Jiang, Recent Progress in Electrothermal Vaporization–Inductively Coupled Plasma Atomic Emission Spectrometry and Inductively Coupled Plasma Mass Spectrometry, *Applied Spectroscopy Reviews* 42 (2007) 203-234

- I.31. M. Popp, S. Hann, G. Koellensperger, Environmental application of elemental speciation analysis based on liquid or gas chromatography hyphenated to inductively coupled plasma mass spectrometry - A review, *Analytica Chimica Acta* 668 (2010) 114–129
- I.32. G.C.Y. Chan, W.T Chan, Plasma-related matrix effects in inductively coupled plasma atomic emission spectrometry by group I and group II matrix-elements, *Spectrochim. Acta B* 58 (2003) 1301–1317
- I.33. R.N. Reeve, *Introduction to Environmental Analysis*, Wiley, 2002, ISBN: 978-0-471-49295-5
- I.34. J. Kenkel, *Anal. Chem. for Technicians. Third Edition*, Southeast Community College, 2002, ISBN: 978-1-566-70519-6
- I.35. M. Iglésias, T. Vaculovic, J. Studynkova, E. Poussel, J.M. Mermet, Influence of the operating conditions and of the optical transition on non-spectral matrix effects in inductively coupled plasma-atomic emission spectrometry, *Spectrochim. Acta B* 59 (2004) 1841–1850
- I.36. J.L. Todoli, J.M. Mermet, A. Canals, V. Hernandis, Acid effects in inductively coupled plasma atomic emission spectrometry with different nebulizers operated at very low sample consumption rates, *J. Anal. At. Spectrom.* 13 (1998) 55–62
- I.37. A. Canals, V. Hernandis, J.L. Todoli, Fundamental studies on pneumatic generation and aerosol transport in atomic spectrometry: effect of mineral acids on emission intensity in inductively coupled plasma atomic, *Spectrochim. Acta B* 50 (1995) 305-321
- I.38. N. Forsgard, E. Nilsson, M. Andersson, J. Pettersson, Investigation of matrix effects in boron determination using organic solvents as modifiers for liquid chromatography coupled to ICP-MS, *J. Anal. At. Spectrom.* 21 (2006) 305–310
- I.39. M.F. Zaranyika, A.T. Chirenje, Interference effects from easily ionizable elements in flame AES and ICP-OES: A proposed simplified rate model based on collisional charge transfer between analyte and interferent species, *Spectrosc. Lett.* 40 (2007) 835–850
- I.40. D.A. Sadler, F. Sun, S.E. Howe, and D. Littlejohn, Comparison of procedures for correction of matrix interferences in the multi-element analysis of soils by ICP-AES with a CCD detection system, *Microchim. Acta* 126 (1997) 301-311
- I.41. I. Llorente, M. Gómez, C. Camara, Improvement of selenium determination in water by inductively coupled plasma mass spectrometry through use of organic compounds as matrix modifiers, *Spectrochim. Acta B* 52 (1997) 1825-1838
- I.42. E.H. Larsen, S. Stürup, Carbon-enhanced inductively coupled plasma mass spectrometric detection of As and Se and its application to As speciation, *J. Anal. At. Spectrom.* 9 (1994) 1099-1105
- I.43. Z. Hu, S. Hu, S. Gao, Y. Liu, S. Lin, Volatile organic solvent-induced signal enhancements in inductively coupled plasma-mass spectrometry: a case study of methanol and acetone, *Spectrochim. Acta B* 59 (2004) 1463-1470
- I.44. J.L. Todolí, J.M. Mermet, Acid interferences in atomic spectrometry: analyte signal effects and subsequent reduction, *Spectrochim. Acta B* 54 (1999) 895-929



- I.45. H. Sigel, A. Sigel, Handbook on Metals in Clinical and Analytical Chemistry Marcel Dekker, 1994, ISBN: 978-0-824-79094-3
- I.46. Y. Cho, Y.N. Pak, Removal of OH spectral interferences from aqueous solvents in inductively coupled plasma-atomic emission spectrometry (ICP-AES) with Ar cryogenic desolvation, B. Kor. Chem. Soc. 26 (2005) 1415-1420
- I.47. Al-Azzawi, Physical Optics, Principles and Practices, Taylor and Francis Group, 2006, ISBN: 978-0-849-38297-0
- I.48. A.F. Lagalante, Atomic emission spectroscopy: a tutorial review, Appl. Spectrosc. Rev. 34 (1999) 191-207
- I.49. C. Zhang, Fundamentals of Environmental Sampling and Analysis, John Wiley and Sons, 2007, ISBN: 978-0-471-71097-7
- I.50. R. Thomas, Practical Guide to ICP-MS, Marcel Dekker, 2003, ISBN: 978-0-824-75319-1
- I.51. R. Thomas, Practical Guide to ICP-MS: A Tutorial for Beginners 2nd edition, Taylor and Francis Group, CRC Press, ISBN: 978-0-8247-5319-1
- I.52. A.A. Ammann, Inductively coupled plasma mass spectrometry (ICP MS): a versatile tool, J. Mass Spectrom. 42 (2007) 419-427
- I.53. K.G. Heumann, Isotope-dilution ICP-MS for trace element determination and speciation: from a reference method to a routine method?, Anal. Bioanal. Chem. 378 (2004) 318-329
- I.54. A.P. Dickin, Radiogenic Isotope Geology, Cambridge University Press, 2005, ISBN: 0 521 53017 2
- I.55. H.E. Taylor, Inductively Coupled Plasma – Mass Spectrometry Practices and Techniques, Academic Press, 2000, ISBN: 978-0-12-683865-8
- I.56. F. Ridder, R. Pintelon, J. Schoukens, J. Navez, L. André, F. Dehairs, An improved multiple internal standard normalisation for drift in LA-ICP-MS measurements, J. Anal. At. Spectrom. 17 (2002) 1461-1470
- I.57. C. Huang, D. Beauchemin, Direct multielemental analysis of human serum by ICP-MS with on-line standard addition using flow injection, J. Anal. At. Spectrom. 18 (2003) 951-952
- I.58. D.L. Sparks, Advances in Agronomy, Elsevier Academic Press, 2005, ISBN: 978-0-12-000783-5
- I.59. S. Landsberger, M. Creatchman, Elemental Analysis of Airborne Particles, Gordon and Brach Science Publishers, 1999, ISBN: 978-9-056-99627-7
- I.60. K. Kawabata, Y. Kishi, R. Thomas, Dynamic reaction cell ICPMS for trace metal analysis of semiconductor materials, Anal. Chem. 75 (2003) 422A-428A
- I.61. Steve J. Hill, Inductively Coupled Plasma Spectrometry and its Applications, Sheffield Academic Press Ltd, 1999, ISBN: 0-8493-9739-1
- I.62. J.S. Becker, Inorganic Mass Spectrometry: Principles and Applications, John Wiley and Sons, 2007, ISBN: 978-0-470-01200-0

- I.63. C.M. Barshick, D. C. Duckworth, D. H. Smith, *Inorganic Mass Spectrometry: Fundamentals and Applications*, Marcel Dekker, 2000, ISBN: 978-0-824-70243-4
- I.64. P.H. Dawson, *Quadrupole mass spectrometry and its applications*, (AVS Classics in Vacuum Science and Technology), American Inst. of Physics, 1997, ISBN: 978-1-563-96455-4
- I.65. J. Sneddon, *Advances in Atomic Spectroscopy* (vol. 7), Elsevier Scientific B, 2002, ISBN: 978-0-444-51033-4
- I.66. J.R. de Laeter, *Applications of Inorganic Mass Spectrometry*, John Wiley and Sons, 2001, ISBN: 978-0-471-34539-8
- I.67. R. Cornelis, J. Caruso, K.G. Heumann, *Handbook of elemental speciation: techniques and methodology*, John Wiley and Sons Ltd, 2003, ISBN: 978-0-471-49214-0
- I.68. K. Warnken, H. Zhang, W. Davison, Chapter 11 In-situ monitoring and dynamic speciation measurements in solution using DGT, *Compr. Anal. Chem.* 48 (2007) 251-278
- I.69. L.Y. Chang, W. Davison, H. Zhang, M. Kelly, Performance characteristics for the measurement of Cs and Sr by diffusive gradients in thin films (DGT), *Anal. Chem.* 3 (1998) 243-253
- I.70. W. Li, F. Wang, W. Zhang, D. Evans, Measurement of stable and radioactive cesium in natural waters by the diffusive gradients in thin films technique with new selective binding phases, *Anal. Chem.* 81 (2009) 5889-5895
- I.71. J.G. Panther, K.P. Stillwell, K.J. Powell, A.J. Downard, Development and application of the diffusive gradients in thin films technique for the measurement of total dissolved inorganic As in waters, *Anal. Chim. Acta* 622(2008) 133-142
- I.72. R. Dahlgvist, H. Zhang, J. Ingri, W. Davison, Performance of the diffusive gradients in thin films technique for measuring Ca and Mg in freshwater, *Anal. Chim. Acta* 460 (2002) 247-256
- I.73. W. Li, C. Li, J. Zhao, R.J. Cornett, Diffusive gradients in thin films technique for uranium measurements in river water, *Anal. Chim. Acta* 592 (2007) 106-113
- I.74. W. Li, J. Zhao, C. Li, S. Kiser, R.J. Cornett, Speciation measurements of uranium in alkaline waters using diffusive gradients in thin films technique, *Anal. Chim. Acta* 575 (2006) 274-280
- I.75. H. Dočekalová, P. Diviš, Application of diffusive gradient in thin films technique (DGT) to measurement of mercury in aquatic systems, *Talanta* 65 (2005) 1174-1178
- I.76. O. Clarisse, D. Foucher, H. Hintelmann, Methylmercury speciation in the dissolved phase of a stratified lake using the diffusive gradient in thin film technique, *Environ. Pollut.* 157 (2009) 987-993
- I.77. C. Pichette, H. Zhang, S. Sauvé, Using diffusive gradients in thin-films for in situ monitoring of dissolved phosphate emissions from freshwater aquaculture, *Aquaculture*, 286 (2009) 198-202

- I.78. P.R. Teasdale, S. Hayward, W. Davison, In situ, high-resolution measurement of dissolved sulfide using diffusive gradients in thin films with computer-imaging densitometry meter, *Anal. Chem.* 71 (1999) 2186-2191
- I.79. B. Dočekal, V. Smetková, H. Dočekalová, Characterization of Czech soils by diffusive gradients in thin films technique, *Chemical Papers*, 57 (2003) 161-166
- I.80. J. Gimpel, H. Zhang, W. Hutchinson, W. Davison, Effect of solution composition, flow and deployment time on the measurement of trace metals by the diffusive gradient in thin films technique, *Anal. Chim. Acta* 448 (2001) 93-103
- I.81. W. Li, P.R. Teasdale, S. Zhang, R. John, H. Zhao, Application of a poly(4-styrenesulfonate) liquid binding layer for measurement of Cu<sup>2+</sup> and Cd<sup>2+</sup> with the diffusive gradients in thin-films technique, *Anal. Chem.* 75 (2003) 2578-2583
- I.82. W. Li, H. Zhao, P.R. Teasdale, R. John, S. Zhang, Application of a cellulose phosphate ion exchange membrane as a binding phase in the diffusive gradients in thin films technique for measurement of trace metals, *Anal. Chim. Acta* 464 (2002) 331-339
- I.83. W. Li, H. Zhao, P.R. Teasdale, R. John, F. Wang, Metal speciation measurement by diffusive gradients in thin films technique with different binding phases, *Anal. Chim. Acta* 533 (2005) 193–202
- I.84. S. Mason, R. Hamon, A. Nolan, H. Zhang, W. Davison, Performance of a mixed binding layer for measuring anions and cations in a single assay using the diffusive gradients in thin films technique, *Anal. Chem.* 77 (2005) 6339-6346
- I.85. C. Naylor, W. Davison, M. Motelica-Heino, G.A. Van Den Berg, L.M. Van Der Heijdt, Simultaneous release of sulfide with Fe, Mn, Ni and Zn in marine harbour sediment measured using a combined metal/sulfide DGT probe, *Sci. Total Environ.* 328 (2004) 275-286
- I.86. H. Zhang, W. Davison, Diffusional characteristics of hydrogels used in DGT and DET techniques, *Anal. Chim. Acta* 398 (1999) 329–340
- I.87. S. Scally, W. Davison, H. Zhang, Diffusion coefficients of metals and metal complexes in hydrogels used in diffusive gradients in thin films, *Anal. Chim. Acta* 558 (2006) 222–229
- I.88. J.R. Lead, K. Starchev, K.J. Wilkinson, Diffusion coefficients of humic substances in agarose gel and in water, *Environm. Sci.* 37 (2003) 482-487
- I.89. N. Odzak, D. Kistler, Ha. Xue, L. Sigg, In situ trace metal speciation in a eutrophic lake using the technique of diffusion gradients in thin films (DGT), *Aquat. Sci.* 64 (2002) 292–299
- I.90. J. Gimpel, H. Zhang, W. Davison, A.C. Edwards, In situ trace metal speciation in lake surface waters using DGT, dialysis, and filtration, *Environ. Sci. Technol.* 37 (2003) 138-146
- I.91. C. Murdock, M. Kelly, L.Y. Chang, W. Davison, H. Zhang, DGT as an in situ tool for measuring radiocesium in natural waters, *Environ. Sci. Technol.* 35 (2001) 4530-4535

- I.92. S. Denney, A comparison of DGT and ASV for measurement of labile metals in river waters, Mining into the next century: environmental opportunities and challenges. Proceedings of the 24th annual environmental workshop, Townsville, October 1999., pp. 295-310
- I.93. S. Denney, J. Sherwood, J. Leyden, In situ measurements of labile Cu, Cd and Mn in river waters using DGT, *The Sci. Total Environ.* 239 (1999) 71-80
- I.94. E. Garofalo, S. Ceradini, M. Winter, The use of diffusive gradients in thin-film (DGT) passive samplers for the measurement of bioavailable metals in river water, *Ann. Chim-Rome* 94 (2004), 515-520
- I.95. R. Cleven, Y. Nur, P. Krystek, G. Van Den Berg, Monitoring metal speciation in the rivers Meuse and Rhine using DGT, *Water Air Soil Poll.* 165 (2005), 249-263
- I.96. N.N. Aung, F. Nakajima, H. Furumai, Trace metal speciation during dry and wet weather flows in the Tama River, Japan, by using diffusive gradients in thin films (DGT), *J. Environ. Monitor.* 10 (2008) 219-230
- I.97. M. Wallner-Kersanach, C.F.F. de Andrade, H. Zhang, M.R. Milani, L.F.H. Niencheski, In situ measurement of trace metals in estuarine waters of Patos Lagoon using diffusive gradients in thin films (DGT), *J. Brazil Chem. Soc.* 20 (2009) 333-340
- I.98. N.C. Munksgaard, D.L. Parry, Monitoring of labile metals in turbid coastal seawater using diffusive gradients in thin-films, *J. Environ. Monitor.* 5 (2003) 145-149
- I.99. V.I. Slaveykova, I.B. Karadjova, M. Karadjov, D.L. Tsalev, Trace metal speciation and bioavailability in surface waters of the Black Sea coastal area evaluated by HF-PLM and DGT, *Environ. Sci. Technol.* 43 (2009) 1798-1803
- I.100. M.R. Twiss, J.W. Moffett, Comparison of copper speciation in coastal marine waters measured using analytical voltammetry and diffusion gradient in thin-film techniques, *Environ. Sci. Technol.* 36 (2002) 1061-1068
- I.101. M. Schintu, L. Durante, A. Maccioni, P. Meloni, S. Degetto, A. Contu, Measurement of environmental trace-metal levels in Mediterranean coastal areas with transplanted mussels and DGT techniques, *Mar. Pollut. Bull.* 57 (2008) 832-837
- I.102. W. Davison, H. Zhang, K.W. Warnken, Chapter 16 Theory and applications of DGT measurements in soils and sediments, *Compr. Anal. Chem.* 48 (2007) 353-378
- I.103. W.M. Last, J.P. Smol, Tracking Environmental Change Using Lake Sediments: Physical and Geochemical, Volume II, Kluwer Academic Publishers, 2001, ISBN: 978-1-4020-0628-9
- I.104. M.P. Harper, W. Davison, W. Tych, Temporal, spatial, and resolution constraints for in situ sampling devices using diffusional equilibration: Dialysis and DET, *Environ. Sci. Technol.* 31 (1997) 3110-3119
- I.105. M.P. Harper, W. Davison, W. Tych, DIFS - a modelling and simulation tool for DGT induced trace metal remobilisation in sediments and soils, *Environ. Modell. Softw.* 15 (2000) 55-66

- I.106. H. Ernstberger, W. Davison, H. Zhang, T.Y.E. Andrew, S. Young, Measurement and dynamic modelling of trace metal mobilization in soils using DGT and DIFS, *Environ. Sci. Technol.* 36 (2002) 349-354
- I.107. J.L. Roullet, M.H. Tusseau-Vuillemin, M. Coquery, O. Geffard, J. Garric, Measurement of dynamic mobilization of trace metals in sediments using DGT and comparison with bioaccumulation in *Chironomus riparius*: first results of an experimental study, *Chemosphere* 70 (2008) 925-932
- I.108. B. Nowack, S.Koehler, R. Schulin, Use of diffusive gradients in thin films (DGT) in undisturbed field soils, *Environ. Sci. Technol.* 38 (2004) 1133-1138
- I.109. H. Ernstberger, H. Zhang, A. Tye, S. Young, W. Davison, Desorption kinetics of Cd, Zn, and Ni measured in soils by DGT, *Environ. Sci. Technol.* 39 (2005), 1591-1597
- I.110. M. Camusso, A. Gasparella, Measuring bioavailable trace metals from freshwater sediments by diffusive gradients in thin films (DGT) in monitoring procedures for quality assessment, *Ann. Chim-Rome* 96 (2006) 205-213
- I.111. V. Kovářiková, H. Dočkalová, B. Dočkal, M. Podborská, Use of the diffusive gradients in thin films technique (DGT) with various diffusive gels for characterization of sewage sludge-contaminated soils, *Anal. Bioanal. Chem.* 389 (2007) 2303-2311
- I.112. N.W. Menzies, B. Kusumo, P.W. Moody, Assessment of P availability in heavily fertilized soils using the diffusive gradient in thin films (DGT) technique, *Plant Soil* 269, (2005), 1-9
- I.113. S. Mason, R. Hamon, H. Zhang, J. Anderson, Investigating chemical constraints to the measurement of phosphorus in soils using diffusive gradients in thin films (DGT) and resin methods, *Talanta* 74 (2008), 779-787
- I.114. I. Cattani, E. Capri, R., Boccelli, A.A.M. Del Re, Assessment of As availability to roots in contaminated Tuscany soils by a diffusion gradient in thin films (DGT) method and uptake by *Pteris vittata* and *Agrostis capillaris*, *Eur. J. Soil Sci.* 60 (2009), 539-548
- I.115. H. Vandenhove, K. Antunes, J. Wannijn, L. Duquène, M. Van Hees, Method of diffusive gradients in thin films (DGT) compared with other soil testing methods to predict uranium phytoavailability, *Sci. Total Environ.* 373 (2007) 542-555
- I.116. C. Naylor, W. Davison, M. Motelica-Heino, G.A. Van Den Berg, L.M. Van Der Heijdt, Simultaneous release of sulfide with Fe, Mn, Ni and Zn in marine harbour sediment measured using a combined metal/sulfide DGT probe, *Sci. Total Environ.* 328 (2004) 275-286
- I.117. H. Zhang, W. Davison, S. Miller, W. Tych, In situ high resolution measurements of fluxes of Ni, Cu, Fe, and Mn and concentrations of Zn and Cd in porewaters by DGT, *Geochim. Cosmochim. Ac.* 59 (1995) 4181-4192
- I.118. M. Leermakers, Y. Gao, C. Gabelle, S. Lojen, B. Ouddane, M. Wartel, W. Baeyens, Determination of high resolution pore water profiles of trace metals in sediments of the Rupel River (Belgium) using DET (diffusive equilibrium in thin films) and DGT (diffusive gradients in thin films) techniques, *Water Air Soil Poll.* 166 (2005) 265-286

- I.119. Y. Gao, M. Leermakers, C. Gabelle, P. Divis, G. Billon, B. Ouddane, J.C. Fischer, M. Wartel, W. Baeyens, High-resolution profiles of trace metals in the pore waters of riverine sediment assessed by DET and DGT, *Sci. Total Environ.* 362 (2006) 266-277
- I.120. Y. Gao, M. Leermakers, M. Elskens, G. Billon, B. Ouddane, J.C. Fischer, W. Baeyens, High resolution profiles of thallium, manganese and iron assessed by DET and DGT techniques in riverine sediment pore waters, *Sci. Total Environ.* 373 (2007) pp. 526-533
- I.121. W. Yao, F.J. Millero, Oxidation of hydrogen sulfide by hydrous Fe(III) oxides in seawater, *Mar. Chem.* 52 (1996) 1-16
- I.122. R. Al-Farawati, C.M.G. van den Berg, Metal-sulfide complexation in seawater, *Mar. Chem.* 63 (1999) 331-352
- I.123. D.E. Canfield, B. Thamdrup, E. Kristensen, *Advances in Marine Biology: Aquatic Geomicrobiology. Volume 48*, Elsevier Academic Press, 2005, ISBN: 978-0-12-026147-5
- I.124. J. Font, J. Gutiérrez, J. Lalueza, X. Pérez, Determination of sulfide in the leather industry by capillary electrophoresis, *J. Chromatogr. A* 740 (1996) 125-132
- I.125. J.P. Amend, K.J. Edwards, T.W. Lyons, Sulfur biogeochemistry – past and present (special paper), *The Geological Society of America*, 2005, ISBN: 978-0-81-3723-795
- I.126. <http://www.atsdr.cdc.gov> (agency for toxic substances & disease registry)
- I.127. A. De Bartolomeo, L. Poletti, G. Sanchini, B. Sebastiani, G. Morozzi, Relationship among parameters of lake polluted sediments evaluated by multivariate statistical analysis, *Chemosphere* 55 (2004) 1323–1329
- I.128. J.S. Lee, J.H. Lee, Influence of acid volatile sulfides and simultaneously extracted metals on the bioavailability and toxicity of a mixture of sediment-associated Cd, Ni, and Zn to polychaetes *Neanthes arenaceodentata*, *Sci. Total Environ.* 338 (2005) 229– 241
- I.129. T. Praharaj, D. Fortin, Determination of Acid Volatile Sulfides and Chromium reducible sulfides in Cu-Zn and Au mine tailings, *Water Air Soil Poll.* 155 (2004) 35-50
- I.130. A.D. Correia, M.H. Costa, Effects of sediment geochemical properties on the toxicity of copper-spiked sediments to the marine amphipod *Gammarus locusta*, *Sci. Total Environ.* 247 (2000) 99-106
- I.131. A.P. Mackey, S. Mackay, Spatial distribution of acid-volatile sulphide concentration and metal bioavailability in mangrove sediments from the Brisbane River, Australia, *Environ. Pollut.* 9, (1996) 205-209
- I.132. D. Rickar, J.W. Morse, Acid volatile sulfide (AVS), *Mar. Chem.* 97 (2005) 141–197
- I.133. M.A.G.T. van den Hoop, H.A. den Hollander, H.N. Kerdijk, Spatial and seasonal variations of acid volatile sulphide (AVS) and simultaneously extracted metals (SEM) in Dutch marine and freshwater sediments, *Chemosphere* 35 (1997) 2307-2316

- I.134. N.S. Lawrence, J. Davis, R.G. Compton, Analytical strategies for the detection of sulfide: a review, *Talanta* 52 (2000) 771-784
- I.135. L. Ferrer, G. De Armas, M. Miró, J. M. Estela, V. Cerdà, A multisyringe flow injection method for the automated determination of sulfide in waters using a miniaturised optical fiber spectrophotometer, *Talanta* 64 (2004) 1119-1126
- I.136. M.S.P. Silva, C.X. Galhardo, J.C. Masini, Application of sequential injection-monosegmented flow analysis (SI-MSFA) to spectrophotometric determination of sulfide in simulated waters samples, *Talanta* 60 (2003) 45-52
- I.137. J.C.C. Santos, E.B.G.N. Santos, M. Korn, A comparison of flow injection methods for sulfide determination based on phenothiazine dyes produced from diverse aromatic amines, *Microchem. J.* 90 (2008) 1-7
- I.138. M.A. Spaziani, J.L. Davis, M. Tinani, M.K. Carrol, On-line determination of sulfide by the 'methylene blue method' with diode-laser-based fluorescence detection, *Analyst* 122 (1997) 1555-1557
- I.139. P.R. Haddad, A.L. Heckenberg, Trace determination of sulfide by reversed-phase ion-interaction chromatography using pre-column derivatization, *J. Chromatogr.* 447 (1998) 415-420
- I.140. D. Tang, P. H. Santschi, Sensitive determination of dissolved sulfide in estuarine water by solid-phase extraction and high-performance liquid chromatography, *J. Chromatogr. A* 883 (2000) 305-309
- I.141. C. Wang, X. Ji, X. Yan, Y. Liu, Determination of sulfide in waste water by 4-amino-dimethyl-aniline spectrophotometry; uncertainty evaluation, *Shiyou Huagong/Petrochemical Technology* 38 (2009) 444-450
- I.142. A. Afkhami, R. Norooz-asl, Cloud point extraction and spectrophotometric determination of sulfide in water samples using ethylene blue formation Reaction, *Separ. Sci. Technol.* 44 (2009) 983-994
- I.143. K. Shanthi, N. Balasubramanian, A Simple spectrophotometric method for the determination of hydrogen sulfide based on Schiff's reaction, *Microchem. J.* 1996, 53, 168-174
- I.144. Z. Baowei, J. Bing, D. Wenjuan, Z. Kun, Study on spectrofluorimetric determination of sulphides in water, *Chemical Journal on Internet* 8 (2006) 47-50
- I.145. A.E. Eroglu, M. Volkan, O.Y. Ataman, Fiber optic sensors using novel substrates for hydrogen sulfide determination by solid surface fluorescence, *Talanta* 53 (2000) 89-101
- I.146. I. Lavilla, F. Pena Pereira, S. Gil, M. Costas, C. Bendicho, Microvolume turbidimetry for rapid and sensitive determination of the acid labile sulfide fraction in waters after headspace single-drop microextraction with in situ generation of volatile hydrogen sulfide, *Anal. Chim. Acta* 647 (2009) 112-116
- I.147. B. Müller, R. Stierli, In situ determination of sulfide profiles in sediment porewaters with a miniaturized Ag/Ag<sub>2</sub>S electrode, *Anal. Chim. Acta* 401 (1999) 257-264

- I.148. B. Vallejo, P. Richter, I. Toral, C. Tapia, M.D. Luque de Castro, Determination of sulphide in liquid and soil samples by integrated pervaporation-potentiometric detection, *Anal. Chim. Acta* 436 (2001) 301-307
- I.149. S.S.M. Hassan, S.A.M. Marzouk, H.E.M. Sayour, Methylene blue potentiometric sensor for selective determination of sulfide ions, *Anal. Chim. Acta* 466 (2002) 47-55
- I.150. S.V. Kovaleva, N.M. Cheremukhina, V.P. Gladyshev, Voltammetric determination of sulfide ions, *J. Anal. Chem+* 59 (2004) 839-842
- I.151. Y. He, Y. Zheng, D.C. Locke, Differential pulse cathodic stripping voltammetric determination of nanomolar levels of dissolved sulfide applicable to field analysis of groundwater, *Anal. Chim. Acta* 459 (2002) 209-217
- I.152. R. Al-Farawati, C.M.G. van den Berg, The determination of sulfide in seawater by flow-analysis with voltammetric detection, *Mar. Chem.* 57 (1997) 277-286
- I.153. G. Roman, A.C. Pappas, D. Kovala-Demertzi, M.I. Prodromidis, Preparation of a 2-(4-fluorophenyl) indole-modified xerogel and its use for the fabrication of screen-printed electrodes for the electrocatalytic determination of sulfide, *Anal. Chim. Acta* (2004) 201-207
- I.154. Y. Yang, M. Yang, H. Wang, J. Jiang, G. Shen, R. Yu, An amperometric horseradish peroxidase inhibition biosensor based on a cysteamine self-assembled monolayer for the determination of sulfides, *Sensors. Actuator. B*, 102 (2004) 162-168
- I.155. R. Hyšpler, A. Tichá, M. Indrová, Z. Kzadák, L. Hyšplerová, J. Gaspari, J. Churáek, A simple, optimized method for the determination of sulphide in whole blood by GC-MS as a marker of bowel fermentation processes, *J. Chromatogr. B* 770 (2002) 255-259
- I.156. T. Ubuka, T. Abe, R. Kajikawa, K. Morino, Determination of hydrogen sulfide and acid-labile sulphur in animal tissues by gas chromatography and ion chromatography, *J. Chromatogr. B* 757 (2001) 31-37
- I.157. G. Becker, A. Colmsjö, Gas chromatography-atomic emission detection for quantification of polycyclic aromatic sulphur heterocycles, *Anal. Chim. Acta* 376 (1998) 265-272
- I.158. I. Sarudi, J. Kelemen, Determination of sulphur and total sulphur dioxide in wines by an ICP-AES method, *Talanta* 45 (1998) 1281-1284.
- I.159. B. K. Mandal, Kazuo T. Suzuki, K. Anzai, K. Yamaguchi, Y. Sei, A SEC-HPLC-ICP MS hyphenated technique for identification of sulfur-containing arsenic metabolites in biological samples, *J. Chromatogr. B* 874 (2008) 64-76.
- I.160. B. Divjak, W. Goessler, Ion chromatographic separation of sulfur-containing inorganic anions with an ICP-MS as element-specific detector, *J. Chromatogr. A* 844 (1999) 161-169.
- I.161. P. Drahotka, M. Filippi, Secondary arsenic minerals in the environment: a review, *Environ. Int.* 35 (2009) 1243-1255
- I.162. Real Decreto 140/2003. BOE num 45, pp 7238
- I.163. A.H. Welch, K.G. Stollenwerk, *Arsenic in Ground Water - Geochemistry and Occurrence*, Kluwer Academic Publishers, 2003, ISBN: 978-1-4020-7317-5



- I.164. C. Reimann, J. Matschullat, M. Birke, R. Salminen, Arsenic distribution in the environment: the effects of scale, *Appl. Geochem.* 24 (2009) 1147–1167.
- I.165. W. Cullen, K. Reimer, Arsenic speciation in the environment, *Chem. Rev.* 89 (1989) (713-764)
- I.166. D. Melamed, Monitoring arsenic in the environment: a review of science and technologies with the potential for field measurements, *Anal. Chim. Acta* 532 (2005) 1–13
- I.167. D. Lièvremon, P.N. Bertin, M.C. Lett, Arsenic in contaminated waters: biogeochemical cycle, microbial metabolism and biotreatment processes, *Biochimie* 91 (2009) 1229–1237
- I.168. J.F. Ferguson, J. Gavis, A review of the arsenic cycle in natural waters, *Water Research*, Pergamon Press, 6 (1972) 1259-1274
- I.169. Y.S. Yusfin, P.I. Chernousov, A.L. Petelin, E.S. Mikhulina, Effect of the removal of arsenic from metal on the environment, *Metallurgist+* 45 (2001) 3-4
- I.170. A.A. Duker, E.J.M. Carranza, M. Hale, Arsenic geochemistry and health, *Environ. Int.* 31 (2005) 631-641
- I.171. J.A. Saunders, M.K. Lee, M. Shamsudduha, P. Dhakal, A. Uddin, M.T. Chowdury, K.M. Ahmed, Geochemistry and mineralogy of arsenic in (natural) anaerobic groundwaters, *Appl. Geochem.* 23 (2008) 3205–3214
- I.172. J. Long, Y. Nagaosa, Determination of trace arsenic (III) by differential-pulse anodic stripping voltammetry with in-situ plated bismuth-film electrode, *Intern. J. Environ. Anal. Chem.* 88 (2008) 51–60
- I.173. M. Kopanica, L. Novotný, Determination of traces of arsenic (III) by anodic stripping voltammetry in solutions, natural waters and biological material, *Anal. Chim. Acta* 368 (1998) 211-218
- I.174. Y. Song, G.M. Swain, Total inorganic arsenic detection in real water samples using anodic stripping voltammetry and a gold-coated diamond thin-film electrode, *Anal. Chim. Acta* 593 (2007) 7–12
- I.175. D.E. Mays, A. Hussam, Voltammetric methods for determination and speciation of inorganic arsenic in the environment - a review, *Anal. Chim. Acta* 646 (2009) 6–16; B. Daus, Topical issue: “The fate of arsenic in the environment”, *Engi. Life Sci.* 6 (2008) 8 571–572
- I.176. D.Q. Hung, O. Nekrassova, R.G. Compton, Analytical methods for inorganic arsenic in water: a review, *Talanta* 64 (2004) 269–277
- I.177. N. Erdem, E. Henden, Inter-element interferences in the determination of arsenic and antimony by hydride generation atomic absorption spectrometry with a quartz tube atomizer, *Anal. Chim. Acta* 505 (2004) 59–65
- I.178. É.C. Lima, J.L. Brasil, J.C.P. Vaghetti, Evaluation of different permanent modifiers for the determination of arsenic in environmental samples by electrothermal atomic absorption spectrometry, *Talanta* 60 (2003) 103-113
- I.179. E. Vassileva, M. Hoenig, Determination of arsenic in plant samples by inductively coupled plasma atomic emission spectrometry with ultrasonic nebulization: a complex, *Spectrochim. Acta B* 56(2001) 223-232

- I.180. Z. Fiket, V. Roje, N. Mikac, G. Kniewald, Determination of arsenic and other trace elements in bottled waters by high resolution inductively coupled plasma mass spectrometry, *Croat. Chem. Acta* 80 (2007) 91-100
- I.181. V. Dufailly, L. Noël, T. Guérin, Optimisation and critical evaluation of a collision cell technology ICPMS system for the determination of arsenic in foodstuffs of animal origin, *Anal. Chim. Acta* 611 (2008) 134–142
- I.182. Y. Morita, T. Kobayashi, T. Kuroiwa, T. Naruka, Study on simultaneous speciation of arsenic and antimony by HPLC–ICP-MS, *Talanta* 73 (2007) 81–86
- I.183. S.N. Ronkart, V. Laurent, P. Carbonnelle, N. Mabon, A. Copin, J.P. Barthélemy, Speciation of five arsenic species (arsenite, arsenate, MMAAV, DMAAV and AsBet) in different kind of water by HPLC-ICP-MS, *Chemosphere* 66 (2007) 738–745
- I.184. J.A. Day, M. Montes-Bayón, A.P. Vonderheide, J.A. Caruso, A study of method robustness for arsenic speciation in drinking water samples by anion exchange HPLC-ICP-MS, *Anal. Bioanal. Chem.* 373 (2002) 664–668
- I.185. F. Zheng, B. Hu, Dual silica monolithic capillary microextraction (CME) on-line coupled with ICP-MS for sequential determination of inorganic arsenic and selenium species in natural waters, *J. Anal. At. Spectrom.* 24 (2009) 1051–106



# OBJECTIVES





The main objective of the present thesis is to develop and improve analytical strategies for the assessment of environmental pollution indicators. More specifically, the works that comprise this thesis try to achieve the following objectives:

1. Design of new methods for sulfide determination based on inductively coupled plasma spectrometry (ICP-MS and ICP-AES) which gives better sensitivity than the potentiometric reference method. Application of these methods to the determination of sulfide in natural waters as well as to the determination of acid volatile sulfides in sediments. To apply the developed methodologies to the analysis of different natural waters as well as to the sediment samples from the abandoned mining area of Cartagena. Moreover, the possibility of the simultaneous determination of sulfide and sulfate is also investigated.
2. Development of a quadrupole ICP-MS based method for arsenic determination in complex aqueous matrices by using different strategies to overcome spectral and non-spectral interferences. These include the use of mathematical corrections, the application of pressurized collision/reaction cell conditions, the employment of internal standards and the effect of carbon-containing addition. Moreover, the interaction between these strategies and the cross effect over each other is discussed.
3. Evaluation of DGT devices to measure labile metals in acidic samples. This includes a systematic study of the effect produced by pH, the calcium content and the fulvic acid presence. Application to acidic waters and mining wastes from the abandoned mining area of Cartagena and comparison to other established availability tests as well as to metal content in *Crithum maritimum* plant grown on these wastes.

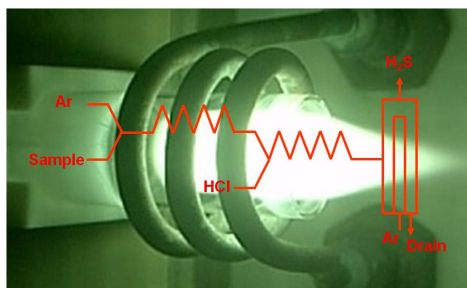


# CHAPTER 1

---

## Determination of sulfide in aqueous and solid samples by hydrogen sulfide-inductively coupled plasma based methods

---



The contents of this chapter are published in:

Colon, M., Iglesias, M., Hidalgo, M., *Development of a new method for sulfide determination by vapor generator-inductively coupled plasma-mass spectrometry*, Spectrochim. Acta B 62 (2005) 470-475.

Colon, M., Todolí, J.L., Hidalgo, M., Iglesias, M., *Development of novel and sensitive methods for the determination of sulfide in aqueous samples by hydrogen sulfide generation-inductively coupled plasma-atomic emission spectroscopy*, Anal. Chim. Acta 609 (2008) 160-168.

Colon, M., Iglesias, M., Hidalgo, M., Todolí, J.L., *Sulfide and sulfate determination in water samples by means of hydrogen sulfide generation-inductively coupled plasma-atomic emission spectrometry*, J. of Anal. At. Spectr. 23 (2008) 416-418.





## 1.1 INTRODUCTION

### 1.1.1 Sulfide in the environment: the importance of being determined

Sulfur is an important element from an environmental point of view as it is one of the major elements in living organisms. It is widely found in natural water and wastewater samples and has been used as a pollution index for water. The toxicity of sulfide in its liberated hydrogen sulfide form ( $\text{H}_2\text{S}$ ) is already well known. The formation of  $\text{H}_2\text{S}$  occurs in a variety of natural waters as a consequence of the decomposition of organic matter and the reduction of sulfate due to bacterial anaerobic respiration [1.1,1.2]. Several industrial processes require the use of sulfide as a reagent or generate it as a by-product. Sulfide and hydrogen sulfide can also be present in thermal waters due to a biological reaction between the sulfates present in such waters and the microorganisms able to reduce them [1.1,1.3].

Inorganic sulfide has received special attention as a metal ligand in anoxic waters, but it has not been traditionally regarded as an environmentally significant species in oxygenated aquatic systems due to the instability of reduced sulfur in the presence of molecular oxygen. However, the occurrence of metastable sulfide in a variety of fully oxygenated marine and freshwater systems has been reported. Sulfide can achieve kinetic stabilization in oxygenated systems through soft metal binding. Thus, sulfide is important for its potential to control trace metal speciation [1.3-1.5].

Under certain pH conditions, sulfide is transformed to hydrogen sulfide ( $\text{pK}_{\text{a}1} = 6.88$ ,  $\text{pK}_{\text{a}2} = 14.15$ ), a toxic gas which is known to be dangerous for health and the environment [1.6].

The high reactivity of sulfide accounts for the large number of determination strategies, and the anion can also act as a versatile intermediate through which other sulfur-based species can be determined. Several techniques have been developed to determine sulfide in natural waters, but a major difficulty here is the lack of stable sulfides. The various approaches that have been considered in the analysis of sulfide are summarized in Figure 1.1.

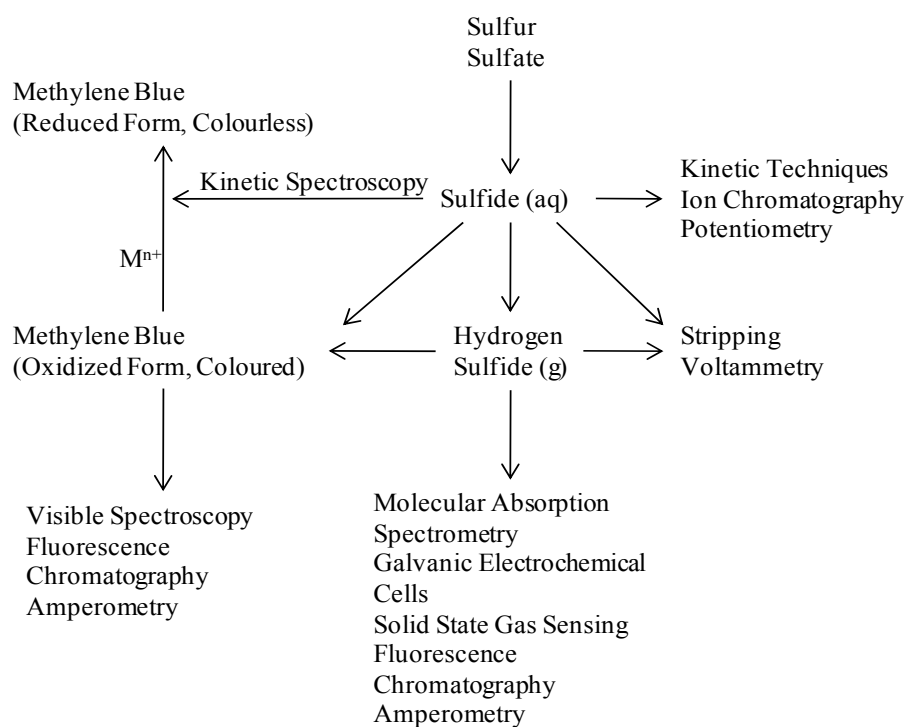


**Figure 1.1** Analytical pathways for the detection of sulfide [1.7].

The role of sulfide in sediments has also been widely reported. It has been found that the transport and distribution of metals between aqueous and solid phases can be regulated by the presence of metal sulfides. Due to the low solubility of some metal sulfides, cations can be immobilized in anoxic sediments. When anoxic sediments are dredged or submitted to natural or forced oxygenation, sulfides can be oxidized with the subsequent release of cations to the aqueous phase. Metal release can also be brought about by lowering the pH [1.8,1.9].

The formation of hydrogen sulfide can be used for the purpose of sulfide determination in sediments. Acid volatile sulfides (AVS), referring to sulfides that are released from the sediment when hydrochloric acid is added, is a parameter widely used to predict the potential toxicity of anoxic contaminated sediments. With this acid medium, some metals called SEM (simultaneous extracted metals) are simultaneously extracted. In general, it is considered that sediment with a SEM/AVS molar ratio higher than one is potentially toxic while sediment with a ratio lower than one is not toxic. Due to the low solubility of metal sulfides in conditions where there is an excess of sulfide, there are no metals available for organisms. However, the AVS model is only valid when it shows

no toxicity ( $AVS \geq SEM$ ); otherwise, it merely indicates that sulfide is not the main metal binding component in the sediment [1.8,1.10].

Besides sulfide, sulfate can also occur in natural waters and many sulfate compounds are readily soluble in water. Most of them originate from the oxidation of sulfate ores or metal sulfide [1.11]. Sulfate is commonly determined in water because at low concentrations (25 to 250 mg/L) it has little effect on the corrosiveness of water with respect to concrete, and increases the water's plumb solvency. Higher concentrations (more than 500 mg/L) can induce diarrhea, and water containing more than 900 mg/L is unsuitable for irrigation. Many methodologies, such as precipitation of barium sulfate followed by ignition and turbidimetric measurement of the collected precipitate, have been developed for sulfate determination. However, ionic chromatography is commonly used nowadays [1.12].

### **1.1.2 Determination of sulfide by ICP-based spectroscopic techniques**

Both ICP-AES and ICP-MS have been used as sensitive techniques for the simultaneous determination of trace elements in different matrices due to their good performance in terms of robustness, sample throughput and simplified sample preparation. Although inductively coupled plasma has been used for the determination of sulfur, it has never been used for sulfide determination in water because it is well known that both ICP-AES and ICP-MS suffer from spectral interferences. When using ICP-AES, low wavelengths (<190 nm) can be hard to achieve because oxygen and water vapor show strong emission below 200 nm [1.13]. To overcome this interference, some mechanism must be used to remove oxygen from the optical chamber. Purge systems have been introduced in some ICP-AES spectrometers; nitrogen or some other inert gas is blown through the chamber to push out the air, which contains oxygen. However, when working with ICP-MS, other spectral interferences besides oxygen also affect sulfide determination. Quadrupole analyzers commonly used in ICP-MS spectrometers have a resolution of 1 uma. Thus, isotopes with a similar mass will be detected as only one isotope. Moreover, polyatomic species with a  $m/z$  ratio similar to the analyte ratio will also cause interference in a quadrupole based system. In Table 1.1, sulfur isotopes together with the most abundant polyatomic interferences are shown. To solve the problem, high resolution spectrometers have been designed, but they are usually very expensive. The introduction of a reaction cell and/or a collision cell device, which

removes interfering ions via chemical reactions by using gases such as H<sub>2</sub>, He or O<sub>2</sub> [1.14-1.18], has proved to be an effective solution. The use of a hexapole collision/reaction cell to determine sulfur isotope ratios in water samples has also been tested, and the studies carried out concluded that the introduction of Xe in hexapole ion optics is necessary to significantly reduce the background produced by the presence of interfering ions [1.19,1.20]. Nevertheless, most commercially available equipment uses H<sub>2</sub> and He gases in the collision/reaction cell, but not Xe. Therefore, the use of this gas is not always possible.

**Table 1.1.** Sulfur isotopes and most abundant polyatomic interferences.

ISOTOPE	INTERFERING SPECIES
<sup>32</sup> S	<sup>16</sup> O <sup>16</sup> O <sup>+</sup> , <sup>14</sup> N <sup>18</sup> O <sup>+</sup> , <sup>15</sup> N <sup>17</sup> O <sup>+</sup> , <sup>14</sup> N <sup>17</sup> O <sup>1</sup> H <sup>+</sup>
<sup>33</sup> S	<sup>16</sup> O <sup>17</sup> O <sup>+</sup> , <sup>15</sup> N <sup>18</sup> O <sup>+</sup> , <sup>14</sup> N <sup>18</sup> O <sup>1</sup> H <sup>+</sup> , <sup>16</sup> O <sup>16</sup> O <sup>1</sup> H <sup>+</sup>
<sup>34</sup> S	<sup>16</sup> O <sup>18</sup> O <sup>+</sup> , <sup>15</sup> N <sup>18</sup> O <sup>1</sup> H <sup>+</sup> , <sup>17</sup> O <sup>17</sup> O <sup>+</sup> , <sup>16</sup> O <sup>17</sup> O <sup>1</sup> H <sup>+</sup>

Another way to avoid interferences is through matrix desolvation, where spectral backgrounds from molecular species associated with a solvent are reduced or eliminated by removing solvent vapor. For this purpose, gas chromatography or cryogenic desolvation systems have been coupled to ICP instruments. A vapor generator has also been used for determining certain elements in aqueous samples as it provides better sensitivity and, in addition, the advantages of matrix elimination [1.20].

### 1.1.2.1 Vapor generator

Arsenic, cadmium, antimony, lead, tin and selenium have been determined by hydride generation because all of them easily form a volatile hydride with high efficiency and velocity. NaBH<sub>4</sub> has been largely used as a reducing agent while HCl is used to form the hydride with the reduced species in a reaction coil. Once the hydride is generated it is separated from the aqueous phase in a gas/liquid separator and it is then swept into the atomizer with a suitable carrier gas.

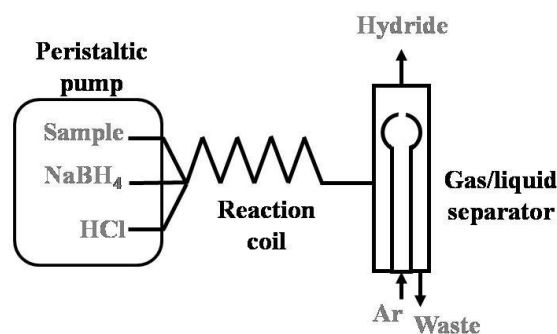


**Figure 1.2** Scheme of a common hydride generator device.

The main advantage of this technique is that the transport of the hydride to the plasma is more efficient, which in turn means the formation of ions in the plasma is also more efficient. Moreover, the separation of the analyte from the matrix samples results in the elimination of or a reduction in interferences [1.21]. Unfortunately, the hydride reaction conditions are not uniform for all the elements, and thus, the capability for the simultaneous determination is decreased. In addition, memory effects can be severe and the use of ultrapure reagents is necessary. Furthermore, some matrix elements can also react with the hydride reactive and suppress the volatile hydride formation [1.22].

In this study, a vapor generator is used for sulfide determination as it easily forms  $H_2S$  when HCl is added, and interferences caused by oxygen present in the water samples can be decreased.

### 1.1.3 Method Optimization

The analytical response obtained using an ICP-QMS can be further affected by different factors related to the collision cell or the mass analyzer. Thus, these factors must be optimized when developing a method, and to this end, different techniques have been used.

#### 1.1.3.1 Experimental design

Experimental design is a methodology based on mathematical tools and statistics. Its main objective is to help the experimenter to select the optimum experimental strategy allowing information to be obtained with the minimum cost and results to be evaluated with guaranteed reliability.

Experimental design is applicable to systems with one or more experimental variables (y), called responses, which depend on the values of one or more independent variables (x), called factors. Factors are controlled by the experimenter and it is not necessary for the relationship between x and y to be known [1.23].

There are different types of experimental design depending on the complexity of the system analyzed. Factorial design is a simple statistical method which, in a few steps, allows the main factors that can influence a response to be discovered [1.24].

**1.1.3.1.1 Complete factorial design**

This type of design allows an area of the experimental domain to be explored and information of use for subsequent optimization to be found. With this methodology, the values of various factors are changed simultaneously, with the result that information about each factor is obtained as well as any possible interaction between them. Each factor is studied at two levels: a lower level (-) and a higher level (+). Experiments take into account all possible combinations of each factor level. In this way, an experimental matrix with  $2^k$  files (number of experiments) and k columns (number of factors) is obtained.

**Table 1.2.** Experimental matrices for complete factorial design  $2^2$ ,  $2^3$  and  $2^4$ .

	$2^2$		$2^3$			$2^4$			
	X <sub>1</sub>	X <sub>2</sub>	X <sub>1</sub>	X <sub>2</sub>	X <sub>3</sub>	X <sub>1</sub>	X <sub>2</sub>	X <sub>3</sub>	X <sub>4</sub>
1	-	-	-	-	-	-	-	-	-
2	+	-	+	-	-	+	-	-	-
3	-	+	-	+	-	-	+	-	-
4	+	+	+	+	-	+	+	-	-
5			-	-	+	-	-	+	-
6			+	-	+	+	-	+	-
7			-	+	+	-	+	+	-
8			+	+	+	+	+	+	-
9						-	-	-	+
10						+	-	-	+
11						-	+	-	+
12						+	+	-	+
13						-	-	+	+
14						+	-	+	+
15						-	+	+	+
16						+	+	+	+

For a factorial design  $2^3$ , eight responses are obtained. These responses can be combined to obtain eight different pieces of information: the average value, three main effects, three interaction effects between two factors, and an interaction effect between the three factors. Each effect can be calculated by adding to or reducing the answer according to the sign in its column as shown in Table 1.3.

**Table 1.3.** Equations used for effect calculation in a complete experimental design  $2^3$ .

EFFECT	EFFECT VALUE
average	$(y_1 + y_2 + y_3 + y_4 + y_5 + y_6 + y_7 + y_8)/8$
$x_1$	$(-y_1 + y_2 - y_3 + y_4 - y_5 + y_6 - y_7 + y_8)/4$
$x_2$	$(-y_1 - y_2 + y_3 + y_4 - y_5 - y_6 + y_7 + y_8)/4$
$x_3$	$(-y_1 - y_2 - y_3 - y_4 + y_5 + y_6 + y_7 + y_8)/4$
$x_1 \cdot x_2$	$(+y_1 - y_2 - y_3 + y_4 + y_5 - y_6 - y_7 + y_8)/4$
$x_1 \cdot x_3$	$(+y_1 - y_2 + y_3 - y_4 - y_5 + y_6 - y_7 + y_8)/4$
$x_2 \cdot x_3$	$(+y_1 + y_2 - y_3 - y_4 - y_5 - y_6 + y_7 + y_8)/4$
$x_1 \cdot x_2 \cdot x_3$	$(-y_1 + y_2 + y_3 - y_4 + y_5 - y_6 - y_7 + y_8)/4$

The average indicates around which value the responses have varied. Generally, it also corresponds to the predicted value in the center of the domain.

The principal effects  $x_1$ ,  $x_2$  and  $x_3$  indicate the average variation of the response when we change from a higher level to a lower level or vice versa, with the sign of the effect giving an idea of the predominant level. Thus, a positive sign indicates that the response of the experiment increases at the higher level of the factor, while a negative sign indicates that the response increases at the lower level.

Interaction effects show whether the effect of a factor depends on the level of another factor. These effects measure the influence that a factor combination has on the response. It is assumed that an interaction exists when a factor effect varies when the level of another factor or factors is changed.

Analysis of variance (ANOVA) and an F test will give an idea of which factors influence the measured response [1.23-1.25].

When there is no interaction, we can conclude that all factors are independent and can be optimized independently. When an interaction exists, an optimization method such as the simplex method is required [1.23-1.26].



### 1.1.3.1.2 Fractional factorial design

Sometimes, when a large number of factors must be evaluated simultaneously, it is reasonable to consider that interactions of a higher order will be very small or negligible. In such cases, fractional factorial design can be applied, and the principal effects and first order interactions can be then evaluated. This methodology allows the evaluation of a large number of factors with a small number of experiments. For example, for a complete  $2^5$  factorial design, 32 experiments would be needed, but if only principal effects and first order interactions were investigated, a fractional factorial design could be applied, and then just 16 experiments would be required.

The effects of each factor can be calculated in the same way as for a complete factorial design.

To evaluate the significance of each effect, an ANOVA or a position diagram can be applied. A position diagram is calculated by ordering effects from the lower to the higher levels and calculating the accumulated observed proportion,  $P_{i,obs}$ , in the following way:

$$P_{i,obs} = \frac{i - 3/8}{n + 1/4} \quad (1.1)$$

Where  $i$  is the order number of the effect in the series and  $n$  is the number of evaluated factors. The calculated value, is then interpolated at the distribution tables to obtain a value of  $z_{i,esp}$ , called Quantile. Finally,  $z_{i,esp}$  values are represented with the effect values. Points which diverge from the principal line are the most important effects [1.27].

### 1.1.3.2 The simplex method

When two or more variables interact, they cannot be optimized independently. In such cases, special optimization methods are needed. Several optimization processes have been described, including simplex methods, central composite designs and the Doehlert design.

Simplex methods are based on an initial design of  $k+1$  trials, where  $k$  is the number of variables. A  $k+1$  geometric figure in a  $k$ -dimensional space is called a simplex. The corners of this figure are known as vertices. With two variables, the first simplex design

is based on three trials, with three variables it is four trials, and so on. The number of trials is also the minimum for defining a direction of improvement, and this makes it a timesaving and economical way to start an optimization project.

Simplex methods follow a step-by-step strategy. The basic method begins with initial trials. The number of initial trials is equal to the number of control variables plus one, and these form the first simplex. The shapes of the simplex in a one-, a two- and a three-variable search space are a line, a triangle and a tetrahedron. The basic simplex algorithm consists of two main rules [1.27]:

- a) **To reject the trial with the least favorable response value in the current simplex.** A new set of control variable levels is calculated by reflection into the control variable space opposite the undesirable result as shown in Figure 1.3. This new trial replaces the least favorable trial in the initial simplex. This leads to a new least favorable response in the simplex that, in turn, leads to another new trial.

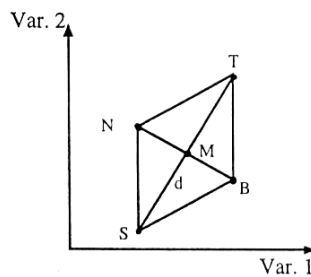


Figure 1.3 Reflection of the undesirable vertex (S) in order to get a new trial (T).

- b) **Never to return to control variable levels that have been rejected.** The reflection calculated in the control variables can also produce a least favorable result. Without this second rule, the simplex would oscillate between the two control variable levels. This problem can be avoided by choosing the second least favorable condition and moving away from it. Thus, the simplex will move towards more favorable conditions as shown in Figure 1.4.

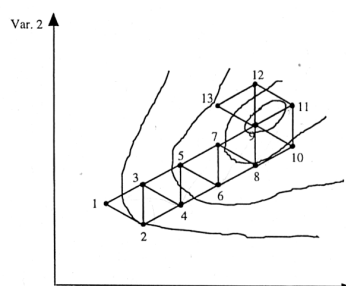


Figure 1.4 Scheme of the simplex method evolving to the optimum response point.

### 1.2 EXPERIMENTAL

#### 1.2.1 Reagents and solutions

All the chemicals used were of analytical reagent grade, and aqueous reagents were prepared in ultrapure MilliQ water obtained from a Millipore system. Sodium sulfide, sodium thiosulfate 5-hydrate, potassium iodate, sodium hydroxide and L(x)-ascorbic acid were purchased from Panreac. Sodium iodide was acquired from Probus. Hydrochloric acid was obtained from Fluka and sulfuric acid from Merck. Hydrochloric acid (10 M) and sulfuric acid (4 M) were both prepared by direct dilution with ultrapure water from a concentrated Suprapur solution.

Sodium sulfide (0.5 M) was prepared by dissolving the necessary amount of solid in previously deoxygenated ultrapure water. This solution was standardized daily [1.28,1.29]. A NaOH buffer was prepared by dissolving appropriate amounts of sodium hydroxide and L(x)-ascorbic acid in ultrapure water to concentrations of 2 M and 0.2 M respectively. A  $\text{NH}_3/\text{NH}_4$  buffer was prepared by dissolving 35g of solid ammonium chloride in 125 mL of ammonia and the total volume was made up to 1 L. L(x)-ascorbic acid was then added to a concentration of 0.2 M.

Sulfide standards were prepared in 50 mL of buffer, a variable amount of standardized sodium sulfide solution and ultrapure water up to 100 mL. Standards containing sulfide and sulfate were prepared in the same way but an appropriate volume of standardized sulfuric acid solution was added. Due to a lack of certified reference materials, spiked samples were prepared using 50 mL of mineral water and the required amount of the standardized sodium sulfide solution, and diluted with buffer to 100 mL.

#### 1.2.2 Sampling procedure

When using ICP-MS, natural waters from a vertical profile (depths of 0, 1 and 2 meters) were collected in Lake Banyoles (Girona, Spain). As sulfide is very unstable in an aqueous solution, it must be preserved in a basic solution with a reducing agent. The EPA [1.29] recommends the use of a SAOB buffer which consists of NaOH, ascorbic acid and ethylenediaminetetraacetic acid (EDTA). Samples were therefore collected immediately and diluted with the same volume of buffer.

With ICP-AES, environmental waters from two different pools were collected in the Alicante region (Spain) and immediately diluted with the same volume of buffer.

In both cases, natural samples were kept at 4 °C until analysis, which was performed within two days after collection.

Sea sediment samples from a vertical profile were collected in the Mar Menor lagoon (Murcia, Spain) using PVC corers 30 cm long, immediately frozen with liquid nitrogen and kept in this state until analysis. In order to extract acid volatile sulfides (AVS) from the sediment, corers were divided into six sections of 5 cm each. Five grams of wet sediment were weighed in a nitrogen atmosphere to avoid oxidation, as shown in Figure 1.5, and submitted to the purge-and-trap procedure proposed by the EPA, depicted in Figure 1.6 [1.29]. The surface part was numbered 1 while the deepest part was numbered 6.



**Figure 1.5** Sampling procedure and manipulation in an N<sub>2</sub> atmosphere.

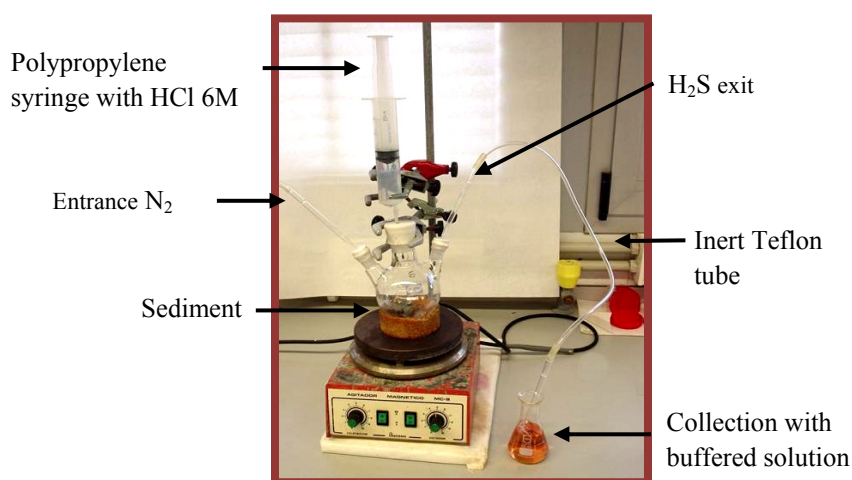


**Figure 1.6** AVS and SEM extraction mounting.

1.2.3 Instrumentation

A Varian VGA 77 vapor generator coupled to an Agilent 7500c ICP-QMS equipped with an octopole reaction cell was used for the first method. A Gilson peristaltic pump was set at the vapor generator drain to maintain a constant flow. Details of the instrumental conditions are given in Table 1.4.

Table 1.4. ICP-MS operating parameters.

PARAMETER	
Rf forward power	1200W
Carrier gas flow rate	1.2 L.min <sup>-1</sup>
Sampling depth	7.7 mm
Plasma gas flow rate	15 L.min <sup>-1</sup>
Isotopes measured	<sup>32</sup> S, <sup>33</sup> S, <sup>34</sup> S
Ion lens settings	Daily adjusted to obtain maximum signal intensity
Nebulizer	Babington
Spray chamber	Scott type double path
Torch	Fassel (Quartz)
Sampling/skimmer cones	Nickel
Collision/reaction gases	He and H <sub>2</sub>
Signal measurement parameter	Sensitivity (slope of the calibration curve)

A Varian (Australia) VGA 76 vapor generator consisting of a reaction coil and a gas separator was used for the ICP-AES methods. Two different systems were employed for H<sub>2</sub>S production. The schemes for both configurations are presented in Figure 1.7.

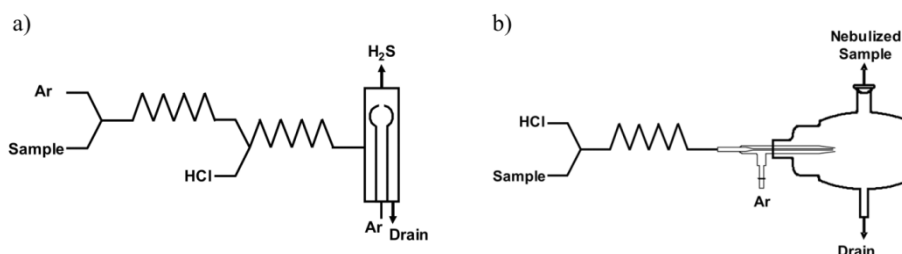


Figure 1.7. Schemes of the sample introduction devices: setup # 1 (a) and setup # 2 (b).

When using setup # 1, only two channels were used, one for the sample and another for the acid solution. The acid was added to the sample flow via a T-piece placed prior to the reaction coil. The generation of H<sub>2</sub>S was completed in a 1 m x 0.8 mm id PTFE capillary. In order to promote the release of H<sub>2</sub>S in the vapor phase, an argon stream was added to the reaction coil. In the second approach (setup # 2), the gas separator was replaced by a conventional liquid sample introduction system consisting of a pneumatic concentric nebulizer (Meinhard Glass Products, CA, USA) coupled to a 40 cm<sup>3</sup> cyclonic spray chamber (Glass Expansion, Australia). In this case, no gas was added in order to avoid degradation of the nebulization process. In both cases, an Optima 4300 DV ICP-AES purged with nitrogen was used; details of the spectrometer instrumental conditions are shown in Table 1.5. Emission intensities were axially measured at 180.669 nm, as these conditions provided the highest sensitivity.

**Table 1.5** ICP-AES Operating Parameters.

PARAMETER	
RF Power <sup>a</sup>	1300 W
Nebulizer gas flow <sup>a</sup>	0.45 L min <sup>-1</sup>
Auxiliary gas flow	0.2 L min <sup>-1</sup>
Plasma gas flow	15 L min <sup>-1</sup>
Integration time	0.1 s
Sample flow rate <sup>a</sup>	7.7 mL min <sup>-1</sup>
Acid flow rate <sup>a</sup>	1.45 mL min <sup>-1</sup>
S wavelength	180.669 nm

<sup>a</sup>Optimized in this work

A Fraunhofer laser diffraction system (model 2600, Malvern Instruments, Malvern, Worcestershire, UK) was used to characterize the aerosol drop size distributions (i.e. the tertiary aerosols) leaving the spray chamber. The sizer was equipped with a 63 mm focal length lens that enabled the system to measure droplets with diameters in the 1.2 to 118 μm range. The spray chamber exit was placed 5 mm from the center of the laser beam.

Potentiometric measurements were carried out using an Orion sulfide electrode (94165c) and a Crison Ag/AgCl reference electrode (cat. 52-41). Both electrodes were connected to a Crison micro-pH 2002 pH meter.

#### 1.2.4 ICP-MS method optimization

A semi-factorial design involving parameters related to the collision cell and the analyzer (octopole bias, quadrupole bias, cell exit, helium flow rate and hydrogen flow rate) was applied to demonstrate that cell exit (between -9 and -13 V) and hydrogen flow rate (between 7 and 1 mL min<sup>-1</sup>) did not affect the results. A 2<sup>3</sup> two-level full factorial design was then developed to investigate the effects of the following instrumental parameters on analyte response: octopole bias (Ob), quadrupole bias (Qb) and helium flow rate (He). These parameters are related to the collision cell and the quadrupole analyzer. The maximum and minimum levels of each factor were established using data from previous experiments and are presented in Table 1.6. Because it is related to sensitivity, the slope of the calibration curve, at m/z 32, was used as the analytical response in the experimental design matrix. The analysis was performed at m/z 32 because this presented the highest signal/background ratio.

**Table 1.6.** Factors and levels used in the factorial design.

VARIABLE	LOW (-)	HIGH (+)
Octopole bias	-12 V	-3.4 V
Quadrupole bias	-10 V	-6 V
Cell Exit	-8 V	-14 V
Helium flow rate	0.5 mL min <sup>-1</sup>	8 mL min <sup>-1</sup>
Hydrogen flow rate	1 mL min <sup>-1</sup>	8 mL min <sup>-1</sup>

Both semi-factorial and full-factorial designs were carried out using a blank solution and a sulfide solution of 60 µg L<sup>-1</sup> in duplicates and in randomized order in order to avoid possible memory effects with the analytical apparatus. These experimental plans allowed evaluation of the effects of the main factors and the possible multi-factor interactions.

Based on the results of the full factorial design, a simplex optimization with octopole bias and helium flow rate was developed.

### 1.2.5 ICP-AES method development

A standard solution of  $500 \mu\text{g L}^{-1}$  of sulfide and  $10 \text{ mol L}^{-1}$  of hydrochloric acid were used in the reaction coil of the vapor generator to form hydrogen sulfide. Different parameters such as gas flow rates of the vapor generating device, sample and acid flow rates, and forward power were studied to achieve a high emission intensity at 180.669 nm.

When using setup # 2, both spiked and real samples were analyzed twice. During the first analysis, sulfate emission was obtained using ultrapure water in the reaction coil. The signal obtained was mainly due to the sulfate present in the sample, because under these circumstances the signal for sulfide was negligible. Note that the sulfide concentration for real samples ( $\mu\text{g L}^{-1}$ ) is much lower than that for sulfate ( $\text{mg L}^{-1}$ ). In the second analysis, hydrochloric acid was added to the reaction coil and the emission intensity was generated by both sulfate and sulfide. The emission due to sulfide was obtained from the difference between these measured intensities. Separate experiments confirmed that sulfate standards gave the same emission intensity whether they were mixed with water or hydrochloric acid in the reaction coil. In the same way, sulfide standards provided negligible emission intensities when they were mixed with water in the reaction coil.

The mass of solvent that reached the plasma per unit of time ( $S_{\text{tot}}$ ) was determined by placing a U tube filled with silica gel, previously weighed, at the exit of either the gas separator or the spray chamber, depending on the method. The solvent which emerged from the gas separator or the spray chamber was trapped on the sorbent over ten minutes. Afterwards, the U tube was weighed again, and the difference in weight showed the mass of solvent that reached the plasma.

## 1.3 RESULTS AND DISCUSSION

### 1.3.1 Sulfide determination by ICP-MS

A method for sulfide determination consisting of a vapor generator coupled to an inductively coupled plasma quadrupole mass spectrometer (VG-ICP-QMS) equipped with a collision/reaction cell was developed.



As pointed out in the introduction section, spectral interferences in sulfur isotopes are already well known. In an attempt to overcome these interferences, a preliminary investigation involving different experiments using He, H<sub>2</sub> or a mixture of both gases in the collision/reaction cell was carried out. In no case was the use of just one gas (He or H<sub>2</sub>) enough to discriminate between the signal of a standard of 1000 µg L<sup>-1</sup> and its background. Although the mixture of both gases in the cell provided a slight difference between the two signals, this difference was very small and suggested the necessity of aqueous matrix elimination. Aqueous matrix elimination was successfully achieved using a vapor generator. Experiments using the vapor generator device with a vented cell showed a signal-to-background ratio that was still low, which led to the conclusion that a vapor generator combined with a pressurized cell was necessary. To determine the best experimental conditions for a collision/reaction cell, an experimental design followed by a simplex optimization was carried out.

### 1.3.1.1 Experimental design and optimization

Initially, 5 variables related to the collision cell and the quadrupole analyzer were taken into account in a semi-factorial design. These were octopole bias (Ob), quadrupole bias (Qb), cell exit (CE), helium flow rate (He) and hydrogen flow rate (H<sub>2</sub>). They are shown in Figure 1.8.

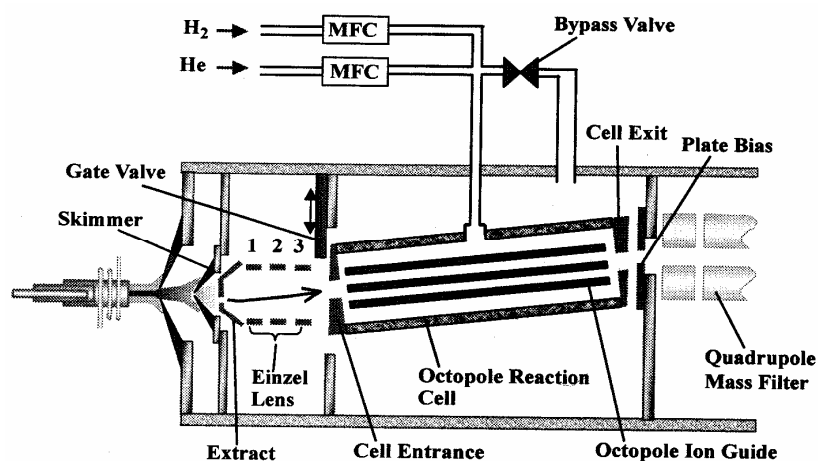


**Figure 1.8** Schem of the interfase, collision cell and analyzer components of the ICP-MS used in these studies.

For a semi-factorial design with 5 variables, 16 experiments were performed in duplicates. Estimated effect for each variable and first order interaction effects between them are shown in Table 1.7.

**Table 1.7** Estimated effect of each factor and the first order interaction effects.

	Ob	Qb	CE	He	H <sub>2</sub>	Ob/Qb	Ob/CE	Ob/He
<b>Estimated effect</b>	-14738	4318	443	-10751	-2953	-2134	741	9041
	Ob/H <sub>2</sub>	Qb/CE	Qb/He	Qb/H <sub>2</sub>	CE/He	CE/H <sub>2</sub>	He/H <sub>2</sub>	
<b>Estimated effect</b>	2242	-186	-1731	-78	-1106	546	1898	

As can be seen, octopole bias and the helium flow rate are the variables with the highest effect, and the interaction between these two variables is also important. To ensure the significance of these variables, a position diagram was developed by calculating the accumulated observed proportion,  $P_{i,obs}$ , for all variables and the corresponding quantile. The resulting diagram, shown in Figure 9, demonstrates that quantiles -2.04, -1.75 and -0.46 are a long way from the position line. These quantiles relate to octopole bias, helium flow rate and the interaction between them respectively. However, as the quadrupole bias effect was considered slightly high, it was decided to develop a full factorial design with those three variables.

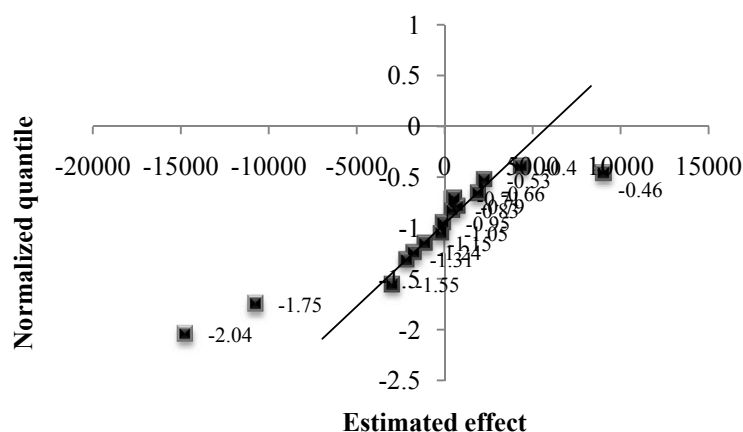


**Figure 1.9** Diagram position of factor effects and their first order interaction

A 2<sup>3</sup> full factorial design was developed with three replicates of the central point, involving the variables octopole bias, quadrupole bias and helium flow rate, and using

the slope of the calibration curve as the analytical response. The results obtained from these experiments were evaluated by analysis of variance (ANOVA). Working at the usual 95% confidence level, a tabulated Student's *t*-value of 2.3 reveals which effects are important. The Pareto chart (Figure 1.10) demonstrates that at the levels studied, octopole bias, helium flow rate and the interaction between them are statistically significant, while quadrupole bias and other interactions are not. In this figure, it can also be observed that better results are obtained working at higher octopole bias voltages and lower helium flow rates. Quadrupole bias can be set at the central point of the interval tested.

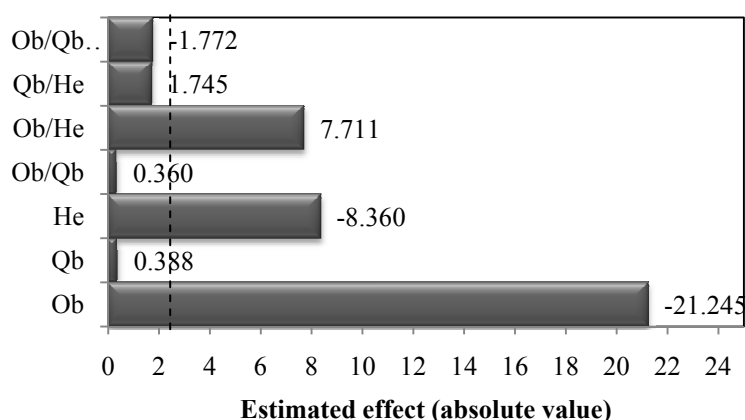


**Figure 1.10** Pareto Chart of the main effects obtained from a  $2^3$  full factorial design. The vertical line defines the 95% confidence interval.

Since octopole bias and helium flow rate interact, these variables can not be assessed individually. Therefore, a simplex algorithm was used to achieve optimum conditions. As the only factor to optimize was sensitivity, the slope between the blank and the standard was chosen as the analytical response. The simplex was moved in the direction given by the rules of the sequential simplex method. The point with the lowest slope was rejected and a new simplex was established by calculating the next reflection vertex. The experiments were performed using the established vertices until no further improvement in sensitivity was observed. These results are shown in Figure 1.11.

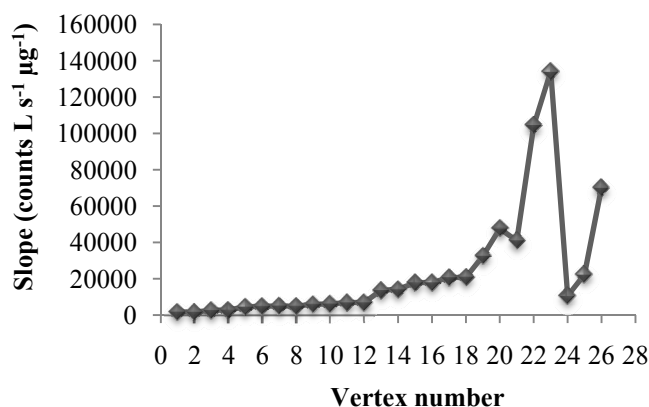


**Figure 1.11** Evolution of the slope of the calibration curve with the trials defined by the simplex method.

The highest slope value was obtained at vertex 23 so the optimum conditions of experiment 23 were selected for further analytical work, these are Octopole bias: -3.8 V and Helium flow rate: 0.7 mL min<sup>-1</sup>.

### 1.3.1.2 Method performance

The calibration curve obtained for the newly developed method shown in Figure 1.12 was obtained using 6 standards and a blank in the range of 1 to 100 µg L<sup>-1</sup>. The working range was increased to 500 µg L<sup>-1</sup> and was found to be linear. The limit of detection (LOD) of the method, calculated as three times the standard deviation of the curve ( $S_{y/x}$ ) divided by the slope of the curve, was 2 µg L<sup>-1</sup> and the limit of quantification (LOQ), calculated as ten times the standard deviation of the curve ( $S_{y/x}$ ) divided by the slope of the curve, was 7 µg L<sup>-1</sup>. For comparison, the LOD obtained for the potentiometric method, calculated according to IUPAC as the intersection of the background signal with the ideal response function [1.30], was 20 µg L<sup>-1</sup>. The relative standard deviations (RSD),  $n = 5$ , were 0.4% and 1.3% for the VG-ICP-QMS and potentiometric methods respectively.

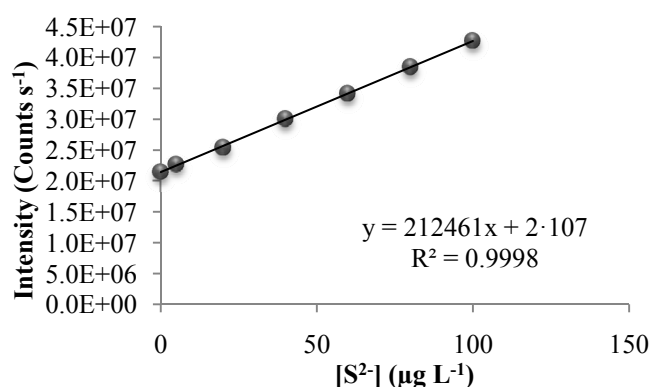


**Figure 1.12** Calibration curve obtained for S<sup>2-</sup> using the VG-ICP-QMS method.

Since natural water reference material with a certified value for  $S^{2-}$  is not commercially available, the proposed VG-ICP-QMS method was evaluated by comparison with the well-established potentiometric method. Three spiked samples with final concentrations of 20, 50 and 90  $\mu\text{g L}^{-1}$  were prepared by transferring 50 mL of buffer and the necessary amount of standardized sodium sulfide and filling up to the mark with mineral water. Three replicates were measured using both methods. The results obtained with VG-ICP-QMS were compared with those obtained by the potentiometric method using an F-test to make sure that there were no significant differences between variances, and then a t-test was applied to determine if the results of the two methods were comparable. These results are shown in Table 1.8. As can be observed, both methods are comparable in terms of precision and accuracy.

**Table 1.8** Determination of sulfide in spiked mineral water by the potentiometric and VG-ICP-QMS methods. Evaluation of the new method, and statistics.

	POTENTIOMETRIC METHOD		VG-ICP-QMS		STATISTICS	
	$\mu\text{g L}^{-1}$	Standard deviation	$\mu\text{g L}^{-1}$	Standard deviation	<i>F</i> -value <sup>a</sup>	<i>t</i> -value <sup>a</sup>
<b>Sample 20 <math>\mu\text{g L}^{-1}</math></b>	< DL	-	14.9	0.4	-	-
<b>Sample 50 <math>\mu\text{g L}^{-1}</math></b>	46.1	0.8	45.1	0.4	4.8	1.8
<b>Sample 90 <math>\mu\text{g L}^{-1}</math></b>	88	1	87.6	0.4	8.4	0.2

<sup>a</sup> The tabulated *F*-value for two degrees of freedom at *P*(0.95) is 19.0 and the tabulated *t*-value for four degrees of freedom at *P*(0.95) is 2.8.

The two methods were then used to measure three different natural waters from Lake Banyoles, in triplicate. The results are shown in Table 1.9.

As can be observed, the results are similar for both methods, but better precision was obtained when using the newly developed VG-ICP-QMS method. The potentiometric method was not sensitive enough for the determination of sulfide in the surface water sample.

**Table 1.9.** Sulfide determination in natural waters by the potentiometric and VG-ICP-QMS methods. Evaluation of the new method and statistics.

Sample depth	POTENTIOMETRIC METHOD		VG-ICP-QMS		STATISTICS	
	$\mu\text{g L}^{-1}$	Standard deviation	$\mu\text{g L}^{-1}$	Standard deviation	<i>F</i> -value <sup>a</sup>	<i>t</i> -value <sup>a</sup>
0 m	<DL	-	14.6	0.4	-	-
1 m	700	30	698	2	15.4	0.6
2 m	1500	100	1520	70	1.7	0.9

<sup>a</sup> Tabulated *F*-value for two degrees of freedom at *P*(0.95) is 19.0 and tabulated *t*-value for four degrees of freedom at *P*(0.95) is 2.8.

Finally, the results obtained for the vertical profile of a sediment sample from the Mar Menor are shown in Table 1.10. They demonstrate that the VG-ICP-QMS method is also applicable to the determination of AVS in sediments.

**Table 1.10.** Determination of AVS in sea sediments.

Sample depth	POTENTIOMETRIC METHOD		VG-ICP-QMS		STATISTICS	
	$\text{mg L}^{-1}$	Standard deviation	$\text{mg L}^{-1}$	Standard deviation	<i>F</i> -test <sup>a</sup>	<i>t</i> -test <sup>a</sup>
0-5 cm	65	2	61.3	0.6	13.45	0.36
5-10 cm	7.0	0.9	4.7	0.6	2.12	0.24
10-15 cm	21	2	18.9	0.2	6.11	0.84
15-20 cm	52	2	48.9	0.5	13.58	0.42
20-25 cm	12	2	11.0	0.5	14.97	0.65
25-30 cm	6	1	4.4	0.8	1.81	0.88

<sup>a</sup> Tabulated *F*-value for two degrees of freedom at *P*(0.95) is 19.0 and tabulated *t*-value for four degrees of freedom at *P*(0.95) is 2.8.

### 1.3.2 SEM/AVS relationship in Mar Menor sediments

When removing sulfide from sediments with hydrochloric acid, a metal fraction is also released. This is the so-called simultaneously extracted metal (SEM) fraction, which can be used together with sulfide content to evaluate the toxicity and potential mobility of

metals in sediments. The SEM/AVS ratio was determined in vertical profiles at five different points. Sulfide was determined by the potentiometric method while simultaneously extracted metals were determined by ICP-AES. The metals identified were zinc, lead and cadmium. The first two were present in those sediments as main metals while the third is a toxic metal which can be present in sediment as an impurity. The results for these experiments are shown in Figure 1.13.

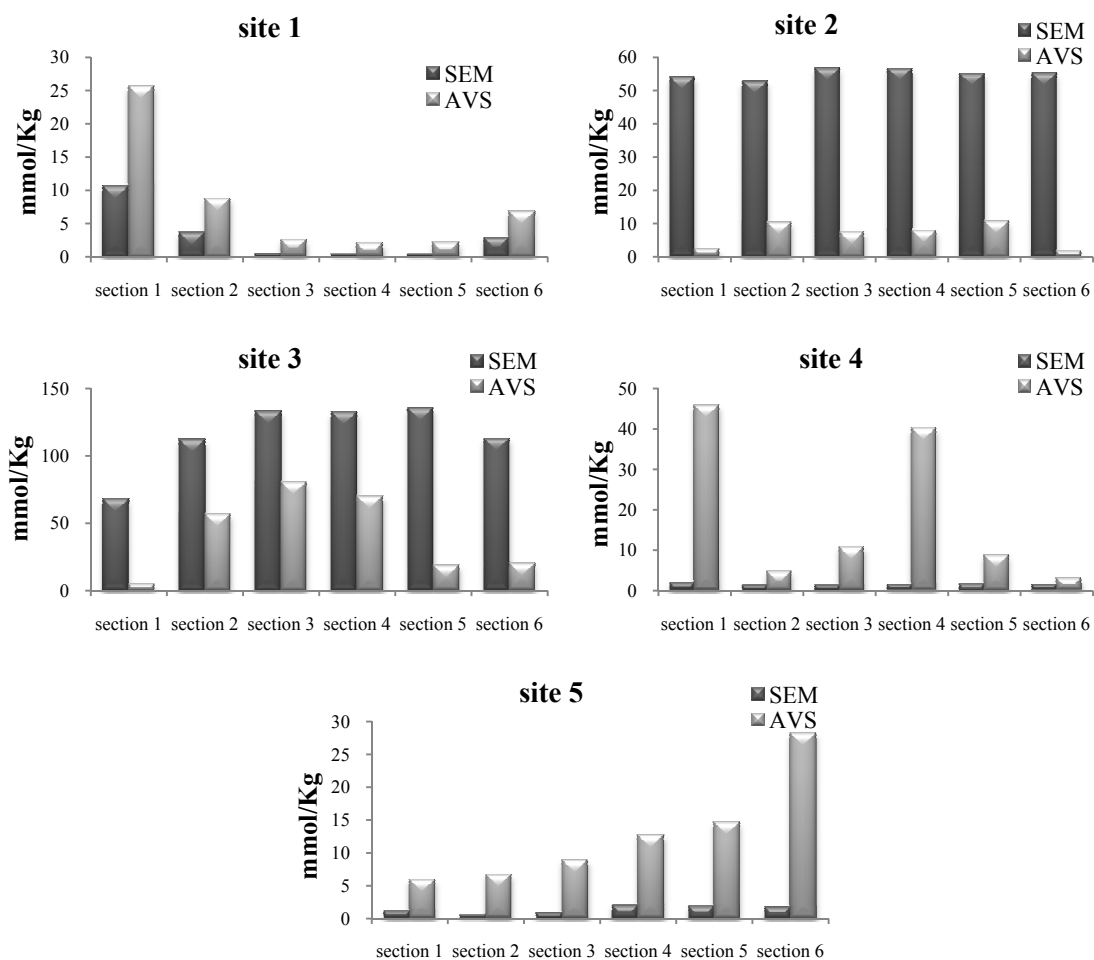


**Figure 1.13** Graphical representation of SEM and AVS results at different sampling points.

In this figure, it can be observed that site 1 and site 4 both have a high AVS concentration in the first section while other sections contain slightly lower concentration, except for the fourth section of site 4 which also contains a high AVS concentration. In site 5, the AVS content increases when depth increases. All these three

points have in common that the SEM/AVS ratio is lower than one, from which it can be concluded that these sediments can be considered as non-toxic.

However, in site 2, AVS concentration is almost constant throughout its vertical profile, although the central sections have a higher content. In this sediment we can observe that the SEM/AVS ratio is much higher than one. Something similar is observed in site 3, where the SEM content is extremely high in all sections and, even though AVS concentrations are also high in central sections, the SEM/AVS ratio is higher than one for the whole of the vertical profile. When a SEM/AVS ratio is higher than one it means that sulfide is not the main binding phase for metals. Those metals could be bound to a more labile phase and, thus, the availability of metals and the potential toxicity of the sediments could be high.

### 1.3.3 Sulfide determination by ICP-AES

#### 1.3.3.1 Buffer selection

With setup # 2, the plasma became extremely orange and was usually extinguished when using SAOB buffer, which contains 2M NaOH. Furthermore, nebulizer tip blocking problems could be observed with this configuration when high sodium content solutions were nebulized. A  $\text{NH}_3/\text{NH}_4^+$  buffer with ascorbic acid was therefore studied and compared with the SAOB buffer. Experiments carried out using both configurations (setup # 1 and setup # 2) and consisting of varying the gas flow rate and the sample or acid flow rate showed similar results for both buffers. By employing setup # 2, two calibration curves were constructed using NaOH and  $\text{NH}_3/\text{NH}_4^+$ . Three aliquots of an environmental water sample were spiked at about  $160 \mu\text{g L}^{-1}$  by transferring 50 mL of each buffer to different containers, adding the necessary amount of standardized sodium sulfide and filling up to 100 mL with the environmental water. Three replicates of each spiked sample were measured and interpolated in the corresponding calibration curve. The results obtained for both buffers were statistically the same and  $\text{NH}_3/\text{NH}_4^+$  was therefore used in the subsequent experiments.

#### 1.3.3.2 Operating parameters

All experiments were carried out using the vapor generator device in both configurations - gas separator (setup # 1) and nebulizer/spray chamber assembly (setup



# 2) - with a  $500 \mu\text{g L}^{-1}$  sulfide standard solution. Different parameters were optimized in terms of sulfur emission intensity. The first variable studied was the sample flow rate/acid flow rate ratio. Three different ratios were tested using acid solution tubing with increasing inner diameters. The ratios studied were 7, 5.3 and 3. This study was performed at a sample flow rate of  $4.8 \text{ mL min}^{-1}$ , forward power of 1300 W and a nebulizer gas flow of  $0.4 \text{ L.min}^{-1}$ . Obviously, the higher this ratio the lower both the acid proportion and the sample dilution factor. The lowest signal was obtained working at a ratio of 7, probably because the acid content was too low. At a ratio of 5.3, the sulfur emission intensity increased slightly but remained constant when the ratio was decreased to 3, which indicates that the acid volume was enough for quantitative  $\text{H}_2\text{S}$  generation. Subsequent experiments were therefore performed at a sample flow rate/acid flow rate ratio of 5.3.

Several sample flow rates were studied at a ratio of 5.3. Results are shown in Figure 1.14.

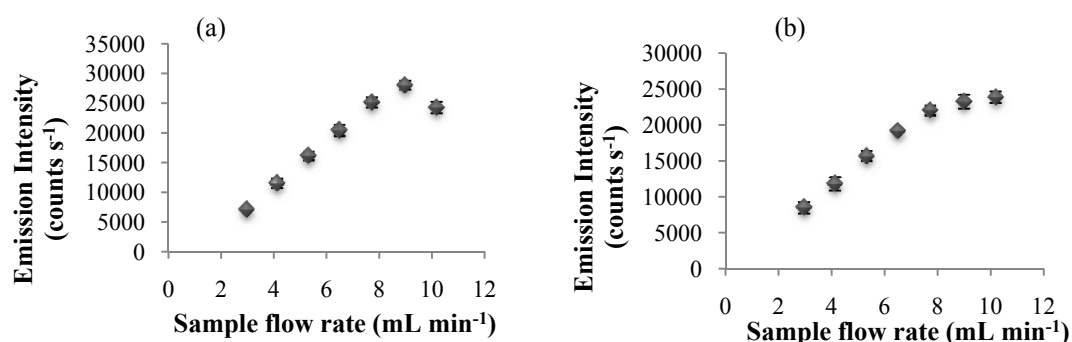


**Figure 1.14** Sample flow rate effect on sulfur emission intensity with setup # 1 (a) and with setup # 2 (b). Forward power is 1300 W and nebulizer gas flow rate is  $0.4 \text{ L min}^{-1}$ .

As can be observed in Figure 1.14a, when the gas separator was used (setup # 1), the sulfur emission intensity increased as the sample flow rate went up to  $9 \text{ mL min}^{-1}$ . Above this value, the signal started to decrease. This result can be accounted for by the decrease in the sample residence time inside the reaction coil at higher flow rates. In contrast, at sample flow rates higher than  $8 \text{ mL min}^{-1}$ , the signal remained constant when the nebulizer/spray chamber combination (setup # 2) was employed. In both cases, below these critical values the signal increase with the flow rate was linear. This result indicates that a mass calibration is possible with only one standard by merely

increasing the liquid flow rate, hence reducing analysis time. To verify this, a standard of  $100 \mu\text{g L}^{-1}$  sulfide was analyzed with setup # 1 at different flow rates, and a mass calibration curve with a slope of  $8674.4$  ( $\text{counts min } \mu\text{g}^{-1} \text{ s}^{-1}$ ) and an intercept of  $477.25$  ( $\text{counts s}^{-1}$ ) ( $r^2 = 0.999$ ) was obtained, as shown in Figure 1.15.

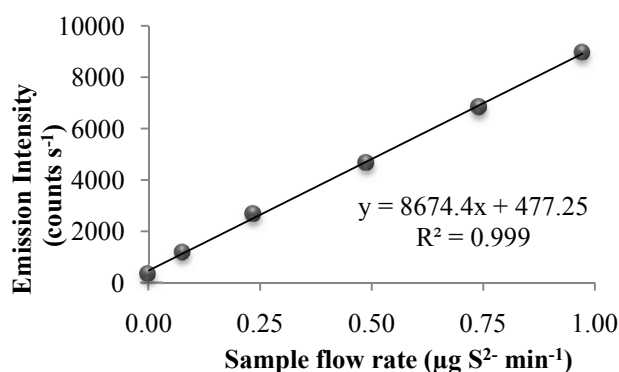


**Figure 1.15** Mass calibration curve for a standard of  $100 \mu\text{g L}^{-1}$  measured at  $180 \text{ nm}$  with setup # 1.

Three standards of  $25$ ,  $49$  and  $99 \mu\text{g L}^{-1}$  were also analyzed and interpolated in this calibration curve, and concentration values of  $25$ ,  $47$  and  $98 \mu\text{g L}^{-1}$  respectively were obtained. These results demonstrate the reliability of the mass calibration procedure.

The fact that the signal increased linearly with the sample flow rate suggests that, for both setups, the analyte was transported towards the plasma in vapor form. It also proves that the reaction efficiency remains unchanged. Note that when a non-volatile analyte is routinely measured with setup # 2, the liquid flow rate has a slight effect on the signal. In the case of the nebulizer coupled to the spray chamber (setup # 2), no argon was added to the liquid flow. Therefore the results in Figure 1.14b were presumably due to the fact that, once the aerosol was produced by the nebulizer, sulfur release in the vapor phase inside the spray chamber was promoted because of the high total liquid surface. At liquid flow rates above  $8 \text{ mL min}^{-1}$ , the sulfur release seemed to be less efficient, resulting in a lower increase in the signal (Figure 1.14b). This mechanism was also confirmed when the sensitivities achieved with both setups were compared. Indeed, Figure 1.14 reveals that fairly similar line slopes were obtained in both cases. Although the best signal was obtained at a flow rate of  $9 \text{ mL min}^{-1}$ , subsequent experiments were carried out at a flow rate of  $7.7 \text{ mL min}^{-1}$ .

When using the gas separator (setup # 1), the vapor generating device had two gas inlets, one located at the reaction coil, which was used to promote the removal of  $\text{H}_2\text{S}$  from the solution, and the other placed at the gas separator, which directed the analyte

towards the plasma. Figure 1.16 shows the intensities registered for different reaction and carrier gas flow rate combinations.

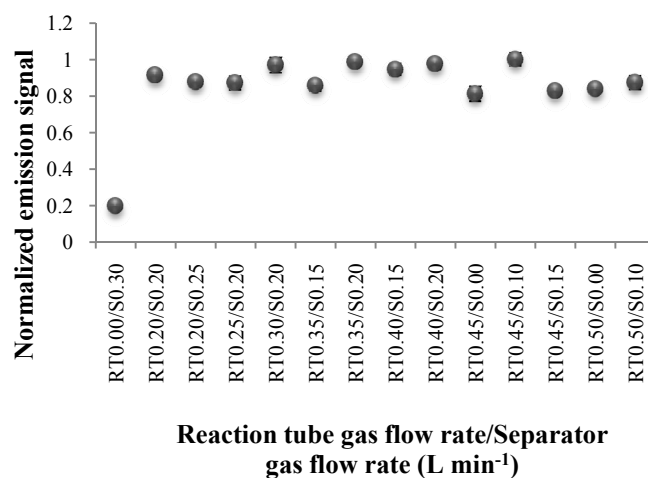


**Figure 1.16** Effect of the two streams of the vapor generator device on the sulfur emission intensity. Forward power 1330 W and sample flow rate 7.7 mL min<sup>-1</sup>.

As can be observed, all gas flow rate combinations led to similar results except when no gas was added at the reaction coil. An argon flow rate of 0.45 L min<sup>-1</sup> in the reaction coil and an argon carrier flow rate of 0.10 L min<sup>-1</sup> were selected for the remaining experiments. In the case of setup # 2, the highest signal for sulfur was obtained when the nebulizer gas flow was set at 0.45 L min<sup>-1</sup>.

Experiments were carried out under these conditions to calculate the percentage of the reaction between sulfide and hydrochloric acid in the vapor generating device. The drainage from the vapor generator's separator was collected and immediately basified. The potentiometric method was then used to determine the concentration of sulfide. The efficiency of the reaction without the gas separator was also studied by collecting and basifying the drainage from the spray chamber. In the first case, setup # 1, 9% of the initial sulfide was found in the drained solution, indicating a reaction yield of 91% (S.D. 0.43, n = 3). In the second case, setup # 2, a similar reaction efficiency was measured (92%; S.D. 0.15, n = 3).

Finally, different forward powers were also studied. As can be observed in Figure 1.17, the highest intensity was obtained at 1300 W when using the gas separating device. Although the signal intensity increased slightly at higher powers when the gas separator was removed, all subsequent experiments were carried out at this power. It is also interesting that in the case of the gas separator, the signal showed a maximum pattern as the power rose, whereas for the nebulizer/spray chamber combination the higher the RF

power, the stronger was the emission intensity. This clearly demonstrates that when a fraction of the solvent was introduced into the plasma as a liquid (Figure 1.17b) it required a higher amount of energy to excite the analyte. Nonetheless, this effect was not severe enough to cause deterioration of the results afforded by the nebulizer spray chamber combination.

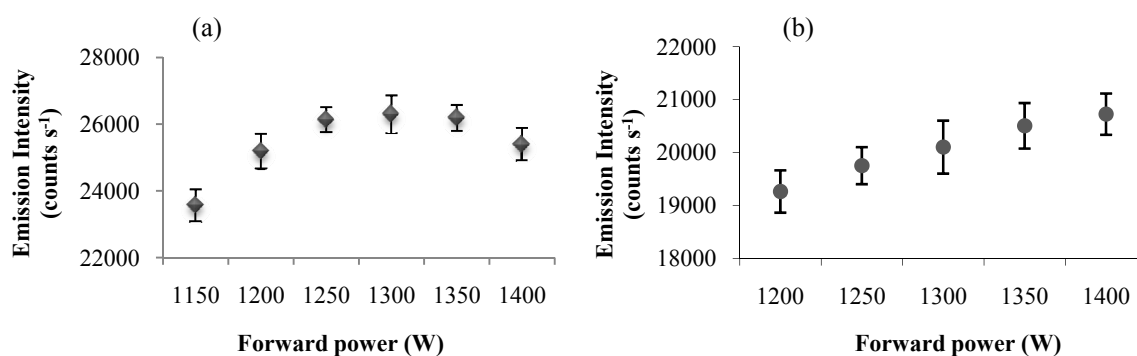


**Figure 1.17** Effect of the Forward power on the sulfur emission intensity with setup # 1 (a) and setup # 2 (b). Sample flow rate 7.7 mL min<sup>-1</sup> and nebulizer gas flow 0.45 L min<sup>-1</sup>.

### 1.3.3.3 Solvent plasma load

One potential drawback of setup # 2 was that, unlike for setup # 1, a fraction of the solvent was transported towards the plasma in liquid form. This could have induced plasma degradation. Several studies were performed to verify that the plasma did not deteriorate when switched from setup # 1 to setup # 2.

The mass of solvent that reached the plasma per unit of time ( $S_{\text{tot}}$ ) was determined under the conditions described in Section 1.2.5. It was found that 10.5 mg min<sup>-1</sup> of solvent arrived at the plasma when the gas separator was used. However, when the nebulizer/spray chamber combination was used, the mass that reached the plasma increased to 21.5 mg min<sup>-1</sup>. The results for the O-H band emission intensities at wavelengths around 309 nm shown in Figure 1.18 supported these results [1.31].

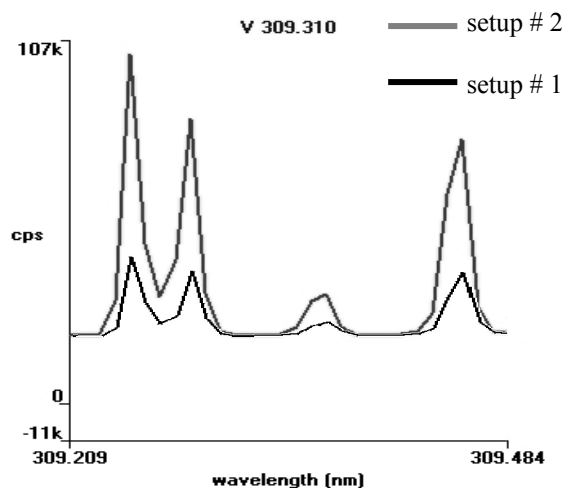


**Figure 1.18** O-H band emission intensities at wavelengths around 309 nm for both configurations setup # 1 to setup # 2.

It was found that the O-H signal was more than two times higher for setup # 2 compared to the results obtained with the gas–liquid separator (Figure 1.18). Several studies have been done on the effect of solvent on ICP-AES. They have demonstrated that the presence of a small amount of water increases electron density and enhances energy transfer in the plasma. A certain amount of water solvent is therefore useful for analyte excitation in an Ar-ICP because hydrogen can be released from the water solvent to enhance energy transfer inside the plasma without destabilizing it [1.32,1.33].

With the system based on the use of a pneumatic nebulizer coupled to the spray chamber (setup # 2), it was possible to determine the fraction of the solvent being transported towards the plasma in both liquid and vapor forms by coupling a laser diffraction system at the exit of the spray chamber. The sizer provides the so-called volume concentration, VC, which corresponds to the fraction of aerosol liquid volume in the beam measurement zone. It was possible to estimate the mass of aerosol reaching the plasma in liquid form by means of the following mathematical relationship:

$$mg\ liquid = VC a \pi r^2 t \quad (1.2)$$

where  $a$  is the width of the aerosol stream at the exit of the spray chamber (i.e., 2 mm),  $\pi r^2$  corresponds to the laser beam cross sectional area ( $r = 5$  mm) and  $t$  is the time (in seconds) that a droplet requires to go through the aerosol measurement zone. When ammonia/ammonium was the buffer used, the aerosol volume concentration was 0.12%.

By applying equation (1) it was found that the total liquid mass flow was close to  $11 \text{ mg min}^{-1}$ . We compared this value with the data corresponding to  $S_{\text{tot}}$  (c.a. 10.5 and  $21.8 \text{ mg min}^{-1}$ , with and without separator respectively) and concluded that the mass of solvent transported in liquid form corresponded to the difference between  $S_{\text{tot}}$  with and without separator. According to theoretical calculations, the mass of water that can evaporate inside the spray chamber at  $20 \text{ }^\circ\text{C}$  ranges from 20 to  $30 \text{ mg L}^{-1}$  of argon [1.34]. By taking into account the nebulizer gas flow rate used (i.e.  $0.45 \text{ L min}^{-1}$ ), the mass of water that could evaporate was within the  $9$  to  $14 \text{ mg min}^{-1}$  range. All these data were in good agreement with the  $S_{\text{tot}}$  results previously discussed.

Another potential risk of setup # 2 relates to the total mass of water delivered to the plasma. It is recognized that the water load that can be accepted by the plasma without degrading its thermal characteristics is somewhere between  $20$  and  $40 \text{ mg min}^{-1}$  [1.35]. The  $S_{\text{tot}}$  results confirmed that the use of a spray chamber did not significantly degrade the plasma with respect to the situation found when a liquid–gas separator was used.

Another interesting issue was the fineness of the aerosols reaching the plasma when sulfide was determined with setup # 2. As has already been mentioned [1.36], the droplets reaching the plasma with diameters above  $12 \text{ }\mu\text{m}$  are incompletely evaporated in the plasma observation zone. These droplets should therefore be prevented from reaching the plasma because they can degrade the sensitivity and induce signal noise increases. The characterization of the aerosols leaving the spray chamber (i.e. tertiary aerosols) revealed that the fraction of aerosol liquid volume contained in droplets above this diameter was 6.5% when only water was nebulized. When the solution contained either sodium or ammonia, this percentage dropped to 4 - 4.5%. Therefore, it can be said that introducing an aerosol into the plasma did not disturb the production of light, provided that fairly fine aerosols were introduced into the excitation cell.

As regards the different sample matrices used, it was found that tertiary aerosol characteristics did not depend on the nature of the buffer. The median of the volume drop size distributions,  $D_{50}$ , was  $4.3 \text{ }\mu\text{m}$  for sodium, ammonium, and hydrochloric matrices. This provided support for the choice of ammonium instead of sodium hydroxide as a buffer for sulfide preservation.

### 1.3.3.4 Method Performance

Calibration curves for ICP-AES developed methods, with and without a gas separator, are shown in Figure 1.19. These were obtained using a blank and seven standards in the range 10 to 500  $\mu\text{g L}^{-1}$ . The working range was increased to 25  $\text{mg L}^{-1}$  and was found to be linear up to this concentration for both methods.

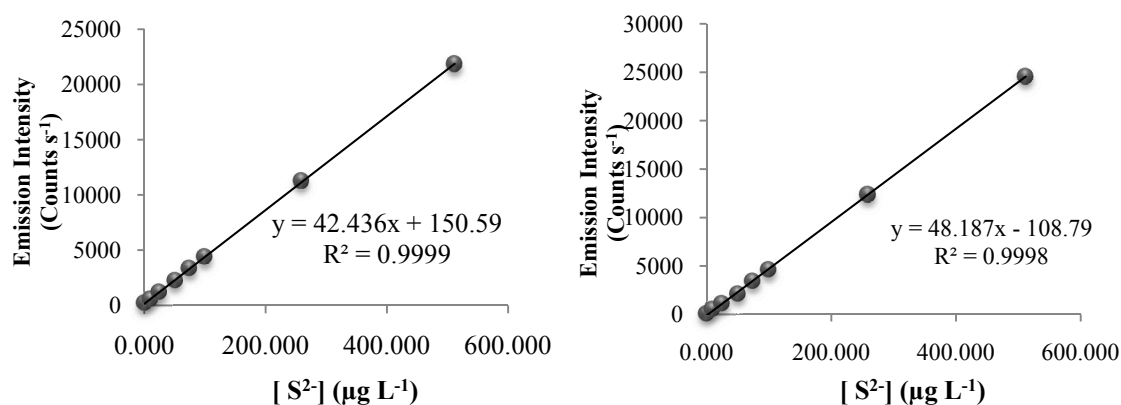


**Figure 1.19** Calibration curves for the VG-ICP-AES methods with setup # 1(a) to setup # 2 (b).

The limits of detection (LOD) were calculated as three times the standard deviation of the curve ( $S_{y/x}$ ) divided by the slope of the curve, and were found to be 5  $\mu\text{g L}^{-1}$  and 6  $\mu\text{g L}^{-1}$  respectively. The limits of quantification (LOQ) were calculated in turn as ten times the standard deviation of the curve ( $S_{y/x}$ ) divided by the slope of the curve. The respective LOQs were 17  $\mu\text{g L}^{-1}$  and 21  $\mu\text{g L}^{-1}$ . A blank and a standard of 2  $\mu\text{g L}^{-1}$  were analyzed and their emission intensities were significantly different, thus suggesting that detection of sulfide at 2  $\mu\text{g L}^{-1}$  was possible with those methods. The proposed VG-ICP-AES methods were evaluated by comparison with the well-established potentiometric method. The LOD obtained for the potentiometric method, calculated according to IUPAC as the intercept of the background signal with the ideal response function [1.30], was 20  $\mu\text{g L}^{-1}$ . The relative standard deviation (RSD), expressed as a fraction of the mean of 5 replicates of a 100  $\mu\text{g L}^{-1}$  standard, was found to be 0.8% and 1% for setup # 1 and setup # 2 respectively, while for the potentiometric method a value of 1.3% was obtained.

With setup # 2, all components of the sample reached the plasma, which means that all sulfur forms (mainly sulfate in environmental waters) contribute to the emission

intensity. Thus, real samples had to be analyzed twice: during the first measurement, the emission of sulfate was obtained by mixing ultrapure water with the sample in the reaction coil. The signal obtained was mainly due to the sulfate present in the sample, because under these circumstances, the signal for sulfide is negligible. Note that the sulfide concentration for real samples ( $\mu\text{g L}^{-1}$ ) is much lower than that for sulfate ( $\text{mg L}^{-1}$ ).

In the second measurement, hydrochloric acid was added to the reaction coil; in this case, the emission intensity corresponded to both sulfate and sulfide, due to the transformation of sulfur into  $\text{H}_2\text{S}$ . Because the second species was released from the aerosol droplets as a vapor, its transport through the spray chamber was more efficient, thus giving rise to an enhancement in the emission signal. Accordingly, a standard of  $5 \text{ mg L}^{-1}$  of sulfate and  $20 \mu\text{g L}^{-1}$  of sulfide gave an emission intensity of  $775 \text{ counts s}^{-1}$  when ultrapure water was used while the emission intensity increased to  $2465 \text{ counts s}^{-1}$  when ultrapure water was replaced by hydrochloric acid.

The emission due to sulfide was obtained from the difference of the two intensities measured:

$$I_{\text{sulfide}} = I_{\text{with acid}} - I_{\text{without acid}} = I_{\text{Sulfate+sulfide}} - I_{\text{sulfate}} \quad (1.3)$$

A number of experiments were performed to verify that sulfate standards gave the same emission intensity both in the presence and the absence of hydrochloric acid in the reaction coil. Five standards containing only sulfate and a blank were measured with and without hydrochloric acid. The results obtained for these experiments are depicted in Figure 1.20. As can be observed, the emission signal produced by sulfate was independent of the medium used in the reaction coil.

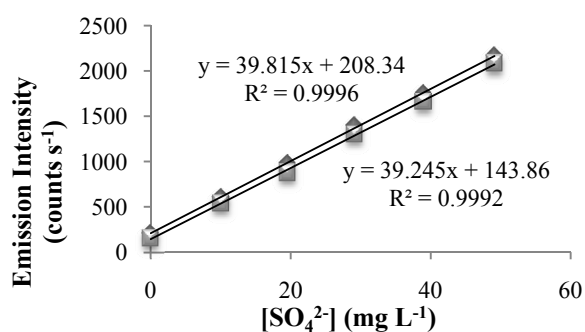


**Figure 1.20** Calibration curve for sulfate when ultrapure water (■) and hydrochloric acid (◆) are introduced in the reaction coil.



Due to the lack of S<sup>2-</sup> certified reference materials, four spiked samples with final concentrations of 25, 75, 100 and 150 µg L<sup>-1</sup> were prepared by transferring 50 mL of buffer solution, the required amount of standardized sodium sulfide, and filling up to 100 mL with bottled mineral water. Five replicates of each sample were measured with the three methods, two VG-ICP-AES methods and the potentiometric method, and results are shown in Table 1.11. Data indicates that there were no significant differences between the results obtained with the three methods for samples spiked at 75, 100 and 150 µg L<sup>-1</sup>. However, there was a slight difference between the spiked value at 25 µg L<sup>-1</sup> and the concentration found with the potentiometric method for this sample, but it must be taken into account that the detection limit for the potentiometric method is 20 µg L<sup>-1</sup> and its quantification limit is higher.

**Table 1.11.** Results obtained for spiked samples by the potentiometric and VG-ICP-AES methods.

Spiked sample	VG-ICP-AES (setup # 1)		VG-ICP-AES (setup # 2)		POTENTIOMETRIC METHOD		SPIKED VALUE µg L <sup>-1</sup>
	µg L <sup>-1</sup>	standard deviation (n = 5)	µg L <sup>-1</sup>	standard deviation (n = 5)	µg L <sup>-1</sup>	standard deviation (n = 5)	
1	22.4	0.6	28	3	19.1	0.6	24.7
2	75	3	75	4	75	3	75.8
3	101	2	114	5	111	6	102.2
4	152.3	0.4	158	2	154	1	152.0

The three methods were also used to measure eight different environmental waters collected in different pools in Alicante, Spain. The results obtained are presented in Table 1.12 with their standard deviation. As can be observed, environmental waters 6 - 8 could be analyzed by all three methods and similar results obtained. In contrast, samples 1 to 5 could not be analyzed by the potentiometric method because their concentrations were under the LOD of this method. Nevertheless, because they are sufficiently sensitive these samples could be analyzed using the newly developed VG-ICP-AES methods, and reliable results were obtained.

**Table 1.12.** Sulfide concentration in environmental waters determined by VG-ICP-AES and Potentiometric methods.

Natural Water	VG-ICP-AES (setup # 1)		VG-ICP-AES (setup # 2)		POTENTIOMETRIC METHOD	
	$\mu\text{g L}^{-1}$	standard deviation (n = 3)	$\mu\text{g L}^{-1}$	standard deviation (n = 3)	$\mu\text{g L}^{-1}$	standard deviation (n = 3)
1	9.8	0.7	13	1	<LOD	-
2	9.9	0.5	10	3	<LOD	-
3	9.3	0.5	12.1	0.9	<LOD	-
4	9.7	0.6	12.3	0.5	<LOD	-
5	10.1	0.7	11.7	0.6	<LOD	-
6	183.3	0.3	186	2	184	1
7	174.3	0.4	178	1	177	1
8	187.6	0.3	187	1	189	1

### 1.3.3.5 Sulfate and sulfide determination

As stated in the previous section, when using the nebulizer, the simultaneous determination of sulfate and sulfide is possible in natural waters when the main oxidized sulfur species is sulfate. Thus, standards containing sulfate and sulfide were prepared in ammonium buffers and analyzed by VG-ICP-AES without the gas separator. Figure 1.21 shows the calibration curves obtained for sulfate and sulfide. The first calibration curve (Figure 1.21a) was obtained when using ultrapure water in the reaction coil. The calibration curve for sulfide (Figure 1.21b) was the result of subtracting the sulfate signal emission from the signal obtained when hydrochloric acid was mixed with the standards, as described above.

The detection limit for both sulfide and sulfate was calculated as 3 times the deviation of the calibration curve divided by its slope. For sulfate, it was found to be  $1 \text{ mg L}^{-1}$ . As previously calculated, the detection limit for sulfide was found to be  $6 \mu\text{g L}^{-1}$ .

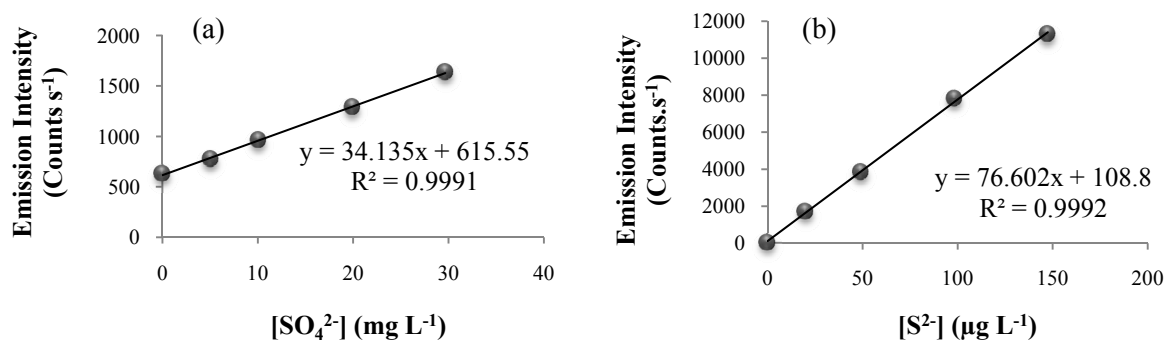


Figure 1.21 Calibration curves for sulfate and sulfide respectively.

Finally, spiked mineral water samples were analyzed also twice. The results are shown in Table 1.13. As it can be observed, in the case of sulfate, the values obtained through this methodology were in good agreement with those indicated in the label of each mineral water bottle. Furthermore, results obtained for sulfide were in concordance with the spiked values.

Table 1.13 Results obtained for spiked samples.

	SULFATE			SULFIDE		
	Label value (mg L <sup>-1</sup> )	Measured concentration (mg L <sup>-1</sup> )	Standard deviation (n = 3)	Spiked value (µg L <sup>-1</sup> )	Measured concentration (µg L <sup>-1</sup> )	Standard deviation (n = 3)
Mineral water 1	18.5	20	2	183.5	183	4
Mineral water 2	11.5	11.1	0.5	173.8	174	1
Mineral water 3	17.3	19	2	187.5	186.7	0.2

## 1.4 CONCLUSIONS

Three rapid, highly sensitive and reliable methods for the determination of low sulfide concentrations in environmental waters based on the use of ICP-QMS and ICP-AES systems have been described.

Results for the VG-ICP-QMS method showed that interfering  $O_2^+$  background ions at  $m/z$  32 could be dramatically reduced through hydrogen sulfide formation with a vapor generator and the consequent elimination of the sample solvent. In addition, the sensitivity of the method could be increased by using  $H_2$  and He gases in the

collision/reaction cell. The reliability of this method was confirmed through comparison with the results from a reference method. Lower concentrations could be determined with the VG-ICP-QMS method, which had a limit of detection of  $2 \mu\text{g L}^{-1}$ . This LOD was almost 10 times lower than that obtained with the potentiometric method.

Two methods using the ICP-AES system were also developed. The first transformed sulfide into  $\text{H}_2\text{S}$ , which was transported towards the plasma after being separated from the remaining solution in a gas-liquid separator. The second used a hydrochloric acid stream and a conventional ICP-AES liquid sample introduction system (i.e. a pneumatic concentric nebulizer coupled to a spray chamber).

The main advantage of the former system over the latter was that the plasma matrix effects were avoided, because the sample concomitants were discarded before the  $\text{H}_2\text{S}$  was introduced, as also happened with VG-ICP-QMS. In the second system, a liquid aerosol was generated and solution droplets reached the excitation cell. This had two important implications: with this assembly matrix effects were noticeable if wastewaters were being analyzed, and it was not advisable to use buffering solutions containing sodium. Fortunately, an ammonia/ammonium solution provided satisfactory results.

The advantage of the system based on the use of a nebulizer coupled to a spray chamber was that it allowed the simultaneous determination of several parameters, thus shortening the time of any eventual water analysis. This system proved to be efficient for the determination of both sulfide and sulfate concentrations. However, the system based on the use of a gas-liquid separator was only applicable to the determination of sulfide.

All methodologies provided similar sensitivities, limits of detection, and dynamic range. These analytical figures of merit were better than those provided by a conventional potentiometric method. The analysis of environmental waters and sediments demonstrated that the results obtained by the methods developed did not differ significantly from those found with a selective electrode, but lower concentration could be determined more accurately.

### 1.5 REFERENCES

- 1.1. W. Yao, F.J. Millero, Oxidation of hydrogen sulfide by hydrous Fe (III) oxides in seawater, *Mar. Chem.* 52 (1996) 1-16
- 1.2. P. Patnaik, *A Comprehensive Guide to the Hazardous Properties of Chemical Substances*, Wiley, New York, 1999
- 1.3. R. Al-Farawati, C. M. G. van den Berg, Metal-sulfide complexation in seawater, *Mar. Chem.* 63 (1999) 331-352
- 1.4. G.W. Luther, E. Tsamakis, Concentration and form of dissolved sulfide in the oxic water column of the ocean, *Mar. Chem.* 27 (1989)165-177
- 1.5. A. Bianchini, K.C. Bowles, Metal sulfides in oxygenated aquatic systems: implications for the biotic ligand model, *Comp. Biochem. Phys. C* 133 (2002) 51-64
- 1.6. <http://www.atsdr.cdc.gov/MHMI/mmg114.html#bookmark02>
- 1.7. N.S. Lawrence, J. Davis, R.G. Compton, Analytical strategies for the detection of sulfide: a review, *Talanta* 52 (2000) 771-784
- 1.8. J.S. Lee, J.H. Lee, Influence of acid volatile sulfides and simultaneously extracted metals on the bioavailability and toxicity of a mixture of sediment-associated Cd, Ni, and Zn to polychaetes *Neanthes arenaceodentata*, *Sci. Total Environ.* 338 (2005) 229-241
- 1.9. A.D. Correia, M.H. Costa, Effects of sediment geochemical properties on the toxicity of copper-spiked sediments to the marine amphipod *Gammarus locusta*, *Sci. Total Environ.* 247 (2000) 99-106
- 1.10. M.A.G.T. Van den Hoop, H.A. Den Hollander, H.N. Kerdiijk, Spatial and seasonal variations of acid volatile sulphide (AVS) and simultaneously extracted metals (SEM) in Dutch marine and freshwater sediments, *Chemosphere* 35 (1997) 2307-2313
- 1.11. M. Csuros, *Environmental sampling and analysis for technicians*, CRS Press, 1994, ISBN: 0-87371-835-6
- 1.12. Assembly of Life Sciences (U.S) Safe Drinking Water Committee, *Drinking water and health, Volume 2*, National Academy of Sciences, 1988, ISBN: 0-309-02619-9
- 1.13. Y. Cho, Y.N. Pak, Removal of OH spectral interferences from aqueous solvents in inductively coupled plasma-atomic emission spectrometry (ICP-AES) with Ar cryogenic desolvation, *Bull. Korean Chem.* 26 (2005) 1415-1420
- 1.14. B. Bouyssiere, P. Leonhard, D. Pröfrock, F. Baco, C.L. Garcia, S. Wilbur, A. Prange, Investigation of the sulfur speciation in petroleum products by capillary gas chromatography with ICP-collision cell-MS detection, *J. Anal. At. Spectrom.* 19 (2004) 700-702
- 1.15. D. Pröfrock, P. Leonhard, S. Wilbur, A. Prange, Sensitive, simultaneous determination of P, S, Cl, Br and I containing pesticides in environmental samples by GC hyphenated with collision-cell ICP-MS, *J. Anal. At. Spectrom.* 19 (2004) 623-631

- 1.16. H. Yang, S.J. Jiang, Determination of B, Si, P and S in steels by inductively coupled plasma quadrupole mass spectrometry with dynamic reaction cell, *Spectrochim. Acta, Part B: Atom. Spectrosc.* 59 (2004) 1389-1394
- 1.17. C.F. Yeh, S.J. Jiang, T.S. His, Determination of sulfur-containing amino acids by capillary electrophoresis dynamic reaction cell inductively coupled plasma mass spectrometry, *Anal. Chim. Acta* 502 (2004) 57-63
- 1.18. B.P. Jensen, C. Smith, I.D. Wilson, L. Weidolf, Directly coupled liquid chromatography with inductively coupled plasma mass spectrometry and orthogonal acceleration time-of-flight mass spectrometry for the identification of drug metabolites in urine: application to diclofenac using chlorine and sulfur detection, *Rapid Commun. Mass Spectrom.* 18 (2004) 181-183
- 1.19. P.R.D. Mason, K. Kaspers, M.J. van Bergen, Determination of sulfur isotope ratios and concentrations in water samples using ICP-MS incorporating hexapole ion optics, *J. Anal. At. Spectrom.* 14 (1999) 1067-1074
- 1.20. D. Pröfrock, P. Leonhard, A. Prange, Determination of sulfur and selected trace elements in metallothionein-like proteins using capillary electrophoresis hyphenated to inductively coupled plasma mass spectrometry with an octopole reaction cell, *Anal. Bioanal. Chem.* 377 (2003) 132-138
- 1.21. J.D. Hwang, G.D. Guenther, J.P. Diomguardi, Hydride generator system for a 1-Kw inductively coupled plasma, *Anal. Chem.* 61 (1989) 285-288
- 1.22. L.K. Olson, N.P. Vela, J.A. Caruso, Hydride generation, electrothermal vaporization and liquid chromatography as sample introduction techniques for inductively coupled plasma mass spectrometry, *Spectrochim. Acta, Part B: Atom. Spectrosc.* 50 (1995) 355-368
- 1.23. <http://www.quimica.urv.es/quimio/general/doecat.pdf>
- 1.24. G.E.P. Box, W.G. Hunter. J.S. Hunter, *Estadística para investigadores. Introducción al diseño de experimentos, análisis de datos y construcción de modelos*, Editorial Reverté, 1989, ISBN: 84-291-5041-2
- 1.25. T. Lundstedt, E. Seifert, L. Abramo, B. Thelin, A. Nyström, J. Pettersen, R. Bergman, *Chemom. and Intell. Lab. Syst.* 42 (1998) 3-40
- 1.26. D.C. Montgomery, *Diseño y análisis de experimentos*, Limusa Wiley, 2004, ISBN: 968-18-6156-6
- 1.27. J.N. Miller, J.C. Miller, *Estadística y quimiometría para químicos*, Pearson Educación S.A., 2002, ISBN: 84-205-3514-1
- 1.28. H.E. Allen, G. Fu, W. Boothman, D.M. DiToro, J.D. Mahony, Draft analytical method for determination of acid volatile sulfide in sediment, United States Environmental Protection Agency Report 821-R-91-100, 1991
- 1.29. C.E. Moore, NSRDS-NBS, 34, Office of Standard Reference Data, National Bureau of Standards, Washington, D.C., 1970
- 1.30. E. Bakker, M. Miller, E. Pretsch, Detection limit of ion-selective bulk optodes and corresponding electrodes, *Anal. Chim. Acta.* 282 (1993) 265-271
- 1.31. J.M. Mermet, in: P.W.J.M. Boumans (Ed.), *Inductively Coupled Plasma Emission Spectroscopy*, John Wiley and Sons, New York, 1987, Chapter 10

- 1.32. Y.Q. Tang, C. Trassy, Inductively coupled plasma: the role of water in axial excitation temperatures, *Spectrochim. Acta B* 41 (1986) 143-150
- 1.33. M. Huang, H. Kojima, T. Shirasaki, A. Hirabayashi, H. Koizumi, Study on solvent-loading effect on inductively coupled plasma and microwave-induced plasma sources with a microliter nebulizer, *Anal. Chim. Acta* 413 (2000) 217-222
- 1.34. J.W. Olesik, J.C. Fister III, Incompletely desolvated droplets in argon inductively coupled plasmas: their number, original size and effect on emission intensities, *Spectrochim. Acta, Part B*, 46 (1991) 851-868
- 1.35. Olesik J.W., Kinzer J.A., Harkleroad, B., Inductively coupled plasma optical emission spectrometry using nebulizers with widely different sample consumption rates, *Anal. Chem.* 66 (1994) 2022-2030
- 1.36. G. Zhu, R.F. Browner, Study of the influence of water vapour loading and interface pressure in inductively coupled plasma mass spectrometry, *J. Anal. At. Spectrom.*, 3 (1988) 781-789

## CHAPTER 2

---

**Determination of arsenic in complex aqueous samples by quadrupole inductively coupled plasma mass spectrometry. Analytical strategies to overcome spectral and non-spectral interferences**

---



The contents of this chapter were submitted in:

Journal of Analytical Atomic Spectrometry:

Colon, M., Hidalgo, M., Iglesias, M., *Correction strategies over spectral interferences for arsenic determination in aqueous samples with complex matrices by quadrupole ICP-MS*, J. Anal. At. Spectr. 24 (2009) 518-521.

Talanta:

M. Colon, M. Hidalgo, M. Iglesias, *Arsenic determination by ICP-QMS with octopole collision/reaction cell. Overcome of matrix effects under vented and pressurized cell conditions*





## 2.1 INTRODUCTION

Arsenic is a naturally occurring element present in the environment in both organic and inorganic forms. It is found in ground and surface waters as well as in many foods, and can be combined with more than 150 different elements such as copper, lead or sulfide. As a result, living organisms are continuously exposed to toxic arsenic species. It has been reported for many years that such exposure can have a variety of adverse health effects, including skin and internal cancers or cardiovascular and neurological disorders depending, principally, on its chemical form. The World Health Organization (WHO) sets a limit of  $10 \mu\text{g L}^{-1}$  on arsenic in drinking water. Inorganic forms are considered to be the more toxic arsenic species. Generally speaking, arsenic is present in the environment due to mineral dissolution, but it can also be present as a result of industrial contamination, insecticides and atmospheric deposition [2.1,2.2]. The arsenic cycle can be summarized as shown in Figure 2.1.

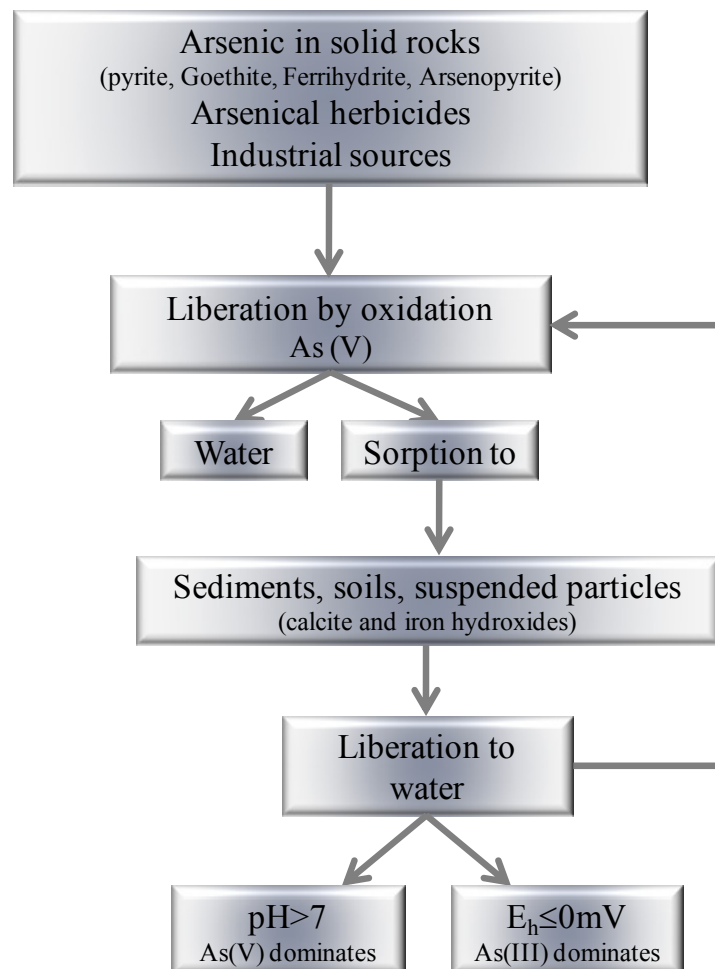


**Figure 2.1** Arsenic cycle in water [2.3].

The accurate measurement of arsenic in water requires expensive and sophisticated instrumentation. The methods usually employed for the determination of trace concentrations include spectrometric techniques and electrochemical procedures. Electrochemical techniques are applicable for the determination of As (III), so As (V) must be reduced to As (III) as the oxidized species is electrically inactive [2.4-2.6]. Some analytical techniques for arsenic determination are summarized in Figure 2.2.

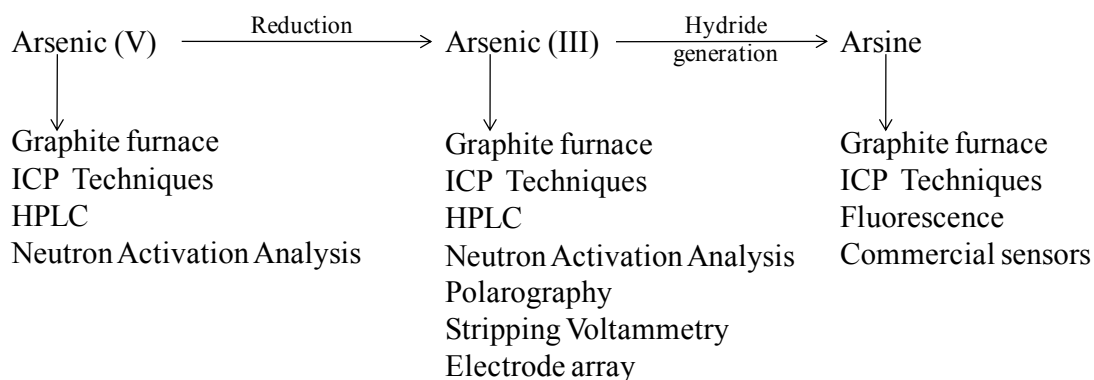


**Figure 2.2** Analytical pathways for the determination of arsenic [2.6].

### 2.1.1 Determination of arsenic by ICP-MS

Inductively coupled plasma-mass spectrometry (ICP-MS) is one of the most widely applied analytical techniques for arsenic detection. However, it is well known that the technique suffers from both spectral and non-spectral interferences. The most important drawback of quadrupole ICP-MS equipped with a direct nebulizer is probably the formation of  $^{40}\text{Ar}^{35}\text{Cl}^+$  interference obtained when moderate chloride ( $\text{mg L}^{-1}$ ) matrices are introduced in the ICP-MS. As this interference has the same mass charge ratio ( $m/z$ ) as arsenic, results can be inaccurate, especially when low levels of arsenic are being determined [2.4,2.7]. Spectral interferences can be avoided by using high resolution ICP-MS but it is an expensive technique and is not always available [2.8,2.9]. Usually, the choice of non-interfered isotopes can solve the problem since most elements have more than one isotope, but this choice is not possible when working with monoisotopic elements like arsenic. Cold plasma conditions have also been used to reduce polyatomic interferences. However, cold plasma cannot be used with elements that have high ionization potentials like arsenic [2.10,2.11]. Other efforts reported as reducing interferences include the use of mixed-gas plasma [2.12] and the separation of some

ions by the ion-exchange method before vapor generation [2.13]. The introduction of ICP-MS equipped with collision/reaction cell devices is another way to overcome problems linked with polyatomic interferences. In collision/reaction cell techniques, various gases such as H<sub>2</sub> or He or a combination of the two can be employed to eliminate argon-based polyatomic ions via chemical reactions or interactions efficiently and without affecting the analyte of interest. Another way to overcome such interference is the use of an interference equation which allows the subtraction of polyatomic interferences on the <sup>75</sup>As signal [2.14-2.17].

It is well known that matrix effects can be very important in plasma based atomic spectrometric techniques, since moderate amounts of matrix ions can significantly change the analyte signal [2.18,2.19]. Several techniques can be used to correct these matrix effects, including standard addition, isotope dilution, the use of an internal standard and the introduction of carbon-containing compounds to the samples [2.20-2.22]. Obviously, as it has only one isotope, arsenic cannot be determined by the isotope dilution technique, although some authors have described an internal standard method that adopts the isotope dilution procedure, assuming <sup>77</sup>Se as a pseudo-isotope of arsenic [2.23].

#### 2.1.1.1 Mathematical corrections

As previously pointed out, mathematical corrections can be used to avoid or correct for spectral overlaps. This procedure can be used whenever the overlapping ion signal/analyte ion signal is not too large, and isobaric corrections are typically provided in quadrupole ICP-MS software. The general mathematical strategy to correct for isobaric interferences in atomic mass spectrometry is to subtract the contribution of interfering isotopes from measurements of non-interfering ones. In the case of polyatomic interferences from two or more species in a particular mass, chemometric approaches require consideration of correction factors calculated using the natural isotope abundances of the atoms from which the interference is formed [2.24].

The US Environmental Protection Agency (EPA) proposes the following equation for arsenic correction [2.25]:

$$^{75}\text{As} = 1.000(^{75}\text{C}) - (3.127)[(^{77}\text{C}) - 0.815(^{82}\text{C})] \quad (2.1)$$

where  $^{75}\text{C}$ ,  $^{77}\text{C}$  and  $^{82}\text{C}$  are counts measured at  $m/z$  75, 77 and 82 respectively. This equation should provide a correction for chloride interference with an adjustment for  $^{77}\text{Se}$  [2.23]. Some authors consider that the contribution of krypton at  $m/z$  82 should be taken into account and have proposed a modified interference equation [2.26,2.27]:

$$^{75}\text{As} = 1.000(^{75}\text{C}) - (3.127)[(^{77}\text{C}) - 0.815(^{82}\text{C}) + 0.883(^{83}\text{C})] \quad (2.2)$$

However, in a recently published work, mass 82 showed strong spectral interferences related to bromine and/or calcium content, which would make these equations unsuitable for correction in arsenic measurements [2.28].

### **2.1.1.2 Internal standard methodology**

Internal standardization is used to correct for changes in sensitivity caused by variations in the concentration or type of matrix components found in the sample, and to correct for instrument drift. An internal standard is a non-analyte element that is added to the blank solution, standards and samples before analysis [2.29]. When using the internal standard technique, it would appear that elements of similar mass give similar signal responses because the transmission of ions to the mass spectrometer depends on the mass of the ions due to the space charge effect. This needs to be taken into account when choosing the element to be used as an internal standard. Some authors state that the ionization potential should also be taken into account [2.30-2.32].

### **2.1.1.3 Effect of carbon-containing compounds on ICP-MS**

The effect of alcohol solutions on the analyte signal in ICP-MS has been reported. The introduction of an organic solvent or a carbon-containing gas such as methane in the nebulizer gas can serve as a chemical modifier and reduce some polyatomic interferences. Signal enhancement of elements with ionization potentials in the range from 9 to 11 eV by the presence of organic solvents (1-5% (v/v) of ethanol, propanol, glycerol, butanol, acetic acid) is a well-known phenomenon in ICP-MS [2.33]. In the presence of different concentrations of organic solvents, signal enhancement factors in the range of 3 to 8 were obtained for arsenic [2.34]. This phenomenon can be attributed to the modification of the ionization equilibrium in the plasma. Some studies have concluded that the enhancement or suppression of analyte signals in the presence of carbon depends on the volatility, mass and ionization potential of the analytes as well as the ICP-MS operating conditions. It has been demonstrated that small amounts of

alcohol enhance the element signal while higher amounts reduce it due to the resultant cooling of the plasma. It is suggested that the introduction of organic compounds into the plasma results in an increased population of  $C^+$  (ionization energy 11.26 eV). The degree of ionization of the analytes is therefore improved by the transfer of electrons to carbon ions from elements with ionization energy lower than carbon [2.34]. However, this enhancement could also be attributable to the improvement in the nebulization transport of the sample and to the shift of the zone of maximum ion density in the plasma [2.33-2.44].

In this chapter, studies on the spectral and non-spectral interferences produced during arsenic determination in complex matrix aqueous samples containing high amounts of sodium and chloride, and strategies to overcome these interferences, are presented. The suitability of applying different internal standards together with approaches to overcome spectral interferences such as pressurized cell conditions and mathematical corrections are assessed. In addition, the effect of the addition of small amounts of alcohol to the samples is evaluated under both vented and pressurized cell conditions, in order to develop a simple procedure to determine arsenic in complicated matrix samples.

## 2.2 EXPERIMENTAL

### 2.2.1 Reagents and solutions

All the chemicals used were of analytical reagent grade, and aqueous solutions were prepared in ultrapure MilliQ water obtained from a Millipore system. Sodium chloride and sodium nitrate were purchased from Panreac; hydrochloric acid with low arsenic content was acquired from Fluka and Suprapur nitric acid from Merck. Ethanol was obtained from Panreac and methanol from Carlo Erba Reagents.  $1 \text{ mg L}^{-1}$  of arsenic solution was prepared by diluting the commercial  $1000 \text{ mg L}^{-1}$  solution from Teknolab A/S. Internal standard solutions were prepared by diluting the necessary amount of each  $1000 \text{ mg L}^{-1}$  element solution from Romil Ltd.

SLEW-3 and CASS-4 certified reference materials (CRM) were obtained from the National Research Council of Canada. SLEW-3 is an estuarine water with a salinity of 15‰ and  $1.36 \text{ } \mu\text{g L}^{-1}$  of arsenic while CASS-4 is a sea water with 30‰ of salinity and  $1.11 \text{ } \mu\text{g L}^{-1}$  of arsenic. Standard reference material 1643e, obtained from the National

Institute of Standards and Technology of the USA, is a synthetic fresh water with 20230  $\mu\text{g L}^{-1}$  of sodium and 59.0  $\mu\text{g L}^{-1}$  of arsenic.

### 2.2.2 Instrumentation

Instrumentation used in this work consisted of an Agilent 7500c ICP-QMS equipped with an octopole collision/reaction cell. The operating parameters are shown in Table 2.1.

**Table 2.1.** Operational parameters of ICP-MS.

PARAMETER	
Plasma potential	1500W
Nebulizer gas flow rate	0.9 L min <sup>-1</sup>
Octopole potential	-14 V
Quadrupole potential	-13 V
Nebulizer	Babington
Nebulizer spray chamber	Scott type double path
Torch	Fassel (Quarz)
Sampling and skimmer cones	Nickel
Collision/reaction gases	He and H <sub>2</sub>

Some other parameters were optimized daily in terms of sensitivity and precision. The oxide level was observed to be a critical value and was therefore maintained under 1 and 3% in vented and pressurized cell conditions, respectively.

### 2.2.3 Effect of collision/reaction gases flow rates

To evaluate this effect, different solutions in 2% HNO<sub>3</sub> with an increasing concentration of chloride coming from HCl were prepared. A solution containing 2  $\mu\text{g L}^{-1}$  of arsenic and a blank in 2% HNO<sub>3</sub> were also prepared.

Two ramps with hydrogen flow rates from 0 to 3 mL min<sup>-1</sup> were applied for each solution. The first ramp was developed without helium gas in the collision/reaction cell, while for the second ramp a 0.5 mL min<sup>-1</sup> He flow rate was set.

### 2.2.4 Interference equation evaluation

In order to evaluate the interference equation used by Brown et al. [2.27], five arsenic solutions with 2% of HNO<sub>3</sub> were analyzed by ICP-MS with and without pressuring the collision/reaction cell. m/z 75, 77, 79, 81, 82 and 83 were determined in both cases for each solution. These solutions consisted of one blank (MilliQ water with 2% HNO<sub>3</sub>), a second solution containing 15000 mg L<sup>-1</sup> of Cl<sup>-</sup> coming from HCl, and a third solution obtained by diluting the necessary amount of NaCl to get 15000 mg L<sup>-1</sup> of Cl<sup>-</sup>, which gave 9800 mg L<sup>-1</sup> of Na<sup>+</sup>. A fourth solution contained the necessary amount of NaNO<sub>3</sub> up to 9800 mg L<sup>-1</sup> of Na<sup>+</sup>. The last solution contained the same amount of HCl and NaNO<sub>3</sub> as the second and fourth solutions respectively.

### 2.2.5 Alcohol effect on m/z signal

Two sets of experiments were carried out at this point to evaluate the effect of alcohol on the <sup>75</sup>As<sup>+</sup> and <sup>40</sup>Ar<sup>35</sup>Cl<sup>+</sup> signals.

For the first set of experiments, solutions containing 10 µg L<sup>-1</sup> of arsenic, 5000 mg L<sup>-1</sup> of Na<sup>+</sup> and 2% HNO<sub>3</sub> were prepared with different amounts of methanol or ethanol. Signals at m/z 75 were determined in these samples at different nebulizer gas flow rates, both with and without pressurizing the collision/reaction cell.

The second set of samples consisted of solutions containing 5000 mg L<sup>-1</sup> of Na<sup>+</sup> and 2% HNO<sub>3</sub>. HCl was added to each sample to obtain four sets of three samples with 5000, 10000, 15000 and 20000 mg L<sup>-1</sup> of Cl<sup>-</sup> in each set. In one of the samples of each set, 4% of methanol was added, while a second sample was spiked with 4% of ethanol and the third sample was not modified. The signal at m/z 75 produced by <sup>40</sup>Ar<sup>35</sup>Cl<sup>+</sup> was determined in these samples with and without pressurizing the collision/reaction cell.

### 2.2.6 Internal standard studies

Solutions containing increasing concentrations of Na<sup>+</sup> were prepared from NaNO<sub>3</sub>. The necessary amounts of As, Ga, Ge, Y, Rh, Ir, Pt, Au and Tl standard solutions were added to each solution to obtain 2 µg L<sup>-1</sup> of each element. Three sets of solutions were prepared in water, 4% ethanol and 4% methanol. Element intensities were measured with and without pressurizing the collision/reaction cell.



### 2.2.7 Sample preparation

Four synthetic samples were prepared in HCl and NaCl solutions containing 10000 mg L<sup>-1</sup> of chloride. For each medium, two aliquots were spiked with rhodium and arsenic to concentrations of 8 and 2 µg L<sup>-1</sup> respectively. Four additional samples were prepared in the same way but with the addition of 10 µg L<sup>-1</sup> of selenium. All the samples were acidified with HNO<sub>3</sub> to 2% of acid. This set of samples was analyzed twice under both vented and pressurized cell conditions. The same set of samples was also prepared in 4% of ethanol and analyzed by ICP-MS twice (with vented and pressurized cells).

Arsenic was determined in three different certified reference materials: CASS-4, SLEW-3 and 1643e. For this purpose, 4 mL of each sample (0.5 mL for 1643e) was spiked with rhodium as an internal standard; Suprapur HNO<sub>3</sub> was also added until an acidity of 2% was reached. Finally, MilliQ water was added to a final volume of 5 mL, and the samples were analyzed by ICP-MS with and without pressurizing the collision/reaction cell. The same procedure was applied to these CRM but adding 4% of ethanol.

Four real samples collected in an abandoned mining area of Cartagena in the Spanish region of Murcia were analyzed to determine arsenic in pressurized cell mode with rhodium as an internal standard, and in the presence and absence of 4% of ethanol.

Four ground waters, collected in the Pannonian Basin, Romania were diluted or remixed by EAWAG (Swiss Federal Institute of Aquatic Science and Technology) to obtain samples with varying element concentrations. Arsenic was determined in those waters in order to participate in the ARS-Interlaboratory program [2.45].

## 2.3 RESULTS AND DISCUSSION

### 2.3.1 Effect of collision/reaction gas flow rates

It is well known that collision/reaction cell devices can be used to reduce spectral polyatomic interferences such as <sup>40</sup>Ar<sup>35</sup>Cl<sup>+</sup>. In such systems, background and analytical signals are affected by the flow rates of collision/reaction gases, thus making it necessary to study these flow rates. As helium is recommended by manufacturers as a collision gas for arsenic determination, it was introduced in the collision/reaction cell at different flow rates varying from 0 to 2 mL min<sup>-1</sup>. The signal at m/z 75 produced by

5000 and 15000 mg L<sup>-1</sup> of chloride solution was always higher than the signal produced by 2 µg L<sup>-1</sup> of arsenic at the same mass-to-charge ratio, demonstrating that the use of helium alone at the collision/reaction cell was not enough to eliminate <sup>40</sup>Ar<sup>35</sup>Cl<sup>+</sup> interference. In light of this, studies including H<sub>2</sub> as a collision/reaction gas were carried out. When no He was introduced in the collision/reaction cell and the H<sub>2</sub> flow rate varied between 0 and 5 mL min<sup>-1</sup>, both interference and analyte signals decreased with an increasing gas flow rate, but in no case was the analyte signal higher than the interference signal. As can be seen in Figure 2.3, when the He flow rate was fixed at 0.5 mL min<sup>-1</sup> and the H<sub>2</sub> flow rate was varied from 0 to 5 mL min<sup>-1</sup>, the interference and analyte signals showed a similar trend. However, between 2 and 3 mL min<sup>-1</sup> of H<sub>2</sub> the arsenic signal was higher than the interference signal and at 2.9 mL min<sup>-1</sup> the interference signal was near the background while the analyte signal for 2 µg L<sup>-1</sup> of arsenic was ten times higher. Thus, flow rates of 0.5 and 2.9 mL min<sup>-1</sup> for He and H<sub>2</sub> respectively were found to give the largest difference between the interference and analyte signals and were used in subsequent experiments, which included the pressurization of the collision/reaction cell. These results are in good agreement with those obtained by Darrouzès et al. [2.16]. In their study, similar gas flow rates gave maximum SBR value for m/z 75 in a 1 g L<sup>-1</sup> NaCl solution.

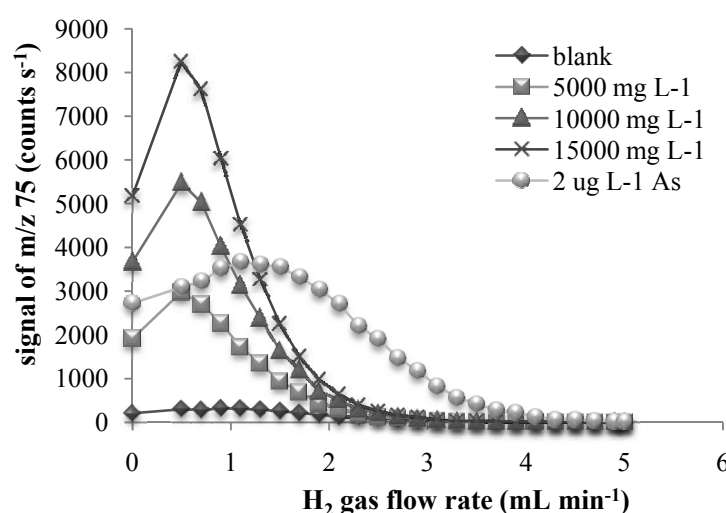
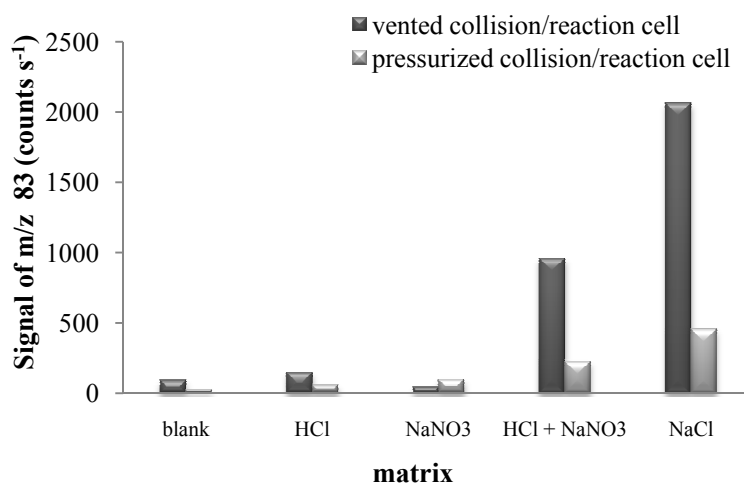


Figure 2.3 H<sub>2</sub> gas flow effect on interference and analyte signals. He was set at 0.5 mL min<sup>-1</sup>.

### 2.3.2 Interference equation evaluation

Contributions from  $^{40}\text{Ar}^{35}\text{Cl}^+$  interference can be corrected by arithmetic means. This type of correction relies on the use of the natural isotopic abundances of chlorine to remove the portion of the  $m/z$  75 peak which is due to  $^{40}\text{Ar}^{35}\text{Cl}^+$ , by measuring the intensity of the  $m/z$  77 ( $^{40}\text{Ar}^{37}\text{Cl}^+$ ) peak, after correcting it for the presence of any selenium and, in turn, krypton [2.27].

In order to evaluate this interference equation, five solutions were prepared as described in Section 2.2.4 and  $m/z$  75, 77, 79, 81, 82 and 83 were monitored. When no gas was added in the collision/reaction cell, it was observed that the signal for  $m/z$  83 was extremely high when  $\text{Na}^+$  and  $\text{Cl}^-$  were both present, while almost negligible for solutions containing just one of these ions. This could be due to the possible formation of polyatomic interference  $^{23}\text{Na}^{23}\text{Na}^{37}\text{Cl}^+$ . However, when the collision/reaction cell was pressurized, the signal for  $m/z$  83 decreased in all cases. These results are shown in Figure 2.4 and demonstrate the need to avoid the correction factor of  $m/z$  83 in the interference equation, as it induced an error.



**Figure 2.4** Signal for  $m/z$  83 in different solutions containing  $\text{Cl}^-$ ,  $\text{Na}^+$  or a combination of both when collision/reaction cell was or was not pressurized with He and  $\text{H}_2$ .

When  $m/z$  82 was monitored, the signal was similar to blank when no gas was added in the collision/reaction cell, and a little higher for HCl solution. However, when the collision/reaction cell was pressurized with helium and hydrogen, a significant increase in the  $m/z$  82 signal was observed in those solutions containing  $\text{Cl}^-$  anion. This effect can be observed in Figure 2.5. It seems that this enhancement is due to the formation of

$^{81}\text{Br}^1\text{H}^+$  in the collision/reaction cell, as bromide is commonly present together with chloride. The presence of bromide was confirmed by measuring the signal at  $m/z$  79 and 81 and calculating the isotope ratio. Thus, the correction factor of  $m/z$  82 should not be used in the interference equation when the collision/reaction cell is pressurized. Alternatively, under these conditions the correction for selenium could be done by using the isotope 78, which suffers from  $^{40}\text{Ar}^{38}\text{Ar}^+$  interference which is practically eliminated under pressurized collision/reaction cell conditions. It was observed that, when pressuring the collision/reaction cell, the signal at  $m/z$  78 was not significant in a solution containing  $15000\text{ mg L}^{-1}$  of chloride coming from NaCl or HCl.

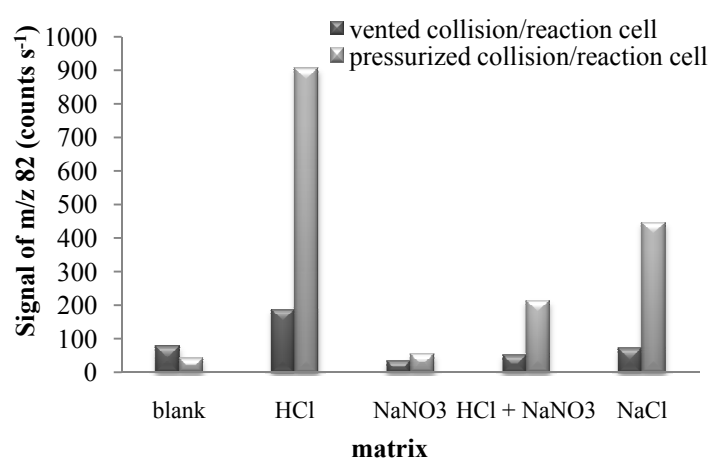


**Figure 2.5** Effect of pressurized collision/reaction cell on  $m/z$  82 signal.

### 2.3.3 Effect of alcohol on the $m/z$ signal

Solutions containing 2% of  $\text{HNO}_3$ ,  $10\text{ }\mu\text{g L}^{-1}$  of arsenic,  $5000\text{ mg L}^{-1}$  of sodium and different percentages of methanol and ethanol were analyzed by using the routine ICP-MS conditions presented in Table 2.1. In Figure 2.6, it can be observed that the signal produced by  $^{75}\text{As}^+$  in those conditions is higher when alcohol is added to the solution, and also that this enhancement is greater in 4% than in 2% of alcohol for both methanol and ethanol.

Some authors have reported that the introduction of small amounts of alcohol (1% of methanol) enhances the analyte signal, whereas higher amounts produce a local cooling effect in the central channel of the plasma that suppresses some analyte signals. Results obtained in these experiments could indicate that the signal enhancement of  $^{75}\text{As}$  is due to a charge transfer reaction between positively charged carbon species and  $^{75}\text{As}$  in the

central channel of the plasma, as some investigators have already observed [2.39,2.43]. It is well known that the position of the zone of maximum  $M^+$  density in the central channel of the ICP depends strongly on the nebulizer gas flow rate [2.39,2.40]. Thus, an optimization of the nebulizer gas flow rate is required. Figure 2.6 illustrates the variation in signal intensity as a function of nebulizer gas flow rate in 2%  $\text{HNO}_3$ , 2-4% methanol and 2-4% ethanol. As depicted in the figure, for all solutions and in both cases, with and without pressurization of the collision/reaction cell, the maximum signal intensity obtained was around  $0.9 \text{ L min}^{-1}$ . Subsequent experiments were therefore carried out using a fix nebulizer gas flow rate of  $0.9 \text{ L min}^{-1}$ .

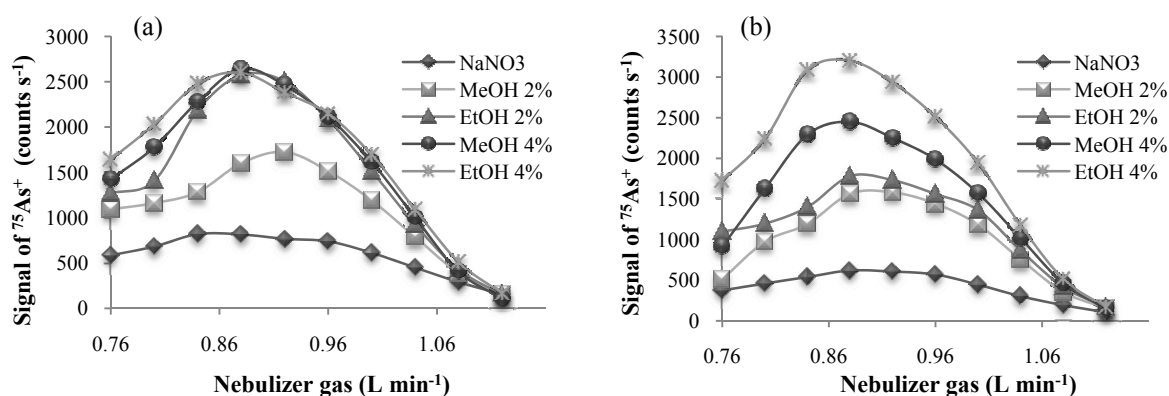


**Figure 2.6** Signal intensities as a function of nebulizer gas flow rate in different percentages of methanol and ethanol using a vented cell (a) and a pressurized cell (b).

When comparing results under vented and pressurized cell conditions, an even greater increase in signal intensity under pressurized cell conditions is seen. This greater increase, which is between 30 and a 60% higher, has been confirmed on different days and at different initial signal intensities. This behavior shows that the presence of alcohol promotes another effect, apart from the charge transfer reaction, that leads to a higher transition of  $^{75}\text{As}^+$  ions in the pressurized cell. This effect could be related with the kinetic energy of the ions reaching the cell.

It has also been reported that the introduction of small amounts of alcohol to the sample solution reduces the formation of  $^{40}\text{Ar}^{35}\text{Cl}^+$  interference. This suppression is mainly attributed to the competitive formation of carbides with Ar or Cl or both [2.41]. The effect of 4% of methanol and ethanol on the  $^{40}\text{Ar}^{35}\text{Cl}^+$  signal in solutions containing different amounts of chloride and a fixed amount of sodium is depicted in Figure 2.7.

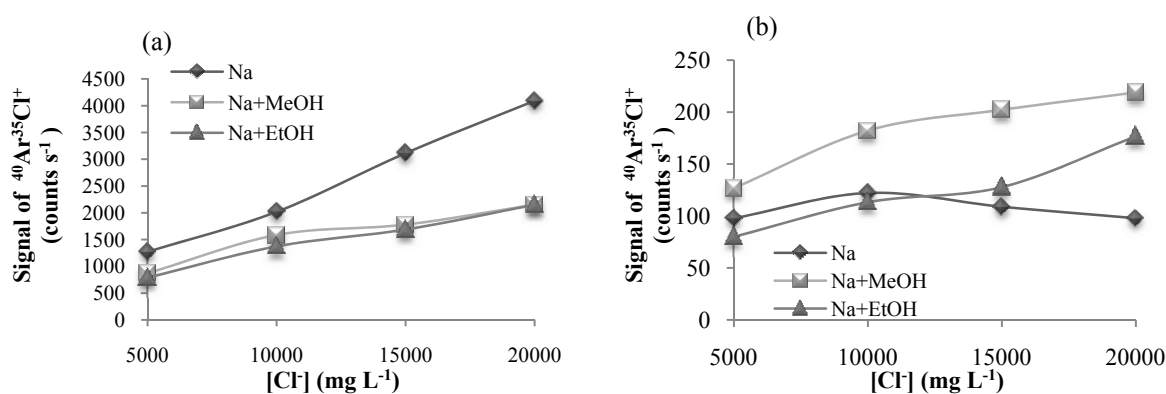


**Figure 2.7**  $^{40}\text{Ar}^{35}\text{Cl}^+$  interferences as a function of  $\text{Cl}^-$  concentration coming from  $\text{HCl}$  in  $5000 \text{ mg L}^{-1}$  of  $\text{Na}^+$  solution and 4% of alcohol with a vented cell (a) and a pressurized cell (b).

As expected, when no gas is introduced in the collision/reaction cell, a decrease in  $^{40}\text{Ar}^{35}\text{Cl}^+$  signal intensity is observed when alcohol is added to the sample solutions. Moreover, it can be seen that this suppression is more noticeable in higher chloride concentrations. In contrast, when  $\text{He}$  and  $\text{H}_2$  are introduced in the collision/reaction cell, the formation of  $^{40}\text{Ar}^{35}\text{Cl}^+$  seems to be similar in both the presence and the absence of alcohol in the sample solutions. However, the signal under these conditions is much lower than the signal obtained when no gas is added to the collision/reaction cell, and cannot be attributed with certainty to  $^{40}\text{Ar}^{35}\text{Cl}^+$ .

Calibration curves have been obtained under four experimental conditions using vented and pressurized cell conditions and in each case using standards with and without a 4% ethanol addition. The more important features of these calibration curves have been summarized in Table 2.2. A clear increase in the sensitivity was observed when ethanol-containing standards were used under both vented and pressurized cell conditions (around 4 times higher) and the sensitivity decreases when using a pressurized cell. Although the addition of ethanol does not improve the limit of detection when using a vented cell, a substantial improvement can be observed under pressurized cell conditions.

**Table 2.2.** Figures of merit of calibration curves using rhodium as an internal standard.

	VENTED CELL		PRESSURIZED CELL	
	Without ethanol	With ethanol	Without ethanol	With ethanol
<b>Slope</b>	0.0827	0.3266	0.05878	0.2505
<b>r</b>	0.9999	0.9998	0.9988	0.9999
<b>LOD (<math>\mu\text{g L}^{-1}</math>)</b>	0.2	0.3	0.7	0.2

### 2.3.4 Internal standard evaluation

The internal standard method has been widely used in ICP-MS to correct for signal drifts and for matrix effects. However there are some factors that have limited the applicability and accuracy of the internal standard method: the internal standard should not be present in the sample at all or only at a negligible amount and the internal standard signal should behave almost in the same manner as the analyte signal in different matrix conditions [2.23].

Eight elements were studied as internal standards for arsenic. The internal standards selected were gallium, germanium, yttrium, rhodium, iridium, platinum, gold and thallium; their elemental mass and ionization potential are described in Table 2.3.

**Table 2.3.** Mass and ionization potential of different isotopes used as internal standards.

ELEMENT	ISOTOPE MASS	IONIZATION POTENTIAL
<b>Ga</b>	69	5.999
<b>Tl</b>	205	6.108
<b>Y</b>	89	6.217
<b>Rh</b>	103	7.459
<b>Ge</b>	72	7.620
<b>Pt</b>	195	8.959
<b>Ir</b>	192	8.967
<b>Au</b>	197	9.226
<b>As</b>	75	9.789

Yttrium and rhodium are two elements commonly used as internal standards in ICP-MS as they both have mid-range masses and ionization potentials. Some authors assert that atomic mass is the most important factor to take into account when choosing an internal standard and that this should be near to the analyte mass [2.32]. However, as some investigators have pointed out, ionization in the plasma depends directly on the ionization potential, so the ionization potential also needs to be considered [2.30]. Germanium and gallium were studied because they are similar in mass to arsenic while iridium, platinum and gold were chosen because they are similar to arsenic in terms of ionization potential. Thallium was included in the internal standard studies because it has a similar ionization potential to yttrium and its mass is similar to those of iridium, platinum and gold.

In Figure 2.8, the signal of each element in different concentrations of sodium (from 5000 to 20000 mg L<sup>-1</sup>) has been normalized by the signal of the element in the absence of sodium, and divided by the normalized arsenic signal, to show which element behaves most similarly to arsenic in the presence of sodium. The signal of arsenic at different concentrations of sodium divided by the signal of this element in the absence of sodium has also been included to make clear the effect of sodium on this element.



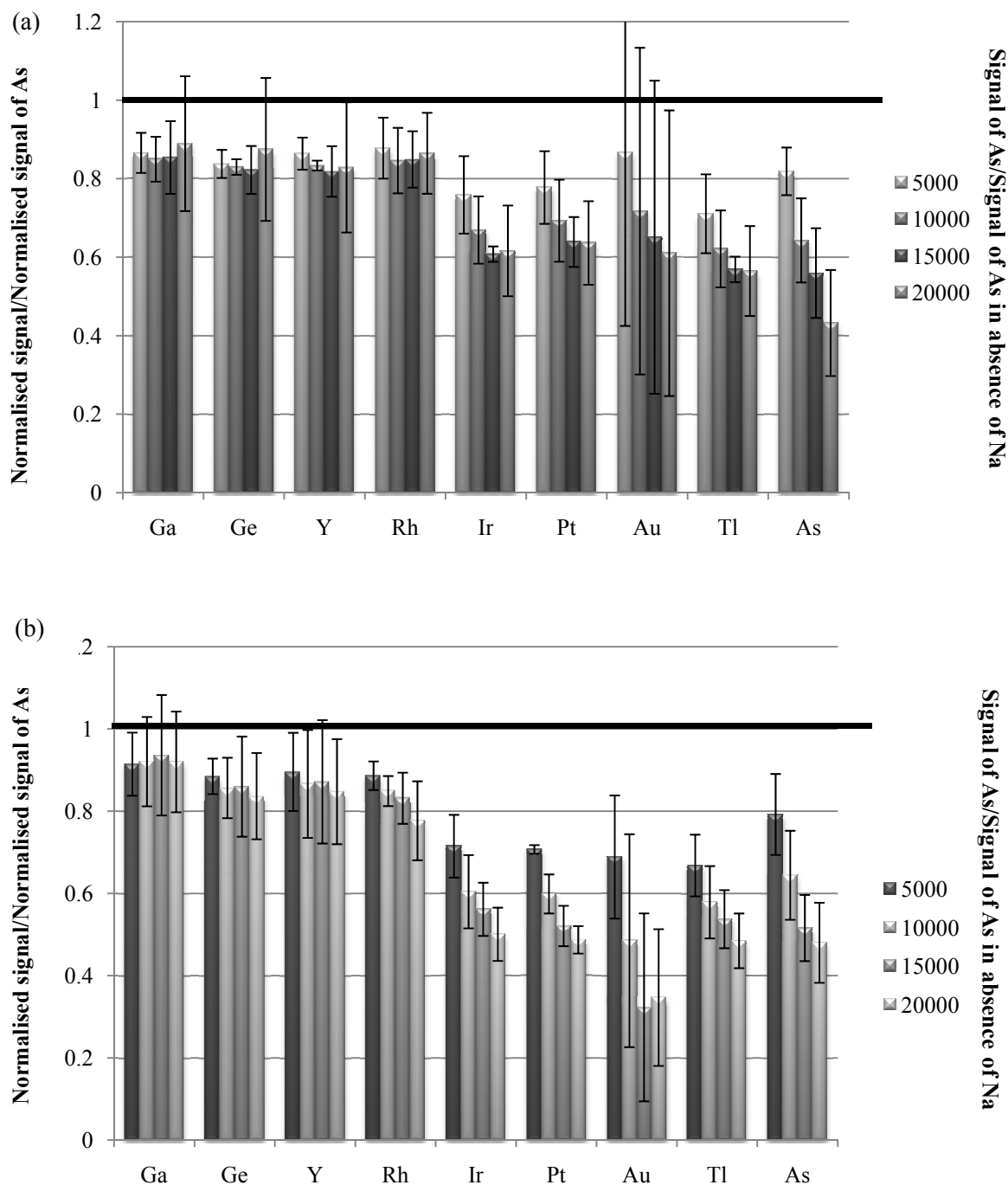


**Figure 2.8** Element signal at different concentration of sodium normalized by the element signal in absence of sodium and divided by normalized arsenic signal in both absence (a) and presence (b) of ethanol.

As can be observed, the presence of different amounts of sodium can reduce the arsenic signal, in some cases by more than 50%. This demonstrates that the use of an internal standard is required. In Figure 2.8, light isotopes with low atomic mass (gallium,

germanium, yttrium and rhodium) behave more similarly to arsenic than heavy ones in the presence of different amounts of sodium under pressurized cell conditions. When 4% of ethanol is added to all solutions the difference between light and heavy elements is even clearer. Moreover, ionization potential does not seem to have an effect, as the behavior of thallium is similar to that of iridium and platinum, which have the most similar ionization potentials to arsenic. These results could lead to the conclusion that gallium, germanium, yttrium and rhodium would be suitable internal standards for arsenic determination. However, it should be taken into account that while yttrium and rhodium are rare elements, gallium and germanium, though in trace concentrations, are present in natural samples. Vented cell conditions give similar results to those observed with the addition of gas in the collision cell.

Based on these results and taking into account its more constant behavior under the different conditions studied (lower S.D. values have been calculated), and the fact that it is usually absent in most matrices, rhodium was used as the internal standard in subsequent experiments.

It should be mentioned that the effect of alcohol, either methanol or ethanol, on the 8 elements studied is very similar, with signal increases around 30-60% and with no relation to either ionization potential or atomic mass, which is in contrast to the results obtained by Hu et al. [2.39]. However, the increase produced in the arsenic signal is around 300-400 %. The charge transfer reaction of the  $C^+$  species to analyte does not totally explain this behavior.

### 2.3.5 Analysis of spiked samples, CRM and real samples

Spiked samples containing selenium, described in Section 2.2.8, were analyzed by ICP-MS twice, under both vented and pressurized cell conditions. The results for these samples are depicted in Figure 2.9. When the collision/reaction cell was not pressurized, the interference equation was required as the amount of  $^{40}\text{Ar}^{35}\text{Cl}^+$  was considerable. The interference equation used in this work took into account signals given by m/z 77 and m/z 82.

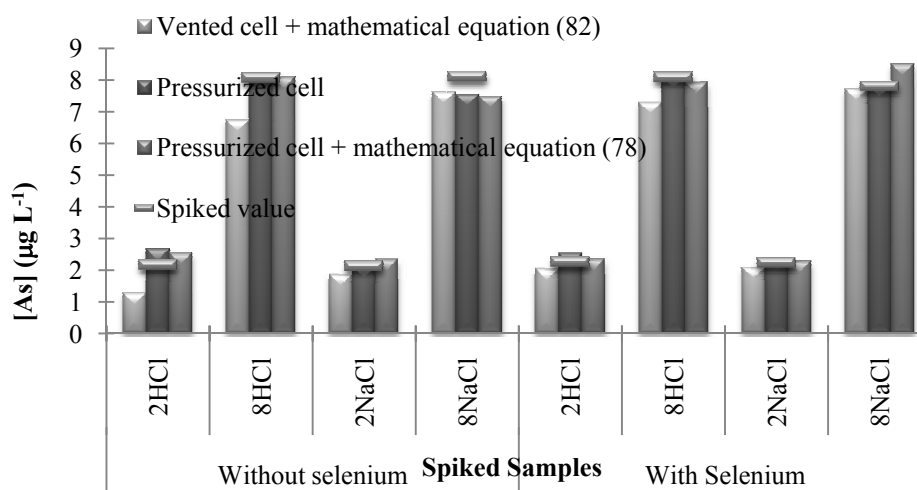


**Figure 2.9.** Arsenic concentration found in spike samples containing 10000 mg L<sup>-1</sup> of chloride coming from HCl or NaCl.

In this case, the recoveries ranged from 59 to 99%. When the collision/reaction cell was pressurized the polyatomic interference was expected to be negligible, so the interference equation was not necessary, and recoveries from 93 to 123% were obtained. However, the values obtained using the interference equation proposed in Section 2.3.2 were also calculated. As can be observed, little improvement in the results was obtained with the proposed correction at low arsenic concentration levels. The recoveries obtained in this case ranged from 92 to 117%.

Spiked samples containing ethanol were also measured twice, with vented and pressurized cell conditions, and it was necessary to correct for  $m/z$  77 and  $m/z$  82 when the collision/reaction cell was vented. As can be observed in Figure 2.10, the results obtained when 4% of ethanol was added were usually more accurate than the results obtained without any alcohol. This effect could be related to the fact that in the presence of small amounts of alcohol, the analyte signal is enhanced while the interference formation in the plasma decreases. It is also possible that the significant matrix effect produced by ethanol, which is corrected thanks to the standards being prepared with the same alcohol content, minimizes other possible matrix effects.

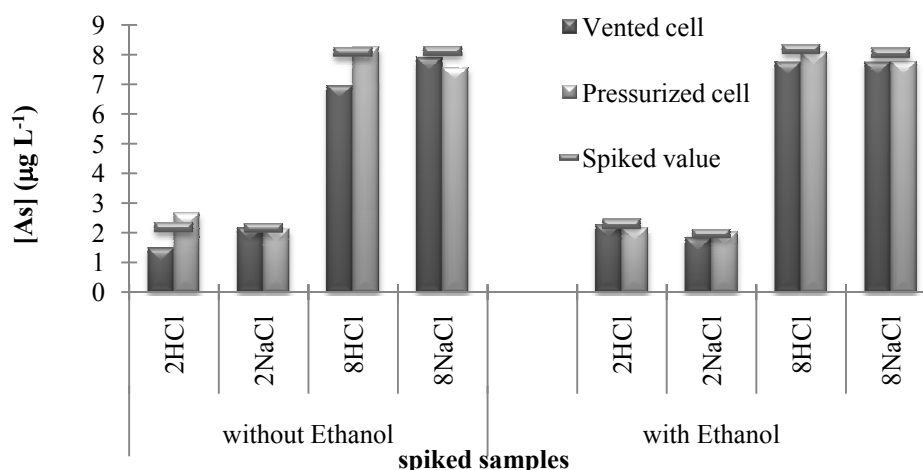


**Figure 2.10.** Arsenic concentration found in spiked samples containing  $10000 \text{ mg L}^{-1}$  of chloride coming from HCl or NaCl with and without addition of 4% ethanol and using rhodium as the internal standard.

Table 2.4 displays the determined concentration of arsenic in three CRM (CASS-4, SLEW-3 and 1643e) with associated specific uncertainty.

**Table 2.4.** Arsenic concentration ( $\mu\text{g L}^{-1}$ ) in certified reference materials using rhodium as internal standard.

	VENTED CELL				PRESSURIZED CELL				CERTIFIED VALUE	
	Without ethanol		With ethanol		Without ethanol		With ethanol		[As]	SD
	[As]	SD	[As]	SD	[As]	SD	[As]	SD		
<b>CASS-4</b>	19.7	0.7	5.1	0.1	1.0	0.1	1.08	0.03	1.1	0.2
<b>SLEW-3</b>	11.5	0.8	3.30	0.03	1.2	0.2	1.48	0.08	1.36	0.09
<b>1643e</b>	52.1	0.8	52.7	0.7	49.0	0.6	52.9	0.1	59.0	0.7

As can be observed, the results obtained when using a vented cell were far more different from the certified value than when a pressurized cell was used, demonstrating that the interference equation does not usually work properly in real samples where the matrix is quite complex. However, the use of 4% of ethanol resulted in a decrease in interference formation in the plasma, as has been previously demonstrated, and, as a consequence, gave more accurate results. On the other hand, when the collision/reaction cell was pressurized, the results obtained for arsenic determination in CRM were in good agreement with the certified value, and were very similar when a 4% ethanol

solution was used. This confirms the absence of spectral polyatomic interferences that decrease in the presence of ethanol.

It should be pointed out that the interference equation proposed in section 2.3.2, which uses the isotope 78 to correct the signal originated from selenium over the mass 77, has also been tested with spiked and CRM samples. Using this equation no differences have been observed with the results obtained when ethanol solutions are used. However, when no ethanol was added, calculated concentrations slightly differed from certified values.

According to results obtained with spiked samples and CRM, four real samples were analyzed in pressurized cell mode with and without ethanol addition and using rhodium as the internal standard. The results are shown in Table 2.5, which also shows the concentrations of chloride and sodium. In a similar way for as the CRM, there is good agreement with the results obtained with and without ethanol, indicating the absence of spectral interferences. Even though in these samples the sensitivity and limit of detection are good enough without ethanol addition, it should be taken into account that some improvement can be obtained when using a 4% ethanol addition in samples and standards.

**Table 2.5.** Arsenic concentration ( $\mu\text{g L}^{-1}$ ) determined in real samples with pressurized cell conditions and rhodium as an internal standard.

	WITHOUT ETHANOL		WITH ETHANOL	
	Average	SD	Average	SD
<b>Site 1</b>	5.5	0.1	4.5	0.1
<b>Site 2</b>	22.1	0.5	20.8	0.3
<b>Site 3</b>	671	9	660	10
<b>Site 4</b>	10400	200	10100	300

Finally, arsenic was determined in samples from annual intercalibration exercise organized by EAWAG [2.45]. The samples (ARS 29-32) were prepared from natural groundwater collected on 03 April 2009 in the Pannonian Basin, Romania and were analyzed by 33 laboratories. The results obtained, together with the indicative values, are summarized in Table 2.6. As can be observed good agreements have been obtained with the indicative values provided by the organisation.

**Table 2.6.** Arsenic concentration ( $\mu\text{g L}^{-1}$ ) determined in ARS using pressurized cell conditions and rhodium as an internal standard.

	WITHOUT ETHANOL		WITH ETHANOL		INDICATIVE VALUES	
	Average	SD	Average	SD	Average	SD
<b>ARS 29</b>	60.3	0.2	60	1	66	7
<b>ARS 30</b>	24.2	0.3	24.3	0.1	28	3
<b>ARS 31</b>	168	2	169	3	185	15
<b>ARS 32</b>	296.9	0.5	292	3	330	26

## 2.4 CONCLUSIONS

A study has been conducted for the accurate determination of arsenic by ICP-MS in complex matrix aqueous samples. The effect of using a pressurized collision/reaction cell together with other strategies to overcome matrix effects has been evaluated.

Octopole collision/reaction cell gas flow rates were adjusted to remove  $^{40}\text{Ar}^{35}\text{Cl}^+$  interference at flow rates of  $2.9 \text{ mL min}^{-1}$  of  $\text{H}_2$  and  $0.5 \text{ mL min}^{-1}$  of He.

The interference equation proposed by USEPA for arsenic determination, Method 200.8, was studied under complex matrix conditions containing high amounts of chloride and sodium. This equation behaved well with spiked samples under vented cell conditions. However, with a pressurized cell, this equation can not be used due to the formation of  $^{81}\text{Br}^1\text{H}$  which interferes with the  $^{82}\text{Se}$  signal, and a modification of the equation has been proposed when pressurized cell conditions are used. Studies carried out in the presence of selenium seem to show a small improvement when the proposed mathematical correction is used.

The presence of different amounts of alcohols enhances the intensity of arsenic at the same time as the formation of polyatomic interferences decreases in the plasma. This enhancement depends on the nebulizer gas flow rate and is more noticeable under pressurized cell conditions. This indicates that the presence of alcohol promotes an effect that leads to a higher transition of  $^{75}\text{As}$  ions in the pressurized cell.

It was found that elements with similar atomic mass behave more similarly to arsenic than elements with similar ionization potential, in the presence of different amounts of sodium and under different experimental conditions, such as the use of pressurized

collision/reaction cells and the addition of carbon containing compounds. Therefore, elements with similar mass can be used as internal standards if they are not present in the samples.

The results obtained in spiked aqueous samples and certified reference materials show that alcohol addition slightly improves accuracy and precision under pressurized collision/reaction cell conditions. Moreover, a comparison of the results obtained with and without alcohol addition can be used to verify the absence of spectral interferences. Good results have been obtained when applying this methodology in an intercalibration exercise.

**2.5 REFERENCES**

- 2.1. T.S. Choong, T.G. Chuah, Y. Robiah, F.L.G. Koay, I. Azni, Arsenic toxicity, health hazards and removal techniques from water: an overview, *Desalination* 217 (2007) 139-166
- 2.2. N Aragonés, M. Palacios, A. Avello, P. Gómez, M. Martínez, M. Rodríguez, Arsenic levels in drinking water supplies from underground sources in the autonomous community of Madrid, *Rev. Esp. Salud Public.* 75 (2001) 421-432
- 2.3. <http://unil.ch/webdav/site/cam/users/jlavanch/public/recherche/arsenic/As-behavior.jpg>
- 2.4. D.Q. Hung, O. Nekrassova, R.G. Compton, Analytical methods for inorganic arsenic in water: a review, *Talanta* 64 (2004) 269-277
- 2.5. J.L. Gómez-Ariza, D. Sánchez-Rodas, I. Giráldez, E. Morales, A comparison between ICP-MS and AFS detection for arsenic speciation in environmental samples, *Talanta* 51 (2000), 257-268
- 2.6. J.H.T. Luong, E. Majid, K.B. Male, Analytical Tools for monitoring arsenic in the environment, *Open Anal. Chem. J.* 1 (2007) 7-14
- 2.7. A.T. Townsend, The determination of arsenic and selenium in standard reference materials using sector field ICP-MS in high resolution mode, *Fresen. J. Anal. Chem.* 364 (1999) 521-526
- 2.8. Z. Fiket, V. Roje, N. Mikac, G. Kniewald, Determination of arsenic and other trace elements in bottled waters by high resolution inductively coupled plasma mass spectrometry, *Croat. Chem. Acta* 80 (2007) 91-100
- 2.9. B. Klaue, J.D. Blum, Trace analyses of arsenic in drinking water by inductively coupled plasma mass spectrometry: high resolution versus hydride generation, *Anal. Chem.* 71 (1999) 1408-1414
- 2.10. J.M. Andrade-Garda, *Basic Chemometric techniques in atomic spectroscopy*, The Royal Society of Chemistry, 2009, ISBN: 978-0-85404-159-6
- 2.11. S.D. Tanner, Characterization of ionization and matrix suppression in inductively coupled "cold" plasma mass spectrometry, *J. Anal. At. Spectrom.* 10 (1995) 905-921
- 2.12. A.T. Townsend, The determination of arsenic and selenium in standard reference materials using sector field ICP-MS in high resolution mode, *Fresen. J. Anal. Chem.* 364 (1999) 521-526
- 2.13. F. Laborda, M.J. Baxter, H.M. Crews, J. Dennis, Reduction of polyatomic interferences in inductively coupled plasma mass spectrometry by selection of instrumental parameters and using an argon-nitrogen plasma: effect on multi-element analyses, *J. Anal. At. Spectrom.* 9 (1994) 727-736
- 2.14. Z. Zhang, S. Chen, H. Yu, M. Sun, W. Liu, Simultaneous determination of arsenic, selenium and mercury by Ion exchange-vapor generation-inductively coupled plasma-mass spectrometry, *Anal. Chim. Acta* 513 (2004) 417-423
- 2.15. M. Niemela, P. Perämäki, H. Kola, J. Piispanen, Determination of arsenic, iron and selenium in moss samples using hexapole collision cell, inductively coupled plasma-mass spectrometry, *Anal. Chim. Acta* 493 (2003) 3-12



- 2.16. S.D. Tanner, V.I. Baranov, D.R. Bandura, Reaction cells and collision cells for ICP-MS: a tutorial review, *Spectrochim. Acta B* 57 (2002) 1361-1452
- 2.17. J. Darrouzès, M. Bueno, G. Lespès, M. Holeman, M. Potin-Gautier, Optimization of ICP-MS collision/reaction cell conditions for the simultaneous removal of argon based interferences of arsenic and selenium in water samples, *Talanta* 71 (2002) 2080-2084
- 2.18. Z. Chen, N.I. Khan, G. Owens, R. Naidu, Elimination of chloride interference on arsenic speciation in ion chromatography inductively coupled mass spectrometry using an octopole collision/reaction system, *Microchem. J.* 87 (2007) 87-90
- 2.19. D. Beauchemin, J.W. McLaren, S. Berman, Study of the effect of concomitant elements in inductively coupled plasma-mass spectrometry, *Spectrochim. Acta B* 42 (1987) 467-490
- 2.20. Y. Kim, H. Kawaguchi, T. Tanaka, A. Mizuike, Non-spectroscopic matrix interference in inductively coupled plasma-mass spectrometry, *Spectrochim. Acta B* 45 (1990) 333-339
- 2.21. E.D. Salin, M. Antler, G. Bort, Evaluation of the simultaneous use of standard additions and internal standards calibration techniques for inductively coupled plasma mass spectrometry, *J. Anal. At. Spectrom.* 19 (2004) 1498-1500
- 2.22. A.S. Al-Ammar, R.K. Gupta, R.M. Barnes, Correction for non-spectroscopic matrix effects in inductively coupled plasma-mass spectrometry by common analyte internal standardization, *Spectrochim. Acta B* 54 (1999) 1849-1860
- 2.23. C. Sartoros, E.D. Salin, Automatic selection of internal standards in inductively coupled plasma-mass spectrometry, *J. Anal. At. Spectrom.* 54 (1999) 1557-1571
- 2.24. C.J. Park, H. Song, Determination of arsenic in biological samples by inductively coupled plasma mass spectrometry with selenium as an internal standard, *J. Anal. Spectrom.* 20 (2005) 436-440
- 2.25. J.M. Andrade-Garda, *Basic Chemometric Techniques in Atomic Spectroscopy*, The Royal Society of Chemistry, 2009, ISBN: 978-0-85404-159-6
- 2.26. USEPA, Method 200.8, Determination of Trace Elements in Water and Wastes by Inductively Coupled Plasma-Mass Spectrometry, Rev. 5.3, US Environmental Protection Agency, 1994
- 2.27. Y. Cai, M. Georgiadis, J.W. Fourqurean, Determination of arsenic in seagrass using inductively coupled plasma mass spectrometry, *Spectrochim. Acta B* 55 (2000) 1411-1422
- 2.28. R.J.C. Brown, R.E. Yardley, A.S. Brown, M.J.T. Milton, Sample matrix and critical interference effects on the recovery and accuracy of concentration measurements of arsenic in ambient particulate samples using ICP-MS, *J. Anal. At. Spectrom.* 19 (2004) 703-705
- 2.29. G.H. Floor, M. Iglesias, G. Roman-Ross, Selenium determination in volcanic soils by ICP-QMS: influence of reaction cell pressurization and methanol addition on the occurrence of spectral interferences, *J. Anal. At. Spectrom.* 24 (2009) 944-948
- 2.30. R. Thomas, *Practical Guide to ICP-MS*, Marcel Dekker, 2003, ISBN: 978-0-824-75319-1

- 2.31. J.J. Thompson, R.S. Houk, A study of internal standardization in inductively coupled plasma-mass spectrometry, *Appl. Spectrosc.* 41 (1987) 801-806
- 2.32. Y. Igarashi, H. Kawamura, K. Shiraishi, Y. Takaku, Determination of thorium and uranium in biological samples by inductively coupled plasma mass spectrometry using internal standardization, *J. Anal. At. Spectrom.* 4 (1989) 71-576
- 2.33. G.R. Gillson, D.J. Douglas, J.E. Fulford, K.W. Halligan, S.D. Tanner, Nonspectroscopic interelement interferences in inductively coupled plasma mass spectrometry, *Anal. Chem.* 60 (1988) 1472-1474
- 2.34. Z. Hu, S. Gao, H. Yuan, X. Liu, Y. Liu, Suppression of interferences for direct determination of arsenic in geological samples by inductively coupled plasma mass spectrometry, *J. Anal. At. Spectrom.* 20 (2005) 1263-1269
- 2.35. P. Kralj, M. Veber, Investigations into nonspectroscopic effects of organic compounds in inductively coupled plasma mass spectrometry, *Acta. Chim. Slov.* 50 (2003) 633-644
- 2.36. E.H. Larsen, S. Stürup, Carbon-enhanced inductively coupled mass spectrometric detection of As and Se and its application to As speciation, *J. Anal. At. Spectrom.* 9 (1994) 1099-1105
- 2.37. L. Llorente, M. Gómez, C. Camara, Improvement of selenium determination in water by inductively coupled plasma mass spectrometry through use of organic compounds as matrix modifiers, *Spectrochim. Acta B* 52 (1997) 1825-1838
- 2.38. J. Goossens, F. Vanhaecke, L. Moens, R. Dams, Elimination of interferences in the determination of arsenic and selenium in biological samples by inductively coupled plasma mass spectrometry, *Anal. Chim. Acta* 280 (1993) 137-143
- 2.39. A.S. Al-Ammar, E. Reitznerova, R.M. Barnes, Feasibility of using beryllium as internal reference to reduce non-spectroscopic carbon species matrix effect in the inductively coupled plasma mass spectrometry determination of boron in biological samples, *Spectrochim. Acta B* 54 (1999) 1813-1820
- 2.40. Z. Hu, S. Hu, S. Gao, Y. Liu, S. Lin, Volatile organic solvent-induced signal enhancements in inductively coupled plasma-mass spectrometry: a case study of methanol and acetone, *Spectrochim. Acta B* 59 (2004) 1463-1470
- 2.41. F. Vanhaecke, R. Dams, C. Vandecastel, "Zone Model" as an explanation for signal behavior and non-spectral interferences in inductively coupled plasma mass spectrometry, *J. Anal. At. Spectrom.* 8 (1993) 433-438
- 2.42. S. Wangkarn, S.A. Pergantis, Determination of arsenic in organic solvents and wines using microscale flow injection inductively coupled plasma mass spectrometry, *J. Anal. At. Spectrom.* 14 (1999) 657-662
- 2.43. M. Kovačević, W. Goessler, Direct introduction of volatile carbon compounds into the spray chamber of an inductively coupled plasma mass spectrometer: Sensitivity enhancement for selenium, *Spectrochim. Acta B* 60 (2005) 135-1362
- 2.44. P. Allain, L. Jaunault, Y. Mauras, J.M. Mermet, T. Delaporte, Signal enhancement due to the presence of carbon-containing compounds in inductively coupled plasma mass spectrometry, *Anal. Chem.* 63 (1991) 1497-1498

- 2.45. M. Berg, C. Stengel, ARS29-32 arsenic reference samples Interlaboratory Quality Evaluation (IQE). Report to participants, Eawag, Swiss Federal Institute of Aquatic Science and Technology, Dübendorf, Switzerland, 2009

# CHAPTER 3

---

## Evaluation of DGT samplers to measure labile and available metals in acidic waters and mining wastes

---



The contents of this chapter were submitted for publishing in:

Analytical Chemistry:

M. Colon, H. Cheng, M. Iglesias, M. Hidalgo, H. Zhang, *Evaluation of DGT samplers for measuring labile metals in acidic waters*

Chemosphere:

M. Colon, M. Iglesias, G. Garcia, H. Zhang, M. Hidalgo, *Diffusive gradients in thin films (DGT) compared with other bioavailability tests for predicting cadmium, lead and zinc bioavailability to *Crithmum maritimum* grown on acidic mining wastes*



### 3.1 INTRODUCTION

Metal pollution is a quickly growing problem for the environment. It is known that such pollution can arise from natural sources but anthropogenic sources, which include industrial effluents, fertilizers or mining and metal processing, are the most important. Some metals have bio-importance as trace elements and it is recognized that they are a threat to human health, animals, plants and the planet itself. While total metal content is a critical measure in assessing risk of a contaminated water or soil, total metal content alone does not provide insights on the bioavailability, mobility, and fate of the metal contaminant. In this way, as different forms of an element may exhibit differing toxicities and mobilities in the environment, it is clearly of importance to be able to distinguish between the individual species present in a particular sample. Natural waters contain a variety of ligands which can form complexes with trace metal ions. Consequently, free metal ions are usually a minor component of the total metal species present. Inorganic and organic metal complexes have very different physical properties, e.g. charge, size and diffusion coefficient. Methods are therefore needed to discriminate between them and in so doing provide valuable environmental information [3.1,3.2,3.3].

High levels of heavy metals can often be found in and around areas where mining activities have taken place. Large amounts of mine waste material are generated as a by-product of the economic extraction of metals from ore deposits [3.4]. During different processes involved in the extraction and in mineral processing to obtain metals, several sub-products such as rocks or metals are overturned to the environment resulting in the presence of waste dump and tailing impoundments. These mine tailing dumps are characterized by high concentrations of heavy metals and thus, they tend to become important sources of air, soil and water pollution [3.5]. Heavy metals contained in these residues are often dispersed by wind and/or water after their disposal. The impact on ecosystems due to wastes from mining and processing activities may appear in groundwater, surface water and soil. It is well known that acidic mine drainage often contains elevated concentrations of potentially toxic metals. Flora, fauna and human beings are all examples of living organisms susceptible to contamination. As heavy metal contamination is widespread, if they are phytoavailable, some toxic metals are potentially accumulated in plants [3.6]. Moreover, there is a risk of transfer of toxic and available metals to humans and animals as well. Vegetation establishment on mine tailings is difficult due to the high level of acidity. Pb/Zn mine tailings may also contain

toxic concentrations of metals such as Pb, Zn and Cd. Moreover, the poor physical structure and excess of salinity can difficult plant grow [3.7]. The mobility of metals in soil systems is dependent on the chemical form of soil-metal interaction. Metal associated with the aqueous phase of the soil can be transported while metals immobilised by adsorption or precipitation mechanisms are retained by soils. Immobilization can be effective until the metal retention capacity is overloaded or when changes in soil conditions occur. Changes of pH, redox potential or organic matter content can result in a remobilization of metals present in the solid phase of a soil [3.8]. Thus, evaluation and characterization of heavy metals pollution near the mine has been one of the major interests in environmental issues for the last years [3.9,3.10].

### **3.1.1 Assessment of metal availability**

In order to estimate bioavailability of trace metals and their toxicity, it is necessary to determine their chemical forms associated with the solid phase. To this end, single and sequential extraction procedures have been largely used to study the fractionation of trace metal content in soils, sediments and related materials. Several procedures have been described for sequential extraction, but all of them consist of treating the sample with a series of reagents selected for their ability to react with different, major, components of the matrix and release associated trace metals [3.11]. The application of sequential extraction schemes on environmental samples provide essential information related to environmental pollution [3.12]. The standardized BCR (Community Bureau of Reference) sequential extraction procedure and the sequential extraction proposed by NIST (National Institute of Standards and Technology) are among the most frequently used methods for predicting trace metal fraction in polluted soils and sediments [3.13,3.14].

On the other hand, the technique of diffusive gradient in thin-films (DGT) is a promising analytical speciation method that has been widely used for the measurements of labile metal species in natural waters as well as for pore water concentrations and remobilisation fluxes of trace-metals in sediments and soils. DGT devices consist of two layers of polyacrylamide gel: a diffusive gel layer and a resin-impregnated gel layer containing Chelex resin. These are placed on a plastic backing plate with the resin layer in contact with the plate. A filter membrane is placed on top to prevent mechanical damage and biological fouling of the gels. Finally, a plastic front plate with an exposure

window is set. This methodology is based on the principle of diffusion of hydrated metal ions and complexes through a hydrogel layer of known thickness and pore size, followed by a progressive immobilization of the metal ions on the chelating resin. Metals that have accumulated on the resin gel can be extracted by acid and their concentration subsequently determined. It has been demonstrated that only metal species that are mobile or labile will diffuse through the hydrogel layer and contribute to the measured metal [3.15-3.17].

The DGT technique has been found to work properly in a pH range of 5 to 10 for a large number of metals, which demonstrates its versatility and explains its widespread use [3.17]. It has been used in rivers, lakes and estuarine waters for in situ trace metal monitoring as a pre-concentration procedure and as a speciation tool [3.18-3.20]. A modification of the thickness of the diffusive gel layer and the use of restricted gels has allowed the application of DGT in waste waters [3.21,3.22]. The concentration, speciation and toxicity of dissolved metals in mine drainage have also been assessed by the deployment of DGT [3.23-3.25]. However, a limitation of the technique is the reduced performance of the chelating Chelex resin at low pH ranges due to competition between metals and hydrogen ions for the binding agent. The effect of pH on Al and Mn sorption on the resin layer has been studied in the range of 2.5 to 4.5 with results suggesting that DGT measurements must be corrected for Mn at pH 3.5 and below, while for Al the correction is necessary below pH 3.0. On the other hand, it has been demonstrated that as it binds very strongly Cu can be measured down to pH 2 with no need for correction [3.23,3.26].

Although Chelex-100 preferentially binds transition metals, it is also able to immobilize  $\text{Ca}^{2+}$  cations. Thus, in hard water, where the calcium concentration can exceed trace metal concentrations by several orders of magnitude, calcium can become a competitor for binding Chelex, and metal concentrations measured by DGT can be affected [3.26].

The diffusion coefficients of metals in simple inorganic solutions are independent of ionic strength (except when it is very low) but they can decrease with increasing ligand size. The contribution of fulvic acid species must therefore be taken into account when deploying DGT in fresh waters and sediments [3.27].

When using this technique in soils and sediments, DGT device is hypothesized to mimic the plant mechanism of uptake by lowering the concentration locally and inducing diffusive supply and release from the solid phase so it can provide an in situ measure of



their bioavailability [3.28-3.30]. The bioavailability of metals is related to their flux into the plant which depends on both their concentration in soil solution and their transport rate through the soil [3.31]. In this sense, copper bioavailability has been commonly investigated in agricultural production using the DGT technique [3.32,3.33]. For efficient fertilizer application, assessment of available phosphorus through DGT has been deeply studied [3.34,3.35]. Bioavailability of selenium, uranium, cadmium and other elements have also been studied by the use of DGT technique [3.36-3.39].

In this chapter, we look at the effect of pH on the adsorption of cobalt, nickel, copper, cadmium, zinc and lead on the resin layer of a DGT sampling device in the pH range of 1.5 to 5.5 under controlled conditions in the laboratory. The effect of different concentrations of calcium on metal adsorption is also tested at pH 2.0 and 3.5, and the effect of the presence of fulvic acid on metal diffusion is studied at pH 5.5, 3.5 and 2.5. The results are compared to predictions obtained by using the WHAM VI speciation program. DGT devices are deployed in the laboratory in acidic mine waters collected in the mining area of Cartagena (Spain). Then, the use of the DGT technique directly on acidic mine spoils is evaluated.

Moreover, the mobility and bioavailability of heavy metals to vegetation specimens is studied. On the other hand, common procedures used for metal mobility and availability such as the first step of BCR protocol, the DTPA (Diethylene triamine pentaacetic acid) procedure and metal extraction with magnesium chloride have been carried out. Possible correlations of these results with those obtained by DGT technique and accumulated metals in a plant species (*Crithmum maritimum*) have been investigated.

## 3.2 EXPERIMENTAL

### 3.2.1 DGT gel preparation

Diffusive gel was prepared by mixing 3.75 mL of acrylamide solution (40%) (BDH Electran) and 4.75 mL of de-ionized water with 1.5 mL of DGT cross-linker (0.3%, measured by weighing 1.5g). This 10 mL of gel solution was well mixed and then 50  $\mu$ L of ammonium persulfate solution (10%) (BDH) and 15  $\mu$ L of N,N,N',N'-tetramethylethylenediamine (TEMED) (99%) (BDH Electran) were added. After mixing, it was immediately cast between two glass plates, which were separated by a 0.5 mm plastic spacer (for a hydrated gel of 0.08 cm) and immediately placed in a 45 °C oven

for 1 hour. Once the gel was completely set, it was removed from the glass plates and placed into a de-ionized water bath, which was changed repeatedly until all the excess polymerization products were removed. Finally, the gel was stored in  $10 \text{ mmol L}^{-1}$   $\text{NaNO}_3$  solution until its use [3.27].

The Chelex-100 resin-gel used in this work was prepared by mixing 10 mL of gel solution, consisting of 3.75 mL of acrylamide (40%), 1.5 mL of DGT cross-linker (0.3%) and 4.7 mL of de-ionized water, with 50  $\mu\text{L}$  of ammonium persulfate solution (10%) and 15  $\mu\text{L}$  of TEMED (99%). A 10 mL aliquot of this mixture was then added to 4 g of Chelex-100 available from Bio-Rad Laboratories. The resin gel solution was well mixed and immediately cast between two plates separated by a 0.25 mm spacer. Setting and hydration procedures then followed those for the diffusive gel.

Polyacrylamide gel sheets were cut into disks and assembled in a gel holder known as a DGT sampling device with a 2.0 cm diameter window and an area exposed to the solution of  $3.14 \text{ cm}^2$ . This device accommodates a 0.08 cm diffusive gel overlying a 0.04 cm resin gel. On the top, a 2.5 cm diameter cellulose nitrate membrane filter (Whatman GmbH), with a reported pore size of  $0.45 \mu\text{m}$ , was used as a protective extension of the diffusive layer [3.40].

### 3.2.2 Experiments with synthetic water

To investigate DGT performance at low pH for Co, Ni, Cu, Zn, Cd and Pb in water, DGT devices were deployed in 2 L of  $0.1 \text{ mol L}^{-1}$   $\text{NaNO}_3$  solutions containing  $10 \mu\text{g L}^{-1}$  of Co, Cd and Pb and  $100 \mu\text{g L}^{-1}$  of Ni, Cu and Zn. The pH was adjusted to 1.5, 2, 2.5, 3, 3.5, 4, 4.5, 5 and 5.5 with suprapure  $\text{HNO}_3$  and  $\text{NaOH}$ . Four DGT devices were deployed together in each solution for 4 h. After deployment, the devices were removed and rinsed with  $18.2 \text{ M}\Omega\text{cm}$  of water, and prised open for removal of the resin gels, which were then placed in a 1.5 mL centrifuge vial. One mL of 1 M  $\text{HNO}_3$  was added to the vial and allowed to stand for 24 h to extract the metals. The solutions were stirred continuously throughout the experiment. The pH and temperature were measured at the beginning and end of the deployment period and samples of the bulk solutions were also taken to determine Co, Ni, Cu, Zn, Cd and Pb. The average temperature, pH and metal concentration were used to represent the solution temperature, pH and metal concentration throughout the deployment period. Before analysis, all the samples were diluted 1:10 and internal standards were added. To determine the effect of calcium,

different synthetic  $0.1 \text{ mol L}^{-1} \text{ NaNO}_3$  solutions containing 0.1, 0.5, 1.0, 5.0 and  $10.0 \text{ mmol L}^{-1}$  of Ca and  $10 \text{ } \mu\text{g L}^{-1}$  of Co, Cd and Pb and  $100 \text{ } \mu\text{g L}^{-1}$  of Ni, Cu and Zn were adjusted to pH 2.5 and 3.5. Four DGT devices were deployed in each solution for 4 hours. Procedure for metal extraction was the same as those described in the above paragraph.

The last series of experiments addressed the effect of the presence of  $10 \text{ mg L}^{-1}$  of fulvic acid. For this purpose, 2 L of MilliQ water containing  $0.1 \text{ mol L}^{-1} \text{ NaNO}_3$  were spiked with the necessary amount of the acid at a final concentration of  $10 \text{ mg L}^{-1}$ . The pH was first adjusted to 5.5 using a NaOH solution and the solution was then spiked with the different metals at the appropriate concentration. The solution was stirred overnight and the four devices deployed the following day. After this deployment, two more deployments were carried out at pH 3.5 and 2.5 using a suprapure  $\text{HNO}_3$  solution to adjust the pH.

Trace metals were analysed using a Thermo Elemental X7 inductively coupled plasma mass spectrometer (ICP-MS), equipped with a high performance interface, Pt-tipped sampler and microskimmer cones. The instrument was optimized daily in terms of sensitivity and precision, and the oxide ( $\text{CeO}^+$ ) and double charged ion ( $\text{Ba}^{2+}$ ) levels were maintained under 2% and 4% respectively. Before sample analysis a 10-min short-term stability check was performed. Accuracy and precision were verified using a river water reference material, SLR-4, available from the National Research Council Canada (NRC). Mass to charge ratio 59, 60, 65, 66, 111 and 208 were monitored for Co, Ni, Cu, Zn, Cd and Pb respectively. Moreover,  $^{45}\text{Sc}$ ,  $^{103}\text{Rh}$  and  $^{209}\text{Bi}$  were used as internal standards.

### 3.2.3 Sampling and analysis of acidic mine drainage waters

The Cartagena-La Union Mining District was an important mining area for more than 2500 years. Mining was the most important economic activity in this zone until 1991 when the mining activity ceased. The wastes from the refining process were traditionally dumped into the water streams that drained the Sierra or into the sea. Nowadays, a large number of mine tailings piles are present in the Cartagena range mountain, called Sierra Minera. The ore deposits of this zone contain large amounts of iron, lead and zinc, as the main metal components [3.41,3.42].

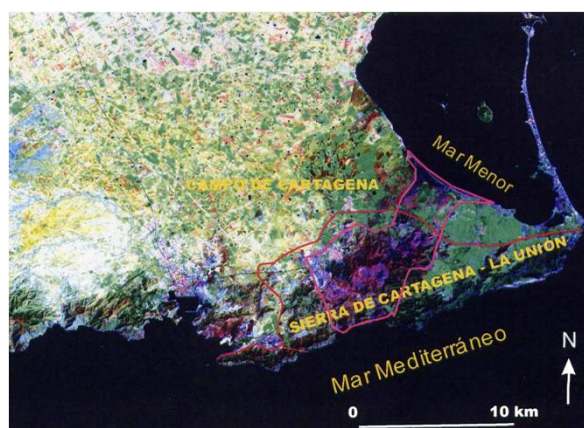


**Figure 3.1** Cartagena-La Unión mining district. In purple, it is shown the area affected by ore deposits containing high amounts of metal [3.43].

Five acidic water samples (2 L of each) were collected from the mining area of Cartagena, Spain, and stored in polyethylene bottles. Three DGT units were deployed together in each sample for 1 h. The temperature and pH were measured just before and just after deployment and the devices were then rinsed thoroughly with 18.2 MΩxcm of water and prised open for removal of the resin gel. Extraction and determination of metals were carried out as in the procedure previously described.

Three small aliquots of each sample were also taken to determine Al, As, Ca, Cd, Co, Cu, Fe, K, Mg, Mn, Na, Pb and Zn by a sequential inductively coupled plasma optical emission spectrometer (ICP-AES) (Liberty RL, Varian Australia, Mulgrave, Victoria, Australia). Dissolved organic carbon (DOC) was measured by a Shimadzu TOC-V<sub>CSH</sub> analyzer and Cl<sup>-</sup>, NO<sub>3</sub><sup>-</sup>, PO<sub>4</sub><sup>2-</sup> and SO<sub>4</sub><sup>2-</sup> were determined by ion chromatography.

### 3.2.4 Sampling and characterisation of mining wastes

Eight mining wastes were collected from eight flotation ponds of the Sierra Minera of Cartagena, using a polypropylene shovel and, subsequently, transferred to clean polypropylene bags. Once at the laboratory, samples were air dried, sieved at <500 μm and stored in polypropylene containers until analysis.

A Crison CLP pH meter was used for pH measurements using a ratio 1:2.5 (waste: MilliQ water). Electrical conductivity was measured in a residue-water extract based on a fixed soil: solution ratio (1:2) using a conductivitymeter Crison Micro CM 2200 [3.44].

Organic carbon was determined by catalytic oxidation of organic matter using a TOC analyzer Shimadzu TOC-V<sub>CSH</sub> with the solids sample module SSM-5000A.

A microwave-assisted digestion procedure, using a Milestone ETHOS PLUS microwave with temperature control, was developed for pseudotoal determination of Pb, Zn and Cd. About 1 g of sample was weighed and placed in a PTFE reactor. 3 mL of 65% HNO<sub>3</sub> Suprapure grade and 9 mL of 37% HCl were added into the reactor. Then it was heated following a two-steps digestion program: 10 minutes to reach 200 °C and 15 min at 200 °C. After cooling, sample digest was filtered with a Whatman 42 filter paper, transferred into a 25 ml flask and brought to volume with MilliQ water.

The first step of the BCR method, a single extraction using DTPA and the first step of NIST sequential extraction were performed to study Pb, Zn and Cd mobility and bioavailability in the mining ore deposits. For BCR method, 0.5 g of each mining waste was weight, placed in a polyethylene container with 20 mL of CH<sub>3</sub>COOH 0.11 M and shacked for 16 h. For DTPA single extraction, 0.5 g of residue and 20 mL of DTPA 0.005 M were placed in a polyethylene container during 2 h. Finally, for the first step of NIST 1 g of sample was placed in a polyethylene container with 16 mL of MgCl<sub>2</sub> 1M for 1 h. To keep samples on suspension during extraction, a rotatory shaker (DINKO systems) was used and a Mixtasel P-Selecta centrifuge was used for separation of extracts.

Both, microwave digests and extracts, were analysed by a sequential ICP-AES (Liberty RL, Varian) with V-groove nebulizer. The selected wavelengths were 202.551 nm (Zn), 220.353 nm (Pb) and 214.438 nm (Cd). Duplicate samples were used in all the analysis done and blank extractions and digests (without sample) were carried out for each set of analysis.

### **3.2.5 Deployment of DGT in mining residues**

About 100 g of each eight mining wastes were saturated, in triplicate, to 100% of the potential water holding capacity with MilliQ water. After 24 h equilibration, DGT units were deployed for 24 h. After deployment, DGT-units were removed and rinsed with MilliQ water before dismantling. The resins were eluted with 1 mL of 65% HNO<sub>3</sub> Suprapure grade. Concentrations of Zn, Pb and Cd in the extracts were determined by ICP-MS (Agilent 7500c) and corrected for pH using the sigmoid 5 parameter curve obtained as it will be explained later. After removal of the DGT units, the mining wastes

saturated with MilliQ water were then centrifuged. Pore water was obtained by decantation and filtrated with 45  $\mu\text{m}$  filter. Concentration of Zn, Pb and Cd was measured by ICP-MS.

### 3.2.6 DGT calculations

According to Fick's first law of diffusion, concentrations of metal in water can be determined from the amount of metal accumulated on the resin gel when the diffusion coefficients of the metal ions are known. Concentrations in solutions measured by DGT can be calculated using Eq. 1:

$$C_{DGT} = M\Delta g/D_{Gel}At \quad (3.1)$$

where  $C_{DGT}$  is the concentration as measured by DGT,  $M$  is the mass of metal accumulated on the resin gel during deployment,  $\Delta g$  is the total thickness of the diffusive gel layer and the membrane filter (0.078 and 0.014 respectively),  $D_{Gel}$  is the diffusion coefficient of the diffusing species within the diffusive gel and prefilter,  $A$  is the sampling window area of 3.14  $\text{cm}^2$  and  $t$  is the deployment time.

The mass of metal accumulated by the DGT sampling device can be calculated using the following equation:

$$M = C_e(V_{Gel} + V_{HNO3})/f_e \quad (3.2)$$

where  $C_e$  is the concentration of metal in the elution sample,  $V_{HNO3}$  is the volume of the elution fluid,  $V_{Gel}$  is the chelating resin volume, typically 0.16 mL. The value of the elution factor  $f_e$  (the percentage of the chelated metal recoverable in 1 mol  $\text{L}^{-1}$   $\text{HNO}_3$ ) was taken to be 0.8 [3.45].

### 3.2.7 Modeling with WHAM VI

The Windermere Humic Aqueous Model VI is a discrete site/electrostatic model of the interactions of protons and metals with fulvic and humic acids [3.46]. Concentrations of free Co, Ni, Cu, Zn, Cd and Pb ions were calculated using the WHAM Model VI for waters. Input values are shown in Table 3.1. When modelling real samples, we assumed DOC to have the ion-binding properties of "default" fulvic acid, FA, as defined in WHAM VI. As suggested in the software guide, we let 50% of the acid groups of FA be active in proton/metal binding.

### 3.2.8 Pot Experiments

*Crithmum maritimum* specimens were grown in non-contaminated soil and then transplanted to the eight mining wastes under laboratory controlled conditions. After 45 days, plants were harvested and submitted to analysis.

Plants were rinsed thoroughly with MilliQ water to remove surficial dust and oven-dried at 55 °C for 72 h. Subsequently, plant samples were milled and digested by a microwave-assisted digestion procedure. About 500 mg of plant sample was weighed and placed in a PTFE reactor. 9 mL of 65% HNO<sub>3</sub> Suprapure grade and 3 mL of H<sub>2</sub>O<sub>2</sub> were added into the reactor. Then it was heated following a two-stage digestion program: 5 minutes to reach 180 °C and 10 min at 180 °C. After cooling, sample digest was transferred into a 25 ml flask and brought to volume with MilliQ water. Zn was measured by a sequential ICP-AES (Liberty RL, Varian), while Pb and Cd were measured by ICP-MS (Agilent 7500c). Duplicate samples and blank reagent digests were carried out for each set of analysis.

## 3.3 RESULTS AND DISCUSSION

### 3.3.1 DGT performance in acidic aqueous solution

In order to evaluate DGT performance in acidic solutions, different experiments were carried out under laboratory controlled conditions. Results are detailed below.

#### 3.3.1.1 Effect of pH on DGT measurements of Co, Ni, Cu, Cd, Zn and Pb

As previously mentioned, it has already been demonstrated that DGT devices work properly in the pH range of 5 to 10 for a large number of inorganic ions. However, at a lower pH, hydrogen ions can compete with metals for the binding agent. In such cases the concentrations given by DGT calculations can be erroneous. To assess the performance of the technique at low pHs, DGT devices were deployed in solutions containing the metals under study at pH values ranging from 1.5 to 5.5. The results for these studies are shown in Figure 3.2.

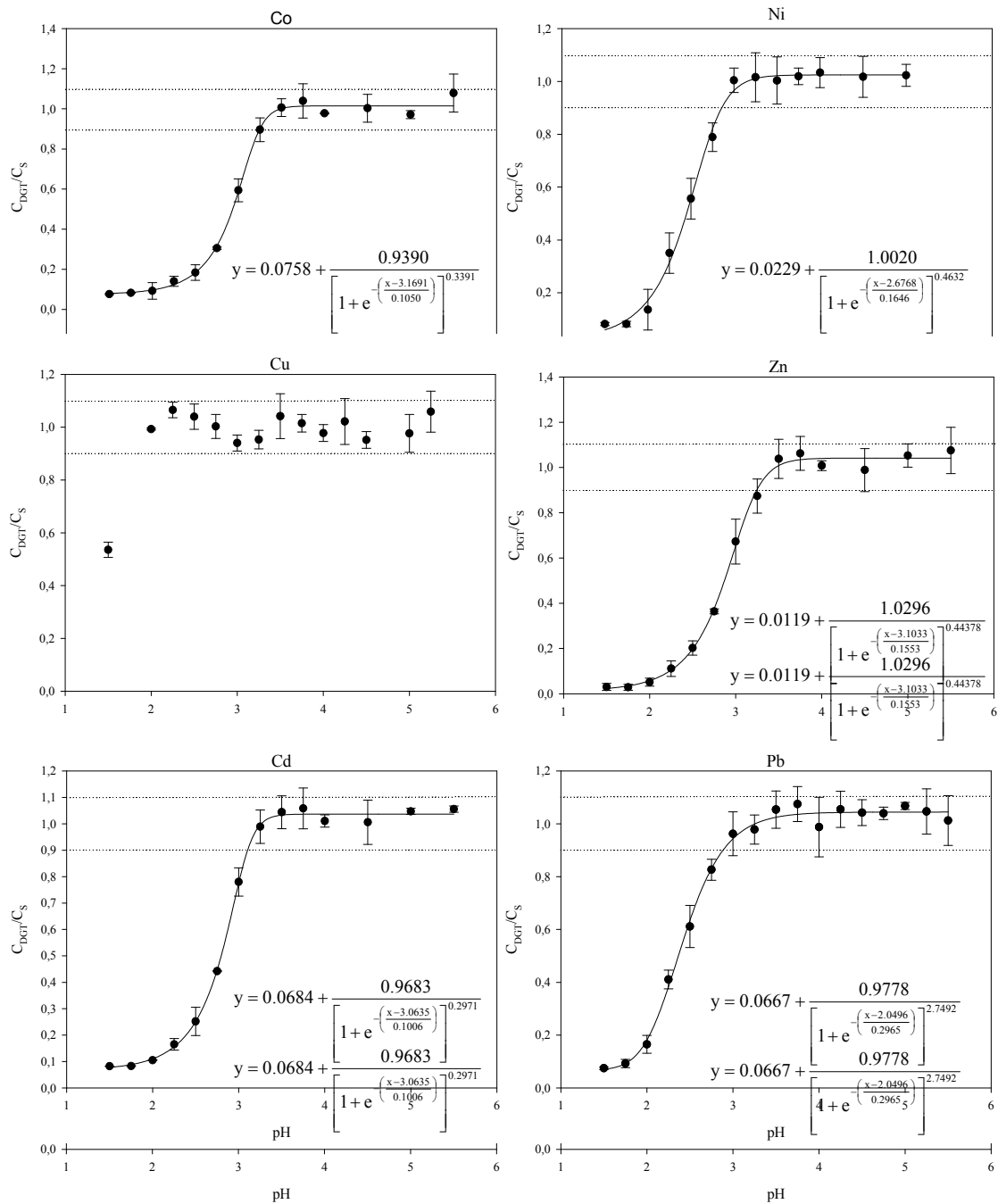


**Figure 3.2** Effect of pH on the measurements of Co, Cd and Pb ( $10\mu\text{g L}^{-1}$ ) and Ni, Cu and Zn ( $100\mu\text{g L}^{-1}$ ) by DGT methodology, plotted as the ratio of concentration given by DGT calculations ( $C_{DGT}$ ) divided by the metal concentration obtained by direct solution measurements with ICP-MS ( $C_s$ ). Each point represents the average of four DGT devices deployed together and their standard deviation. Dotted lines represent a deviation of 10% from a  $C_{DGT}/C_s$ , which is the accepted error in this technique.



The ratio of the metal concentration measured by DGT,  $C_{DGT}$ , to the mean concentration measured directly by ICP-MS in solution,  $C_S$ , systematically varied from a low value at pH 1.5 to a value close to 1 at pH 5.5 (Figure 3.2). A sigmoid 5 parameters curve provided a good fit to the data for each element except for Cu, which binds to Chelex so strongly that DGT performance is only affected at pH lower than 2. The concentrations given by DGT measurements applying the explained calculations agreed very well with solution concentrations determined by ICP-MS for all metals in solutions with pH greater than 3.5. Binding to the resin-gel works efficiently down to pH 3.5 for Co and Zn, but below this pH, concentrations calculated by DGT must be corrected using the sigmoid equations that fitted the data very well (correlation coefficient,  $r = 0.9982$  and  $0.9984$ , respectively). Similarly, Ni and Pb, can be determined without any correction down to pH 3, but below this pH,  $C_S$  of Ni and Pb must be determined using the sigmoid equations ( $r = 0.9984$  and  $0.9979$ , respectively). The concentration given by DGT does not require any correction for Cd until pH 3.25, but it should be corrected for lower pH using the sigmoid equation ( $r = 0.994$ ). As Cu binds efficiently to the resin down to pH 2, no correction is required.

### **3.3.1.2 Effect of calcium on DGT measurements of Co, Ni, Cu, Zn, Cd and Pb**

Chelex resin binds Ca, but less strongly than the preferential binding of transition metals. However, due to its much higher concentration in natural waters the possible interference of calcium should be considered when measuring transition metals by DGT. DGT performance was investigated in solutions containing Ca in the concentration range of 0.1 to 10 mmol L<sup>-1</sup> at pH 2.5 and 3.5. Measured DGT-labile concentrations were corrected for the reduced DGT response at low pH by applying the 5 parameter sigmoid curves found previously. Results for these experiments are shown in Figure 3.3. At pH 3.5, low concentrations of Ca have no effect on the binding of any metal to the resin-gel. However, at a concentration of Ca of 0.5 mM and above, cadmium, which binds less strongly to Chelex than other transition metals, seems to be affected by calcium. At 10 mM of Ca,  $C_{DGT}$  for Cd is almost 25% lower than the concentration measured when no calcium is present in the solution. At pH 2.5 it seems that calcium has little effect on metal-Chelex binding. Only at a concentration of 10 mM of Ca,  $C_{DGT}$  for Co, Ni, Cd and Pb is slightly lower than the expected concentration.

It can be concluded that the presence of calcium does not significantly affect DGT performance except when it is at very high concentrations (10 mmol L<sup>-1</sup>) for the measurement of Cd at pH 3.5. These Ca concentrations are usually only found in sea water, but the pH in such samples is usually higher than 7 and it has been previously demonstrated that under these conditions competition by Ca is not a problem [3.26].

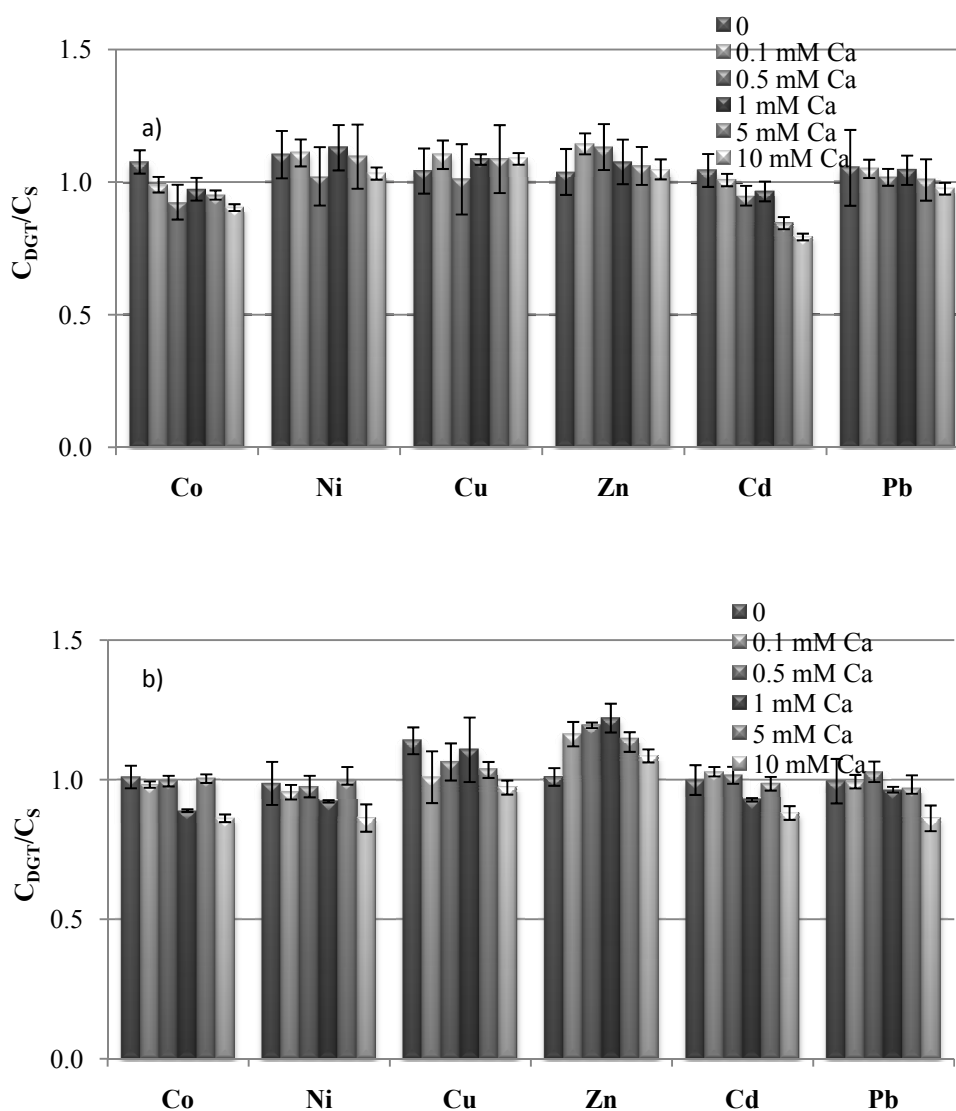


**Figure 3.3** Effect of Ca on the measurement of trace metals by DGT, determined by the ratio of corrected metal concentrations measured by DGT to the concentrations obtained by direct ICP-MS measurement in solution at pH 3.5 (a) and 2.5 (b). Error bars represent the standard deviation of the results of the four devices deployed together.

### 3.3.1.3 Effect of fulvic acid on DGT measurements of Co, Ni, Cu, Zn, Cd and Pb

In natural waters, as different ligands can interact with metal ions, metal complexes can have a range of diffusion coefficients. Diffusion coefficients of complexes with fulvic and humic acids are substantially lower than those of simple inorganic complexes. Moreover, those diffusion coefficients may not have a unique value, as they depend on parameters such as pH, ionic strength or concentration, which affect conformation changes and aggregation effects [3.47].

The WHAM VI modeling program can be used to predict the fraction of metal that binds to organic matter in a solution where the analytical composition is known. DGT measurements were made in the presence of  $10 \text{ mg L}^{-1}$  of fulvic acid at pH 5.5, 3.5 and 2.5. DGT-labile concentrations measured at pH 2.5 and 3.5 were corrected using the 5 parameter sigmoid fits found previously. Results for these experiments are shown in Figure 3.4 where maximum dynamic concentrations,  $C_{\text{dynmax}}$ , are also represented. This parameter is calculated as the concentration of inorganic species plus 0.2 times the concentration of the metal-fulvic acid species which is the percentage expected to diffuse through the DGT device [3.48]. According to WHAM VI predictions, at low pH (2.5 and 3.5) almost all of Cd, Co, Ni and Zn are present as inorganic species. The DGT measurements agree within reasonable error limits with  $C_s$ , in line with predictions. WHAM VI predicts that at pH 2.5, 20% of Cu is bound to fulvic acid and at pH 3.5 50% is bound, but DGT-labile concentrations for Cu are similar to the total dissolved metal at pH 2.5 and 3.5. Similarly, 20% of Pb is predicted to be bound to fulvic acid at pH 3.5 according to WHAM VI model. However, according to DGT results, only 10% of Pb is as non-available form. At pH 5.5, according to WHAM VI results, Co and Ni should be 10% and 15%, respectively, as Co-FA and Ni-FA, 30% and 35% of Zn and Cd, respectively, should be also bind to fulvic acid. Almost all Cu and Pb (96%) should be as metal-FA form according to WHAM VI model. It can be seen that DGT results are in good agreement with those results given by WHAM VI for Co, Ni, Zn and Cd. However, results obtained for Cu are quite higher than those we should expect; these results could be explained due to fact that fulvic substances are able to diffuse through the APA gel even though they have much lower diffusion coefficients than simple metal ions [3.47].

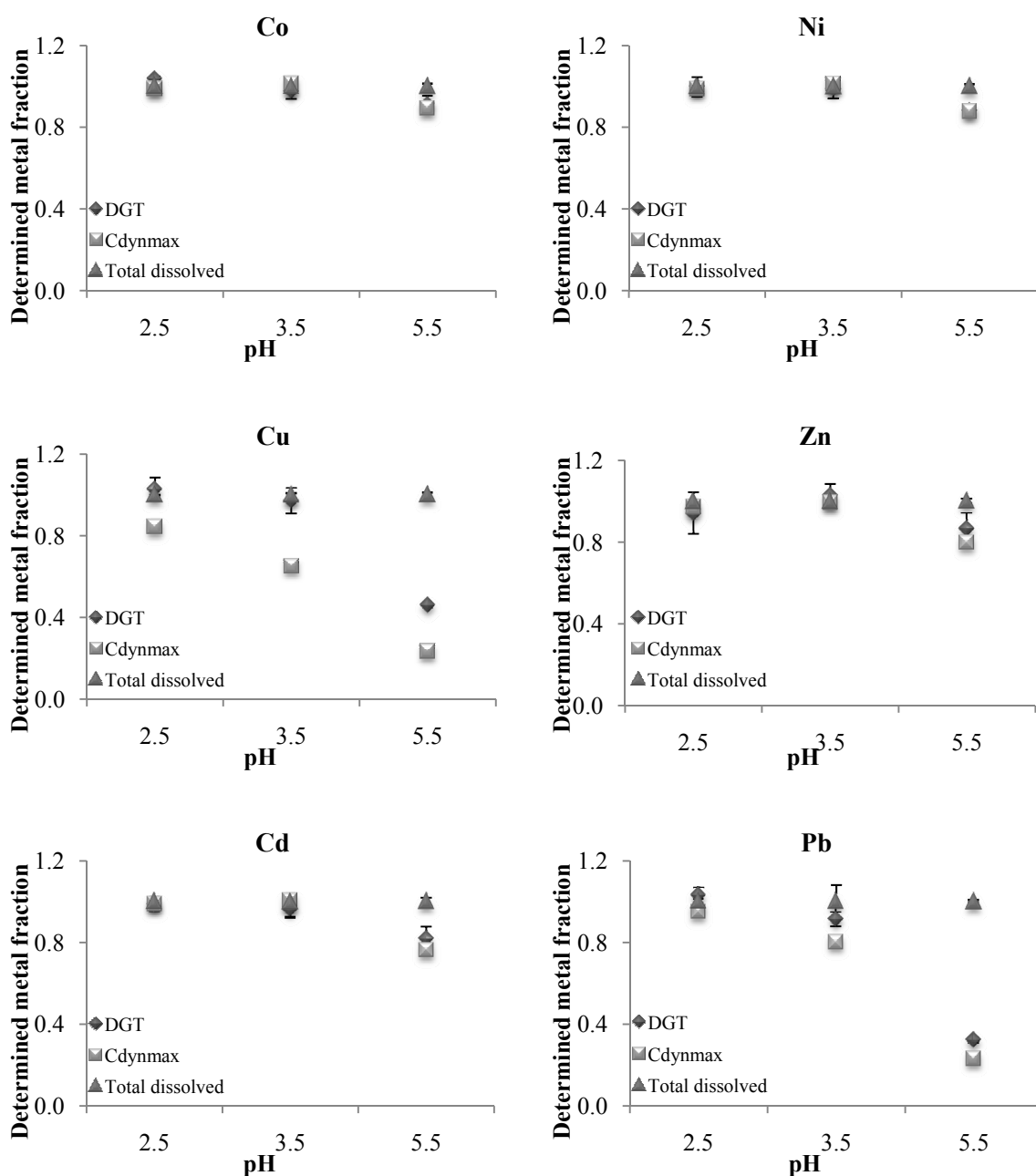


**Figure 3.4** Speciation of different metals at different pH values in laboratory experiments. Points represent the mean values and standard deviation of measured total dissolved concentrations ( $\triangle$ ), DGT-labile concentrations ( $\diamond$ ) and concentrations of inorganic species modeled using WHAM VI + 20 % of species bound to fulvic acid ( $\square$ ).

#### 3.3.1.4 Acidic mine drainage (AMD) waters

Acidic waters coming from mine drainage collected at five sites in The Sierra de Cartagena, Spain, were analyzed. The composition of these samples is shown in Table 3.1. As can be observed, their pH range from 1.8 to 2.8. All the samples have very high

concentrations of metals and other inorganic ions, such as sulfate and chloride, compared to most natural waters, consistent with their pH.

**Table 3.1** Element concentrations in waters collected from different sites in the Cartagena mining area. Results are given in mg L<sup>-1</sup>.

Site no.	pH	NO <sub>3</sub> <sup>-</sup>	Cl	PO <sub>4</sub> <sup>3-</sup>	SO <sub>4</sub> <sup>2-</sup>	DOC	Ca
1	2.57	-	288	2	6092	1.35	485
2	2.13	3.5	503	69	40425	4.64	486
3	2.50	0.7	44	56	1157	2.76	224
4	2.77	0.9	852	50	2170	1.79	226
5	1.80	-	330	10	11832	26.43	753
Site no.	K	Na	Al	As	Mg	Fe	Mn
1	846	165	5	-	872	532	155
2	4680	62	58	0.04	166	151	29
3	759	3	146	0.14	37	235	7
4	336	61	359	0.4	16	199	8
5	7229	27	3717	10.2	7493	25904	1299
Site no.	Co	Ni	Cu	Zn	Cd	Pb	
1	0.426	0.344	0.045	430	0.686	0.575	
2	0.467	1.848	0.3	153	0.206	0.111	
3	0.263	1.033	0.709	123	0.36	0.034	
4	1.135	3.934	0.446	232	0.031	0.006	
5	4.896	5.607	9.592	2648	5.614	0.056	

Among the transition metals studied in this chapter, Zn has particularly high concentrations, from 127 to 2648 mg. L<sup>-1</sup>. DGT-labile concentrations of Co, Ni, Cd, Pb and Zn were measured and corrected using the appropriate sigmoid fit. Average DGT-labile concentrations of Cu were used directly. WHAM VI predicted very low FA-metal concentration which means that almost all metal is found as free metal at these low pH values. Thus, results obtained by DGT were compared to the total dissolved metals obtained by ICP (Figure 3.5).

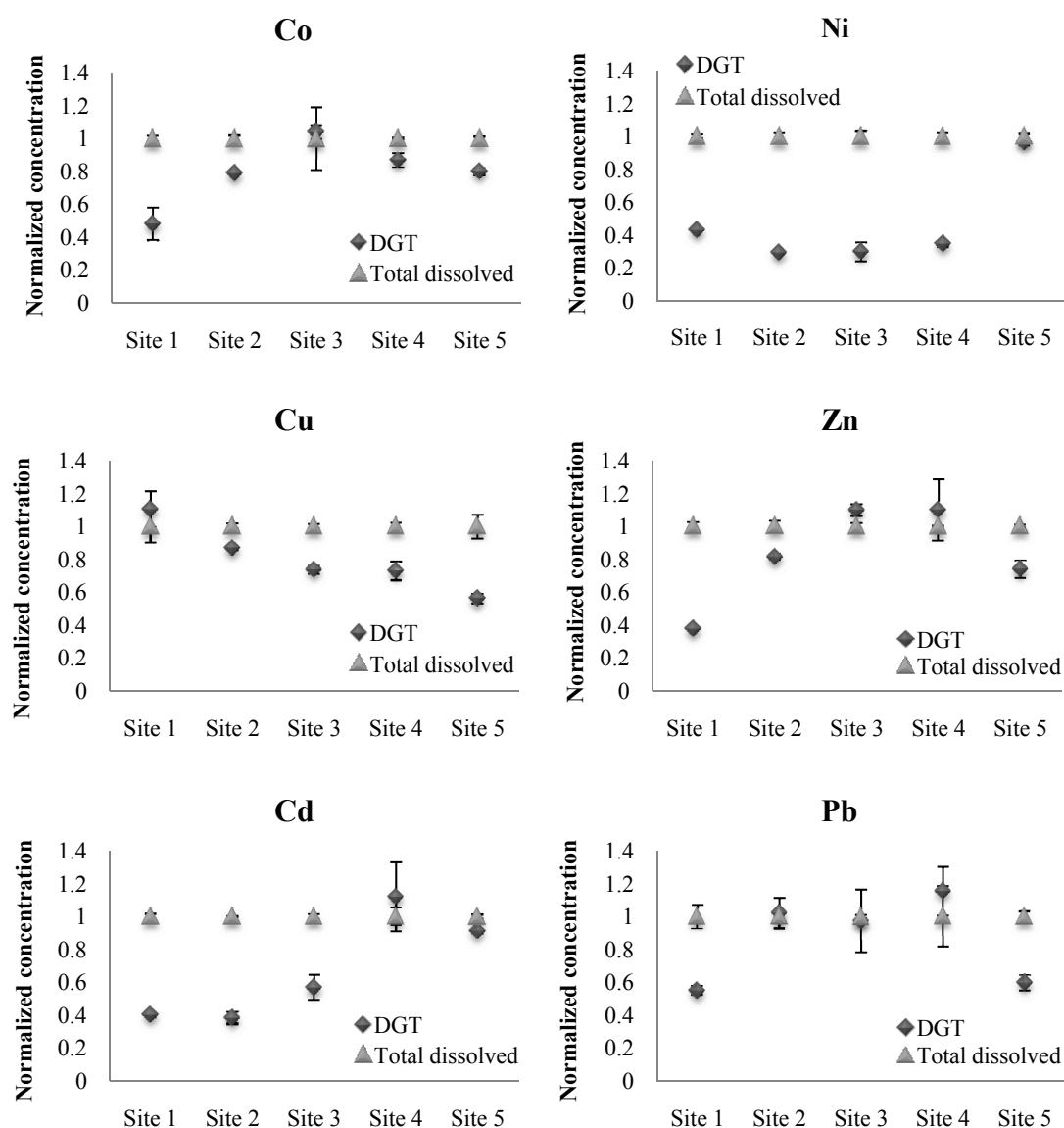


**Figure 3.5** Speciation of different metals at different sites of the mining area of Cartagena, Spain. Points represent mean values divided by Total dissolved concentration and standard deviation of measured DGT-labile concentrations ( $\diamond$ ) and Total dissolved concentrations ( $\triangle$ ).

Generally, results obtained by DGT were lower than those predicted by WHAM for most metals studied, especially at sites 1 and 5 where the highest metal concentrations were found. This lower DGT measurement may be due to (1) the presence of colloids that are not measured by DGT, (2) inaccurate corrections of the pH effect or (3) saturation of the Chelex causing inaccurate measurements. A very short deployment time of 1 h was used to try to prevent saturation effects. However, the metal concentrations are high and therefore the proportion occupation of binding sites might

be high. Any approach to saturation will affect the most weakly binding metal, namely Cd, first. There is evidence that the DGT measurements are proportionally lower for Cd and Ni than for the other metals.

There is no reason to suspect inaccuracies in the correction procedure used at low pH. The sigmoidal relationships fitted the data very well (Figure 3.2) and when they were used to obtain corrected values of  $C_{DGT}$  in the Ca and fulvic acid experiments, good agreement was obtained with  $C_S$  where it was appropriate.

Acidic mine drainage waters are usually finely poised with respect to the precipitation of iron, which can be induced by a very slight change in pH. The presence of colloids is therefore reasonable and DGT provides a good method to establish their presence. Actually, samples from sites 1 and 5 were brown coloured with high content colloids and therefore interfering with the DGT metal measurements.

### 3.3.2 DGT performance in acidic mining wastes

Once DGT performance was tested in acidic aqueous samples and a pH-depending correction was established using sigmoid 5 parameters curve fitted for each metal, DGT performance was tested in acidic mining wastes also collected at eight sites in the Sierra Minera de Cartagena. Moreover, relationships between DGT results and metal concentration found in plants grown in such residues were investigated. Results for these experiments are presented below.

#### 3.3.2.1 pH of mining wastes

pH values of the studied wastes are shown in Table 3.2. The pH of tailings ranged from 2.1 to 7.5. Almost all of them present an acidic pH. Using the classification system of the U.S.D.A. (2010) [3.49], mining tailings from, “Esperanza”, “Brunita” and “Belleza” can be considered ultra acid (pH 1.8-3.4). “Cabecera Avenque” mining waste is classified as extremely acid (pH 3.5-4.4). “Portmán” showed strongly acid pH (pH 5.1-5.5) while “El Galo” is considered moderately acid (pH 5.6-6.0). Finally, “El Lirio” is classified as neutral (pH 6.6-7.3) whereas “La Unión” is considered slightly alkaline (pH 7.4-7.8).

From a general point of view, low values of pH could mean that metals might be potentially available.

**Table 3.2** pH, conductivity and total organic carbon (TOC) values obtained for the different studied residues.

<b>SITE</b>	<b>pH</b>	<b>CONDUCTIVITY (mS/cm)</b>	<b>TOC (%)</b>
<b>Unión</b>	7.5	1.47	1.64
<b>Lirio</b>	7.2	1.23	0.51
<b>Galo</b>	5.9	1.07	0.33
<b>Portmán</b>	5.3	5.02	0.45
<b>Cabecera Avenque</b>	3.6	1.84	0.42
<b>Esperanza</b>	2.5	1.94	0.47
<b>Belleza</b>	2.4	2.92	0.21
<b>Brunita</b>	2.1	5.07	0.3

Usually, electrical conductivity is related to pH because under acidic conditions, the tailing matrix will dissolve more salts. Thus, electrical conductivities at Belleza and Brunita are high because they are points with ultra acid pH. Surprisingly, conductivity at Portmán is higher than those found at Cabecera Avenque, Esperanza and Brunita which are more acidic sites. However, as it will be discussed in next section, total metal content at Portmán is also higher, this could explain the high conductivity of Portmán waste. Finally, all eight zones have low levels of organic carbon.

### 3.3.2.2 Pseudototal heavy metal content

High pseudototal heavy metal concentrations were found at all studied sites, especially lead and zinc. These metals were accompanied with cadmium as a minor element which is also contained in the ores. The high concentration of zinc can be attributed to the large amounts of sphalerite (ZnS), goslarite (ZnSO<sub>4</sub>) and smithsonite (ZnCO<sub>3</sub>) present in the ores. Lead occurs in galena and in carbonates and sulfates as well also present in the mining tailings. Moreover, both, zinc and lead can be present in manganese or iron oxides as impurities [3.50].



**Table 3.3** Pseudototal metal content at the different studied sites.

SITE	PSEUDOTOTAL METAL (mg kg <sup>-1</sup> )		
	Cd	Pb	Zn
<b>Unión</b>	11.1±0.6	2400±400	950±40
<b>Lirio</b>	24±1	2920±80	7300±300
<b>Galo</b>	34.1±0.1	5400±80	11360±40
<b>Portmán</b>	54.3±0.3	3790±20	11530±60
<b>Cabecera Avenque</b>	29±0.1	3690±20	8840±50
<b>Esperanza</b>	24.9±0.7	2800±100	2200±100
<b>Belleza</b>	41.1±0.3	3009±3	5420±90
<b>Brunita</b>	14.8±0.2	1730±80	1280±20

The values are means ± standard deviation (n = 2).

As it can be observed in Table 3.3, the highest concentrations were found at “Galo” and “Portmán” sites which are considered moderately and strongly acid respectively. The lowest metal concentrations were found at sites with the extreme pHs, “Brunita” which is ultra acid, and “Unión” which is slightly alkaline.

### 3.3.2.3 Single Extractions

Besides determination of total metal contents, to assess metal pollution is also very important to gain information on metal mobility. Single extractions methods have proved to be very useful to this end.

The first extract of the BCR sequential extraction procedure (CH<sub>3</sub>COOH 0.11 M as extractant) is suggested to correspond to the more mobile metal fraction. In this sense, metal extracted in this fraction is supposed to be bound in exchangeable positions, water soluble or carbonate-bound. Results obtained for this procedure are depicted in Table 3.4.

In general, it is observed that large amounts of zinc were released in this fraction in wastes with pH above 5 which correspond to high percentage of the pseudototal metal

content (about 50 %). The same trend is observed for cadmium. Although the concentrations of cadmium are much lower than those for lead or zinc, almost 50% of total cadmium was extracted in this fraction in samples with pH above 5. Percentages of lead obtained in mining wastes with higher pHs were lower than zinc and cadmium percentages, but higher in comparison to percentages extracted for wastes with very low pHs. In general, low metal concentration were released in very acidic wastes which translate into low percentages of the pseudototal metal content (lower than 10%) except for zinc in “Brunita” which is almost 35%.

**Table 3.4** Acetic acid extractable fraction and percentages respect of pseudototal metal.

SITE	ACETIC ACID EXTRACTABLE FRACTION (mg kg <sup>-1</sup> )		
	Cd	Pb	Zn
<b>Unión</b>	1.22±0.03 (11%)	206±8 (8.5%)	166±8 (17.5%)
<b>Lirio</b>	12.2±0.4 (51%)	420±30 (14%)	3600±100 (49%)
<b>Galo</b>	16.1±0.4 (47%)	260±10 (5%)	6000±100 (53%)
<b>Portmán</b>	13±0.7 (24%)	71±2 (2%)	3000±300 (26%)
<b>Cabecera Avenque</b>	1.0±0.1 (3.5%)	430±90 (12%)	152±8 (2%)
<b>Esperanza</b>	1.118±0.001 (4.5%)	26±8 (1%)	5±2 (0.22%)
<b>Belleza</b>	0.89±0.07 (2%)	7±0.9 (0.23%)	60±20 (1%)
<b>Brunita</b>	1.264±0.007 (8.5%)	17±2 (1%)	440±10 (34%)

The values are means ± standard deviation (n = 2).

DTPA single extraction procedure has been widely used for predicting plant uptake of different metals. Results obtained for DTPA extractions in this work are summarized in Table 3.5.

**Table 3.5** DTPA-extractable fraction and the percentages related to the pseudototal metal.

SITE	DTPA-EXTRACTABLE FRACTION (mg kg <sup>-1</sup> )		
	Cd	Pb	Zn
<b>Unión</b>	0.394±0.002 (3.5%)	374±9 (16%)	35.7±0.4 (4%)
<b>Lirio</b>	4.72±0.08 (20%)	410±8 (14%)	550±20 (8%)
<b>Galo</b>	5.2±0.2 (15%)	38±3 (0.7%)	910±20 (8%)
<b>Portmán</b>	3.35±0.08 (6%)	4.4±0.2 (0.1%)	577±6 (5%)
<b>Cabecera Avenque</b>	0.14±0.02 (0.5%)	490±70 (13%)	82±5 (1%)
<b>Esperanza</b>	0.14±0.02 (0.6%)	1.6±0.7 (0.05%)	0.50±0.1 (0.02%)
<b>Belleza</b>	0.14±0.01 (0.34%)	0.66±0.05 (0.02%)	10.7±0.8 (0.2%)
<b>Brunita</b>	0.81±0.04 (5.5%)	1.0±0.2 (0.05%)	290±20 (23%)

The values are means ± standard deviation (n = 2).

A relatively high percentage of the total metal content was extracted by DTPA in mining wastes with pH above 5. An average of 10% of the total cadmium content was DTPA-extractable. For zinc, these percentages were lower, around 5%. Quite different percentages were calculated for lead which varies from 0.1% to 15%. For very acidic wastes, the DTPA-extractable fraction was less than 1% in almost all cases, except for lead at “Cabecera Avenque” (13%) and cadmium and zinc at “Brunita” (6% and 22% respectively), the most acidic site. It must be mentioned that DTPA is a polyamino carboxylic acid consisting of a diethylenetriamine backbone with five carboxymethyl groups with pKa values of 1.9, 2.9, 4.4, 8.7 and 10.9. Thus, its metal complexing efficiency decrease when decreasing pH and, moreover, at pH lower than 2, DTPA is completely protonated. This could explain the low DTPA-extractable fraction obtained for very acidic wastes.

The first step of NIST sequential extraction consists on the use of MgCl<sub>2</sub> as extractant reagent. It is supposed that exchangeable metal or water soluble metal is released in this fraction. In this sense, metals that may become environmentally bioavailable via

changes in ionic strength can be identified in this fraction [3.14,3.51]. Results obtained for these set of experiments are collected in Table 3.6.

**Table 3.6** MgCl<sub>2</sub>-extractable fraction and the percentages related to the pseudototal metal.

SITE	MgCl <sub>2</sub> -EXTRACTABLE FRACTION (mg kg <sup>-1</sup> )		
	Cd	Pb	Zn
<b>Unión</b>	0.58±0.02 (5%)	3.4±0.1 (0.14%)	0.49±0.02 (0.05%)
<b>Lirio</b>	2.4±0.1 (10%)	3.1±0.3 (0.10%)	24±2 (0.3%)
<b>Galo</b>	4.4±0.1 (13%)	3±2 (0.06%)	218±9 (2%)
<b>Portmán</b>	3.6±0.1 (7%)	3±2 (0.08%)	243±1 (2%)
<b>Cabecera Avenque</b>	0.541±0.002 (2%)	566±6 (15%)	101.1±0.4 (1%)
<b>Esperanza</b>	0.565±0.005 (2%)	23±2 (0.8%)	1.6±0.3 (0.07%)
<b>Belleza</b>	0.63±0.07 (1.5%)	18.3±0.5 (0.6%)	32.1±0.9 (0.6%)
<b>Brunita</b>	0.82±0.04 (6%)	20±3 (1%)	298.4±0.8 (23%)

The values are means ± standard deviation (n = 2).

It is observed that these results are quite similar to those obtained with DTPA extraction, except for lead. For cadmium, comparable results were obtained at low acidic and neutral pH wastes, but higher percentage is extracted in this fraction in mining wastes with extremely to ultra low pH. Something similar is observed for lead, where percentage for very acidic wastes is quite higher than those obtained with DTPA extraction. In contrast, for acidic to neutral wastes, percentages of lead extracted with MgCl<sub>2</sub> are far lower than percentages obtained with DTPA. This could be explained due to the high affinity that DTPA has for lead.

Although the pseudototal metal concentration in acidic wastes is very high, the general low values obtained for DTPA-extractions and MgCl<sub>2</sub>-extractions in that residues could indicate that most labile metal fraction was previously mobilised through weathering,

therefore the remaining metals in such wastes are strongly bind to the solid phase and, thus, they are not mobile and, subsequently, they are not available for organisms.

### 3.3.2.4 DGT-measured metal concentration in mining wastes

As it has been mentioned in section 3.3.1, DGT performance is influenced by pH. At low pH, competition between hydrogen ions and metal ions is established and thus, metal concentration given by DGT must be corrected using the equations found in such section when soil pH is under 3.5 for cadmium and zinc and, under 3 for lead. Corrected measured metal concentrations by DGT for the mining wastes are shown in Table 3.7.

**Table 3.7** Measured DGT-metal concentration corrected according to pH.

SITE	DGT CONCENTRATION ( $\mu\text{g L}^{-1}$ )		
	Cd	Pb	Zn
<b>Unión</b>	0.135±0.009	2.1±0.2	7±1
<b>Lirio</b>	1.0±0.3	4±1	29±1
<b>Galo</b>	4.3±0.3	8±2	280±20
<b>Portmán</b>	6±1	6.4±0.5	670±30
<b>Cabecera Avenque</b>	0.71±0.07	271±3	170±10
<b>Esperanza</b>	0.427±0.007	9.0±0.9	50±10
<b>Belleza</b>	1.58±0.06	8.82±0.04	280±30
<b>Brunita</b>	6±1	8±2	250±50

The values are means  $\pm$  standard deviation for DGT measurements (n = 3).

It is remarkable the high concentration found by the DGT method for lead at “Cabecera Avenque” site and it is observed that zinc concentration found by this methodology at “Portmán” site is also remarkably high.

In order to study the variation of the metal content in DGT according to the estimated metal mobility and availability of the mining tailings evaluated, single correlation

analyses were performed between the pseudototal metal content and  $\text{MgCl}_2$ -extractable metal contents with the metal concentration given by DGT as it is shown in Figure 3.6.

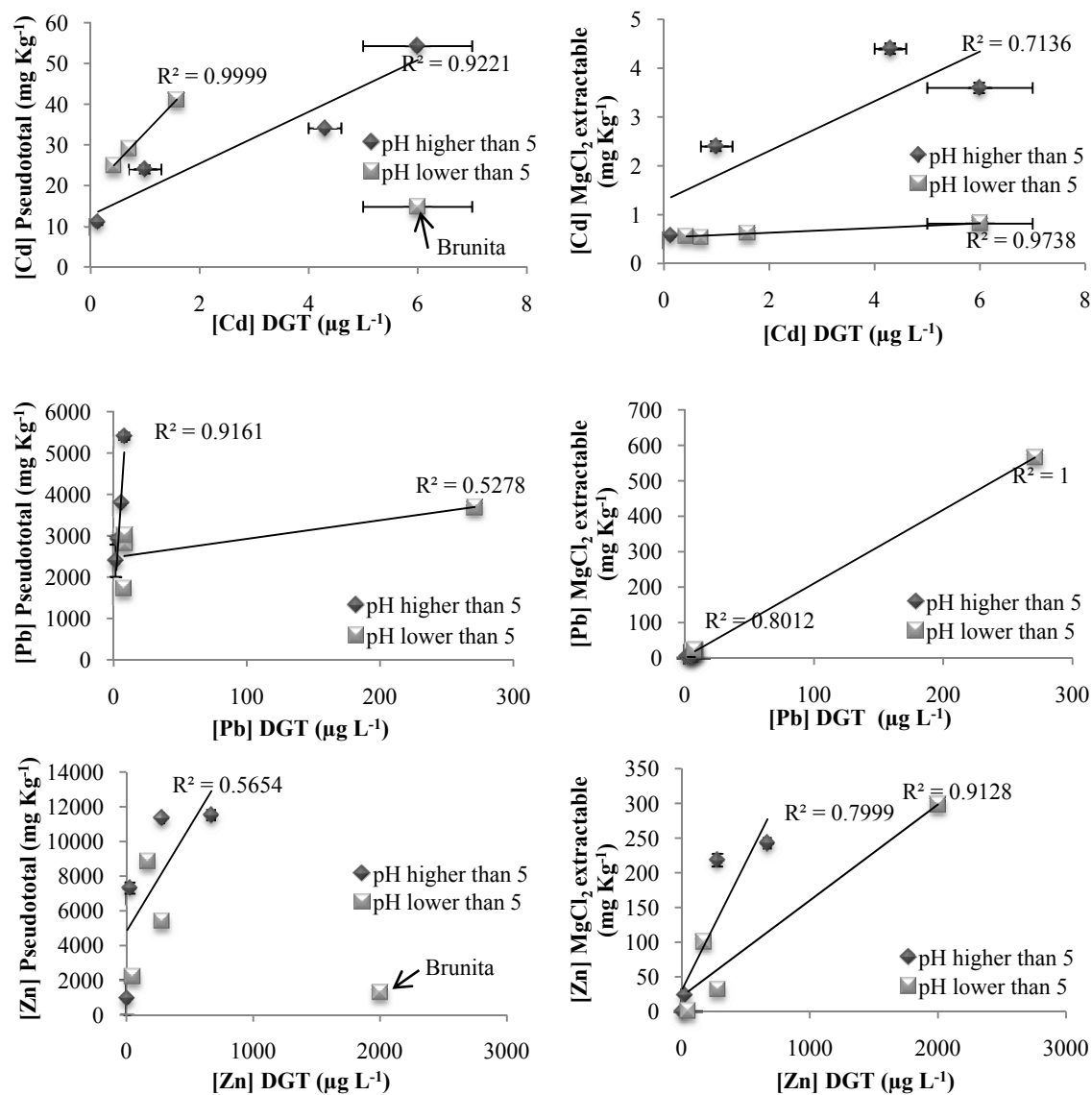


**Figure 3.6** Relationships between DGT metal content and pseudototal and  $\text{MgCl}_2$ -extractable metals in mining wastes.

Metal concentration obtained with the DGT method correlated quite well with the pseudototal metal concentrations, especially for cadmium and lead. However, mining tailings with low pH values show less linearity. “Brunita” site, which is the most acidic waste lies further from linearity in all cases. Also a high correlation for all metal concentration was found between DGT and the first step of NIST extraction procedure.

However, between DGT-concentration and the first step of BCR there was not a good correlation, this could be attributed to the fact that acetic acid also extracts metals bound to carbonates while metals trapped in DGTs mostly originated from easily exchangeable metals and metals weakly bound to labile organic matter. Something similar is observed when correlating DGT results with DTPA procedure.

Pore water of mining waste moisture was collected after removing the DGT-units. As the amount of water that could be recovered by centrifugation was too small for a duplicate analysis, just a single analysis was done in that case. Results for pore water metal concentration are summarized in Table 3.8.

**Table 3.8** Measured metal concentration in pore water.

SITE	PORE WATER CONCENTRATION ( $\mu\text{g L}^{-1}$ )		
	Cd	Pb	Zn
<b>Unión</b>	9.5	11.8	18.3
<b>Lirio</b>	10.2	14.1	250.3
<b>Galo</b>	9.9	11.3	377.4
<b>Portmán</b>	10.1	10.9	4249.5
<b>Cabecera Avenque</b>	9.0	112.6	1487.1
<b>Esperanza</b>	8.1	89.8	500.4
<b>Belleza</b>	12.1	40.2	1536.4
<b>Brunita</b>	14.6	16.2	3087.8

The values are means  $\pm$  standard deviation (n = 3).

Concentrations found in pore water are higher than those given by DGT methodology. This can be easily explained by the fact that pore waters are not well mixed resulting in a depletion of the concentration adjacent to the DGT device. The ratio between DGT-concentration and pore water concentration is always lower than 0.1 for cadmium except at “Galo”, “Portmán” and “Brunita” sites. This could mean that there is no resupply of cadmium at the studied sites except at the three mentioned wastes where there is a significant resupply but insufficient to sustain fully pore water concentration. Something similar is observed for zinc, it can be considered that no resupply occurs in

any case except for “Unión” and “Galo”. In contrast, ratios for lead suggest that resupply of lead is partially sustained at all sites. Moreover, at “Cabecera Avenque”, the ratio is higher than one, but no explanation has been found for this fact. It is possible that, as just one replicate could be measured for pore water, this high value could be attributed to an isolate analysis error.

### 3.3.2.5 Metal content in vegetation specimens (*Crithmum maritimum*)

Plant species and populations differ widely in their ability to accumulate heavy metals. *Crithmum maritimum* specimen has been found to grow in high salinity soils. Thus, this specimen was chosen for our experiments. Plants were grown in non-contaminated soil and then transplanted to the eight mining studied wastes under controlled conditions. However, the high metal content of some wastes produced that, after 45 days, some of the specimens started to die. Specimens grown in moderately acidic to neutral wastes showed higher stability than the ones that were ground at wastes with very low pH. Once harvested, plants were mashed, mixed and roots, shoots and leaves were measured together. Metals determined in *Crithmum maritimum* specimens are reported in Table 3.9.

**Table 3.9** Measured metal concentration in plant.

SITE	PLANT CONCENTRATION (mg kg <sup>-1</sup> )		
	Cd	Pb	Zn
<b>Unión</b>	6.5±0.6	48±7	73±2
<b>Lirio</b>	9±1	85±10	120±10
<b>Galo</b>	6.6±0.3	101±8	190±20
<b>Portmán</b>	6.3±0.2	78±6	390±50
<b>Cabecera Avenque</b>	14.0±0.6	410±50	190±20
<b>Esperanza</b>	7.0±0.6	180±20	130±10
<b>Belleza</b>	5.3±0.7	39.3±0.3	73±3
<b>Brunita</b>	10±1	66±3	162±50

The values are means ± standard deviation (n = 2).



Concentration for zinc varied from 73 to 390 mg kg<sup>-1</sup>, being “Portmán” the specimen with highest accumulated zinc concentration. Lead accumulation ranged from 39 to 410 mg kg<sup>-1</sup>. Lower accumulation was found for cadmium, which ranged from 5 to 14 mg kg<sup>-1</sup>. “Cabecera Avenque” showed the highest accumulation for cadmium and lead while “Belleza”, with ultra acid pH, showed the lowest metal accumulation.

### 3.3.2.6 DGT-plant relationships

In order to establish whether DGT derived concentrations can be used as a bioavailability index for cadmium, lead and zinc at mining wastes, single correlation analyses were performed between the plant content and the metal concentration given by DGT. The DGT device contains a resin which induces a flux of ions from the soil to the resin and thus, it should mimic the action of a plant root. Results are shown in Figure 3.7.

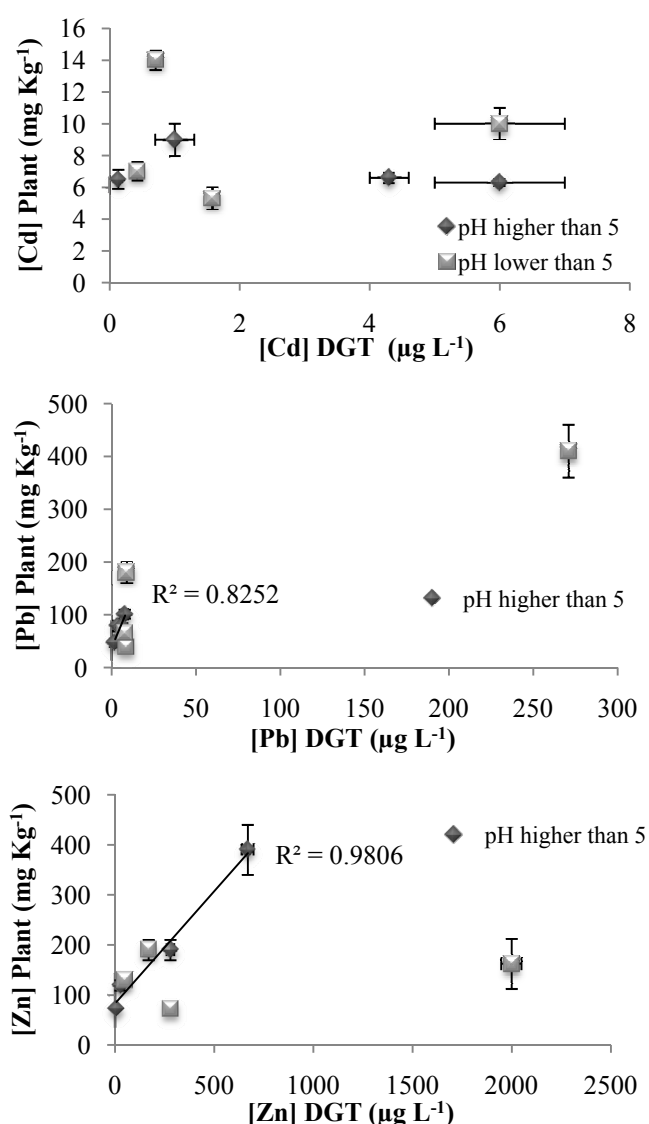


Figure 3.7 Relationships between DGT metal content in mining wastes and plant content.

It is observed that in the case of cadmium, there is not a direct relationship between DGT-measured concentrations and uptake by *Crithmum maritimum* neither in wastes with pH lower than 5 nor in wastes with pH higher than 5, this could be explained due to the low and similar concentrations found at all eight studied waste, with these similar concentrations is difficult to find any correlations between plant and DGT results. In contrast, two different trends are observed in the case of lead and zinc according to the pH of the wastes. For mining wastes with pH higher than 5, a high correlation is established which should suggest that DGT measured lead and zinc concentrations were good for predicting zinc and lead bioavailability in this type of soils. However, at sites with pH lower than 5 no significant correlations were found which indicates that DGT measured concentration is not a good predictor of zinc and lead availability of *Crithmum maritimum* at pH lower than 5.

### 3.4 CONCLUSIONS

In this chapter, it has been demonstrated that the DGT technique can be used to measure labile metal concentrations in acidic waters. The resin gel works properly for Cu at pH 2 and above. Although resin gel efficiency decreases with decreasing pH below 3.5 for Co, Ni, Zn, Cd and Pb, a sigmoid 5 parameters curve could be fitted for each metal and a pH-dependent correction could be applied.

High concentrations of calcium do not affect measurements of metals by DGT at low pH, with the possible exception of Cd, which suggests that DGT devices can be used for speciation technique in such waters.

Experiments with solutions containing fulvic acid demonstrated that at low pH, almost all Cd, Ni, Co and Zn are found as inorganic metal and determined by DGT. However, Cu and Pb bind to some extent to fulvic acid at pH 3, while at pH 5 all metals can bind appreciably to fulvic acid (from 10 to 90%, depending on the metal). Interpretation of the DGT measurement is then more complicated, as the lower diffusion coefficients of metal-fulvic complexes, by about 20% compared to that of inorganic complexes, affects the sensitivity of the measurement.

The performance of DGT as a bioavailability predicting tool has been tested for the first time on acidic mining wastes and pH-dependent corrections have been used for wastes with very acid pH.

Bioavailability studies based on the use of the conventional DTPA single extraction procedure and the first steps of the well established BCR and NIST procedures have also been carried out at the eight mining wastes. Moreover, pseudototal metal content has been determined at those sites.

Significant correlations have been found between the first step of NIST sequential extraction procedures and the DGT-calculated concentrations. Likewise, high correlations have been found between DGT measured concentration and pseudototal metal content. However, it has not been possible to determine clear relationships between metal extracted by the DTPA or BCR procedures with the DGT measured concentration.

Finally, cadmium, lead and zinc have been measured in *Crithmum maritimum* grown on the mining wastes under controlled conditions. Neither DTPA single extraction procedure nor the first step of BCR correlate well with concentrations determined in the vegetation specimens and it can be concluded that, in this case, DTPA and BCR procedures are poor indicators of bioavailability. Correlations between plant metal content with DGT measured metal demonstrate that lead and zinc bioavailability for the *Crithmum maritimum* at pH higher than 5 can be predicted with the DGT methodology. However, in this kind of mining wastes, bioavailability of these two metals at very acid pH and bioavailability of cadmium can not be estimated by the use of DGT.

### 3.5 REFERENCES

- 3.1. T.M. Florence, G.M. Morrison, J.L. Stauber, Determination of trace-element speciation and the role of speciation in aquatic toxicity, *Sci.Total Environ.* 125 (1992) 1-13
- 3.2. B.L. Rivas, I. Moreno-Villoslada, Evaluation of the counterion condensation theory from the metal ion distributions obtained by ultrafiltration of a system poly(sodium 4-styrenesulfonate)/Cd<sup>2+</sup>, *J. Phys. Chem. B* 102 (1998) 11024-11028
- 3.3. J.J. D'Amore, S.R. Al-Abed, K.G. Scheckel, J.A. Ryan, Methods for speciation of metals in soils: a review, *J. Environ. Qual.* 34 (2005) 1707–1745
- 3.4. J.V. García-Meza, A. Carrillo-Chávez, O. Morton-Bermea, Sequential extractions on mine tailings samples after and before bioassays: implications on the speciation of metals during microbial re-colonization, *Environ. Geol.* 49 (2006) 437–448
- 3.5. X. Wang, Y. Liu, G. Zeng, L. Chai, X. Xiao, Xi. Song, Z. Min, Pedological characteristics of Mn mine tailings and metal accumulation by native plants, *Chemosphere* 72 (2008) 1260–1266
- 3.6. A. Boularbah, C. Schwartz, G. Bitton, J.L. Morel, Heavy metal contamination from mining sites in South Morocco: 1. Use of a biotest to assess metal toxicity of tailings and soils, *Chemosphere* 63 (2006) 802–810
- 3.7. Z.H. Ye, W.S. Shu, Z.Q. Zhang, C.Y. Lan, M.H. Wong, Evaluation of major constraints to revegetation of lead/zinc mine tailings using bioassay techniques, *Chemosphere* 47 (2002) 1103–1111.
- 3.8. F. Pagnanelli, E. Moscardini, V. Giuliano, L. Toro, Sequential extraction of heavy metals in river sediments of an abandoned pyrite mining area: pollution detection and affinity series, *Environ. Pollut.* 132 (2004) 189-201
- 3.9. Z. Dang, C. Liu, M. Haigh, Mobility of heavy metals associated with the natural weathering of coal mine spoils, *Environ. Pollut.* 118 (2002) 419-426
- 3.10. M.C. Jung, Heavy metal contamination of soils and waters in and around the Imcheon Au-Ag mine, Korea, *Appl. Geochem.* 16 (2001) 1369-1375
- 3.11. K.F. Mossop, C.M. Davidson, Comparison of original and modified BCR sequential extraction procedures for the fractionation of copper, iron, lead, manganese and zinc in soils and sediments, *Anal. Chim. Acta* 478 (2003) 111-118
- 3.12. A. Baig, T.G. Kazi, M.B. Arain, A.Q. Shah, R.A.Sarfraz, H.I. Afridi, G.A. Kandhro, M.K. Jamali, S. Khan, Arsenic fractionation in sediments of different origins using BCR sequential and single extraction methods, *J. Hazard. Mater.* 167 (2009) 745-751
- 3.13. A. Vaněk, T. Grygar, V. Chrastný, V. Tejnecký, P. Drahota, M. Komárek, Assessment of the BCR sequential extraction procedure for thallium fractionation using synthetic mineral mixtures, *J. Hazard. Mater.* 4 (2009) 913-918

- 3.14. M.K. Schultz, K.G.W. Inn, Z.C. Lin, W.C. Burnett, G. Smith, S.R. Biegalski, J. Filliben, Identification of radionuclide partitioning in soils and sediments: determination of optimum conditions for the exchangeable fraction of the NIST standard sequential extraction protocol, *Appl. Radiat. Isotopes* 49 (1998) 1289-1293
- 3.15. H. Zhang, W. Davison, Performance Characteristics of diffusion gradients in thin films for the in situ measurement of trace metals in aqueous solution, *Anal.Chem.* 67 (1995) 3391-3400
- 3.16. H. Zhang, W. Davison, S. Miller, W. Tych, In situ high resolution measurements of fluxes of Ni, Cu, Fe, and Mn and concentrations of Zn and Cd in porewaters by DGT, *Geochim. Cosmochim. Ac.* 59 (1995) 4181-4192
- 3.17. M.P. Harper, W. Davison, H. Zhang, W. Tych, Kinetics of metal exchange between solids and solutions in sediments and soils interpreted from DGT measured fluxes, *Geochim. Cosmochim. Ac.* 62 (1998) 2757-2770
- 3.18. B. Vrana, I.J. Allan, R. Greenwood, G. A. Mills, E. Dominiak, K. Svensson, J. Knutsson, G. Morrison, Passive sampling techniques for monitoring pollutants in water, *Trac-Trend. Anal. Chem.* 24 (2005) 845-868
- 3.19. S. Denney, J. Sherwood, J. Leyden, In situ measurements of labile Cu, Cd and Mn in river waters using DGT, *Sci. Total Environ.* 239 (1999) 71-80
- 3.20. W. Li, H. Zhao, P.R. Teasdale, F. Wang, Trace metal speciation measurements in waters by the liquid binding phase DGT device, *Talanta* 67 (2005) 571-578
- 3.21. T. Yapici, I.I Fasfous, J. Murimboh, C.L. Chakrabarti, Investigation of DGT as a metal speciation technique for municipal wastes and aqueous mine effluents, *Anal. Chim. Acta* 622 (2008) 70-76
- 3.22. R. Buzier, M. Tusseau-Vuillemin, J. Mouchel, Evaluation of DGT as a metal speciation tool in wastewater, *Sci. Total Environ.* 358 (2006) 277-285
- 3.23. J. Søndergaard, In situ measurements of labile Al and Mn in acid mine drainage using diffusive gradients in thin films, *Anal. Chem.* 79 (2007) 6419-6423
- 3.24. J. Søndergaard, B. Elberling, G. Asmund, Metal speciation and bioavailability in acid mine drainage from a high arctic coal mine waste rock pile: temporal variations assessed through high-resolution water sampling, geochemical modelling and DGT, *Cold Reg. Sci. Technol.* 54 (2008) 89-96
- 3.25. L.S. Balistrieri, R.R. Seal, N.M. Piatak, B. Paul, Assessing the concentration, speciation, and toxicity of dissolved metals during mixing of acid-mine drainage and ambient river water downstream of the Elizabeth copper mine, Vermont, USA, *Appl. Geochem.* 22 (2007) 930-952
- 3.26. J. Gimpel, H. Zhang, W. Hutchinson, W. Davison, Effect of solution composition, flow and deployment time on the measurement of trace metals by the diffusive gradient in thin films technique, *Anal. Chim. Acta* 448 (2001) 93-103
- 3.27. K.W. Warnken, H. Zhang, W. Davison, Theory and applications of DGT, *Environ. Monitor. Elsevier* (2007) 251-278

- 3.28. W. Davison, H. Zhang, K.W. Warnken, Chapter 16 Theory and applications of DGT arsenic measurements in soils and sediments, *Comp. Anal. Chem.* 48 (2007) 353-378
- 3.29. H. Zhang, W. Davison, B. Knight, S. McGrath, In situ measurement of solution concentrations and fluxes of trace metals in soils using DGT, *Environ. Sci. Technol.* 32 (1998) 704–710
- 3.30. H. Zhang, W. Davison, Performance characteristics of diffusion gradients in thin films for the in situ measurement of trace metals in aqueous solution. *Anal. Chem.* 67 (1995) 3391–3400
- 3.31. P.S. Hooda, H. Zhang, W. Davison, A.C. Edwards, Measuring bioavailable trace metals by diffusive gradients in thin films (DGT): soil moisture effects on its performance in soils, *Eur. J. Soil Sci.* 50 (1999) 285-294
- 3.32. J. Song, F.J. Zhao, Y.M. Luo, S.P. McGrath, H. Zhang, Copper uptake by *Elsholtzia splendens* and *Silene vulgaris* and assessment of copper phytoavailability in contaminated soils, *Environ. Polluti.* 128 (2004) 307-315
- 3.33. I. Cattani, G. Fragoulis, R. Boccelli, E. Capri, Copper bioavailability in the rhizosphere of maize (*Zea mays* L.) grown in two Italian soils, *Chemosphere* 64 (2006) 1972-1979
- 3.34. S. Mason, R. Hamon, H. Zhang, J. Anderson, Investigating chemical constraints to the measurement of phosphorus in soils using diffusive gradients in thin films (DGT) and resin methods, *Talanta* 74 (2008) 779-787
- 3.35. N.W. Menzies, B. Kusumo, P.W. Moody, Assessment of P availability in heavily fertilized soils using the diffusive gradient in thin films (DGT) technique, *Plant Soil* 269 (2005) 1-9
- 3.36. T.A. Sogn, S.Eich-Greatorex, O. Røyset, A.F. Øgaard, A.R. Almås1, Use of diffusive gradients in thin films to predict potentially bioavailable selenium in soil, *Commun. Soil Sci. Plant* 39 (2008) 587-602
- 3.37. L. Duquène, H. Vandenhove, F. Tack, M. Van Hees, J. Wannijn, Diffusive gradient in thin films (DGT) compared with soil solution and labile uranium fraction for predicting uranium bioavailability to ryegrass, *J. Environ. Radioactiv.* 101 (2010) 140-147
- 3.38. H. Vandenhove, K. Antunes, J. Wannijn, L. Duquène, M. Van Hee, Method of diffusive gradients in thin films (DGT) compared with other soil testing methods to predict uranium phytoavailability, *Science of the Total Environment*, 373 (2007) 542-555
- 3.39. A.L. Pérez, K.A. Anderson, DGT estimates cadmium accumulation in wheat and potato from phosphate fertilizer applications, *Sci. Total Environ.* 407 (2009) 5096-5103
- 3.40. K.W. Warnken, H. Zhang, W. Davison, Trace metal measurements in low ionic strength synthetic solutions by diffusive gradients in thin films, *Anal. Chem.* 77 (2005) 5440-5446
- 3.41. H.M. Conesa, R. Schulin, B. Nowack, Mining landscape: a cultural tourist opportunity or an environmental problem? The case of the Cartagena-La Unión Mining District (SE Spain), *Ecol. Econ.* 64 (2008) 690–700

- 3.42. H.M. Conesa, B.H. Robinson, R. Schulin, B. Nowack, Metal extractability in acidic and neutral mine tailings from the Cartagena-La Unión Mining District (SE Spain), *Appl. Geochem.* 23 (2008) 1232–1240
- 3.43. C. García-García, Impacto y riesgo ambiental de los residuos mineros metalúrgicos de la Sierra de Cartagena-La Unión (Murica-España) (Tesis Doctoral), 2004, Universidad Politécnica de Cartagena
- 3.44. K. Gartley, Chapter 10: Recommended Soluble Salts Tests. In J. T. Sims, A. Wolf (eds.) *Recommended Soil Testing Procedures for The Northeastern United States*. Northeast Regional Bulletin 493, Agricultural Experiment Station University of Delaware, Newark, DE (2009).
- 3.45. K.W. Warnken, H. Zhang, W. Davison, In-situ monitoring and dynamic speciation measurements in solution using DGT, Elsevier (2005)
- 3.46. E. Tipping, M.A. Hurley, A unifying model of cation binding by humic substances, *Geochim. Cosmochim. Acta* 56 (1992) 3627-3641
- 3.47. H. Zhang, W. Davison, Diffusional characteristics of hydrogels used in DGT and DET techniques, *Anal. Chim. Acta* 398 (1999) 329-340
- 3.48. E.R. Unsworth, K.W. Warnken, H. Shang, W. Davison, J. Buffle, J. Cao, R. Cleven, J. Galceran, P. Gunkel, E. Kalis, D. Kistler, H.P. Van Leeuwen, M. Martin, S. Noel, Y. Nur, N. Odzak, J. Puy, W. Van Riemsdijk, L. Sigg, E. Temminghoff, M. Tercier-Waeber, S. Toepperwien, R.M. Town, L. Weng, H. Xue, Model predictions of metal speciation in freshwaters compared to measurements by in situ techniques, *Environ. Sci. Technol.* 40 (2006) 1942-1949
- 3.49. USDA (United States Department of Agriculture). Natural resources conservation service. National soil survey handbook. [Online] <http://soils.usda.gov/technical/handbook/contents/part618.html#48> (1 January 2010)
- 3.50. G. Garcia, J.M. Peñas, J.I. Manteca, Zn mobility and geochemistry in surface sulfide mining soils from SE Spain, *Environ. Res.* 106 (2008) 333-339
- 3.51. M.K. Schultz, W.C. Burnett, Partitioning of radioactive elements in NIST natural matrix standards, NIST Speciation Workshop, *J. Res. Natl. Inst. Stan.* 101 (1996) 707-715

# GENERAL DISCUSSION

---







Novel procedures based on inductively coupled plasma (ICP) spectroscopic techniques have been developed in this thesis, as well as other analytical existing methodologies have been applied to the assessment of pollution indicators in the environment. The use of diffusive gradients in thin films (DGT) technique has also been proved for the first time in acidic contaminated mining samples. The developed methodologies have been applied to the analysis of different types of samples from the abandoned mining area of Cartagena.

Over the last 25 years, inductively coupled plasma (ICP) has become an indispensable tool for chemical elemental analysis. The ICP quadrupole mass spectrometry (ICP-QMS) has been used as a sensitive technique for the simultaneous determination of trace elements in different matrices due to its good performance in terms of robustness, sample throughput and simplified sample preparation. However, it is well known that it suffers from both, spectral and non-spectral interferences. Spectral interferences in ICP-MS occur in two forms, the overlap of one isotope with another (isobaric interference), or the overlap of one isotope with a species derived from the ion beam sampling process (polyatomic interference and double charged species). Isobaric interference is a result of equal mass isotopes of different elements present in the sample solution. Polyatomic interferences are due to the recombination of sample and matrix ions with other matrix components or elements from the air such as O, N, H, etc or with Ar from the plasma. Some examples of such interferences are  $^{14}\text{N}_2^+$  on  $^{28}\text{Si}^+$ ,  $^{40}\text{Ar}_2^+$  on  $^{80}\text{Se}^+$ ,  $^{16}\text{O}_2^+$  on  $^{32}\text{S}^+$  or  $^{40}\text{Ar}^{35}\text{Cl}^+$  on  $^{75}\text{As}^+$ . Non-spectral interferences appear when matrix induces changes in signal intensity which are related not to the presence of a spectral component but to the presence of certain components affecting nebulization, transport and ionization processes. It is well known that sodium causes a decrease in the analyte signal while small amounts of organic compounds enhance the element signal. Some strategies have been developed for alleviating these interferences. Usually, non-spectral interferences are overcome by the use of internal standards or the standard addition method. An internal standard is a non-analyte element that is added to the blank solution, standards and samples before analysis and it is supposed to behave the same as the analyte. Its selection is a very important step as all results will depend on the internal standard behavior. Spectral interferences can be solved or reduced using mathematical

corrections, cool plasma, desolvation of the aerosol, matrix elimination, collision or reaction cells or using high resolution (HR) mass spectrometers.

Some elements can be released from its matrix before being introduced into the ICP. In this sense, hydride generation has been used to form volatile hydrides with high efficiency and velocity as a sample introduction technique, not only to avoid interferences from matrix but also to enhance sensitivity. A collision reaction cell consists of a multipole (octopole, hexapole or quadrupole) where a collision/reaction gas is introduced to promote ion-molecule reactions or collisions with the aim of eliminating spectral interferences arising from air, argon, matrix or solvent. The analytical response can be further affected by different factors related to the collision cell. Therefore, an optimization of the collision/reaction cell must be always done: collision and reaction gases flow rates must be optimized as well as the potential applied in the cell. On the other hand, in this thesis, sulfide and arsenic have been determined by ICP-QMS applying the above strategies to overcome spectral and non-spectral interferences.

Sulfide has received special attention as a metal ligand in anoxic waters and it has been considered an important pollution index for different types of waters. However, sulfur isotopes are particularly difficult to measure accurately by ICP-QMS due to the large interference from  $^{16}\text{O}^{16}\text{O}^+$  on  $^{32}\text{S}^+$  as well as  $^{16}\text{O}^{17}\text{O}^+$  on  $^{33}\text{S}^+$  and  $^{16}\text{O}^{18}\text{O}^+$  on  $^{34}\text{S}^+$ . In the present thesis, it has been demonstrated that sulfide can be easily determined by ICP-QMS by removing it from the matrix and using a collision/reaction cell to reduce such spectral interferences. In a vapor generator (VG), sulfide reacts with hydrochloric acid to form hydrogen sulfide which can be removed from the matrix and introduced to the ICP as a gas. The elimination of the sample solvent results in a dramatic reduction of the interfering  $\text{O}_2^+$  background ions at  $m/z$  32. Moreover, when pressuring the collision reaction cell with  $\text{H}_2$  and He gases, the sensitivity of the method can be increased. However, an optimization of some instrumental parameters must be done. To this end, a  $2^3$  full factorial design, involving the variables octopole bias, quadrupole bias and helium flow rate, and a simplex method have been developed; the optimum conditions have been found when octopole bias was set at -3.8 V, helium flow rate at  $0.7 \text{ mL min}^{-1}$  and quadrupole bias at -8.0 V. The reliability of this method has been confirmed through comparison with the results from a reference method. Lower concentrations can be determined with the developed VG-ICP-QMS method, which has a limit of detection

of  $2 \mu\text{g L}^{-1}$ . This LOD is almost 10 times lower than that obtained with the potentiometric method of reference.

On the other hand, the interest on arsenic has gained importance during the last decades due to its potential toxicity. It has been reported for many years that exposure to arsenic can have a variety of adverse health effects, including skin and internal cancers or cardiovascular and neurological disorders. It is well known that arsenic determination by ICP-MS suffers from both spectral and non-spectral interferences. Possibly, the most important drawback of ICP-QMS equipped with a pneumatic nebulizer is the formation of  $^{40}\text{Ar}^{35}\text{Cl}^+$  interference obtained when moderate chloride ( $\text{mg L}^{-1}$ ) matrices are introduced into the ICP-MS. As this interference has the same mass charge ratio ( $m/z$ ) as arsenic, results can be inaccurate, especially when low levels of arsenic are determined. The optimization of collision/reaction gas flow rates has been carried out and a mixture of  $2.9 \text{ mL min}^{-1}$  of  $\text{H}_2$  and  $0.5 \text{ mL min}^{-1}$  of  $\text{He}$  has been found to be suitable for the removal of  $^{40}\text{Ar}^{35}\text{Cl}^+$  interference. The use of mathematical corrections has also been studied to overcome spectral interferences on arsenic. In this sense, the interference equation proposed by USEPA for arsenic determination, Method 200.8, and its modification proposed by Cai et. al. have been studied under complex matrix conditions containing high amounts of chloride and sodium. Although the use of arithmetic corrections is necessary when no gas is used in the collision/reaction cell, it does not completely eliminate persistent interferences produced in the plasma. First equation behaved reasonably well with spiked samples under vented cell conditions. However, with a pressurized cell, this equation can not be used due to the formation of  $^{81}\text{Br}^1\text{H}^+$  which interferes on the  $^{82}\text{Se}^+$  signal. In this sense, a modification of the arithmetic equation must be made when it is used together with a pressurised collision/reaction cell. The second equation can not be used neither under vented cell conditions nor under pressurized cell conditions due to the formation of  $^{35}\text{Cl}^{23}\text{Na}^{23}\text{Na}^+$  which interferes on the  $^{83}\text{Kr}^+$  signal.

For alleviating the non-spectral interferences and enhancing sensitivity, alcohol addition and internal standard technique have been applied for arsenic determination by ICP-QMS. It has been verified that the presence of 4% (v/v) of ethanol or methanol results in an increase in arsenic sensitivity, this enhancement depends on the nebulizer gas flow rate and it is more important under pressurized cell conditions. This indicates that the presence of alcohol promotes an effect that leads to a higher transition of  $^{75}\text{As}^+$  ions in

the pressurized cell. Under vented cell conditions the addition of alcohol also results in a decrease of the formation of polyatomic interference ( $^{40}\text{Ar}^{35}\text{Cl}^+$ ). However, this decrease has not been observed under pressurized cell conditions as the interference is almost totally eliminated. Eight elements have been studied as internal standards for arsenic determination taking into account their atomic mass and ionization potential. The internal standards selected were gallium, germanium, yttrium, rhodium, iridium, platinum, gold and thallium. It has been found that elements with similar atomic mass behave more similarly to arsenic than elements with similar ionization potential, in the presence of different amounts of sodium and under different experimental conditions, such as the use of a pressurized collision/reaction cell and the addition of carbon containing compounds. Therefore, elements with similar mass can be used as internal standards if they are not present in the samples. In this case, rhodium has been found to be the most suitable element for arsenic determination in the presence of sodium and ethanol, under both vented and pressurized cell conditions. The reliability of the method has been proved by analyzing spiked aqueous samples and certified reference material under the described conditions. These results showed that alcohol addition slightly improves accuracy and precision under pressurized collision/reaction cell conditions. Moreover, a comparison of the results obtained with and without alcohol addition can be used to verify the absence of spectral interferences.

ICP atomic emission spectrometry (ICP-AES) is one of the most common techniques for elemental analysis due to its high specificity, multi-element capability, robustness and rapid sample throughput. However, it suffers from interferences. Non-spectral effects such as matrix effects are also common in ICP-AES and spectral interferences are usually caused by overlap of a spectral line from another element, or by unresolved overlap of molecular spectra, from background contribution or stray light from the line emission of high-concentration elements. Moreover, wavelengths below 190 nm are absorbed by oxygen or water vapor; in such case, spectrometers must be evacuated or purged. Vacuum optical systems for ICP spectrometry have the problem that they are often not able to attain a perfect vacuum and that back-streaming vapours from the oil-filled vacuum pumps cause coatings on the optical surfaces of the spectrometer. A successful approach to avoid these disadvantages is a nitrogen-filled optical system. This technique allows element determinations down to a wavelength of 120 nm. Sulfide

can be determined by ICP-AES, but as the spectral sulfur emission lines are below 190 nm, its determination by means of ICP-AES requires purging the path between the plasma and the monochromator with N<sub>2</sub>. Moreover, the elimination of the aqueous matrix through a vapor generator, as it has been described above, enhances the sensitivity due to the elimination of water vapor which can absorb sulfur wavelengths. However, hydrogen sulfide formed in a hydrochloric acid stream can be introduced using a conventional ICP-AES liquid sample introduction system (i.e. a pneumatic concentric nebulizer coupled to a spray chamber). With this configuration a liquid aerosol is generated and solution droplets reach the excitation cell. This has two important implications: with this assembly matrix effects are noticeable if complex samples like wastewaters are being analyzed, and it is not advisable to use buffering solutions containing sodium. Fortunately, an ammonia/ammonium buffer solution also provides satisfactory results. The advantage of such configuration is that it allows the simultaneous determination of several parameters, thus shortening the time of any eventual water analysis. This system has been proved to be efficient for the determination of both sulfide and sulfate concentrations. However, the system based on the use of a gas-liquid separator is only applicable to the determination of sulfide.

All methodologies provide similar sensitivities, limits of detection, and dynamic range. These analytical figures of merit are better than those provided by the conventional potentiometric method. The analysis of environmental waters and sediments has demonstrated that the results obtained by the developed methods do not differ significantly from those found with a selective electrode; in addition, lower concentration can be determined more accurately.

The last technique applied in this thesis is the diffusive gradients in thin films (DGT). This technique has been widely used for in situ dynamic trace metal measurement in liquid and solid samples. Moreover, DGT was proposed as a speciation device. The technique is based on the diffusion of dissolved metal species in a polyacrylamide gel and measures the free metal ion and labile complexes. Because DGT is a selective sampler, this technique can remove interferences encountered with other techniques such as electrochemical techniques. The device can be used with different kinds of diffusive gels and binding agents. The pore size of the diffusive gel can be controlled, and thus, the size of complexes that cross the gel can be also controlled. Chelex-100 is

generally used as a binding agent as it can bind a large number of metals. However, other binding phases have been studied for trace metal speciation. DGT technique has already been used for labile metal measurements in waters with pH in the range from 5 to 10. However, a limitation of DGT is the reduced performance of the chelating Chelex resin at low pH, due to the competition between metals and hydrogen ions for the binding agent. In this thesis, it has been demonstrated that the DGT technique can be used to measure labile metal concentrations in acid waters. Resin gel efficiency decreases with decreasing pH. Hence, below 3.5 for cobalt, nickel, zinc, cadmium and lead, a sigmoid 5 parameters curve can be fitted for each metal and a pH-dependent correction can be applied. The resin gel works properly for copper at pH 2 and above. The effect of calcium and fulvic acid on the adsorption of different metals on the resin gel has also been studied under controlled laboratory conditions. The presence of calcium does not significantly affect DGT performance except when it is at very high concentrations ( $10 \text{ mmol L}^{-1}$ ) for the measurement of cadmium at pH 3.5. These calcium concentrations are usually only found in sea water, but the pH in such samples is usually higher than 7 and it was previously demonstrated that under these conditions competition by calcium is not a problem. Experiments with solutions containing fulvic acid demonstrated that at low pH, almost all cadmium, nickel, cobalt and zinc are found as inorganic metal and they are determined by DGT. However, copper and lead bind to some extent to fulvic acid at pH 3. At pH 5 all metals can bind appreciably to fulvic acid (from 10 to 90%, depending on the metal). Interpretation of the DGT measurement is then more complicated, as the lower diffusion coefficients of metal-fulvic complexes, by about 20% compared to that of inorganic complexes, affects the sensitivity of the measurement. The experimental results have compared well with predictions of speciation made using the speciation program WHAM VI. DGT has been used with correction for low pH to measure metals in waters from acid mine drainage containing high amounts of lead, zinc and cadmium. Generally, results obtained by DGT were lower than those predicted by WHAM for most metals studied. These lower values could be explained taking into account the matrix complexity of the samples analyzed, with high contents of elements that could lead to the saturation of the chelex resin and high values of ionic strength which could affect DGT performance. However, for cobalt, zinc and lead there is a quite good agreement between DGT measured concentrations and WHAM VI predictions for the samples containing these metals at lower concentrations. These results indicate that DGT can be used to measure these

elements at trace level in acid mining drainage even in the presence of high amounts of calcium and other metals at pH as low as 2.

For the first time, DGT devices have been also deployed in acidic mining wastes with pH ranging from 2 to 7 to assess zinc, lead and cadmium availability to vegetation. Eight residues from the abandoned mining area of Cartagena, Spain, have been studied. The results obtained with the DGT device have been compared with other bioavailability tests such as metal concentration in pore water or in selective extracts. In this way, the DTPA extraction protocol and the first steps of BCR and NIST standardized sequential extraction procedures have been carried out. Pseudototal metal content has been also determined at the eight studied sites. Significant relations have been found between the first step of NIST sequential extraction procedures and the DGT-calculated concentrations. Likewise, high correlations have been found between DGT measured concentration and pseudototal metal content. However, it has not been possible to determine clear relationships between metal extracted by neither DTPA nor BCR procedures with the DGT measured concentration.

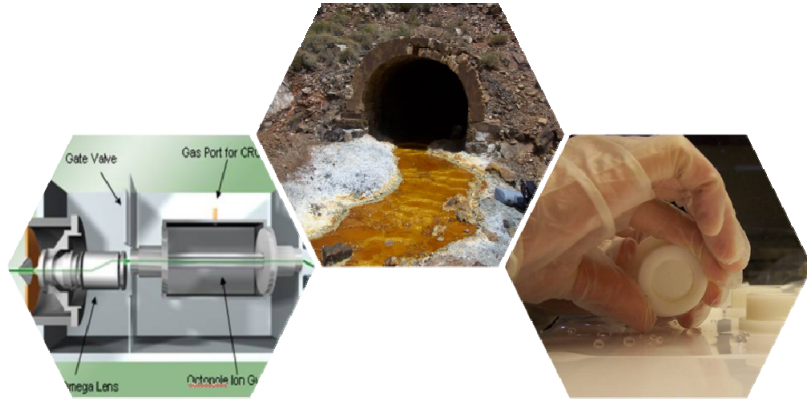
Finally, the DGT-recovered metal concentration has been also correlated with metal content in *Crithmum maritimum* species grown on the mining wastes under controlled laboratory conditions. It has been observed that in the case of cadmium, there is not a direct relationship between DGT-measured concentrations and uptake by *Crithmum maritimum* neither in wastes with pH lower than 5 nor in wastes with pH higher than 5. In contrast, significant relation between the lead concentration in the DGT-device and the lead concentration in *Crithmum maritimum* has been observed. Thus, it can be concluded that the DGT measured lead concentration is a good predictor of availability for *Crithmum maritimum* grown in mining wastes even at very low pH. Two different trends have been observed in the case of zinc according to the pH of the wastes. For mining wastes with pH higher than 5, a high correlation has been observed, meanwhile at sites with pH lower than 5 no significant correlation has been found. These observations indicate that DGT measured zinc concentrations were good for predicting zinc bioavailability on *Crithmum miritimum* in soils with pH higher than 5 but not for soils with lower pH.





# GENERAL CONCLUSIONS

---





In this thesis, the development of analytical methods based on spectroscopic ICP techniques for sulfide and arsenic determination has been carried out and they have been applied to different types of environmental samples. Moreover, the use of DGT technique in acidic aqueous and soil samples has also been deeply studied.

Even though detailed conclusions from the present work have been included in each chapter, the main conclusions are highlighted below:

1. The determination of sulfide in aqueous matrix can be carried out by means of ICP spectroscopy through the formation of hydrogen sulfide in a vapor generator. Different approaches have been used for this purpose:
  - a) ICP-MS can be used for sulfide determination with a previous separation of the matrix. The use of a collision/reaction cell improves the sensitivity of the method when it is pressurized with H<sub>2</sub> and He gases. Moreover, sulfide in sediments can also be determined with the developed method using the purge-and-trap procedure proposed by EPA.
  - b) Sulfide in water can also be determined using ICP-AES after being transformed to hydrogen sulfide. On one hand, it can be determined after being separated from the aqueous matrix in a vapor generator. On the other hand, a hydrochloric acid stream and a conventional liquid sample introduction system can be used for sulfide introduction in the ICP-AES; in this case hydrogen sulfide is not released from the matrix.
2. The reliability of these three developed methodologies, based on ICP spectrometry, for sulfide determination was confirmed through comparison with the results obtained with the conventional potentiometric method. In all cases lower detection and quantification limits were achieved.
3. The use of a conventional liquid sample introduction system allows the simultaneous determination of sulfide and sulfate as the aqueous matrix is not eliminated. For sulfate determination, acid stream must be substituted by a water stream.
4. The determination of arsenic in complex aqueous matrices has been achieved by means of ICP-MS equipped with a collision/reaction cell and the application of different strategies to overcome spectral and non-spectral interferences:

- a) A modification of the USEPA mathematical correction for arsenic determination by ICP-MS allows the determination of such element in complex matrix aqueous samples when the collision/reaction cell is pressurized.
  - b) Although  $^{40}\text{Ar}^{35}\text{Cl}^+$  interference is almost totally eliminated by using a collision/reaction cell, it has been observed that the presence of small amounts of alcohol improves this reduction and, moreover, carbon-containing compounds produce an enhancement of the analyte signal when the collision/reaction cell is pressurized.
  - c) It has been demonstrated that, under all studied conditions, internal standards with similar mass to arsenic behave more similar to this metalloid than elements with similar ionization potential.
5. pH-depending correction curves have been fitted for the determination of different metals in acidic water with the DGT technique at low pH. Moreover, the effects of calcium and fulvic acid at these low pHs have been studied and successfully compared with the speciation program WHAM VI predictions. DGT devices have been successfully applied for the determination of Co, Ni, Cu, Zn, Cd and Pb in different acid mining drainage waters.
  6. DGT units have been applied to acid mining wastes as a predicting tool for zinc, cadmium and lead bioavailability. Moreover, the DTPA single extraction procedure and the first step of BCR and NIST sequential extraction procedures have been used as approaches to predict mobility of metals in the mining wastes. Pseudototal metal content has also been determined in such residues. Results obtained for DGT measurements correlated well with results obtained for pseudototal metal content and the first step of NIST extraction procedure while neither DTPA single extraction nor the first step of BCR correlated well with DGT measured concentrations.
  7. Metal content in *Crithmum maritimum* grown on the mining wastes under controlled laboratory conditions has been also measured and correlated to DGT results. Lead and zinc bioavailability can be predicted by DGT at pH higher than 5, but no good correlations were observed at lower pHs.





Finalment ha arribat el moment dels agraïments. Això significa que la tesi ja està gairebé enllestida, que tanco una etapa de la meua vida. Ara mateix, són tantes les sensacions que experimento, que el meu cap va més ràpid que els meus dits. Però no puc passar pàgina sense abans donar les gràcies a totes aquelles persones que directament o indirectament m'han ajudat a tirar endavant aquesta tesi.

Tots sabem que darrere una tesi, a part del doctorand, hi ha altres persones que són tan o més importants, els directors de tesi. Jo no hauria començat mai aquest treball si la Nela i la Mònica no m'haguessin oferit fer un doctorat a la seva àrea. Uns quants anys després els haig de donar les gràcies per donar-me aquesta oportunitat, per haver confiat en mí en aquell moment i per no haver-me abandonat mai durant la recerca. Gràcies per la vostra ajuda, guia i experiència. Permet-me Nela, un agraïment especial per la Mònica, perquè aquesta és la seva primera tesi com a directora, i jo he tingut la sort de ser la seva primera doctoranda.

Hi ha molts moments en la investigació en què les coses no surten tal com voldries, és per això que és molt important tenir al teu voltant persones que sàpiguen com animar-te i ajudar-te. És fonamental estar rodejat d'un bon equip i crec que jo no n'hauria trobat cap de millor fora de l'Àrea de Química Analítica on, a part de companys, he trobat amics. Gràcies a tots per aquests anys, els que hi sou i els que ja n'heu anat marxant. Victòria, Juanma, Enriqueta i Clàudia, gràcies per oferir sempre la vostra experiència i aconsellar en tots aquells dubtes científics i no tan científics que es van plantejant. Eva, gràcies per encomanar les teves ganes de treballar, et desitjo molta sort en aquest món. Chantal i Ester, moltes gràcies per totes les hores que m'heu dedicat, pels moments que hem passat juntes i per escoltar-me sempre que ho he necessitat,



*molta sort a totes dues pel que us espera. Marta (tal com deies tu, la meua parella de fet) gràcies per ajudar a fer més curts els llargs viatges que ens ha tocat fer durant les nostres tesis. Gràcies també, junt amb la Mercè, pels berenars que hem compartit i per les vegades que hem intentat arreglar el món; Mercè, espero que tu, un dia no gaire llunyà, passis també per aquest moment en el qual estic jo ara. I a la resta de l'Àrea, que no deixa de créixer cada any, molts ànims i molta sort en la vostra carrera investigadora. En aquest moment també vull agrair a la Lluïsa Matas el fet d'haver-me facilitat la feina tant amb l'ICP-MS com amb el microones.*

*Part d'aquesta tesi es va fer al "Departamento de Química Analítica, Nutrición y Bromatología" de la Universitat d'Alacant. A tots ells els vull agrair la seva acollida i integració, especialment al meu director de recerca, en José Luis, i a l'Edu, investigador i amic excel·lent.*

*My days at Lancaster were really special. There, I found really nice people. Bill and Hao, thank you very much for your supervision, wellcome and attention, I won't forget neither the nice meals at your home nor the excursions to the Lake Districts. Debbie, Jacqui, Mohammed and Øyvind, thank you very much for the nice time spent together, at home and around Lancaster.*

*Als SCT de l'ICRA, moltes gràcies per aquest mesos que he passat amb vosaltres. Marta i Àlex, espero que aviat us trobeu també en aquest moment. Olga, gràcies pels ànims, els consells i les hores de laboratori que hem compartit. Sara, gràcies perquè, a més d'una gran "jefa", ets una gran amiga. Molta sort a tots.*

*Diuem que els amics van i vénen, però també n'hi ha d'aquells que són per sempre. D'aquests últims en tinc uns quants; alguns ja els he anomenat, però n'hi ha d'altres que indirectament també m'han*

*ajudat molt aquests anys i també mereixen que ara els doni les gràcies. Gràcies a la Taula del Fons per tots els moments que hem compartit i seguirem compartint, especialment a la Núria perquè hi és sempre. Laura, Iòlix i Yolí, gràcies per l'amistat que ens uneix, espero que la sort us acompanyi. Enric, Montse i petits, moltes gràcies per l'atenció i l'amistat que en tot moment rebem de vosaltres. A tota la colla d'Aiguafreda, gràcies pels bons moments que ens feu passar.*

*Un agraïment molt especial a tota la meva família, perquè ells són els que sempre han cregut en mí, m'han ajudat en els pitjors moments i m'han animat sempre a realitzar els meus somnis. Gràcies als meus pares per haver-me donat sempre tot el suport que he necessitat. Gràcies també per haver sigut pares quan calia i ser amics ara. Gràcies a les meves germanes i els meus cunyats per ser els millors amics que tinc, gràcies per ser-hi sempre que us he necessitat. Gràcies a les alegries de la casa, l'Irma i la Neus, que sense fer res especial, sempre ens fan sentir millor. Gràcies als avis i padrins per creure sempre en les meves possibilitats. Gràcies també a la Margo i a l'Antonio per la seva alegria i confiança.*

*Finalment, moltes gràcies Ton per acompanyar-me cada dia. A tu et vull dedicar aquesta tesi. Gràcies per la teva energia i la paciència. Gràcies per saber-me arrencar somriures fins i tot en els moments més difícils. Gràcies per recordar-me cada dia que no estaré mai sola.*

*Moltes gràcies a tots per ser una peça del meu trencaclosques.*

MiReia